THE UNIVERSITY
of EDINBURGH

Identification of novel genes interacting with *DVAP*, the causative gene of ALS8 in humans

Mario Andrés Sanhueza Cubillos

Doctor of Philosophy

Centre for Integrative Physiology

School of Biomedical Science

University of Edinburgh

2015

Declaration

I declare that this thesis was composed by myself and that the work contained herein is my own, except where explicitly stated otherwise in the text. This work has not been submitted for any other degree or professional qualification except as specified.

Mario Sanhueza

Febraury 2015

Abstract

Amyotrophic lateral sclerosis (ALS) is a major neurodegenerative disease caused by the death of motor neurons leading to paralysis. Mechanisms underlying the pathogenesis of the disease remain unknown but with the identification of causative genes from ALS patients, some processes have been linked to the disease. One of these genes is *VAPB*, a highly conserved protein involved in lipid transfer, vesicle metabolism and synaptic morphology. We modeled in *Drosophila* the disease-linked P56S mutation (*DVAP-P58S*) and observed with the expression of this allele neurodegeneration in the eye and loss of motor performance. These phenotypes provide an excellent opportunity to use fly's genetics to find novel genetic interactors of DVAP and understand ALS pathomechanism. Therefore, we carried out a large scale genetic screen by crossing the ALS model with a collection of P-element overexpression lines. After the analysis of 1183 lines, we obtained 71 modifier lines that suppress DVAP-induced neurodegeneration and 14 lines that enhance this phenotype, decreasing furthermore the eye size and viability of the offspring. To confirm that the effect of modifier lines was caused by a specific gene, we validated them with independent alleles of those genes. Using different sources, we were able to confirm the effect of 63 of the 85 modifiers, providing a strong confirmation of their effect. When we studied the effect of the modifier genes co-expressed with DVAP-P58S in the nervous system, we detected that 46 lines presented the same modifying effect in adult viability and 58 in the motor performance of the adult offspring. Considering the stronger readouts, we obtained 42 genes as novel high confidence DVAP genetic interactors. To understand furthermore the way they are affecting DVAP neurodegeneration, we carried out a series of bioinformatic analyses using *Drosophila* and human databases. Lipid droplets, vesicle metabolism and cell proliferation appear as the most important categories found in the screen, all processes conserved when analysed with human orthologs of the modifiers. Further characterisation of the endocytosis-linked modifier Rab5 and the predicted DVAP-interactors Rab7 and Rab11, showed that the suppression effect is not only confirmed *in vivo* but is also conserved in human tissue from ALS patients. These data validate our genetic screen and at the same time open novel opportunities to understand ALS mechanisms and find possible therapeutic targets.

Acknowledgments

Firstly, I would like to thank my supervisor Giusy Pennetta for the opportunity to be part of her lab, her guidance throughout my PhD and for explaining me all the details needed to become a Drosophilist. I have to thank my colleagues Stuart Forrest and Vin Sahota for the help and support on the first stages of my project, and Raquel Mendez-Castro and Luigi Zechini for their company and technical support in different parts of this period.

Many thanks to Andrew Jarman and his group, who constantly supported my research and project with ideas and feedback in our lab meetings, especially Lynn, Petra, Kasia and Daniel. Also, I have to thank all the honour and summer students that worked in our lab. Special mentions to Alistair and Mohammed that worked in part of this project.

I also would like to thank enourmously to the Euan MacDonald Centre for motor neurone disease research, who have funded my PhD. I really hope the data presented in this thesis provide ideas and hope for the cure of these dramatic diseases.

A huge thank you to all my family back in Chile. My Dad and Mum that had the chance to understand my new world and enjoy part of my life in Edinburgh. Also my siblings Cristian, Felipe and Nicole, which with eternal love supported me in every step and encourage me to persue my dreams. Thanks for leading me to this stage.

Finally, my most important acknowledgement and gratitude are for my wife Natalia. Her personal and scientific support in every step of my project, the constant company in the hardest moments and especially the unconditional love that backs all our plans are the main reason why I reached this point. Ultimately, these words, plans and thoughts are for Matilda and our future.

Table of contents

List of figures

List of tables

List of abbreviations

ALS	amyotrophic lateral sclerosis
ANOVA	analysis of variance
APP	amyloid precursor protein
ATP	adenosine triphosphate
BDSC	Bloomington *Drosophila* stock center
BSA	bovine serum albumin
C9orf72	chromosome 9 open reading frame 72
CA	constitutively active
CC	coiled-coil
CG	Computed gene
CMT	Charcot-Marie-Tooth
CTRL	Control
Cy3	indocarbocyanine
DAVID	Database for annotation, visualization and integrated discovery
DENN	differentially expressed in normal and neoplasia
DIOPT	DRSC integrative ortholog prediction tool
DN	dominant negative
DNA	deoxyribonucleic acid
DRSC	*Drosophila* RNAi screening center
DVAP	*Drosophila* VAMP-associated protein
EGF	epidermal growth factor
ELAV	embryonic lethal abnormal vision
EMS	ethylmethane sulphonate
ER	endoplasmic reticulum
fALS	familial amyotrophic lateral sclerosis
FDR	False discovery rate
FFAT	diphenylalanine in an acidic tract
FESEM	field emission scanning electron microscope
FITC	fluorescein isothiocyanate
FRT	flp recombinase target
FTD	frontotemporal dementia
FUS	fused in sarcoma
GAP	GTPase activating protein
GDP	guanosine diphosphate
GEF	guanine nucleotide exchange factor
GFP	green fluorescent protein
GMR	Glass multimer reporter
GTP	guanosine triphosphate
GO	Gene Ontology
GWAS	Genome-wide association studies
HE	haematoxylin and eosin
HD	Huntington’s disease
HRP	horseradish peroxidase
HSP	heat-shock protein
IPA	Ingenuity pathway analysis

JNK	Jun N-terminal kinase
KASH	Klarsicht, ANC-1, Syne Homology
kb	kilobase
kDa	kilodalton
LD	lipid droplets
MND	motor neurone disease
mRNA	messenger ribonucleic acid
MSP	major sperm protein
NGS	normal goat serum
NIG-Fly	Fly stocks of National institute of Genetics
NMJ	neuromuscular junction
NSF	N-ethylmaleimide sensitive fusion
OMIM	Online Mendelian Inheritance in Man
ORF	open reading frame
OST	One-sample t-test
PANTHER	Protein Analysis through evolutionary relationships
PBS	phosphate buffered saline
PBT	phosphate buffered saline + Triton X-100
PCR	polymerase chain reaction
PH	pleckstrin homology
PI	phosphatidyl inositol
PI3K	PI 3-kinase
PI3P	PI 3-phosphate
PI(3,5)P2	PI (3,5) bisphosphate
PI4P	PI 4-phosphate
RIR	RAF-inhibitory region
RNA	ribonucleic acid
RNAi	RNA interference
RT	room temperature
sALS	sporadic amyotrophic lateral sclerosis
SCA	spinocerebellar ataxia
SDS	Sodium dodecyl sulfate
SNARE	soluble NSF attachment protein receptor
SOD1	superoxide dismutase 1
TAR	transactive response
TDP-43	TAR DNA-binding protein of 43 kDa
TGN	trans-Golgi network
TM	transmembrane
TRiP	transgenic RNAi project
UAS	upstream activating sequence
UPR	unfolded protein response
UPS	ubiquitin-proteasome system
VAPB	VAMP associated protein B
VAMP	vesicle-associated membrane protein (Synaptobrevin)
VDRC	Vienna *Drosophila* Resource Center
WT	wild-type

Chapter 1:
Introduction

1.1 Amyotrophic lateral sclerosis and motor neuron diseases

Amyotrophic lateral sclerosis (ALS) is a progressive adult-onset disorder, characterized by the selective death of upper and lower motor neurons leading to paralysis and muscle atrophy (Pasinelli & Brown, 2006). Most clinical symptoms appear when axons show retraction and denervation, effect slowered through subsequent lateral sprouting and reinnervation. After the failure of this last response, neurons die leading to development of the disease (Robberecht & Philips, 2013). ALS is the most common motor neuron disease and one of the major neurodegenerative diseases alongside Alzheimer's disease and Parkinson's disease, with an incidence rate of 1-2 per 100,000 people affected per year and a uniform distribution in Europe of 2.16 per 100,000 persons (Kiernan *et al.*, 2011).

The overall population-based lifetime risk of ALS is 1:400 for women and 1:350 for men. The peak age at onset is 58–63 years for sporadic disease and 47–52 years for familial disease (Kiernan *et al.*, 2011). In most cases, respiratory failure causes the death of patients usually within 5 years after the onset of clinical symptoms (Pasinelli & Brown, 2006). These include limb spasticity, fasciculation and weakness, slow and distorted speech caused by bulbar dysfunction, and defects in bulbar lower motor neurons, leading to tongue wasting and dysphagia (Kiernan *et al.*, 2011). Evaluations of all these symptoms are required to distinguish between different ALS types and other pathologies with similar symptoms as endochrinopathies, infections and intoxication (Kunst, 2004).

Studies of familial cases of ALS (fALS) have identified thirty genetic loci as causative to the disease (Figure 1), including among others, mutations in the genes *VAPB, ALS2, TARDBP* and *SOD1* (Nishimura *et al.*, 1994; Hadano *et al.*, 2001; Neumann *et al.*, 2006; Rosen *et al.*, 1993). Mutations in these genes share the same pathological features as sporadic ALS (sALS), which represent 90% of the cases (Chen *et al.*, 2010) (Figure 1). The diversity of gene functions means that different processes have been implicated in the pathogenesis of ALS, including apoptosis, mitochondrial defects, altered axonal transport and RNA processing (Cleveland &

A

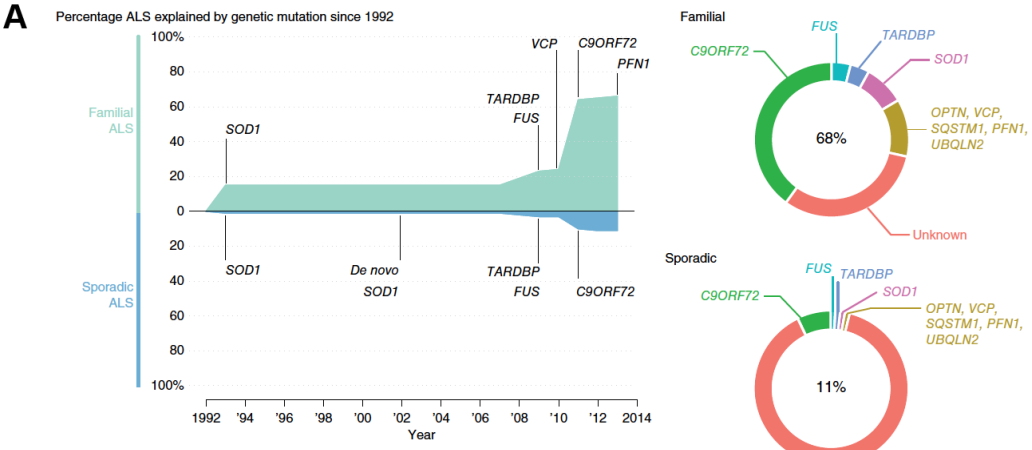

B

Locus	Gene symbol	Gene name	Chromosome
ALS 1	*SOD1*	Superoxide dismutase 1, soluble	21q22.11
ALS 2	*ALS2*	Amyotrophic lateral sclerosis 2 (juvenile)	2q33.2
ALS 3	Unknown	Unknown	18q21
ALS 4	*SETX*	Senataxin	9q34.13
ALS 5	*SPAST*	Spastin	2p24
ALS 6	*FUS*	Fused in sarcoma	16p11.2
ALS 7	Unknown	Unknown	20p13
ALS 8	*VAPB*	VAMP (vesicle-associated membrane protein)-associated protein B and C	20q13.33
ALS 9	*ANG*	Angiogenin, ribonuclease, RNase A family, 5	14q11.1
ALS 10	*TARDBP*	TAR DNA-binding protein	1p36.22
ALS 11	*FIG4*	FIG4 homologue, SAC1 lipid phosphatase domain containing (*Saccharomyces cerevisiae*)	6q21
ALS 12	*OPTN*	Optineurin	10p13
ALS 13	*ATXN2*	Ataxin 2	12q23–q24.1
ALS 14	*VCP*	Valosin-containing protein	9p13
ALS 15	*UBQLN2*	Ubiquilin 2	Xp11.21

Locus	Gene symbol	Gene name	Chromosome
ALS 16	*SIGMAR1*	Sigma non-opioid intracellular receptor 1	9p13
ALS 17	Unknown	Unknown	3p11.2
ALS 18	*PFN1*	Profilin 1	17p13.3
ALS–FTD 1	Unknown	Unknown	9q21–q22
ALS–FTD 2	*C9orf72*	Chromosome 9 open reading frame 72	9p21.2
ALS–FTD 3	*CHMP2B*	Charged multivesicular body protein 2B	3p12.1
ALS	*UNC13A*	Unc-13 homologue A (*Caenorhabditis elegans*)	19p13.12
ALS	*DAO*	D-amino-acid oxidase	12q24
ALS	*DCTN1*	Dynactin 1	2p13
ALS	*NEFH*	Neurofilament, heavy polypeptide	22q12.1–q13.1
ALS	*PRPH*	Peripherin	12q12
ALS	*SQSTM1*	Sequestosome 1	5q35
ALS	*TAF15*	TAF15 RNA polymerase II, TATA box binding protein (TBP)-associated factor, 68 kDa	17q11.1–q11.2
ALS	*SPG11*	Spastic paraplegia 11 (autosomal recessive)	15q14
ALS	*ELP3*	Elongator acetyltransferase complex subunit 3	8p21.1

Figure 1. ALS causative genes. (A) Timeline of gene discoveries in familial and sporadic ALS. Values represent the proportion of ALS explained by each gene in populations of European ancestry. In the charts at the right, percentages represent the amount of cases explained by known genetic mutations. Taken from Renton *et al.*, 2013. (B) Genes thought to cause or increase risk of ALS and their location in the human genome. FTD, frontotemporal dementia. Taken from Al-Chalabi & Hardiman, 2013.

Rothstein, 2001). However, even considering all these functions, the molecular mechanism underlying this disease remains elusive. The study of these individual pathways and the search and characterisation of new causative genes are the best way to move forward in the comprehension of the disease.

1.2 ALS causatives genes

1.2.1 Cu/Zn-superoxide dismutase (SOD1)

Twenty years ago, Rosen *et al.* (Rosen *et al.*, 1993) linked for the first time genetic mutations with ALS. Thirteen different families showed different mutations in the gene that encodes the cytoplasmic copper/zinc-binding superoxide dismutase SOD1, an enzyme that catalyses the conversion of the toxic O_2^- anions into O_2 and H_2O_2. Being the first gene associated with the disease, several studies in patients have found more than 100 mutations throughout the years, but only a subset of these mutations shows a link to a pathogenic effect of the protein (Andersen *et al.*, 1996). Also, these mutations, which account for over 10% of all the familial cases of the disease (Chio *et al.*, 2008), exhibit a broad range of phenotypes and penetrance. These effects stretch from the one caused by the aggressive A4V allele that leads to death in less than one year from the symptom onset, to the milder D90A form, which causes respiratory failure only after 10 years of the onset (Andersen *et al.*, 1996).

SOD1 is an important protein in the respiratory metabolism, involved in free radical scavenging. However, pathogenesis caused by the mutation does not seem to be associated with a loss-of-function mechanism, but more likely to an increase in the aggregation and misfolding of the protein (Robberecht & Philips, 2013). Most SOD1 mutations are missense and not truncations, suggesting that most of the protein length must be present in the cell to trigger a pathogenic effect. Misfolded SOD1 proteins carrying these mutations escape from ubiquitylation process and affect proteasomal pathway and autophagy clearance pathways (Bendotti *et al.*, 2012; Chen *et al.*, 2012).

Misfolded protein aggregates cause failure of several cellular processes and trigger ER stress response and apoptotic signals (Pasinelli & Brown, 2006). Processes related to SOD1 toxicity include axonal transport and cytoskeleton defects (Williamson & Cleveland, 1999; Farah *et al.*, 2003), DNA/RNA metabolism (Pasinelli & Brown, 2006) and mitochondrion dysfunction (Pasinelli *et al.*, 2004). However, all these processes seem to be related to protein stability and aggregation more than to the original function of the enzyme and its lack of function in the affected cell (Pasinelli & Brown, 2006). The relevance of the aggregation in the death of cells has led to several studies to propose SOD1 as a potential prion-like protein. In this hypothesis, a misfolded version of SOD1 would seed the transformation of wild-type SOD1 into fibrils that can be then transmitted to other cells. These fibrillar species represent a toxic state of the protein that would lead to cellular death, developing the whole pathology (Chia *et al.*, 2010; Grad *et al.*, 2011). These novel features, far from elucidating the complex genetics of SOD1 mutations, open extra questions in terms of cross-seeding process, exportation of the toxic aggregates to other cell types and discrimination between toxic and wild type forms of the protein (Polymenidou & Cleveland, 2011).

Different animal models have been generated to understand SOD1-induced pathogenesis, but none of them has completely clarified the picture. Studies with the first SOD1 transgenic mouse elucidated relevant interactions and cellular mechanisms (Pasinelli *et al.*, 2004) but the model has failed as a target of proposed human therapies (Ludolph *et al.*, 2010). Wang *et al.* observed that overexpression of wild-type version of SOD1 accelerated the disease onset and pathogenesis in mice expressing a mutant form of the protein (Wang *et al.*, 2009). They suggest that wild-type SOD1 may be recruited to toxic aggregates caused by the mutant version. Other rodent models however, have not improved these aspects (Turner & Talbot, 2008) and currently, SOD1-ALS is treated independently of other types of ALS, mainly for its absence of TDP43-related phenotypes (Renton *et al.*, 2013). Watson *et al.* generated the first *Drosophila* model for SOD1 and observed motor defects, upregulation of the heat shock protein 70 and reduction of synaptic transmission. These phenotypes are also present when the wild type form of the protein is

overexpressed (Watson *et al.*, 2008). However, no effect was observed in motor neuron survival and life span. Expression of three different ALS-related SOD1-mutations in *C. elegans* also showed aggregates formation and mild cellular dysfunction. Interestingly, this toxicity was enhanced when proteins that destabilize the cellular folding machinery were co-expressed. This indicates that SOD1 toxicity may not be completely dependent of its own misfolding activity but also depends on genetic interactions with other cellular pathways (Gidalevitz *et al.*, 2009).

1.2.2 Transactive response DNA-binding protein (TDP-43) and Fused in sarcoma (FUS)

RNA processing dysfunction appeared to be a cause of ALS pathogenesis when the Transactive response DNA-binding protein (TARDBP, TDP-43) was found to be a major component of ALS-associated protein aggregates in neurons (Neumann *et al.*, 2006). Mutations in this gene account for 4% of ALS familial cases (Sreedharan *et al.*, 2008) and since the original discovery in 2006, several other mutations have been linked to sporadic cases of ALS and FrontoTemporal dementia (FTD). TDP-43 is a protein involved in RNA processing that normally presents a nuclear localisation but shuttles to cytoplasmic protein aggregates where then blocks mRNA translation as a response to starvation or oxidative stress (Dewey *et al.*, 2011). In ALS patients, the protein is located mostly in stress granules, which are cytoplasmic aggregates composed by proteins and inactive mRNA and induced by cellular stress. TDP-43 translocation to these structures potentially initiates neurodegenerative effects in neurons and glia (Ferraiuolo *et al.*, 2011).

One hypothesis that explains TDP-43 toxicity highlights the exact amount of protein needed for the normal function of TDP-43. ALS-linked mutations enhance the aggregation ability of the protein, increasing toxic aggregation and formation of stress granules that includes also the wild-type form of the protein in a gain-of-function mechanism. This translates at the same time, in the decrease of the TDP-43 amount available in the nucleus, implying a loss of TDP-43 normal function as an RNA processing protein (Johnson *et al.*, 2009; Blokhuis *et al.*, 2013) This two-step

gain-of-function/loss-of-function mechanism may be related to functions of other proteins and has been proposed as a central explanation for ALS pathomechanism (Robberecht & Philips, 2013).

The discovery of Fused in Sarcoma (*FUS*) as an ALS causative gene also fortified the role of RNA metabolism in the disease (Vance *et al.*, 2009; Kwiatkowski *et al.*, 2009). This protein, just as TDP-43, is involved in transcriptional regulation and RNA processing. FUS ALS-linked mutations generally alter the nuclear localisation of the protein, inducing the formation of FUS aggregates in the cytoplasm (Dormann *et al.*, 2010). Just as in the case of TDP-43, the mechanism underlying the disease is not known and it can be due to a combination of loss of FUS nuclear function and gain of toxic function in the cytoplasm.

Compared to SOD1, TDP-43 animal models have been more successful mirroring hallmarks of the disease, but they still do not provide a complete picture of the disease mechanism. Neuromuscular phenotypes and motor dysfunction have been observed in *Drosophila*, zebrafish and mice models (Feiguin *et al.*, 2009; Laird *et al.*, 2010; Kraemer *et al.*, 2010). In rodent models toxicity phenotypes have been detected with the overexpression of mutants and wild type versions of the protein, implying that TDP-43 pathogenesis may be dosage dependent (Stallings *et al.*, 2010). In zebrafish and fly models however, mutant TDP-43 overexpression causes a greater degeneration than the wild type version (Liachko *et al.*, 2010; Laird *et al.*, 2010). An interesting result was observed in a conditional rat model that presented motor performance dysfunction when TDP-43 was overexpressed. The observed paralysis was however, suppressed in the same animal when the overexpression was transiently removed, result that can give insights into a potential reversible pathogenic effect of the protein (Huang *et al.*, 2012).

The association of TDP-43 and RNA metabolism with the disease changed the initial idea of a disease based exclusively on protein dysfunction. At the same time this protein linked even more ALS and FTD as similar genetic diseases. The

connection between the two diseases and the relevance of RNA processing as an associated pathway in the diseases were supported later on with the identification of novel mutations in other RNA metabolism-related genes such as C9orf72 (Robberecht & Phillips, 2013).

1.2.3 Chromosome 9 open reading frame 72 (C9orf72)

An important shift in the research of the ALS occurred a couple of years ago when two different groups reported that in the genetic locus *C9orf72*, a GGGGCC hexanucleotide repeat expansion was the cause of the ALS and FTD cases linked to the chromosomal region 9p21 (DeJesus-Hernandez *et al.*, 2011; Renton *et al.*, 2011). This breakthrough constituted the first time that a repeat expansion is linked to ALS but more importantly, this expansion appeared to be the most frequent cause of the disease. Only considering the familial cases, expansions in C9orf72 now account for up to 48% of the ALS cases (Woollacott & Mead, 2014). Interestingly, expansions in this gene are also linked to 25% of the familial FTD cases, explaining genetically the overlap between these two diseases (Majounie *et al.*, 2012).

The increasing relevance of this protein in the disease has not been translated yet to a definitive pathomechanism. C9orf72 function is not clear yet, but *in silico* research suggested that it may be related to Differentially Expressed in Normal and Neoplasia (DENN), a GDP/GTP exchange factor (GEF) protein that regulates Rab-GTPases activation and vesicular trafficking (Levine *et al.*, 2013). Patients with ALS-carrying expansions in the gene show RNA foci, also found in TDP43-linked patients. RNAi foci suggest a link to RNA metabolism disruption and sequestering of RNA binding proteins (DeJesus-Hernandez *et al.*, 2011) but the mechanism in which hexanucleotide are toxic in neurons still has not been completely understood. Recently however, the link between C9orf72 and endocytic transport was confirmed *in vivo*, suggesting that the role of this protein in RNA metabolism and protein degradation may be an important pathway in ALS pathogenesis (Farg *et al.*, 2014)

A current hypothesis for hexanucleotide toxicity involves the disorganised recruitment of splicing factors during the C9orf72 mRNA production, which translates in a loss-of-function mechanism. The presence of RNA G-quadruplexes, guanine-rich nucleic acids sequences that form four-stranded structures (Bugaut and Balasubramanian, 2012), alters the RNA splicing and disrupts the production of one of the three mature transcripts for this gene. At the same time, this expansion can generate toxic insoluble dipeptide repeats that may affect in a direct form the cellular metabolism in a gain-of-function mechanism (Fratta *et al.*, 2012; Robberecht & Philips, 2013). This hypothesis implies two different mechanisms for the C9orf72-linked toxicity, with loss- and gain-of-function mechanisms. These are not mutually exclusive but still unclear whether both of them contribute to the degeneration and how they are connected to other ALS-linked mutations.

Considering the recent discovery of *C9orf72* as an ALS causative gene, big efforts have been made to construct animal models and characterise the effect of the hexanucleotide repeat expansion. So far, studies have shown that loss-of-function of C9orf72 is linked with motor deficits in zebrafish (Ciura *et al.*, 2013) but also that a decrease of 70% of its transcription is not enough to produce a phenotypic effect in mice (Lagier-Tourenne *et al.*, 2013). Even though there is not a *Drosophila* homologue for C9orf72, strong structural homology can be found with other DENN-like proteins (Stepto *et al.*, 2014). Additionally, studies have related overexpression of G_4C_2 hexanucleotide repeats with neurodegeneration in *Drosophila* eye and motor neurons (Xu *et al.*, 2013). The confirmation of these results in Zebrafish, where RNAi foci were also found (Lee *et al.*, 2013) supports the idea of animal modeling. However the lack of strong evidence suggests a long period before complete characterization of the C9orf72 pathomechanism.

1.2.4 Alsin (ALS2)

ALS2 is one of the three genes causative of a juvenile form of ALS (altogether with *SETX* and *SPG11*) and also the only one where recessive loss-of-function mutations are responsible for the disease. Mutations in this gene, identified originally in a

Tunisian family in 2001 (Hadano *et al.*, 2001), are also associated with other MNDs but they represent less than 1% of known ALS cases (Hadano *et al.*, 2007). ALS2 protein has multiple domains associated with regulation of small GTPases, including Rac, Rho and Rab families. Small GTPases function as molecular switches, changing from a GTP-bound active state to an inactive GDP-bound state. This GTP-depending control is regulated also by the guanine nucleotide exchange factor (GEF) and GTPase activating protein (GAP) proteins, which improve the GTP binding and hydrolysis respectively (Zhang *et al.*, 2007). In vitro, ALS2 shows a GEF activity on Rab5, through its VPS9-containing C-terminal domain. The presence of the vacuolar protein sorting 9 (VPS9) domain suggests an involvement of ALS2 in membrane dynamics and cytoskeletal structure of the cell (Hadano *et al.*, 2007).

ALS2 is also related to ALS because of its interaction with SOD1. ALS2 binds mutant but not wild type forms of SOD1, through its RhoGEF domain (Kanekura *et al.*, 2004). Morever, ALS2 suppress SOD1-induced toxicity in a mouse model, activating Rac1 and the PI3K/Akt prosurvival pathway (Kanekura *et al.*, 2005). A parallel work confirmed this finding reporting an exacerbation of motor dysfunction in a SOD1 mutant by loss of ALS2 function (Hadano *et al.*, 2010).

1.2.5. Other causative genes

A constantly increasing number of at least 30 genetic loci have been associated with ALS so far (Robberecht & Philips, 2013). Some of these loci have not been completely validated and others have been strongly linked with other similar syndromes. Nevertheless, detailed study of each of these genes can potentially provide important clues and connections to understand the disease mechanism.

Found originally in Japanese families (Maruyama *et al.*, 2010), mutations in Optineurin (*OPTN*) were also associated with other disorders not closely linked to ALS such as primary open angle glaucoma and Paget's disease of bone (Rezaie *et al.*, 2002; Albagha *et al.*, 2010). The molecular function of OPTN is related to protein secretion, membrane trafficking and cell division. The recent association of

the gene with ALS and the low frequency in the total of familial cases (lower than 1%) translate in a lower interest in the characterisation of OPTN pathomechanism at the moment.

Other gene found mutated in only 1% of the familial ALS cases is the Valosin-containing protein (*VCP*). Connected to the disease for the first time in 2010 (Johnson *et al.*, 2010), mutations in VCP were previously linked with FTD (Watts *et al.*, 2004) supporting furthermore the similarities between this disease and ALS. These mutations seem to affect the respiratory metabolism and levels of ATP produced due to mitochondrial uncoupling (Bartolome *et al.*, 2013). The mechanism recapitulates deficiencies observed with SOD1 mutations, indicating that different causative genes can be involved in converging pathways. Interestingly, the discovery of VCP mutations in 2010 was the first obtained using exome sequencing of affected patients, a technique that will help to study known and novel mutations in families without abundant availability of genetic data (Renton *et al.*, 2013).

UBQLN2 and *SQSTM1* that encode Ubiquilin 2 and p62 respectively, are two genetic loci associated with protein degradation, which were recently linked to less than 1% of patients with the disease (Deng *et al.*, 2011; Gal *et al.*, 2009). P62 directs and ubiquilin transports polyubiquitinated proteins to the protein degradation systems ubiquitin-proteasome and autophagy. In this way, p62 and ubiquilin link these two systems and accentuate the relevance of this pathway in the disease pathogenesis (Ling *et al.*, 2013). Protein aggregation and accumulation appear as an important cause of neurodegeneration for most ALS-linked mutations. Therefore, the presence of UBQLN2 and SQSTM1 in protein inclusions found in ALS patients provides extra evidence for that mechanism (Ling *et al.*, 2013). Whether protein aggregation is an initial trigger or a consequence of toxicity caused by other proteins is not completely understood although.

Finally, an important group of genes is associated with cellular transport defects, a cause also related to the most studied loci (Ferraiuolo *et al.*, 2011). Only two years ago, mutations in Profilin 1 (*PFN1*) were found in several ALS kindred

(Wu *et al.*, 2012). This gene plays an important role in cytoskeletal architecture, functioning as an actin-monomer binding protein (Witke, 2004). PFN1 also interacts with VCP, the spinal muscular atrophy causative gene *SMN*, and Huntingtin, the causative of Huntington's disease. This suggests that cytoskeleton regulation can be a misregulated pathway shared between different disorders (Wu *et al.*, 2012). Mutations in Dynactin (*DCTN*), Neurofilament heavy polypeptide (*NEFH*), phosphoinositide phosphatase (*FIG4)*, Charged multivesicular body protein 2b (CHMP2B) and peripherin (*PRPH*) have all been linked to ALS (Munch *et al.*, 2004; Figlewicz *et al.*, 1994; Chow *et al.*, 2009; Parkinson *et al.*, 2006; Gros-Louis *et al.*, 2004). These genes are connected to both axonal and vesicular transport in neurons. However, despite the fact that all of them could potentially be part of a crucial mechanism to explain the disease, these genes have been less studied than the previously mentioned causative loci. The lack of patients carrying a mutation in this group of genes has been associated with a lower relevance in the whole picture of ALS mechanism. This tendency can be risky if we consider that they may possess an equally high importance in the disease pathogenesis and their underestimation in favour of the most studied genes can lead to an incomplete map of the disease. Commonalities between the previously mentioned neurodegenerative disorders could be explained by similar pathomechanisms, where all these described causative genes should play an important role. A similar situation is observed with mutations in the protein VAPB, a transport-related protein that will be the central focus of this study.

1.3 VAP proteins

Vesicle-associated membrane protein (VAMP) associated protein, VAP, is another important ALS-linked protein. A mutation in this gene was first isolated from an ALS Brazilian kindred and therefore, research with animal models and patients have increased in the last decade. VAP relevance in several key cellular processes has transformed this protein in a crucial player in different mechanisms associated with neurodegeneration.

1.3.1 VAP primary organization exhibits three conserved domains

First isolated from *Aplysia californica* (Skehel *et al.*, 1995), VAP-33 was proposed to be a SNARE (soluble N-ethylmaleimide-sensitive factor attachment protein receptor) associated protein. These proteins are relevant in synaptic fusion (Lev *et al.*, 2008) and autophagic degradation and regulation (Furuta *et al.*, 2010).

After being identified in *Aplysia*, VAP genes were found in humans (Weir *et al.*, 1998), mice (Nishimura *et al.*, 1999), *Drosophila* (Pennetta *et al.*, 2002), yeast (Loewen *et al.*, 2003) and *C. elegans* (Tsuda *et al.*, 2008). This highly conserved gene has two isoforms in mammals, *VAPA* and *VAPB*. A third one, *VAPC*, was found to be a shorter splicing variant of *VAPB* without known data of expression or function (Nishimura *et al.*, 1999). VAP proteins are ubiquitously expressed in tissues, organs and cell types with a higher expression in the nervous system (Skehel *et al.*, 2000). In the human nervous system, five splice variants of VAPB have been found but the alternative versions are barely detected and quickly degraded through the proteasomal system (Nachreiner *et al.*, 2010).

VAP proteins share highly conserved sequences and three relevant domains (Figure 2). Facing the cytoplasm, the N-terminal region exhibits a sequence that is highly similar functionally and structurally to *C. elegans* Major Sperm Protein (MSP) (Kuwabara, 2003). MSP is a dimeric protein that forms non-polar cytoskeletan filaments and mediates amoeboid motility. The dimerization of recombinant MSP domain observed in VAPB suggests that this domain may contribute to VAP oligomerisation (Lev *et al.*, 2008). Inside this MSP domain, there is a FFAT (diphenylalanine in an acidic tract) binding site formed by the consensus aminoacid sequence EFFDAxE. FFAT works as a targeting signal motif and localises proteins to the cytosolic side of the ER and nuclear membranes (Kaiser *et al.*, 2005). FFAT binding site is highly conserved among VAP proteins but not in MSP proteins, indicating that this sequence activity is important for VAPB biological function (Lev *et al.*, 2008).

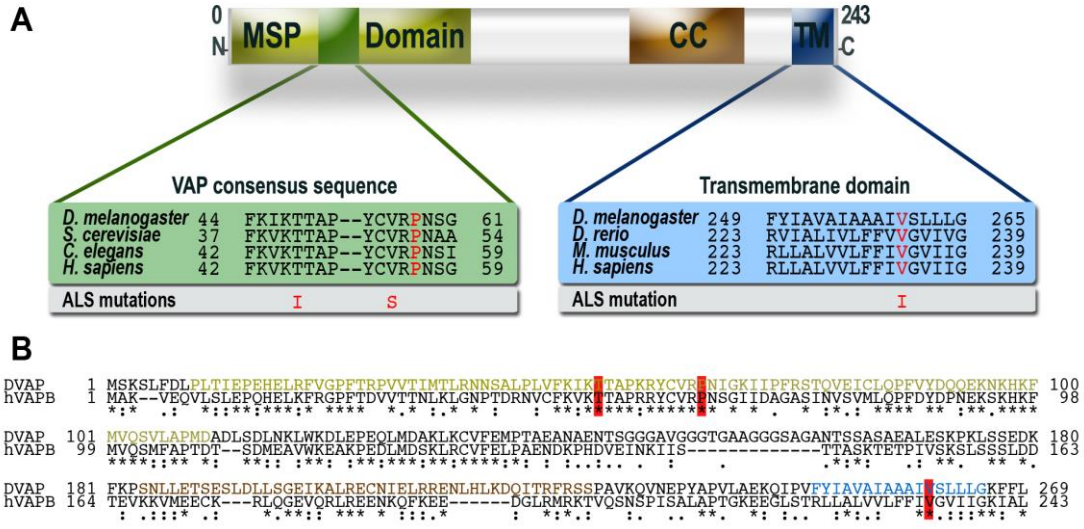

Figure 2. VAP proteins sequence and conserved domains. (A) Predicted domains in VAP proteins: major sperm protein (yellow), coil-coiled (brown) and transmembrane domains (blue). The high degree of homology in the VAP consensus (pale green box) and transmembrane (pale blue box) sequences are specified for different species. The three ALS-linked mutations (gray box) are presented in these conserved sequences. (B) Alignment of the sequences from human VAPB (hVAPB) protein and its *Drosophila* orthologue DVAP. Asterisks indicate an identity match; colons indicate conservation between amino acids with strongly similar properties and periods indicate a conserved substitution between amino acids with weakly similar properties. Red boxes highlight the amino acid residues changed by the ALS8 causing mutations identified so far. Adapted from Sanhueza *et al.*, 2013.

The central part of the protein shows a variable coiled-coil domain (CCD) that is also present in other VAMPs and SNARE proteins (Nishimura *et al.*, 1999). VAPA and VAPB form homo- and hetero-dimers mediated by both the CCD and the dimerization site located in the C-terminal transmembrane region of the protein. The similarity of VAP protein in the transmembrane region also is less conserved from yeast to humans compared to the MSP domain. The GxxxG dimerisation site is present from humans down to *C. elegans* and the lack of this sequence in the yeast VAP homolog explains its failure to form dimers (Russ & Engelman, 2000).

Different studies have found that VAP proteins localize in the ER and several other intracellular membrane such as endosome, Golgi, neuromuscular junction and plasma membrane (Lev *et al*., 2008). ER membranes can reach mostly every intracellular organelle through membrane conctact sites or ER junctions, explaining in this way the multiple localisation of VAP proteins (Levine and Loewen, 2006). Through these junctions, VAPB can regulate not only ER structure but also calcium homeostasis at the mitochondria and lipid transfer at the Golgi (De Vos *et al*., 2012; Peretti *et al.,* 2008). VAPB mutations that lead protein aggregation disrupt the normal VAPB localization. The formation of aggregates in immobile ER clusters (Teuling *et al*., 2007) and in non-ER compartments (Kanekura *et al.,* 2006) explains the toxicity and associate neurodegeneration of this structural change of the protein.

1.3.2 VAP functions affect several cellular processes

VAP proteins are linked with several important cellular processes including lipid transfer, vesicular trafficking, synaptic regulation, calcium metabolism and ER morphology (Amarilio *et al.*, 2005; Teuling *et al.*, 2007; Soussan *et al.*, 1999; Skehel *et al.*, 2000; Kuijpers *et al.,* 2013). A relation between VAP proteins and lipid transfer was originally observed in the yeast homologue SCS2. Opi1p, a transcriptional regulator of phospholipid biosynthesis, binds SCS2 through its FFAT domain. This binding was proposed as a common ER targeting mechanism for lipid-related proteins containing FFAT motif (Loewen *et al.*, 2003). Following this, different groups reported interactions between VAP and the FFAT motif-containing

proteins Oxysterol-binding protein (OSBP), ceramide transport protein (CERT) and phosphatidylinositol transfer protein (Nir2) (Wyles *et al.*, 2002; Kawano *et al.*, 2006; Amarilio *et al.*, 2005). Last year, we characterised the interaction between the *Drosophila* VAPB homologue and the phosphoinositide phosphatase Sac1 (Forrest *et al.*, 2013). Phosphoinositides (PI) are lipids that localise in specific cellular organelles according to their reversible phosphorylation state. Each one of these lipid pools can bind specifically different effector proteins regulating their intracellular concentrations (Blagoveshchenskaya & Mayinger, 2008). Sac1 is an evolutionarily conserved protein that mainly dephosphorylates PI4P pools, affecting actin organization and sphingomyelin synthesis (Foti *et al.*, 2001; Brice *et al.*, 2009). *Drosophila* DVAP is necessary to regulate phophoinositide levels through its interaction with Sac1, and the lack of this complex affects synaptic structure and causes neurodegeneration (Forrest *et al.*, 2013). OSBP and CERT interacts in the ER with VAPB through their pleckstrin homology domain (PH), and with the Golgi-specific PI4P pool through their FFAT motif. Disruption of the Sac1/DVAP complex could potentially alter not only phosphoinositide metabolism but also sphingolipid and sterol metabolism, regulated by CERT and OSBP proteins respectively (Raychaudhuri & Prinz, 2010, Forrest *et al.*, 2013).

Calcium homeostasis is another process regulated by VAPB. Wild type version of the protein interacts with the tyrosine phosphatase-interacting protein 51 (PTPIP51), an outer mitochondrial protein implicated in cell morphology and apoptosis (De Vos *et al.*, 2012). The mutant version of VAPB found in patients with ALS (VAPB-P56S) does not show interaction with PTPIP51, increasing the mitochondrial calcium uptake obtained from ER reservoirs. VAPB-P56S also disrupts Ca^{++} concentrations by the disruption of the mitochondrial Rho GTPase-1 Miro1/kinesin-1 complex. Affected binding affinity of Miro1 for tubulin leads to failure of anterograde axonal mitochondria transport, a phenotype also observed in the ALS-linked mutations of SOD1 (Morotz *et al.*, 2012). Calcium homoeostasis has been underlined as a possible explanation of the selective neuronal vulnerability. Specifically, motor neurons are more susceptible to calcium-overload due to limited

expression of the calcium-regulator glutamate receptor 2 (GluR2) (Van Damme *et al.*, 2007) and reduced calcium-buffering capacity (Vanselow & Keller, 2000).

Most VAP interactors are located at the ER, a fact that underlines the relevance of the protein in this organelle's function. ER-Golgi recycling protein YIF1A is a VAPB interactor that regulates intracellular trafficking into dendrites and ER morphology (Kuijpers *et al.*, 2013). Mutant VAPB disrupts this regulation and affects the localisation of both proteins. Alteration of the ER structure was also shown to be a consequence of VAPB-P56S-mediated aggregates that affect wild type VAPB availability and its interaction with other ER proteins (Teuling *et al.*, 2007; Fasana *et al.*, 2010). Increase of VAPB-associated inclusions was observed by down-regulating the ATPase VCP, another ALS-linked protein (Johnson *et al.*, 2010) and reduction of non-aggregated VAPB levels is one of the features shared with SOD1 mutant cells, another aggregation-prone ALS-causative protein (Teuling *et al.*, 2007).

Recently, VAPB was also linked to cell growth and cancer. When primary and metastatic breast tumor were analysed, VAPB appears overexpressed and this increase in mRNA levels correlates with a lower survival in patients with breast cancer (Rao *et al.*, 2012). Authors not only observed cell growth or inhibition with VAPB up- or down-regulation respectively, but also showed that modulation of AKT mediates this growth regulation. AKT forms part of a pathway altogether with mTOR and PI3K, which regulates phosphoinositide metabolism, autophagy and cell survival (Bitting & Armstrong, 2013; Fruman & Rommel, 2014). As mentioned before, VAPB is tightly associated with phosphoinositide metabolism; therefore, this study can present a still unknown relevance of VAPB in cell growth and cancer.

1.3.3 VAP MSP domain is cleaved and secreted

A recent hypothesis for VAP function suggests that the N-terminal MSP domain is secreted to regulate energy metabolism in muscles (Tsuda *et al.*, 2008; Han *et al.*, 2012; Han *et al.*, 2013). This highly conserved domain has been deeply studied in *C.*

elegans where it works as signaling molecule that controls oocyte maturation and fertility (Miller *et al.*, 2003). In *Drosophila,* Tsuda *et al.* showed that the DVAP-MSP domain is cleaved and secreted to bind postsynaptic Eph receptors. The ALS-linked DVAP mutation disrupts the cleavage of the domain and triggers the protein accumulation (Tsuda *et al.*, 2008). The same group later proved that the secreted MSP domain binds to Roundabout and Lar-like protein-tyrosine phosphatase receptors in muscles. These growth cone guidance pathways regulate actin remodeling and mitochondrial localisation via Arp2/3 complex. Therefore, secretion of DVAP-MSP domain can support energy production and ALS-linked VAP mutants can affect mitochondrial metabolism deregulating localisation and function of the protein (Han *et al.*, 2012).

Recently, the same authors proposed that an up-regulation of the FoxO pathway could compensate the metabolic dysfunction caused by the lack of VAPB-MSP domain secretion (Han *et al.*, 2013). DAF-16, the *C. elegans* FoxO homolog, presents an up-regulation when secreted MSP is low. This transcription factor activates ATP and triacylglycerol production in muscles, increasing lifespan and compensating VAPB-associated energy metabolism defects. DAF-16 acts downstream of Arp2/3 complex, therefore the up-regulation of the transcription factor and its fat-related downstream targets could explain the observed lipid accumulation in muscles and the recovery of mutants phenotypes observed in their previous work.

Lipid accumulation is an important aspect observed in VAPB related phenotypes. However, these previous works have not elucidated completely the implication of MSP domain secretion with lipid metabolism. Other lipid-related VAPB interactors may play an important role in the final mutant phenotype in a MSP-independent way, explaining in a better form the VAPB-linked neurodegeneration.

1.3.4 VAP interacting proteins include lipid- and synapsis-related proteins

The structure of VAP proteins and the presence of conserved domains facilitate an important number of interactions with other proteins. Mostly, these have been found in high-throughput approaches aimed at finding VAPB physical interactors in different organisms. However, VAPB genetic interactors have been not extensively characterized so far. In *S. cerevisiae*, different studies have found physical interactors of the yeast VAP homologue, Scs2p, including the proteins Num1, Rpn10 and the lipid-related proteins Stt4, Osh1, Osh2 and Erg2, 9 and 11 (Kagiwada & Zen, 2003; Chao *et al.*, 2009; Wilson *et al.*, 2011; Manford *et al.*, 2012). Most interactors originally were linked to the group of SNARE proteins, triggered by the initial finding that VAPB interacts with the synaptic SNARE VAMP (Lev *et al.*, 2008). Therefore, other proteins related to synaptic vesicles were found as VAPB interactors such as Rbet1, Rsec22, tSNARe, NSF and αSNAP (Weir *et al.*, 1998).

However, the most characterised VAPB interactions are the ones with proteins containing the FFAT-motif. The interaction in yeast between Sc2 and Opi1p, a transcriptional regulator of phospholipid synthesis, was the first link between VAP proteins and lipids (Lowren *et al.*, 2003). Later, this was supported by the confirmation of the interaction of VAP proteins and the previously discussed lipid-related proteins OSBP, CERT and Nir2.

Other studies have found genetic interactors in genes related to processes including autophagy, vesicle and nuclear migration, GTP exchange and lipid metabolism (Costanzo *et al.*, 2010; Schuldiner *et al.*, 2005; Aguilar *et al.*, 2010). According to the Biological General Repository for Interaction Datasets, BioGrid (Chatr-aryamontri *et al.*, 2012) 313 unique interactions have been found only in yeast and some of these proteins have been confirmed in more complex organisms. The same database informs of 49 interactions found in *Drosophila* and humans, which confirm the same protein functions previously described in yeast (Table 1). These

interactions represent a central core of the known VAP functions and could provide insights into the potential mechanisms in which the protein associates to pathogenesis in ALS.

1.4 VAP mutations cause ALS

Initially, *VAPB* was found to be an ALS causative gene with the discovery of a Brazilian family carrying the substitution Pro56Ser in the gene (Nishimura *et al.*, 2004a). This mutation causes a predicted structural change of the MSP domain and disrupts the seven-strand β-sandwich conformation present in the wild type form of the protein. This change transforms the protein to an insoluble state (Shi *et al.*, 2010) with an enhanced oligomerisation conformation (Kim *et al.*, 2010). Also, the substitution converts the MSP domain to a highly helical conformation in a membrane environment that potentially can explain ER rearrangements (Qin *et al.*, 2013).

Later studies indicated that the P56S mutation was not the only way in which VAPB was associated with the disease, as it was shown that VAPB expression is down-regulated in spinal cord tissue and pyramid tract of sporadic ALS patients (Anagnostou *et al.*, 2010) and SOD1 mutants mice (Teuling *et al.*, 2007). More recently, other VAPB mutations have been found in ALS patients, supporting furthermore the link between the protein and the disease's pathomechanism. A threonine to isoleucine substitution in *VAPB* position 46 was found in a 73 year old British ALS patient who presented classical signs of the disease. Located in the MSP domain, this mutation presented a pathogenesis index even larger than the previously characterized P56S mutation (Chen *et al.*, 2010). As observed in P56S expressing cells, T46I mutation triggered protein aggregation that also included the wild type form of the protein. Protein aggregation caused cell death, ubiquitin-labeled inclusions and a disruption of UPR system activation via IRE1. Interestingly, they showed a non-cell autonomous effect of VAPB toxicity and aggregation in neighbor cells, which supports the idea of ALS as a disease that is not exclusive to motor neurons. All these phenotypes were confirmed in a *Drosophila* model that expressed

Interactor	Organism	Experimental Evidence	Reference	Throughput
HNRNPC	*H. sapiens*	Co-fractionation	Havugimana *et al.*, 2012	HT
INSIG1	*H. sapiens*	Affinity Capture-Western	Gong *et al.*, 2006	LT
MPST	*H. sapiens*	Co-fractionation	Havugimana *et al.*, 2012	HT
MTNR1A	*H. sapiens*	Affinity Capture-MS	Daulat *et al.*, 2007	LT
NRF1	*H. sapiens*	Co-localization	Satoh *et al.*, 2013	HT
OSBPL9	*H. sapiens*	Affinity Capture-MS	Sowa *et al.*, 2009	HT
OXCT1	*H. sapiens*	Co-fractionation	Havugimana *et al.*, 2012	HT
PITRM1	*H. sapiens*	Co-fractionation	Havugimana *et al.*, 2012	HT
PRKACA	*H. sapiens*	Affinity Capture-MS	Varjosalo *et al.*, 2013	HT
PRKACB	*H. sapiens*	Affinity Capture-MS	Varjosalo *et al.*, 2013	HT
S100A16	*H. sapiens*	Co-fractionation	Havugimana *et al.*, 2012	HT
SCAF4	*H. sapiens*	Co-fractionation	Havugimana *et al.*, 2012	HT
SEC22B	*H. sapiens*	Co-fractionation	Havugimana *et al.*, 2012	HT
SEPT9	*H. sapiens*	Co-fractionation	Havugimana *et al.*, 2012	HT
STX1A	*H. sapiens*	Reconstituted Complex	Li *et al.*, 2003	LT
STX1B	*H. sapiens*	Reconstituted Complex	Li *et al.*, 2003	LT
STX2	*H. sapiens*	Reconstituted Complex	Li *et al.*, 2003	LT
STX4	*H. sapiens*	Reconstituted Complex	Li *et al.*, 2003	LT
STX5	*H. sapiens*	Reconstituted Complex	Li *et al.*, 2003	LT
TJP1	*H. sapiens*	Co-fractionation	Havugimana *et al.*, 2012	HT
UBC	*H. sapiens*	Affinity Capture-MS	Danielsen et al., 2011	HT
UBL4A	*H. sapiens*	Affinity Capture-MS	Xu *et al.*, 2012	HT
UQCRFS1	*H. sapiens*	Co-fractionation	Havugimana *et al.*, 2012	HT
USP20	*H. sapiens*	Affinity Capture-MS	Sowa *et al.*, 2009	HT
VAMP1	*H. sapiens*	Reconstituted Complex	Nishimura *et al.*, 1999	LT
VAMP2	*H. sapiens*	Reconstituted Complex	Nishimura *et al.*, 1999	LT

VAPA	*H. sapiens*	Reconstituted Complex	Nishimura *et al.*, 1999	LT
VCL	*H. sapiens*	Co-fractionation	Havugimana *et al.*, 2012	HT
VDAC3	*H. sapiens*	Co-fractionation	Havugimana *et al.*, 2012	HT
VHL	*H. sapiens*	Reconstituted Complex	Lai *et al.*, 2012	LT
VKORC1	*H. sapiens*	Two-hybrid	Schaafhausen *et al.*, 2011	LT
EPHA4	*M. musculus*	Affinity Capture-Western	Tsuda *et al.*, 2008	LT
CG1513	*D. melanogaster*	Two-hybrid	Giot *et al.*, 2003	HT
CG2064	*D. melanogaster*	Affinity Capture-MS	Guruharsha *et al.*, 2011	HT
CG4729	*D. melanogaster*	Affinity Capture-MS	Guruharsha *et al.*, 2011	HT
CG5742	*D. melanogaster*	Affinity Capture-MS	Guruharsha *et al.*, 2011	HT
CG8188	*D. melanogaster*	Affinity Capture-Western	Tsuda *et al.*, 2008	LT
CG8765	*D. melanogaster*	Affinity Capture-MS	Guruharsha *et al.*, 2011	HT
CG9205	*D. melanogaster*	Affinity Capture-MS	Guruharsha *et al.*, 2011	HT
CG9723	*D. melanogaster*	Affinity Capture-MS	Guruharsha *et al.*, 2011	HT
CG13220	*D. melanogaster*	Affinity Capture-MS	Guruharsha *et al.*, 2011	HT
CG33523	*D. melanogaster*	Affinity Capture-MS	Guruharsha *et al.*, 2011	HT
CCT2	*D. melanogaster*	Affinity Capture-MS	Guruharsha *et al.*, 2011	HT
DL	*D. melanogaster*	Two-hybrid	Formstecher *et al.*, 2005	HT
MRG15	*D. melanogaster*	Affinity Capture-MS	Guruharsha *et al.*, 2011	HT
NF-YA	*D. melanogaster*	Two-hybrid	Giot *et al.*, 2003	HT
RAB7	*D. melanogaster*	LC-MS/MS	McCray *et al.*, 2010	LT
REL	*D. melanogaster*	Affinity Capture-MS	Fukuyama *et al.*, 2013	HT
SAC1	*D. melanogaster*	Two-hybrid	Giot *et al.*, 2003	HT

Table 1. VAP physical interactors found in *Drosophila* and human-based experiments. According to BioGrid, forty nine unique proteins have physical interaction confirmed through different approaches. These proteins are related to vesicle recycling, synaptic structure and lipid metabolism, among other cellular functions. HT: High throughput experiments; LT: Low throughput.

the corresponding mutation DVAP-T48I. Additionally, disruption of ER protein distribution, heat shock response and neurodegeneration in the eye were observed in the fly model (Chen *et al.*, 2010).

Two years later, a novel mutation was found in a Dutch familial ALS patient. In contrast to the previous substitutions, the mutation V234I was located in an evolutionary conserved sequence in the VAPB transmembrane domain (van Blitterswijk *et al.*, 2012b). The pathogenicity of the mutation calculated *in-silico* is similarly high to the one found in T46I, mainly due to the structural change predicted in the transmembrane domain of the protein. Interestingly, this fALS patient also carries the expansion in the C9orf72 gene, which supports the oligogenic origin of the disease (van Blitterswijk *et al.*, 2012a). Only some months ago our group reported a characterisation of this mutation in a *Drosophila* model (Sanhueza *et al.*, 2013). Surprisingly, the synaptic and microtubule phenotypes observed in this model go in the opposite direction to the ones observed with the two previous VAPB mutations. However, aggregate formation, abnormal locomotion behavior and up-regulation of HSP stress response were observed, all phenotypes present with the previous mutations. The fact that overexpression of wild-type alleles of DVAP also produces similar phenotypes than those observed with DVAP-V260I implies that the overexpression of the protein is enough to cause neurodegeneration and that a gain-of-function mechanism may be involved in VAPB-induced ALS (Sanhueza *et al.*, 2013).

These three mutations have been characterised and neurodegenerative phenotypes were found reminiscent to those observed in ALS-linked phenotypes. However, VAPB mutations are sometimes treated as a rare cause of ALS without a strong number of cases from different origins, despite the presence of European and Japanese patients with the VAPB-P56S mutations (Millecamps *et al.*, 2010; Funke *et al.*, 2010). Recent reviews of the molecular causes of ALS (Renton *et al.*, 2013; Robberecht & Philips, 2013; Al-Chalabi & Hardiman, 2013) underestimate the relevance of VAPB based on the lack of novel mutations and on studies that found less pathogenic VAPB alleles in ALS patients (Ingre *et al.*, 2013; Conforti *et al.*,

2006; van Blitterswijk *et al.*, 2012b). However, these reviews avoid important facts that strongly link VAPB with ALS pathology including the lower VAPB levels in ALS patients and the neurodegeneration observed in the previously described VAPB models (Anagnostou *et al.*, 2010; Chai *et al.*, 2008). Additionally, we cannot discard that the decrease in protein levels may be caused by unknown mutations in VAPB regulatory regions that may lead to pathogenic forms difficult to find by studies that search mutations in gene exons. Finally, the association of VAPB mutants with defects in protein clearance links this gene with a group of other ALS causative genes and suggests that further studies of this pathway and VAPB can provide important insights into the disease pathogenesis (Ling *et al.*, 2013)

1.5 *Drosophila* is a powerful animal model

In the last century, the fruit fly played a pivotal role in crucially advancing areas of biology. Landmark studies in *Drosophila* include the initial work of Thomas Hunt Morgan studying the chromosomal theory of inheritance, advances in learning (Quinn *et al.*, 1974), visual system (Pak *et al.*, 1970) and embryonic development (Nüsslein-Volhard & Wieschaus, 1980). In the last two decades however, the use of *Drosophila* as an animal model to study human diseases has increased enormously (Bilen & Bonini, 2005). Despite the significant evolutionary distance between fruit flies and humans, their genomes share a considerable similarity. Half of the *Drosophila* genes show a significant homology to human genes and furthermore, 77% of human genes associated with diseases have an ortholog in the fruit fly (Reiter *et al.*, 2001).

Normally, the easier a genetic model is to work with, the worse it is to mimic human characteristics (St Johnston, 2002). In that regard, *Drosophila* exhibits one of the best balances between these two aspects. Also, with an important repertoire of genetic techniques, it is fair to consider *Drosophila* as an important animal model. Fruit fly's low cost, simple maintenance, short generation time and well-known anatomy are vital advantages of *Drosophila* compared to major organisms and a central reason to use it for large-scale studies (St Johnston, 2002; Bellen *et al.*, 2004;

Bilen & Bonini, 2005). On the other hand, the use of *Drosophila* as animal model implies some drawbacks as well. Fruit flies need constant stock maintenance at controlled temperatures compared to unicellular models that can be frozen and revived afterwards (St Johnston, 2002). *Drosophila* also lacks some organs and tissues present in humans, which affects the modeling of some human diseases (Razell *et al.*, 2011). Finally, developmental difference between flies and human nervous systems is large enough to make difficult the study of some cognitive and behavioral hallmarks of neurodegenerative diseases (Prubing *et al.*, 2013).

Genetic simplicity is another key aspect of *Drosophila* advantages. In the last two decades, a strong effort from the *Drosophila* community has generated a valuable number of stock collections that cover most its genome. P-element insertions, deletions, RNAi and overexpression lines are all publicly available and are the basis of a productive scientific communication between Drosophilists (Drysdale & FlyBase Consortium, 2008; Bellen *et al.*, 2004; Dietzl *et al.*, 2007; Cook *et al.*, 2012). These stock lines are constantly studied, mapped and conserved to help the *Drosophila* community. The genetic simplicity of *Drosophila* also is useful as there are less evolutionary duplication events that in other animal models. This makes more challenging the study of a gene function in animals with more than one copy for that gene (O'Kane, 2003; O'Sullivan *et al.*, 2012).

Finally, the evolutionary distance between *Drosophila* and humans can be evaded with the insertion of human genes into the fly's genome. Mechanisms involved in human diseases can be confirmed with this approach using *Drosophila* genetic tools repertoire. Also, it can be useful to express human genes without orthologs in the *Drosophila* genome as an alternative way to use the previously listed advantages of this organism. The exploitation of this idea has led to several models of human diseases that successfully provide crucial data (Chai *et al.*, 2008; Li *et al.*, 2010; Greeve *et al.*, 2004).

1.6 Other neurodegenerative disease models

Fly models have been successfully constructed for the most relevant human neurodegenerative diseases. Polyglutamine diseases include a group of at least 9 different diseases that share the expansion of a CAG repeat in their genes (Gusella & MacDonald, 2000). The study of one of these diseases, spinocerebellar ataxia type 1 (SCA1) was enormously benefited by the generation of a *Drosophila* model expressing the full-length human *SCA1* gene. A genetic screen looking at modifiers of the SCA1-induced neurodegenerative phenotype led to understand the participation of protein misfolding and clearance along with aberrations in RNA processing as main aspects of disease pathogenesis (Fernandez-Funez *et al.*, 2000). Subsequent reports have deepened the understanding of these mechanisms and supported the relevance of flies as an SCA1 model (Chen *et al.*, 2003; Lam *et al.*, 2006; Park *et al.*, 2013). Similar results were observed with the models for SCA2 and SCA3, where the expression of either full-length, truncated or expanded versions of these proteins in *Drosophila* lead to neurodegeneration and protein aggregation (Warrick *et al.*, 2005; Warrick *et al.*, 1998; Satterfield *et al.*, 2002).

Another polyglutamine-caused disorder is Huntington's disease (HD). Expression of the N-terminal portion of the causative gene *htt* in *Drosophila* was linked to progressive neurodegeneration. As observed in humans, the pathogenicity was proportional to the length of polyQ repeats (Jackson *et al.*, 1998). Further studies proved that expression of the full-length version of the protein in *Drosophila* nervous system generated neurodegeneration due to an increased release of neurotransmitter. This finding indicates a possible pathomechanism for HD (Ross *et al.*, 2014; Rozas *et al.*, 2011). Other two models based on the truncated version of htt showed that the pathomechanism was explained in part by transcriptional deregulation and fast axonal transport (Steffan *et al.*, 2001; Lee *et al.*, 2004). Furthermore, *Drosophila* models were used to identify chemicals with potential pharmaceutical effects (Auluck & Bonini, 2002; Miller *et al.*, 2012).

Parkinson disease is a more common disorder affecting 2.5 per 100.000 persons (Savica *et al.*, 2013). Feany and Bender were able to express in *Drosophila* the human α-synuclein, one of the causative genes of the disease (Feany & Bender, 2000). This model presented adult onset neurodegeneration, protein accumulation and motor dysfunction, as observed in humans. Models based on another causative gene, parkin, presented oxidative stress sensitivity and abnormal wing phenotypes (Greene *et al.*, 2003; Pesah *et al.*, 2004). Recently, specific dopaminergic neurons were identified in *Drosophila*'s mushroom bodies as the cause of locomotor deficits (Riemensperger *et al.*, 2013).

However, the most common neurodegenerative disease is Alzheimer' disease. The main mechanism associated with the disease is the cleavage of the amyloid precursor protein (APP) by the γ-secretase, encoded by the presenilin 1 and 2 genes (*PS1* and *PS2*). This cleavage releases the Aβ40 and Aβ42 products found in protein aggregates (Huang & Mucke, 2012). Mutations in the *APP*, *PS1* and *PS2* genes are associated with familial cases of the disease (Vassar *et al.*, 2014). All the components of the APP cleavage machinery are not present in *Drosophila* genome and the APP protein does not present the Aβ domain. Despite that, fly models for the disease have provided important insights into the disease pathomechanism, such as the link of cell death and cell-cell adhesion (Ye *et al.*, 1999; Fossgreen *et al.*, 1998). When the human APP is coexpressed with the γ-secretase precursor in flies, Aβ40 and Aβ42 are produced causing neurodegeneration (Greeve *et al.*, 2004). Neurodegeneration also is observed in fly models expressing mutant forms of Tau, another Alzheimer's disease-associated protein (Nishimura *et al.*, 2004b; Wittmann *et al.*, 2001).

1.7 Genetic screens using fly models

The genetic power of *Drosophila* as animal model has been a key aspect of its success in the identification of novel gene functions using genetic screens. From mutagenesis analyses based on ethylmethane sulphonate (EMS) and P-transposable

elements, to more specific approaches including transgenic and clonal screens, these studies are a strong way to use the power of *Drosophila*.

Traditional studies were based on the generation of mutant lines using EMS, which causes specifically point mutations in the genome. The first ground-breaking study of this kind was the screen designed by the Nobel Prize recipients Christiane Nusslein-Volhard and Eric Wieschaus (Nüsslein-Volhard & Wieschaus, 1980). In this screen were identified mutants that affected embryonic positional information. It became one of the first screens that used the embryo as model to find genes in a single process (St Johnston, 2002). In this work, authors were able to define three different segmentation processes and associate them with most of the genes that control them such *Hedgehog, Fused, Wingless, Cubitus interruptus, patched* and other 10 central genes.

A further step forward in the searching for novel gene functions was reported in the characterisation of *sevenless*, a gene that controls cell fate in photoreceptor cells. Most loss-of-function mutations are recessive and only one copy is enough to show a wild type phenotype. However, when additionally another gene from the same process is already mutated, the single copy of the original gene may not be enough and a phenotype may be detected. Changes in gene dosage are used in this way to find novel genes that modify the mutant phenotype of a known protein. The screen that found downstream targets of sevenless had extra advantages compared to previous screens, especially the possibility to screen the offspring directly after the original cross and not to wait for homozygous mutant flies as in the previous screens (idea known as a F1 screen, Figure 3) (Simon *et al.*, 1992; Simon, 1994).

Another way to analyse recessive mutations that show phenotype in homozygous cells are the screens based on mitotic clones. This technique involves the use of the yeast recombinase Flp and transgenic lines with specific sites of recombination (Flp recombinase target, FRT). With these elements, recombination occurs in homologous chromosomes that after segregating in mitosis, produce cells with the desired mutation in homozygosis. This technique also is a F1 screen, which

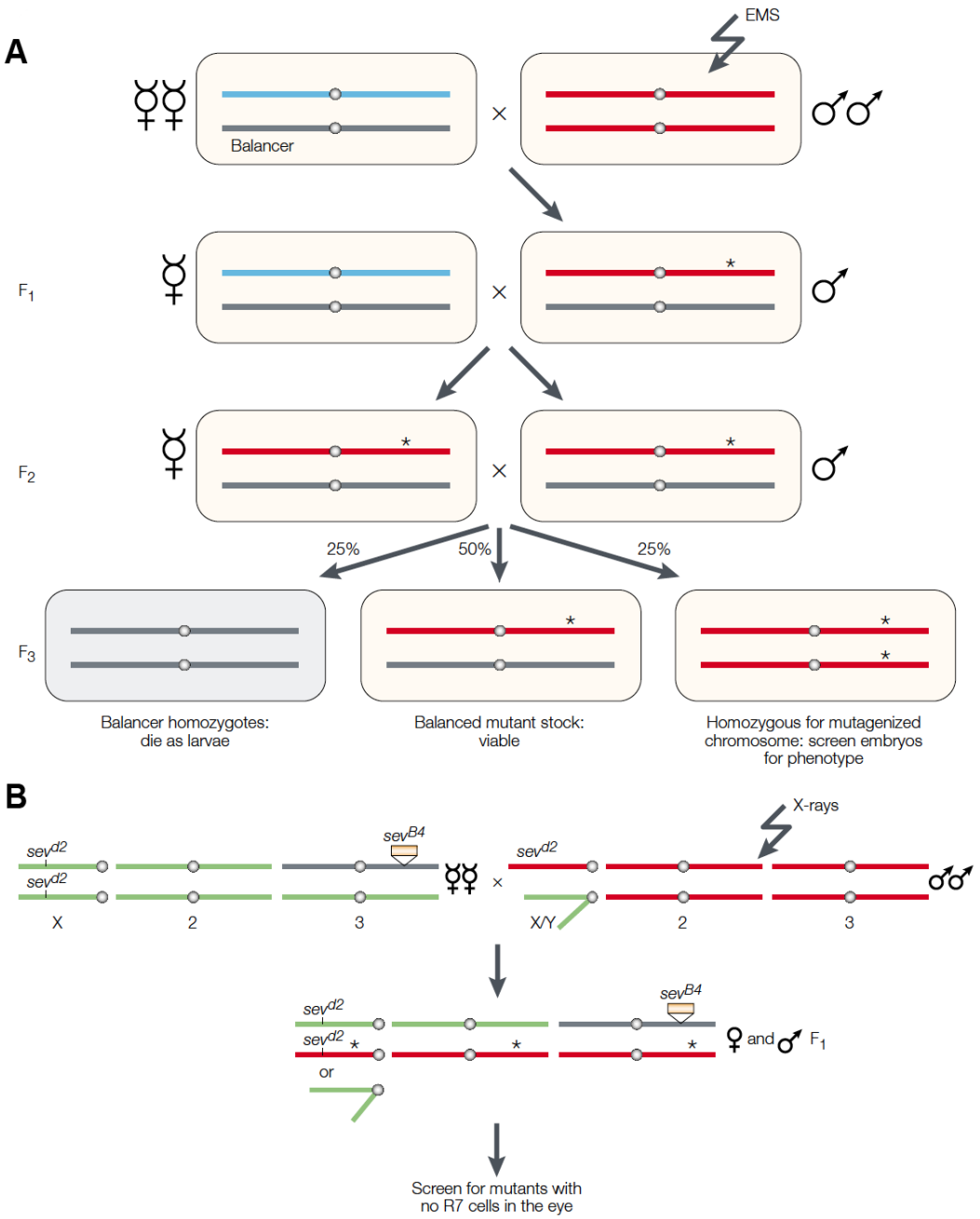

Figure 3. Schemes of classic genetic screens in *Drosophila.* (**A**) Mutagenesis-based screen published by Nüsslein-Volhard & Wieschaus, which found for the first time mutations that affect patterning of the embryo. Male flies are fed EMS to induce mutations. As the mutations are induced in mature spermatids, each F1 male inherits a mutagenized chromosome (red) carrying a different spectrum of mutations. Single F1 males that carry a mutagenized chromosome are then backcrossed to balancer stock to generate F2 males and females that carry the same mutagenized chromosome. (B) Scheme for the screen for enhancers of sev, published by Simon *et al*. Males that are hemizygous for sev^{d2} were mutagenized with X-rays and crossed to sev^{d2} homozygous females that carry a temperature-sensitive allele of sev as a transgene inserted on TM3. The F1 TM3 flies were then screened for a reduction in the number of R7 photoreceptor cells in the eye. Taken from St Johnston, 2002.

provides the advantage of a faster search for new functions. Originally used for the search of tumour related genes (Xu *et al.*, 1995), the clonal analysis has been optimized in following studies that direct the recombination in specific tissues (Chou & Perrimon, 1996; Newsome *et al.*, 2000) or others that improve the recombination efficiency removing non-recombinant cells (Stowers & Schwarz, 1999).

To address the situation of a lack of phenotype in several genes when presented as loss-of-function, an effective type of screen was designed by Pernille Rørth (Rørth, 1996) using the modular expression technique UAS-Gal4 (Brand & Perrimon, 1993). With the creation of transgenic lines carrying upstream activating sequences in a target gene, Rørth was able to upregulate several genes and observe a specific phenotype or the modulation of a previous one. This was exemplified by the phenotype observed with the misexpression of Ras GAP in the eye. Proposed as the best way to screen genes, due to the possibility to observe effects in previously silent genes, misexpression screens have been successfully performed throughout the last decade to understand different processes (Franciscovich *et al.*, 2008; Paik *et al.*, 2012; Stofanko *et al.*, 2008; Ambegaokar & Jackson, 2011). The generation of novel collection of transgenic misexpressing lines constantly improves these screens (Staudt *et al.*, 2005; Bellen *et al.*, 2004; Beinert *et al.*, 2004; Bellen *et al.*, 2011).

From these screens, the eye appears as the most popular way to find genetic modifiers of an existing process or mutant phenotype. The non-essential condition of this organ and the easy readout that is associated with it allow testing in the eye lethal genes in a quick manner. More importantly, genes that do not present a known eye-specific function can still be tested if they show a specific rough phenotype in the eye (St Johnston, 2002). *Drosophila* eye is composed of approximately 750 ommatidia, a unit that clusters differentiated eye cells. When a protein produces a toxic effect, the severity of its associated degeneration can be observed in different degrees, according to the number of ommatidia damaged (Thomas & Wassarman, 1999). Several studies have successfully used eye screens to find genetic modifiers that alter this degree of degeneration (Bonini, 1999; Fernandez-Funez *et al.*, 2000; Barrett *et al.*, 1997).

Finally, another effective way to test modification phenotypes is behavioural performance analysis, specially testing motor performance changes in model flies. Feany's work modeling Parkinson in *Drosophila* used the motor performance measurement to detect late-onset loss of dopaminergic neurons (Feany & Bender, 2000). Later, similar assays were reported for other neurodegenerative diseases including SCA1 and HD, where novel genetic interactors of the causative genes Ataxin 1 and huntingtin respectively, were found to affect *Drosophila*'s behaviour (Branco *et al.*, 2008; Kaltenbach *et al.*, 2007). In the study of ALS, behaviour has been tested in fly models for two genes. Li reported a TDP-43 model that presented late-onset motor defects with the overexpression of the human form of the protein in *Drosophila* (Li *et al.*, 2010). This same gene and technique were the center of multisystemic works that discovered Taf15 and ataxin-2 as TDP-43 genetic interactors (Couthouis *et al.*, 2011; Elden *et al.*, 2010). SOD1 mutants also present motor performance defects first described by Watson *et al*. (Watson *et al.*, 2008) and confirmed by a different model recently (Bahadorani *et al.*, 2013). However, for SOD1 and other causative genes, no further characterisations have been made linking disease-related mutations with relevant hallmarks of the diseases like motor defects. The potential use of this analysis, together with other gene discovery tools could lead to an incremental understanding of the disease pathomechanism.

1.8 Experimental aims

The lack of understanding of VAP biology and its relation with ALS pathogenesis are the driving forces to start this study. A gain of knowledge regarding interactions and phenotypes of this protein will significantly improve our comprehension of the mechanism behind motor neuron death. *Drosophila* as a simple animal model gives us the chance to perform genome-wide projects that are basically impossible in other systems. Curiously, the search for genetic interactors is something not performed yet for VAPB and ALS. Therefore, we plan to perform a high-scale genetic screen to find modifiers of DVAP-P58S-associated neurodegeneration, and discover potential pathways and mechanisms currently hidden in the study of this protein. For that purpose, we aim to characterise and

optimise the ALS *Drosophila* model based on DVAP-P58S to then carry out a misexpression screen to find potential DVAP genetic modifiers. The confirmation and further characterisation of these novel interactors will not only increase DVAP spectrum of mechanisms inside the cell, but also will potentially allow us to identify future therapeutic targets for the VAPB-linked ALS.

Aim 1. Characterisation and optimisation of the ALS model. Before start a genome-wide screen, it is mandatory to characterise the phenotypes associated with DVAP mutants and pinpoint the exact conditions to perform following experiments in an optimal way. For this purpose, we plan to study the expression of DVAP mutants in different tissues and temperatures, and test our parameters in small-scale pilot experiments.

Aim 2. Perform a primary screen based on the expression of DVAP-P58S in the eye. Using changes in the fly's eye phenotype as a quick and reliable readout, we plan to analyse more than one thousand misexpression lines to search for genes that modify DVAP-P58S phenotype. The selection and further confirmation of these genetic interactors will be the central part of this study and the genes discovered at this stage should provide us novel information about the role of DVAP in the cell.

Aim 3. Perform a secondary screen based on the expression of DVAP-P58S in the whole nervous system. After filtering positive interactors with our previous aim, we plan to study the behaviour of these modifiers in the *Drosophila* nervous system under the control of the *elav-GAL4* driver. Analysing different paradigms, we will be able to confirm results informed previously. Importantly, we will observe the behaviour of these interactions in assays that resemble relevant human hallmarks of the disease such as the loss of motor performance.

Aim 4. Bioinformatic studies of the DVAP-neurodegeneration modifiers. Currently, an important area of scientific research involves the data prediction and organization of the available information. We plan to use different approaches to obtain further information, with our set of novel interactors as the starting point.

These analyses will not only allow us to understand previously reported information but also, will unveil relevant functions and pathways associated now to DVAP-linked neurodegeneration.

Aim 5. Characterisation of functional pathways enriched in the genetic screen. From the myriad of novel DVAP-interactors found in the previous stages, some will highlight due to their known connection to DVAP and their integration with other modifiers. We propose the characterisation of some of these modifiers with the purpose to validate our list of modifiers but also to provide a potential link of DVAP with important cellular functions. The study through immunohistochemical assays and furthermore, the translation of our results to human samples will accomplish these aims and provide data for further studies.

Chapter 2:
Materials & Methods

2.1 Antibodies

2.1.1 Primary antibodies used for immunohistochemistry

Antibody	Source
Guinea Pig α-DVAP	Giusy Pennetta
Rabbit α-Rab5	Giusy Pennetta
Rabbit α-human RAB5A	Novus Biologicals
Chicken α-Syx7	David Bilder

Table 2. Primary antibodies

2.1.2 Secondary antibodies used for immunohistochemistry

Antibody	Source
Goat α-guinea pig FITC	Jackson Immunoresearch
Goat α-rabbit Cy3	Jackson Immunoresearch

Table 3. Secondary antibodies

2.2 Fly genetics

2.2.1 *Drosophila* stocks

Stocks were maintained on standard cornmeal food at room temperature. Flies were raised at specific temperatures according the experiment. Four groups of stocks were used in this study: general *Drosophila* stocks, 1183 misexpression stocks tested in the genetic screen (Bloomington *Drosophila* Stock Center, BDSC), RNAi stocks used to validate positive results from the screen (BDSC and Vienna *Drosophila* resource center, VDRC) and transgenic lines used for the same purpose, obtained from other labs.

Line	Source	Description
yw	Bloomington *Drosophila* Stock center	Wild type line
Canton S	Bloomington *Drosophila* Stock center	Wild type line
elav^{c155}-GAL4	Bloomington *Drosophila* Stock center	Nervous system expression driver
GMR-GAL4	Bloomington *Drosophila* Stock center	Eye expression driver
eyeless-GAL4	Bloomington *Drosophila* Stock center	Eye expression driver
BG57-GAL4	Bloomington *Drosophila* Stock center	Muscle expression driver
UAS-DVAP-P58S	Chai *et al.*, 2008	Transgenic DVAP allele
UAS-DVAP-T48I	Chen *et al.*, 2010	Transgenic DVAP allele
ey-GAL4, UAS-DVAP-P58S/CyO-GFP	Giusy Pennetta	Recombinant line
elav-GAL4; UAS-DVAP-P58S/CyO-GFP	This study	Recombinant line
UAS-mCD8:GFP	Bloomington *Drosophila* Stock center	GFP control line
Δ2-3	Robertson *et al.*, 1988	Transposase source line
Lpin/CyO-GFP	Andrew Jarman	CyO-GFP Balancer line
UAS-Sac1	Giusy Pennetta	Sac1 overexpression
Stt4RNAi	Khuong *et al.*, 2010	Stt4 RNAi line
FwdRNAi	Yavari *et al.*, 2010	Fwd RNAi line
UAS-DIAP1	Bloomington *Drosophila* Stock center	Inhibitor of Apoptosis 1
Jnk-DN	Bloomington *Drosophila* Stock center	Basket dominant negative
UAS-Puc	Bloomington *Drosophila* Stock center	Puc overexpression
UAS-DIAP2	Ribeiro *et al.*, 2007	DIAP2 overexpression

Line	Source	Description
UAS-Ric	Harrison *et al.*, 2005	Ric overexpression
UAS-Sir2	Burnett *et al.*, 2012	Sir2 overexpression
UAS-Rho	Strisovsky *et al.*, 2009	Rho overexpression
$Klar^{1}$	Elhanany-Tamir *et al.*, 2012	Klar loss of function
DAP160Δ1/CyO-GFP	Koh *et al.*, 2007	DAP160 loss of function
UAS-Drp(I)	McPhee *et al.*, 2010	Draper overexpression
UAS-$Rab7^{WT}$-Flag	McCray *et al.*, 2010	Rab7 WT overexpression
UAS-$Rab7^{Q67L}$-Flag	McCray *et al.*, 2010	Rab7 constitutively active
UAS-$Rab7^{T22N}$-Flag	McCray *et al.*, 2010	Rab7 dominant negative
UAS-$Rab7^{L129}$-Flag	McCray *et al.*, 2010	Rab7 CMT mutation
UAS-Rab11-GFP	Bloomington *Drosophila* Stock center	Rab11 WT overexpression

Table 4. General Stocks and *Drosophila* tools used in this study.

2.2.2 Genetic screen

Virgins females from the recombinant line ey-Gal4,DVAP-P58S/CyO-GFP ("tester line") were crossed with males from misexpression stocks. Embryos from these crosses were collected at RT for 48 hours. Parents were transferred and embryos were heat-shocked at 30ºC to maximize the expression of the Gal4 activator. This temperature was maintained in a termoregulated water bath, in which the food vials showed better condition, humidity levels and larger offspring, in comparison to an air incubator at the same temperature. The offspring was sorted by phenotype, counted and their eyes were photographed using a Nikon D5100 camera attached to a SZX9 Nikon stereomicroscope. The lines showing a modifying activity compared to controls were re-tested and stocks with negative results were discarded.

2.2.3 P-Element excision

To confirm that the modifying effect was due to the P-element insertion, we excised the P-element from the original misexpression stocks and tested if this revertant line loses its effect over ey-GAL4,DVAP-P58S. As a transposase source, we used the P{Δ2-3} line (*w-; Sp/CyO; P{ry+Δ2-3}(99B), Dr/TM6B,Tb*) (Robertson *et al.*, 1988), which increases the mobilisation frequency of other elements but remains stable itself. P-elements inserted in the second chromosome were excised following this genetic scheme:

P: ♂ $\frac{P\ (EP)}{P\ (EP)}$; $\frac{+}{+}$ *x* ♀ $\frac{Sp}{CyO}$; $\frac{\Delta\ 2\text{-}3,\ Dr}{TM6B,Tb}$

↙

F1: ♂ $\frac{P\ (EP)}{CyO}$; $\frac{\Delta\ 2\text{-}3,\ Dr}{+}$ *x* ♀ $\frac{L,\ Pin}{CyO\text{-}GFP}$

↙

F2: ♂ $\frac{P\ (\Delta EP)}{CyO\text{-}GFP}$ *x* ♀ $\frac{+}{CyO}$

↙

F3: $ $\frac{P\ (\Delta EP)}{CyO}$

Virgin Δ2-3 females were crossed with males from the original P-element modifier line. Males with the markers Curly (on the chromosome CyO) and drop (Dr) were selected from the offspring. One hundred males were individually crossed with virgin CyO-GFP females. From the offspring of those crosses, the revertant male was selected for the lack of eye colour and presence of GFP signal. The stock was constructed after crossing that male with virgins CyO and selecting for the lack of GFP marker. This revertant was tested against ey-GAL4,DVAP-P58S to confirm the lack of modifying effect and therefore, excision of the element.

2.2.4 Viability assay

To investigate the effect of DVAP mutant in the adult viability, we analysed the number of eclosed flies expressing *DVAP-P58S* under the control of the pan-neural driver elav^{C155}-GAL4. Crosses between elav;DVAP-P58S virgin females and males from lines with potential modification effect were performed in the same way as previously detailed. All the eclosed flies were sorted in two groups: flies co-expressing *DVAP* mutant allele and the target studied gene (flies without the CyO chromosome, CyO^{+}) and flies expressing exclusively the target gene (CyO flies). If the co-expression of both genes is not toxic for flies, we could assume that the amount of flies that would come out from both phenotypes is the same. Therefore, the ratio between observed (CyO^{+}) and expected (CyO) flies would be 1.0 for non-toxic co-expression. A value lower than 1.0, indicated a toxicity effect. Modification ratios were then compared to the ratio observed for the tester line (*elav-GAL4/+; DVAP-P58S/+*). The modification effect was plotted and statistically analysed using unpaired, two-tailed Student's T-test.

P: ♂ $\frac{P\,(EP)}{P\,(EP)}$ x ♀ $\frac{elav\text{-}Gal4\ ;\ DVAP\text{-}P58S}{elav\text{-}Gal4 \qquad Cyo}$

F1: Co-expressing flies: (Cyo^{+}) $\frac{elav\text{-}Gal4\ ;\ DVAP\text{-}P58S}{+ \qquad P(EP)}$ ♀

Y $\frac{elav\text{-}Gal4\ ;\ DVAP\text{-}P58S}{\ \ P(EP)}$ ♂

Non-DVAP flies: (Cyo) $\frac{elav\text{-}Gal4\ ;\ P(EP)}{+ \qquad Cyo}$ ♀

$\frac{elav\text{-}Gal4\ ;\ P(EP)}{Y \qquad Cyo}$ ♂

2.2.5 Motor performance assay

Motor performance of the DVAP-mediated toxicity modifier lines was tested using the climbing assay (Branco *et al.*, 2008). Misexpression stocks were crossed with elav;DVAP-P58S flies virgin females at 28ºC. A set of 10 age-matched adult females

was raised at the same temperature and every 2 days was tested to score how many flies could climb 8 cm high in an empty vial in 15 seconds. After this period, flies were tapped to the bottom and the trial was repeated ten times to calculate the average. These averages were plotted and statistically analysed using Two-way ANOVA with Bonferroni as Post-Hoc test to compare samples with control flies performance. Flies were transferred to a new vial every two days to avoid death of flies or loss of mobility due to sticky food.

2.3 *Drosophila* eye structure

2.3.1 Light microscopy images and modification levels

To characterise the eye morphology of the different lines, two-dimensional images were obtained using a Nikon D5100 Camera attached to a SZX9 Nikon stereomicroscope. To quantify the eye surface area of flies, images were analysed with ImageJ software. The percentage of modification was calculated to reflect the difference of area between stocks and controls. If we assume that level of modification occurs between the tester line ey-Gal4,DVAP-P58S/+ (T, 0%) and the control ey-Gal4/+ as maximum level of eye size (C,100%), we can calculate the specific modification ratio of each stock (S) as: (AreaS - AreaT) / (AreaC - AreaT). A perfect suppressor will show the same area of the control (Ratio=1), a no-effect stock will show the same area of the tester line (Ratio=0) and an enhancer line will show smaller area than positive control (Ratio $\leq$ 0). The same principle was used for enhancement assays at 28ºC, where the percentage of decrease from the tester line was calculated for each stock as: 1 - (AreaS /AreaT). All these values were then analysed statistically to confirm modifying effects.

2.3.2 Histology

To analyse the internal eye structure of adult flies, 10 heads were fixed overnight using a mix of formaldehyde, ethanol and acetic acid (10:85:5). After dehydration, the samples were embedded in paraffin and sliced to obtain thin sections. These

sections were stained with hematoxylin-eosin and then visualised on a stereomicroscope.

2.3.3 Scanning electron microscopy

Fly heads were fixed with 3% glutaraldehyde in 0.1M sodium cacodylate buffer pH 7.4 for at least 3 hours. After wash with the same buffer for 1 hour, the heads were incubated in 1% osmium tetroxide for 2 hours and then dehydrated in 50%, 70%, 90% and 100% acetone for 10 minutes each. Finally, samples are sputter coated with 20nm gold/palladium (60/40) to be visualised with a Hitachi 4700 FESEM.

2.4 Plasmid rescue

DNA was extracted from 15 adult flies using the alkaline method (Roberts, 1986). Flies were smashed in 1% SDS buffer and incubated for 30 min at 65ºC, followed by DNA extraction using 8M potassium acetate and precipitation with isopropanol. Genomic DNA was digested using 10U EcoRI and checked in a 1% agarose gel with ethidium bromide. Completely digested DNA was ligated overnight at 15ºC using T4 DNA ligase, extracted with phenol-chloroform-isoamyl alcohol (25:24:1) and precipitated with 3M sodium acetate solution.

Circular DNA obtained was transformed into XL10 Gold Ultracompetent *e. coli* cells (Agilent), following a heat pulse of 42ºC for 45 s. Transformants were selected by Kanamycin resistance over LB plates (30ng/mL) and positive colonies were rescued and grown overnight in LB-Kanamycin media. Plasmidial DNA was extracted from these cultures using standard alkaline lysis method (Russell & Sambrook, 2001), linearised by digestion with EcoRI and analysed in a 1% agarose gel. The plasmid size was calculated by comparison with the DNA 1kb ladder (Invitrogen) and compared with the expected genomic region of the P element insertion of each stock. This region comprises the EcoRI 3' end fragment from the EP cassette (Rørth, 1996) plus the genomic sequence downstream of the insertion site, reported in FlyBase for each line. This DNA sequence was virtually digested

using NEB Cutter 2.0 (New England Biolabs website) and the resulting fragments compared with the one observed from the linearised plasmid.

2.5 Statistical analysis

Statistical analysis was performed and graphs were generated using GraphPad Prism 5.0. For experiments with more than two samples, a one-way ANOVA test was applied. Tukey's multiple comparison test was then used as a post hoc-test when a significant difference was found in the ANOVA test. For experiments with only two samples a two-tailed un-paired Student's t-test was applied. For the climbing assay data, two-way ANOVA and Bonferroni as post-hoc test were used to compare difference between time points and genotypes with the motor performance of each line. Finally, one-sample t-test was used to compare the observed value of a sample with an expected value.

2.6 Bioinformatics

2.6.1 PANTHER

To classify the modifiers found in the screen, we used the Protein Analysis Through Evolutionary Relationships system, PANTHER (Thomas *et al.*, 2003). The protein and gene classification performed by this system is both human curated and bioinformatically sorted. Data obtained include Family and Subfamily levels from PANTHER classification, GeneOntology terms and the closer human ortholog, if available.

2.6.2 DIOPT

The search of human orthologs for the *Drosophila* DVAP genetic interactors was performed with the DRSC Integrative Ortholog Prediction Tool (DIOPT). This tool developed by the *Drosophila* RNAi screening center at the Harvard medical school

(Hu *et al.*, 2011) uses ten different algorithms to find orthologs for one specific gene. The number of positive results for one ortholog is associated with a score, reflecting the strength of the result as well. With this tool, we tried to avoid conflicting results originated by the use of different approaches that led to unrepresentative results.

2.6.3 DAVID

The Database for Annotation, Visualization and Integrated Discovery, DAVID, was used to identify enriched Gene Ontology terms from the genes found in the screen. For a large number of input genes, DAVID provides number of genes linked to a specific function, related genes and groups to each function and a statistical representation of the significance of the enrichment (Huang *et al.*, 2008). Connections are discovered using a knowledge database that recalls information from public genomic resources, including NCBI, SWISS-PROT, GO, OMIM, PubMed and others. For the representation we selected non-redundant Gene Ontology terms with a significance level of $P < 0.05$.

2.6.4 GeneMANIA

The set of modifier genes was further analysed to search for previously reported functional links. GeneMANIA (Warde-Farley *et al.*, 2010) finds genes that are related to the input using a large set of functional association data. These specifically include physical interaction, co-expression and co-localisation data. We searched for connection between the 85 modifiers, without predicting related nodes. Interactions and categories were graphed in a network using the GeneMANIA plug-in for the bioinformatical tool Cytoscape 3.1.0. Genes were also ranked according their false discovery rate (FDR) corrected, enrichment Benjamin-Hochberg test. Weighting method for the interactions was selected automatically according to software parameters.

2.6.5 STRING

In order to predict other proteins that may be involved in the DVAP-modifiers network, we used the database STRING (Jensen *et al.*, 2009). Similar to the way GeneMANIA connect nodes, STRING uses previously reported data and predicts other relevant proteins in the input network. An interaction network was created with all the modifier lines plus DVAP using *Drosophila* datasets. Parameters were calculated automatically and 20 predicted interactors plus 10 white nodes were added using a medium confidence of 0.25.

2.6.6 Ingenuity pathway analysis

To explore if the relation of modifiers observed with the *Drosophila* data was conserved in human data and proteins, we searched biological connection of the human orthologs of our data set using Ingenuity Pathway Analysis, IPA (Ingenuity systems, Quiagen). Most relevant functional categories and canonical pathways were selected using an adjusted Benjamin-Hochberg test, with a significance level of $P<0.05$. They were classified according to their functional category and enrichment level. Modifiers were also connected using a network analysis, including only input modifier genes plus VAPB. Finally, an expanded VAPB interaction network was built connecting the whole modifier list to VAPB using the "Shortest path" method from IPA, which includes predicted interactors of these proteins.

2.7 Dissection and antibody staining of *Drosophila* eye imaginal discs

Eye imaginal discs were extracted from wandering third-instar larvae expressing DVAP-P58S and its control. Collected larvae were washed in PBS and cut in the middle. Anterior half was turned inside out pushing the head end in on itself, exposing the imaginal discs still attached to cuticle. Samples were transferred to an eppendorf tube and fixed with Bouin's fixative (15:5:1 saturated picric acid: 37% formaldehyde: glacial acetic acid) for ten minutes. After several washes with 0.1% solution of phosphate buffered Triton (PBT), samples were blocked with 10%

normal goat serum (NGS) for 2h at room temperature. Staining with primary antibodies was performed overnight at 4ºC at a concentration of 1:1000 in a solution of 5% NGS. After 8 rinses of 15 min with PBT, samples were incubated for 2h at room temperature with the secondary antibodies at a concentration of 1:500 in a 5% NGS solution. Excess of antibody was then removed washing 8 times for 15 min with PBT. Eye imaginal discs were carefully separated from the remaining tissue using fine tipped tweezers and a syringe needle. Finally, samples were transferred to a microscope slide with drops of Vectashield, covered and sealed using nails varnish to avoid drying out.

2.8 Immunohistochemistry on post-mortem human spinal cord tissue

Human tissue was obtained from the MRC Edinburgh Brain Bank with full ethical approval for research studies. Human spinal cord tissue fixed in 10% neutral-buffered formalin was processed into paraffin. 7 µm sections were cut and de-paraffinised with xylene before being rehydrated through graded ethanol solutions. Sections were pre-treated using heat-induced epitope retrieval with Novocastra pH6 retrieval buffer in a decloaking chamber by heating to 125°C for 10sec, cooling to 90°C before washing in running tap water. Slides were then stained on a Leica Vision Biosystems Bond robot using the refine polymer detection kit (Leica) as follows. Endogenous peroxidase was blocked with 3% hydrogen peroxide in TBST for 10 min. Sections were incubated with rabbit anti-Rab5 (1:250, Bethyl laboratories) primary antibody in 0.1% TBST for 2 hours at 25°C and then incubated with anti-rabbit HRP polymer for 15 minutes at 25°C. Staining was visualized using 3,3'-diaminobenzidine as chromogen. Tissue was finally subjected to haematoxylin staining, dehydrated through graded ethanol, cleared in xylene and mounted in Pertex (Cellpath).

Chapter 3: ALS model: DVAP-P58S expression causes neurodegeneration

3.1 Introduction

These initial experiments were designed to explore the effect of the expression of *DVAP* alleles in the eye and nervous system of flies. Having performed so, we tried to find the best condition to observe clear degenerative phenotypes and optimize the use of this ALS model as a way to search for DVAP-interactor genes in a genome-wide screen.

3.2 *DVAP* mutant alleles cause neurodegeneration in the *Drosophila* eye

The biology of VAPB has been systematically studied since its original characterisation in *Aplysia* (Skehel *et al.*, 1995). Functional homologues found in *Drosophila,* mice and humans improved the understanding of this protein and its relation with synaptic vesicles. However a major turning point occurred with its linkage to ALS in patients from a Brazilian family (Nishimura *et al.*, 2004a). Since then, the causative mutation has been modeled in different organisms and the relation between structural changes in the protein and neurodegenerative phenotypes has been strengthened. One of these models was developed by our group (Chai *et al.*, 2008) using the expression of the *Drosophila* homolog of the human Pro56Ser mutation, DVAP-P58S. Expression of the causative allele in flies has been shown to cause altered synaptic remodeling, decrease in viability and recapitulation of other ALS hallmarks. This *Drosophila* ALS model will be the pivot of this project and as a first step, we have determined the best combination of parameters to perform a genome wide genetic screen.

DVAP-P58S expression in the eye was previously associated with roughness and reduction in size (Forrest *et al.*, 2013). These same phenotypes were also observed with the expression of another ALS-linked mutation, DVAP-T48I (Chen *et al.*, 2010). The aim of this chapter was to report the characterization of DVAP expression in the eye and analyse neurodegenerative phenotypes associated with

different alleles, GAL4-drivers and temperature. The optimal combination of these variables was used to carry out the screen.

3.3 UAS-GAL4 system can direct DVAP expression specifically in the eye

In *Drosophila,* to drive the expression of a transgene in a tissue- and time-specific manner, the best available tool is the UAS-GAL4 system designed by Andrea Brand and Norbert Perrimon (Brand & Perrimon, 1993). With this technique, the level of expression and activity of the GAL4 protein and consequently, the expression of the transgene, can be modulated by changing the temperature at which flies are raised. This system is based on two components: the yeast transcriptional activator GAL4, which is expressed under the control of tissue specific promoters, and the target gene that possess in its regulatory region GAL4 binding sites (Upstream activator sequences, UAS) that activate the expression of this gene in the tissues where the GAL4 activator is present. In this way, the target transgene will be expressed exclusively in the tissue where the GAL4 was transcribed. The discovery and construction of different tissue-specific GAL4 lines ("driver" lines) and the increasing availability of transgenic UAS alleles, allow a myriad of possibilities to study *Drosophila* genes in an efficient and clean way (St Johnston, 2002)

To examine DVAP-associated neurodegeneration specifically in the eye, we explored the use of the two eye specific drivers: *eyeless-GAL4* and *GMR-GAL4*. *Eyeless-GAL4* is a transgenic line based on the *eyeless* gene (*ey*), which encodes the homolog to the mouse transcription factor Pax6. Initially, *ey* is expressed in the embryonic ventral nerve cord and in some regions of the brain. In the larval stages it is expressed in eye imaginal discs and only in the third larval stage, the expression is restricted to undifferentiated cells from imaginal discs, becoming the master gene for the *Drosophila* eye development (Halder *et al.*, 1995). The *ey-GAL4* driver was originally reported as a way to express specifically a target gene in the eye imaginal disc. Then, it has become a relevant tool for the study of lethal genes without affecting massively the offspring viability (Tseng & Hariharan, 2002). However, a

low level of expression in other tissues has been observed in previous studies as well (Callaerts *et al.*, 2001).

Glass multimer reporter or *GMR-GAL4* driver was constructed to drive the expression in the developing eye (Freeman, 1996). Opposite to *ey,* which is expressed in the region anterior to the morphogenic furrow area of undifferentiated cells (Halder *et al.*, 1995), *GMR* is expressed in the posterior area, where ommatidia cells are starting to differentiate. Nevertheless, both genes have shown expression in tissues outside this area. Both drivers are widely used as tools to perform genetic screens in the eye (Tseng & Hariharan, 2002; Fernandez-Funez *et al.*, 2000). We decided to test whether any of them could be used to drive the expression of *DVAP* alleles in the eye to perform a genetic screen.

3.4 Expression of *DVAP-P58S* under the control of *ey-GAL4* driver presents a consistent degenerative phenotype

Light microscopy images of flies expressing both *DVAP* mutant alleles under *GMR-GAL4* control at 30ºC revealed degeneration in the eye, but unfortunately a similar phenotype was also observed in the control cross carrying one copy of the driver (Figure 4A). With the same driver, a slight rough eye phenotype was observed in mutants but not in control flies when they were raised at 28˚C. However, the mutant phenotype was too weak to be used for a screen and when raised at lower temperatures, the phenotype vanished. The degenerative effect of the driver by its own was confirmed using paraffin eye sections stained with hematoxylin and eosin (HE) at 30ºC (Figure 4B). Toxicity caused by *GMR-GAL4* on its own has been previously reported (Kramer & Staveley, 2003), so the use of this driver has been useful only for genes with a strong phenotype that is not masked by the one of the driver.

Conversely, using *ey-GAL4* driver, a robust and specific phenotype was observed in mutant transgenic lines when compared to controls. Although a reduction in eye size was already evident for both transgenic lines at 28˚C, a stronger

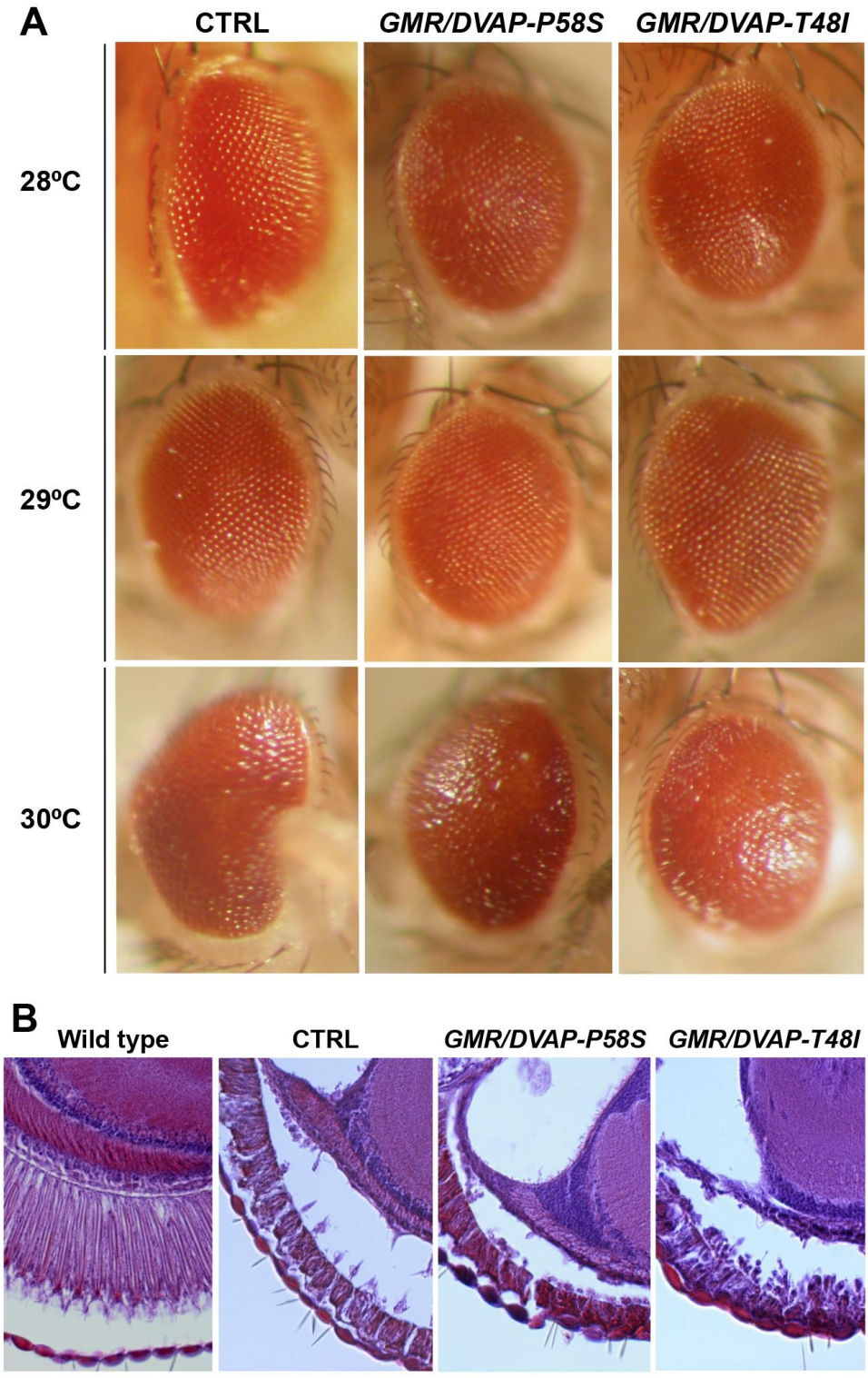

Figure 4. Expression of *DVAP* mutant alleles under the control of *GMR-GAL4*. (**A**) Representative light microscope images of eyes from control (*GMR-GAL4/+*), *GMR/DVAP-P58S* and *GMR/DVAP-T48I* adult flies raised at 28, 29 and 30ºC. (**B**) Paraffin sections of heads from adult flies from these phenotypes raised at 30ºC. Roughness in the eye is present not only in flies carrying the mutant alleles but also in controls expressing the driver by its own.

effect was observed at 30˚C (Figure 5A). Under the microscope, eyes of flies *DVAP-P58S/ey-GAL4* looked smaller than *DVAP-T48I/ey-GAL4* ones. This neurodegeneration was confirmed with the analysis of HE stained sections (Figure 5B). At 30ºC, eyes of adult flies expressing DVAP-P58S looked comparatively smaller and showed fusion and disorganisation of ommatidia as well. This was also previously reported in detail using scanning electronic microscopy images and paraffin eye sections (Andrea Chai thesis). These phenotypic changes can be analysed and as previously reported, they represent an interesting readout for a genetic screen (Branco *et al.*, 2008; Fernandez-Funez *et al.*, 2000).

Eye size differences were easily noticeable but there was variability at different temperatures. The model selected for the genetic screen must show a consistent phenotype but also display a low variability for data reproducibility. To address this issue, we quantified the eye size area of the previous crosses. At least 20 eyes were photographed from independent adult flies using a light microscope. These were processed with the software ImageJ to quantify their eye surface area and then statistically analysed with Graphpad Prism.

The difference between mutant alleles and control areas was larger at 30ºC (Figure 6A), and less clear at 29ºC and 28ºC (Figure 6B and C, respectively). Another relevant difference was the larger variability in the area of eyes from flies carrying the *DVAP-T48I* allele compared to those with *DVAP-P58S*. This was clearly noticeable at 30ºC, where the former presents individuals with wild-type size eyes and others with almost no eyes. DVAP-P58S flies on the other hand, present a more consistent and narrow data distribution, clustering near the mean value. This crucial parameter for reproducibility of a screen, plus the higher reduction of eye size compared to controls, led us to select the expression of *DVAP-P58S* driven by *ey-GAL4* as a model to search for modifiers of neurodegeneration in the eye.

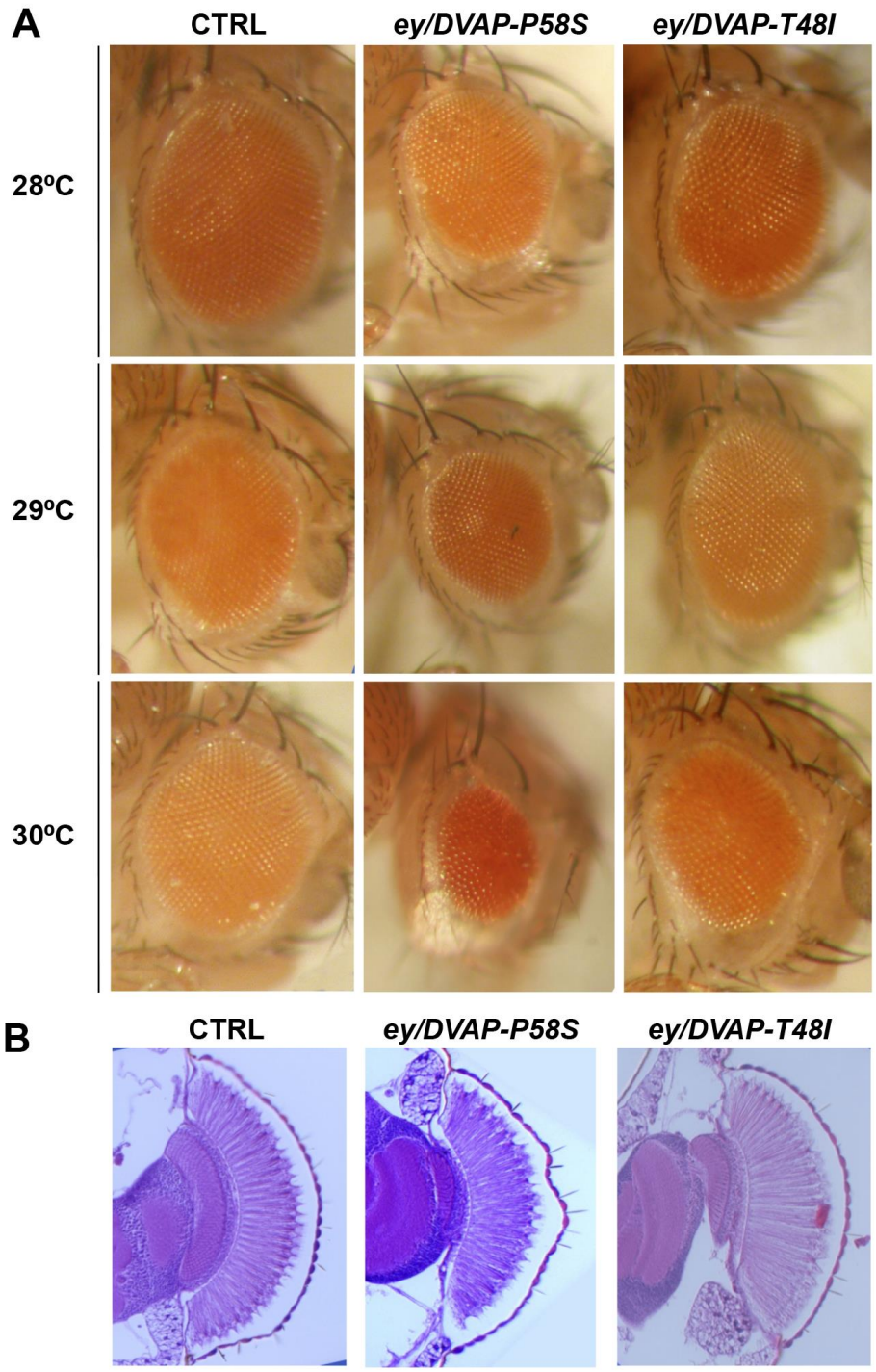

Figure 5. Expression of *DVAP* mutant alleles under the control of *ey-GAL4*. (**A**) Representative light microscope images of eyes from control (*ey-GAL4/+*), *ey/DVAP-P58S* and *ey/DVAP-T48I* adult flies raised at 28, 29 and 30ºC. (**B**) Paraffin sections of heads from adult flies from these phenotypes raised at 30ºC. A significant roughness and decrease in the eye size is observed in ey/DVAP-P58S flies raised at 30ºC.

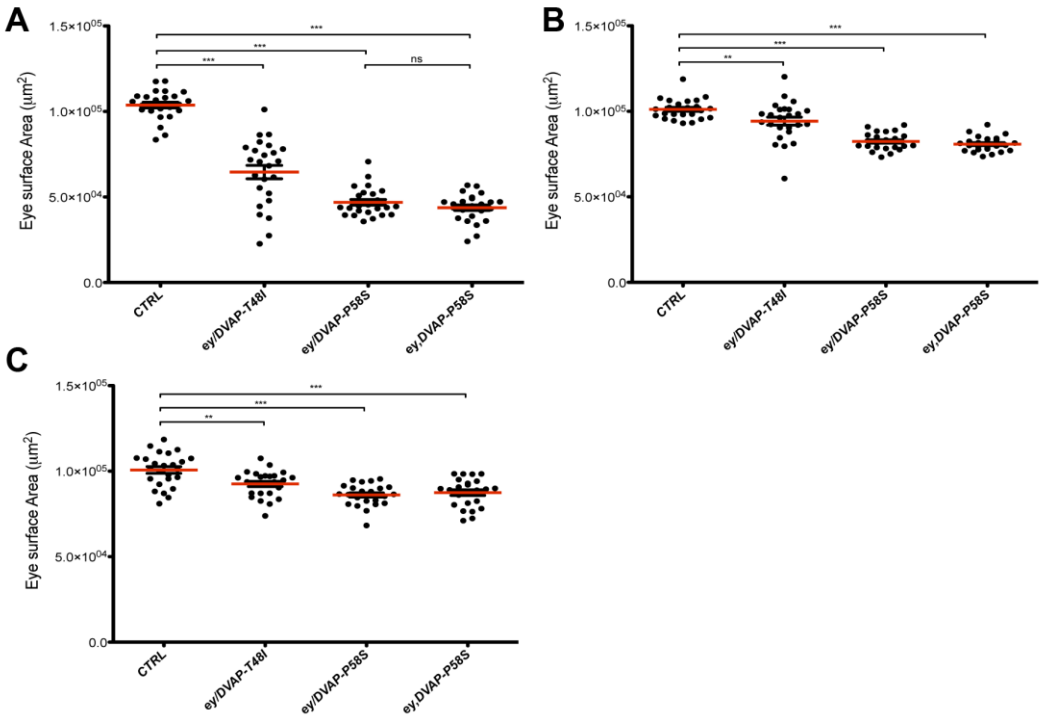

Figure 6. Quantification of the eye surface area of flies carrying *DVAP* mutant alleles. Scatter plot displaying eye size area of CTRL (*ey-GAL4/+*), *ey/DVAP-T48I (ey-GAL4,DVAP-T48I/+), ey/DVAP-P58S (ey-GAL4/DVAP-P58S)* and recombinant *ey,DVAP-P58S (ey-GAL4,DVAP-P58S/+)* adult flies raised at 30ºC (**A**), 29ºC (**B**) and 28ºC (**C**). Each point corresponds to the measurement of an individual eye and the red line display the average of the population. When raised at 30ºC, the expression of DVAP-P58S in the eye presents a significant and consistent decrease in surface area. The same output is also observed in the recombinant line *ey,DVAP-P58S*. *** P<0.001, ** P<0.01 (One-way ANOVA).

3.5 Recombinant *ey-GAL4,DVAP-P58S* works consistently as a useful ALS model

To achieve the *DVAP-P58S* expression, the UAS version of the allele must be present at the same time with the *ey-GAL4* driver. This can be established either by crossing two parental lines each of them carrying one of the two elements, or by the construction of a recombinant line carrying both elements on the same chromosome. All these lines were available in our lab and we searched for differences in neurodegeneration induced by these two genetic possibilities. Quantification of eye surface area of flies obtained from a cross between ey-GAL4 males and UAS-DVAP-P58S virgin females (*ey-GAL4/DVAP-P58S*) showed no significant differences when compared to eyes from flies obtained by crossing of the recombinant line and a wild type line (*ey-GAL4,DVAP-P58S/+*) (Figure 6A). Moreover, these two crosses presented the same narrow distribution at three different tested temperatures. Thus, the recombinant line *ey-GAL4,DVAP-P58S* represents a more convenient line as it provides the option to add a third element in the offspring (i.e. Misexpression EP line) to test its effect in the DVAP-P58S-expressing eye. This line was maintained throughout the screen, based on the solid results observed in these analyses.

3.6 Expression of *DVAP-P58S* in the whole nervous system causes lethality at 30ºC

After dissecting the DVAP-P58S-induced neurodegeneration in the eye, we studied the effect of the expression of this allele in the whole nervous system and compared the phenotype of the *Drosophila* model with some classical hallmarks of the disease in humans. ALS is a neurodegenerative disease that affects the motor system; therefore, expression in the whole *Drosophila* nervous system represents a closer approximation to the real degeneration mechanism compared to the analysis in the eye.

A different GAL4 driver was selected for nervous system expression. *Elav-GAL4* is based on the gene *embryonic lethal abnormal vision*, which codifies for a RNA-binding protein expressed in all neurons (pan-neural expression, Yannoni & White, 1997). This protein is required for maintenance and differentiation of the nervous system as it regulates splicing forms of different central genes like *ewg, nrg* and *armadillo*. Although DVAP protein is ubiquitously expressed, by using *elav-GAL4* we can regulate and mimic its deregulation in the nervous system.

As a first step we wanted to assess whether DVAP expression alters the viability of adult flies. Previous reports have shown that expression of DVAP-P58S forms intracellular protein aggregates containing both mutant and wild type versions of the protein (Teuling *et al.*, 2007). This phenotype is central in several neurodegenerative diseases (Vabulas *et al.*, 2010) and is related to cell death and decrease in the number of viable organisms. To study the effect of DVAP expression on the viability of adult flies, we expressed mutant DVAP alleles under the control of elav-GAL4. Flies failed to eclose when the mutant alleles *DVAP-P58S* and *DVAP-T48I* were expressed at 30ºC (Figure 7A). Another line expressing low levels of the wild type form of the protein (DVAP-WT) showed a decrease in viability but not as severe as observed with mutant levels. When the expression of the alleles was reduced by decreasing the temperature, adult flies expressing the mutant alleles were able to eclose, but at a reduced ratio compared to controls and the DVAP-WT line. In the case of DVAP-P58S, the number of adult flies was almost 70% of the expected number observed in controls at 27ºC. These flies carry the mutant DVAP allele but still eclose as normal flies. This indicates that a progressive neurodegenerative effect can be observed after the flies eclose and not exclusively a defect at developmental level is presented. This was an important aspect of the next analysis, where mutant flies were tested for other neurodegenerative phenotypes.

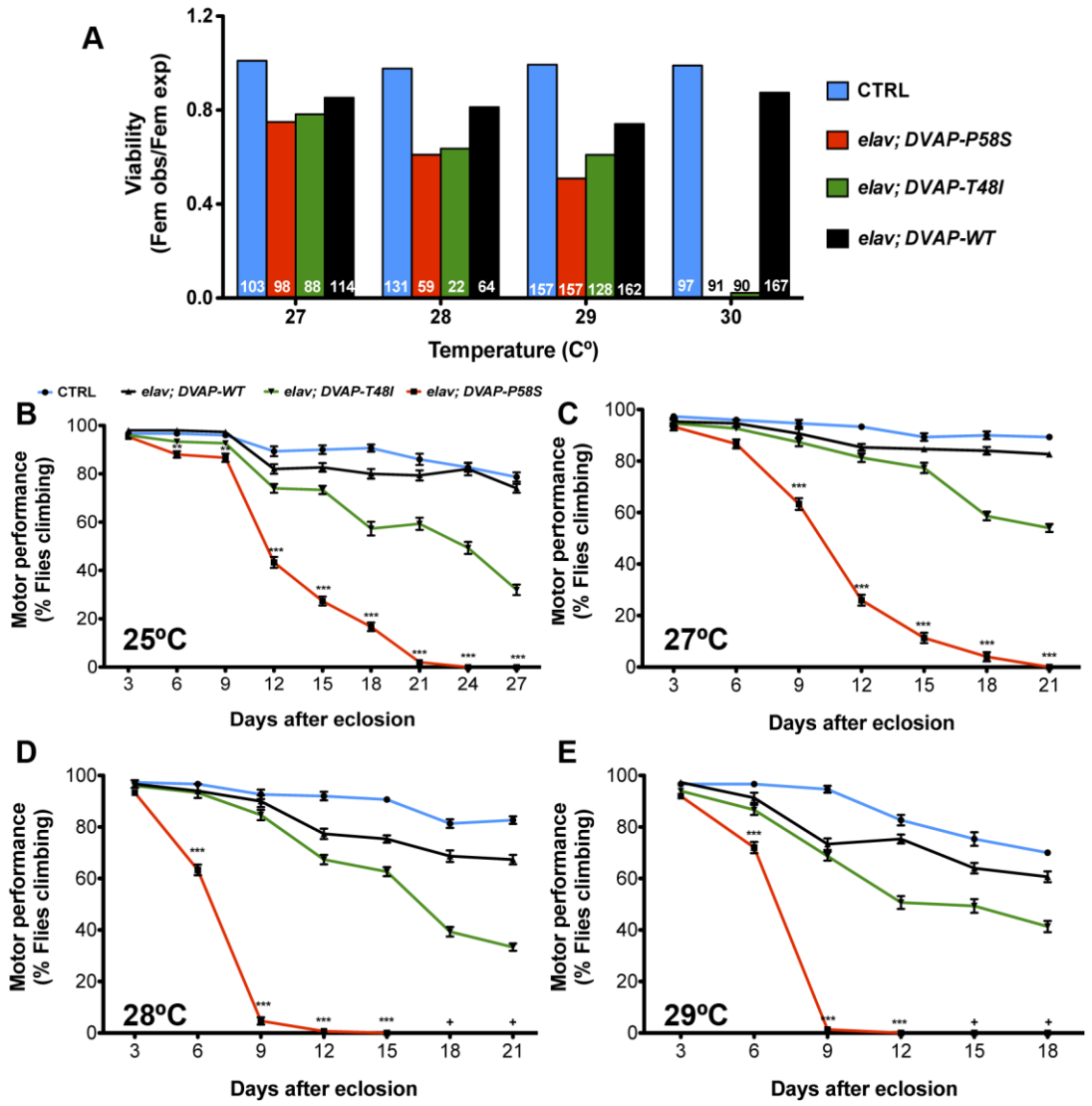

Figure 7. Expression of *DVAP* mutant alleles in *Drosophila* nervous system is toxic. (**A**) Viability ratios expressed as the number of observed adults females from control (in blue, *elav-GAL4/+;+/+*), *elav;DVAP-P58S* (red, *elav-GAL4/+*; *DVAP-P58S/+*), *elav;DVAP-T48I* (green, *elav-GAL4/+*; *DVAP-T48I/+*), and *elav;DVAP-WT* (black, *elav-GAL4/DVAP-WT*; *+/+*) flies raised at 27, 28, 29 and 30ºC. Number of females counted is displayed at the bottom of each bar. (**B-E**) Motor performance assay in DVAP-expressing adult flies. Flies expressing DVAP mutant alleles in the nervous system (red and green) lose progressively motor performance after eclosion. Compared to control flies (blue) *elav;DVAP-P58S* flies show a dramatic phenotype even before ten days after eclosion when raised at 28ºC. Each point represent the average of 10 repetitions of the percentage of flies able to reach 8 cm in 15 seconds (n=10). *** $P < 0.001$, ** $P < 0.01$ (Two-way ANOVA).

3.7 Motor performance progressively deteriorates with the expression of *DVAP-P58S* in the nervous system

A central hallmark of ALS observed in patients is the progressive loss of motor performance, which finally leads to paralysis of vital organs such as heart and lungs (Pasinelli & Brown, 2006). This symptom is related to the progressive death of motor neurons through a mechanism not completely understood yet. If *DVAP* is an ALS causative gene and causes neurodegeneration, will be likely affecting motor performance in ALS models such as *Drosophila*. This has not been tested yet in this model, but has been consistently proved in other screens for neurodegenerative diseases, as a powerful tool to determine neuronal death (Branco *et al.*, 2008; Kaltenbach *et al.*, 2007).

To analyse this, we tested both *DVAP* mutant alleles at different temperatures to determine which level of expression would exhibit a specific and consistent phenotype. Males overexpressing DVAP were crossed with *elav-GAL4* virgin females and the offspring was collected and raised at different temperatures: 25, 27, 28 and 29 ºC. The different amount of DVAP expressed in the nervous system can alter the level and speed of neurodegeneration in adult flies. Therefore, we tried this range of temperatures to increase the possibility to obtain a clear phenotype.

Only female individuals were selected, as they show different climbing speed than males, likely due to their different size. Also, only virgin females were chosen due to two important observations: eggs inside non-virgin females may affect their weight and motor performance, and collection of virgin females in one day provides a narrow difference in age between the different individuals from the same group.

The tested females were kept at the specific temperature and every three days were tested to quantify the proportion of flies that were able to climb 8 cm in 15 s, inside a clear polyethylene tube. The number of flies who reached this height was counted, flies were tapped to the bottom and the measurement was repeated ten times. The flies were then transferred to a new vial of food and kept at the original

temperature until the time curve was complete. Every day before recording data, a trial run of ten non-recorded repetitions was performed to stabilise flies behaviour and climbing ability.

All DVAP lines showed normal motor performance in the first three days compared to controls; however they progressively started to lose this ability, implying that this phenotype had a neurodegenerative and not only a developmental origin (Figure 7B). Flies expressing DVAP-P58S in the nervous system showed a worse motor performance than other alleles at all temperatures tested, with an average of ten days before losing climbing capability. At 25ºC, flies expressing *elav;DVAP-P58S* showed wild-type level of climbing ability during the first nine days before losing it progressively ten days after. At this point, wild-type controls and overexpression of DVAP-WT exhibit an almost perfect motor performance. When the temperature was increased, the lack of motor performance in DVAP-P58S appeared even earlier, probably due to an increase in the toxic accumulation of this mutant protein in the nervous system. When tested at 29ºC, maximum temperature at which flies can eclose, the motor performance of individuals expressing DVAP-P58S was drastically lost before ten days, while flies expressing the other two DVAP alleles still performed at a climbing ratio over the 50%.

With these results, we showed for the first time the use of this important assay that can link expression of DVAP mutants and neurodegeneration. DVAP-P58S-expressing flies mimic a central hallmark of the disease in humans and this validates even more the model as a relevant tool to study ALS. Considering that we plan to use this test to analyse several lines as part of our screen, it could be desirable to express DVAP at high temperatures to follow a shorter time curve that could supply data in a consistent way but in a shorter period of time. On the other hand, it is desirable to have a progressive decline in motor performance, which might bring less consistency and more variability as a negative effect. After several steps of optimisation, we decided to perform the climbing assay at 28ºC and in a time window between 4 and 12 days. A significant suppression or enhancement of DVAP-P58S-associated

toxicity can be tested in this time frame and could represent a critical way to filter possible candidates.

3.8 DVAP genetic modifiers can be found using the expression of its mutant allele in the eye

We showed that the *DVAP-P58S* allele causes neurodegeneration in the eye as well as in the rest of the nervous system, and that driven under specific conditions, a consistent phenotype can be obtained. This phenotype could be the key to start the search of modifiers of DVAP-linked toxicity and at the same time, determine potential novel interactions of DVAP with ALS-related proteins. Before deciding to start this genome-wide search, we wanted to determine whether the ALS model can be used for that purpose, studying the genetic interaction of DVAP with pathways that other studies suggested could be involved in its toxicity. For this aim, we planned to study changes in DVAP-mediated toxicity under the effect of alleles of genes related to phosphoinositide metabolism and components of the JNK Pathway.

Phosphoinositides (PI) are membrane-related lipids involved in regulation and movement of different effector proteins. This function is crucial inside the cell and controls several pathways, based on the concentration of different versions of these lipids. The specific phosphorylation of 3 different positions in the molecule can form seven altered molecules that differ in concentration and localisation inside the cell. These small pools can relocate and concentrate diverse proteins to achieve their function in that specific area. For this reason, not only is relevant the PI concentration, but also the phosphatases and kinases that reversibly transform these molecules (Blagoveshchenskaya & Mayinger, 2008; Nakatsu *et al.*, 2012).

Sac1 (Suppressor of Actin 1) is a phosphoinositide phosphatase that preferably dephosphorylates PI4P pools, but also can catalyse the conversion of PI3P and PI3,5P2. Previously, this protein has been listed as a DVAP physical interactor (Giot *et al.*, 2003). This large-scale yeast two-hybrid result was recently confirmed by our group (Forrest *et al.*, 2013), identifying at the same time that the transmembrane

domain of DVAP was necessary for this interaction. To understand the biological relevance of this physical interaction and concurrently, test our previously optimised ALS model, we analysed the effect of Sac1 alleles in the DVAP-linked neurodegeneration.

The co-expression of *UAS-Sac1* in flies expressing *DVAP-P58S* under the control of *ey-GAL4* suppresses the neurodegeneration in the eye (Figure 8). The eye size increased to an almost wild-type level. Additionally, ommatidia organization presented a normal organization compared to the roughness of the flies expressing *DVAP-P58S*, as observed in scanning electronic microscopy and paraffin sections of fly heads (Figure 8). This result suggests that the increase of PI or the decrease of PI4P could ameliorate the DVAP-P58S linked toxicity. If any of these is true, we should observe a suppression of the neurodegeneration by decreasing the formation of PI4P molecules. To confirm this, we co-expressed altogether with *DVAP-P58S* two loss-of-function alleles of the *Drosophila* PI4P kinases, Fwd and PI4KIIIα. As expected, we confirmed the result detected with the overexpression of Sac1 and reduction of kinases levels produced a normal eye structure, even when co-expressed with *DVAP-P58S*. These results (Figure 8) suggest the novel idea that accumulation of PI4P may be involved in DVAP toxicity, but more importantly for this project, reveal that changes in levels of DVAP genetic interactors can alter DVAP-P58S phenotype. The results also validate the expression of this allele under the control of *ey-GAL4* as a useful model to search for genetic modifiers of its toxicity.

With the idea of confirming this last point and obtain novel data associated with DVAP mechanism, we studied components of another pathway related to PIs. In 2003, Wei *et al.* showed that Sac1 regulates apoptosis via JNK pathway. The Jun-N-terminal kinase (JNK) is a stress-activated kinase that is conserved throughout the evolution and is the central step of a cascade system that responds to environmental stress stimuli. Even though in mammals each step of this system associates to a large family of genes that codifies different kinases, in *Drosophila* there is only one JNK protein (Basket) and two JNK Kinases (Hemipterous and dMKK4). These proteins can activate the transcription factors AP-1 and Foxo and start different cellular

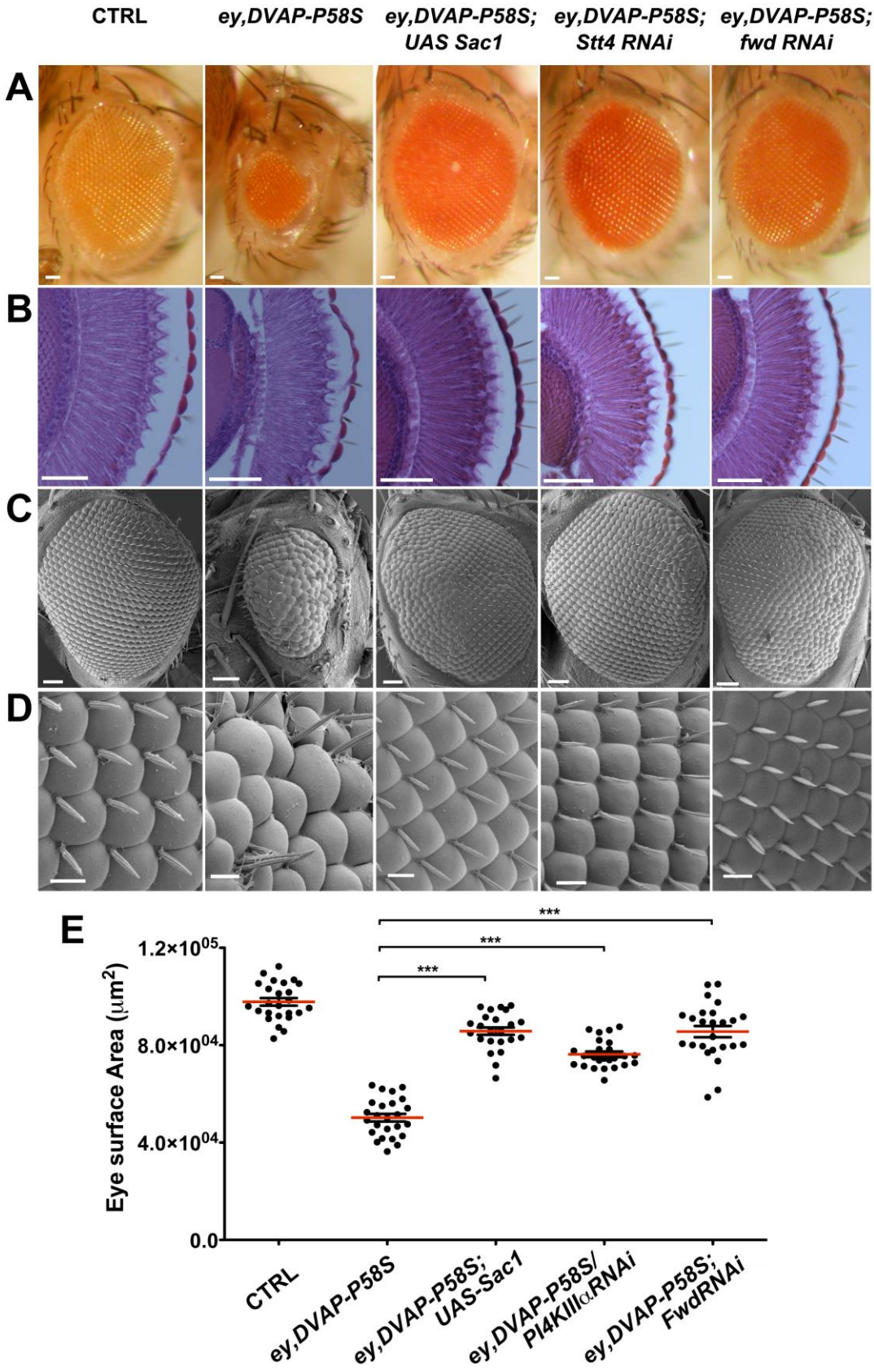
CTRL
ey,DVAP-P58S
ey,DVAP-P58S; UAS Sac1
ey,DVAP-P58S; Stt4 RNAi
ey,DVAP-P58S; fwd RNAi
A
B
C
D
E
Eye surface Area (μm²)
1.2×10^05
8.0×10^04
4.0×10^04
0.0
***
***
***
CTRL
ey,DVAP-P58S
ey,DVAP-P58S; UAS-Sac1
ey,DVAP-P58S/ PI4KIIIαRNAi
ey,DVAP-P58S; FwdRNAi

Figure 8. DVAP-P58S-linked neurodegeneration is suppressed by downregulating PI4P formation. (**A**) Stereo microscope images, (**B**) frontal sections and (**C,D**) scanning electron micrographs of controls (*ey-Gal4/+*), *ey,DVAP-P58S (ey-GAL4,DVAP-P58S/+;+/+), ey,DVAP-P58S;UAS-Sac1 (ey-GAL4,DVAP-P58S/+;UAS-Sac1/+), ey,DVAP-P58S/PI4KIIIaRNAi (ey-GAL4,DVAP-P58S/PI4KIIIaRNAi;+/+)* and *ey,DVAP-P58S;FwdRNAi (ey-GAL4,DVAP-P58S/FwdRNAi;+/+)* adult fly eyes. Wild type structure of the control eye is affected as ey,DVAP-P58S eyes are smaller, with missing bristles and occasionally fused ommatidia. The ey,DVAP-P58S-mediated neurodegeneration is rescued by upregulating Sac1 phosphatase or by downregulating either PI4KIIIa or Fwd kinases. (E) Quantification of the eye surface area of these genotypes. Scale Bar = 50 um in (A), (B) and (C) and 10 um in (D). *** P<0.001 (One-way ANOVA).

responses such as apoptosis, autophagy, cell proliferation and growth (Biteau *et al.*, 2011). Sac1 was linked to this pathway as a cooperative protein for the JNK suppressor *Puckered*, regulating negatively the pathway (Wei *et al.*, 2003). They also suggested that this repression is mediated by the alteration of PI pools through the regulation of the cytoskeleton. To analyse whether this PI pool alteration also links the JNK pathway and DVAP toxicity, we crossed flies expressing different components of the JNK pathway with our ALS model. Interestingly, we did not find any modification of the DVAP neurodegeneration by downregulating the central component Jnk (Basket), or overexpressing the repressor Puc (Figure 9). However, we observed a strong suppressive effect when we tested the Inhibitor of apoptosis gene, DIAP1. This protein is required for survival of somatic cells in *Drosophila* embryos, inactivating different caspases that execute apoptosis via autoubiquitylation and proteasomal degradation (Hawkins *et al.*, 1999). Our data suggest that the suppression of DVAP toxicity by DIAP1 is directed through a JNK-independent mechanism, possibly by blocking apoptosis effectors located downstream of DVAP.

In both validation assays, we observed a decrease in the toxic effect of the UAS-DVAP-P58S construct. It can be thought that this effect was due to a dilution of GAL4 when we crossed the construct with a different one. To discard this idea, we crossed DVAP-P58S flies with a line expressing a GFP construct (UAS-mCD8:GFP). We observed the same phenotype of DVAP-P58S by its own (Figure 10), indicating that the suppression effects previously showed are not due to a dilution effect from a non-interacting protein, validating at the same time these results.

Considering the previous data, we successfully tested the interaction of different alleles with the DVAP mutant allele. The clear neurodegeneration observed with the expression of this protein in the eye is a strong approach to analyse genetic interactions with those proteins involved in DVAP-toxicity mechanism. This idea will be the central part of this project, as we aim to search for novel modifiers of DVAP-linked neurodegeneration in a genome-wide screen.

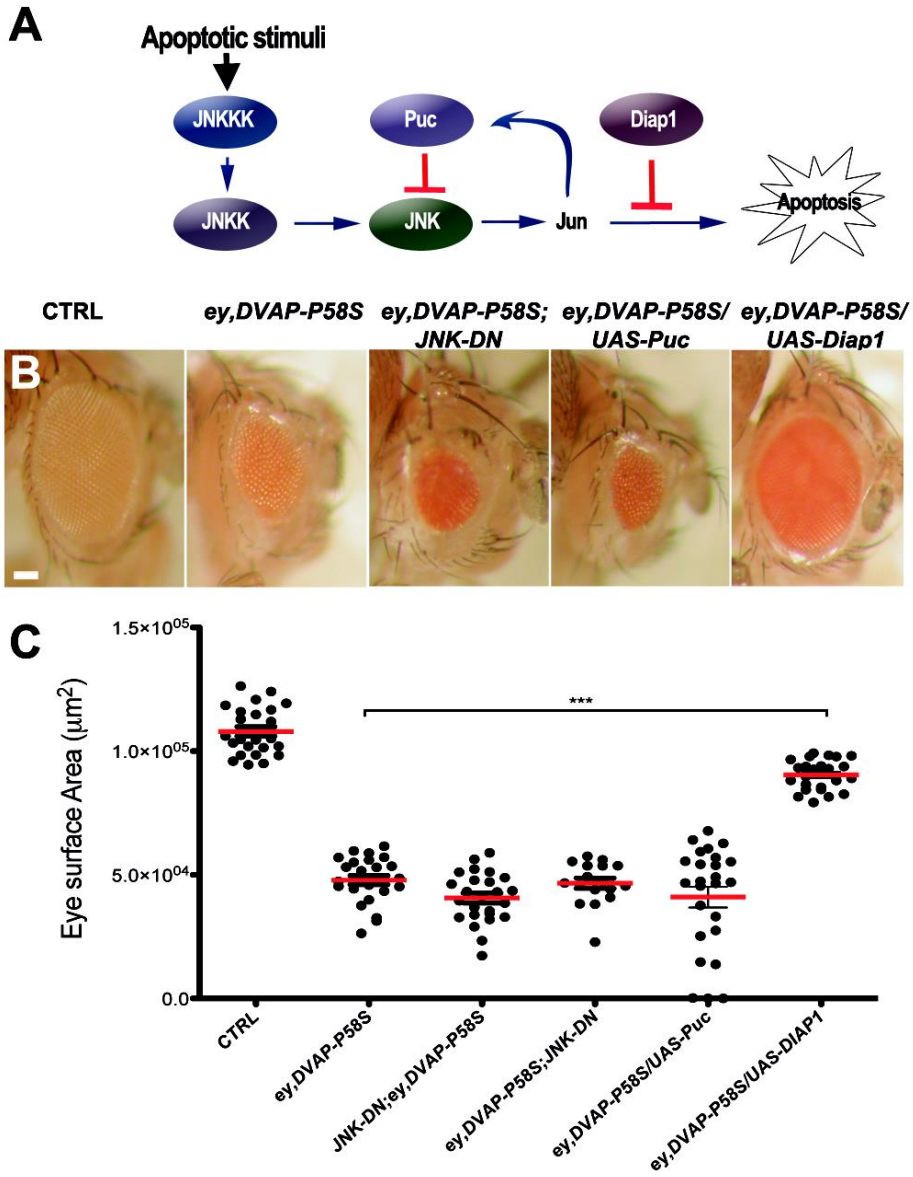

Figure 9. JNK Pathway components do not modify DVAP-linked neurodegeneration. (**A**) The JNK pathway, composed of three consecutive kinases that activate different apoptosis effectors. Puc is a direct repressor of the pathways and DIAP1 can also suppress apoptosis at other levels. The balance of these activities is important for cell growth and development. (**B**) Light microscopy images of control flies (*ey-GAL4/+;+/+*) and flies co-expressing in the eye *DVAP-P58S* and different JNK pathway mutant lines: *ey,DVAP-P58S (ey-GAL4,DVAP-P58S/+;+/+*), *ey,DVAP-P58S;JNK-DN (ey-GAL4,DVAP-P58S/+;JNK-DN/+*), *ey,DVAP-P58S ey,DVAP-P58S/UAS-Puc (ey-GAL4,DVAP-P58S/UAS-Puc;+/+*) and *ey,DVAP-P58S/UAS-Diap1 (ey-GAL4,DVAP-P58S/UAS-Diap1;+/+*). Suppression is only observed with the overexpression of *DIAP1*, suggesting that the DVAP toxicity does not go through JNK pathway. (**C**) Quantification of eye surface area of the previous crosses. Only *ey,DVAP-P58S/UAS-DIAP1* presented a comparable eye size with control (*ey-Gal4/+*) and significantly different from the ALS model (*ey-Gal4,DVAP-P58S/+*). Scale Bar = 50 um. *** P<0.001 (One-way ANOVA).

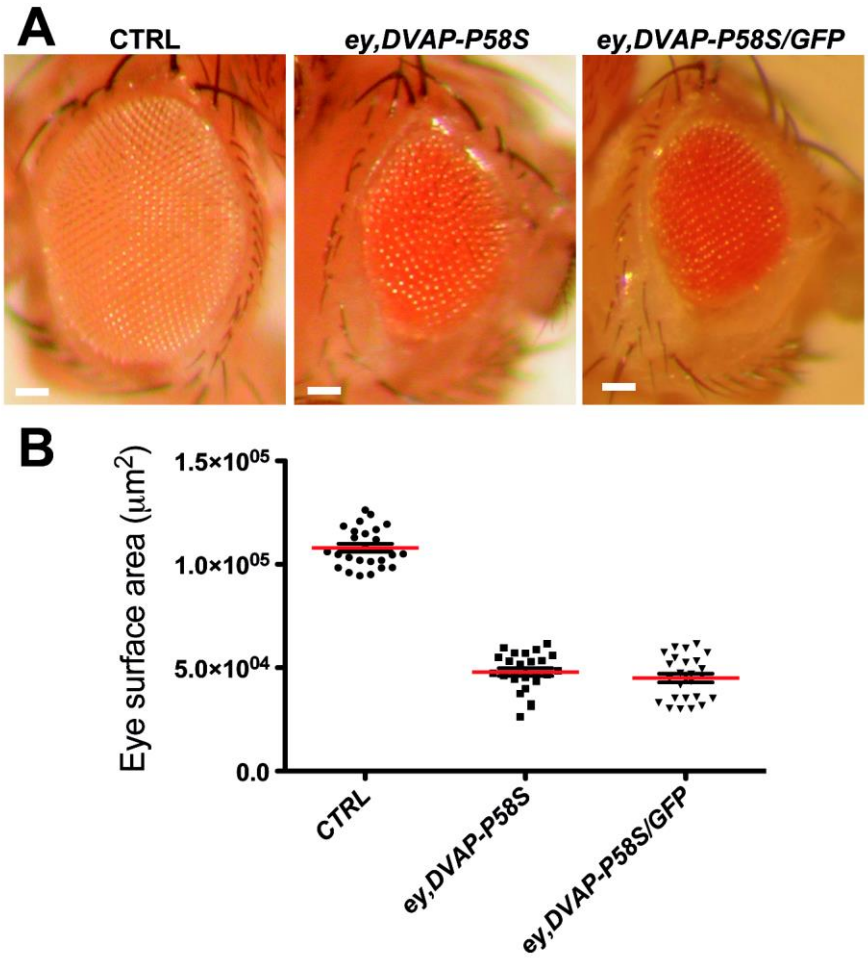

Figure 10. Expression of a GFP construct does not affect DVAP-P58S phenotype. (**A**) Light microscopy images of Controls (*ey-Gal4/+*), *ey,DVAP-P58S (ey-GAL4,DVAP-P58S/+*), and *ey,DVAP-P58S/GFP (ey-GAL4,DVAP-P58S/UAS-GFP*) eyes. (B) Quantification of the eye surface area in flies of the indicated genotypes. *DVAP-P58S* expression in the eye displays same phenotype over a wild type chromosome or when co-expressed with the GFP construct. This confirms the lack of a GAL4 dilution effect in DVAP-P58S phenotype when another transgene is co-expressed. Scale bars = 50 µm.

Chapter 4: Genetic screen to find modifiers of DVAP-P58S-induced neurodegeneration

4.1 Introduction

After optimising and validating the expression of DVAP-P58S in the eye as a proper model to study ALS, we performed a functional screen to discover genetic modifiers of the neurodegeneration associated with DVAP mutant allele. The lines that showed a significant modification level were then tested in a series of validation analyses that confirmed their effect in DVAP-P58S toxicity.

4.2 Genetic screening as a powerful approach to study ALS

Historically, the use of *Drosophila* has provided several crucial findings in the genetic field. In comparison with other models, probably the most practical advantage of the fruit fly is its genetic flexibility, which can lead to strong findings without redundancies or complications linked to higher organisms. This aspect has been successfully exploited throughout the years with designs of genetic functional screens, which stand out as a powerful approach successfully tested in other neurodegenerative diseases such as ataxias, Huntington's disease and tauopathies (Fernandez-Funez *et al.*, 2000; Kaltenbach *et al.*, 2007; Shulman & Feany, 2003). Nevertheless, this idea has never been used to find unbiased functional interactors of ALS-causative genes.

Over the last years, other non-functional and biased screens have been performed with ALS-linked genes (Couthouis *et al.*, 2011; Yang *et al.*, 2013; Zhan *et al.*, 2013). However, the strong characterisation performed in our model and the supporting evidence of it as a useful model for the study of the disease, directed us to start this functional screen. This characterisation has unveiled interesting processes and phenotypes associated with DVAP-P58S neurodegeneration. Among these parameters, neurodegeneration in the eye highlights as an easy and fast readout, not only for the consistent smaller eye compared to controls, but also for a clear disorganisation of the internal structure. This phenotype constitutes a good approach to test a high number of lines without excessive amount of resources involved in determining whether a modification effect is present.

4.3 Overexpression-based screens are an improved approach to find genetic interactions

As an initial step, it was crucial to decide which type of line will be tested. Successful screens have mostly been performed based on three different *Drosophila* stocks: lines that misexpress transgenic constructs, loss-of-function lines of individual genes through expression of specific RNAi, and deletions of a genomic region using previously mapped stocks. Even considering the high availability of tools for the two loss-of-function techniques, these present important drawbacks and fewer advantages that the overexpression approach.

The expression of RNAi lines can be conveniently controlled. In the last years, different groups and stock centers have constructed RNAi lines for most *Drosophila* genes, turning this technique into a strong approach for genetic studies. However, an important problem with the expression of these constructs is the probability of non-specific down-regulation of other genes. This off-target suppression affects the effect in the expected gene, and is necessary the use of additional RNAi lines to confirm a phenotype (Ma *et al.*, 2006; Mohr *et al.*, 2010). This is not ideal in a large scale screen, when the same resources could be used to investigate an additional gene and not a different allele for the first one. Additionally, RNAi-based results depend on the strength of the construct on the target gene. Therefore, different misleading phenotypes can be observed if the used RNAi line has a partial knock-out effect, compared to a complete loss of function allele. This also implies an extra detail in the background of the screen and the rate of false discovery that can affect the outcome of an RNAi screen (Mohr *et al.*, 2010).

On the other hand, the search of modification using deletion stocks can provide important data in a faster way. A deletion line is constructed after the removal of a genomic region that includes a variable number of genes. A phenotype observed crossing the studied model with one of the deletion stocks may be caused by any of the missing genes in that specific line or even by two genes simultaneously. This is a main drawback of this technique for large scale studies, as it is necessary to

determine which of these genes is affected. This process may require several other stocks, resulting in a similar problem as the RNAi approach. Additionally, these techniques need a genetic background sensible enough to observe minor phenotypic differences, issue that can be difficult after handle an important number of stocks (Rørth, 1996).

The third technique, the use of missexpression lines, is our preferred choice for this study. Introduced for the first time in 1996 for the detection of tissue-specific phenotypes (Rørth, 1996), this genetic approach became the best way to find genetic modifiers as it was able to detect an important number of dominant interactions that were overlooked with the loss-of-function screens. This first generation of misexpression screen was based on the UAS-GAL4 system and random insertions of a P-element carrying a promoter with the potential to overexpress neighbor genes.

The P-transposable element inserted in the middle of a gene still worked as a loss-of-function insertion, disrupting the expression of the original gene. However if the P-element was inserted upstream of an open reading frame, the GAL4-responsive Upstream Activator Sequence enhances the transcription of the neighbour gene, resulting in lines that overexpresses their target. This concept was successfully proved originally by Rørth and later, expanded with the creation of other optimised P-elements (Staudt *et al.*, 2005), building an important collection of misexpression stocks. These collections gathered a number of advantages that supported the system as an advanced screen approach: the detection of genes with phenotypes overlooked by previous screens (crucial point considering that two thirds of *Drosophila* genes do not posses a clear loss of function phenotypes), the tissue and temperature specific overexpression controlled by the UAS-GAL4 system, and the modular idea of the technique, which encouraged constant expansion of the system.

4.4 DVAP-P58S expression in the eye at 30ºC favours the finding of suppressor lines

Temperature and tissue specific expression, parameters relevant in the UAS-GAL4 system, were tested in the optimisation presented in our previous chapter. Temperature increase enhances the GAL4 transactivator activity in the target tissue and thus, increases the expression of the transgene under the control of the UAS-GAL4 binding sequences (Duffy, 2002).

We observed a spectrum of phenotypes over 25ºC, but we decided to express the target genes at 30ºC, which constitutes a strong phenotype. The reason for selecting this temperature was that in this condition a more severe neurodegenerative phenotype is observed in the eye. This phenotype is characterized by disorganised ommatidia, loss and supernumerary bristles and a significant reduction in size (Forrest *et al.*, 2013). This phenotype allowed us an easy and quick readout, relevant decision for a large scale screen considering resources and time scales.

This strong phenotype sets a threshold where the probability to find modifiers that suppress this neurodegeneration is higher than the ones that enhance it even more. This selection is desirable because, even although all modifiers are potentially useful, suppression of the phenotype can give us stronger clues for possible mitigation of ALS pathology. On the other hand, we consider that a possible enhancer line will show a narrower modification effect compared to the suppressors, basically because the eye in our model is already severely damaged. To address this problem we plan to double check potential enhancer lines repeating the cross at 28ºC, a lower temperature where the eye size of the model is less affected and a potential enhancer line will show a bigger difference than at 30ºC. Additionally, another parameter was observed and consequently considered as a complement of the eye structure readout. Eyeless-GAL4 driver shows a leaky expression outside the eye (Callaerts *et al.*, 2001). This may translate into a toxic effect in the rest of the nervous system and leads to a decrease in viability of crosses carrying the *DVAP-P58S* allele. The viability ratio of *ey-GAL4,DVAP-P58S/+* is lower than 1.0, but in

crosses with potential enhancers this ratio was even less, in addition to a smaller eye size. Reduction in eye size observed altogether with a decrease in viability gave us a stronger indication of a potential enhancement of the DVAP-P58S toxicity. With these parameters we expect to cover in a fast way, both directions of toxicity modification in flies expressing DVAP-P58S in the eye.

4.5 Potential misexpression insertion stocks tested in the genetic screen

The important amount of research and collaborative efforts achieved with *Drosophila* explain another central advantage of this model: the high number of stocks and genetic tools available for the community. Beside the already mentioned RNAi lines and deletion stock collections, an important number of P-element lines are publicly available in *Drosophila* stock centers. Bloomington *Drosophila* Stock Center at Indiana University is the largest one, offering different services, genetic tools and stocks. Their Potential Misexpression collection, comprising 5340 lines (34% of the *Drosophila* genome) include different lines carrying a P-element that potentially can overexpress or down-regulate a specific gene. Throughout the years, this list has been curated to remove redundant lines and characterised to add relevant information, such as genes affected, exact genetic location of the insertion and references associated. This information, available in FlyBase (Drysdale & FlyBase consortium, 2008), will be key in this study to filter and select the best lines that potentially can overexpress a specific target.

The Potential Misexpression collection comprises six groups of stocks carrying a different transgene each. The consortium in charge of the Gene disruption project, led by the Rubin, Bellen and Spradling groups, has mostly constructed these collections in the last two decades (Bellen *et al.*, 2004). These collections, illustrated in Figure 11, differ in structure and final phenotype observed. Three of them (P{EP}, P{EPgy2} and P{Mae-UAS.6.11}) carry an independent promoter next to the UAS sequence in the construct. The promoter increases the chances of a potential overexpression if they are inserted in the same orientation upstream the target gene

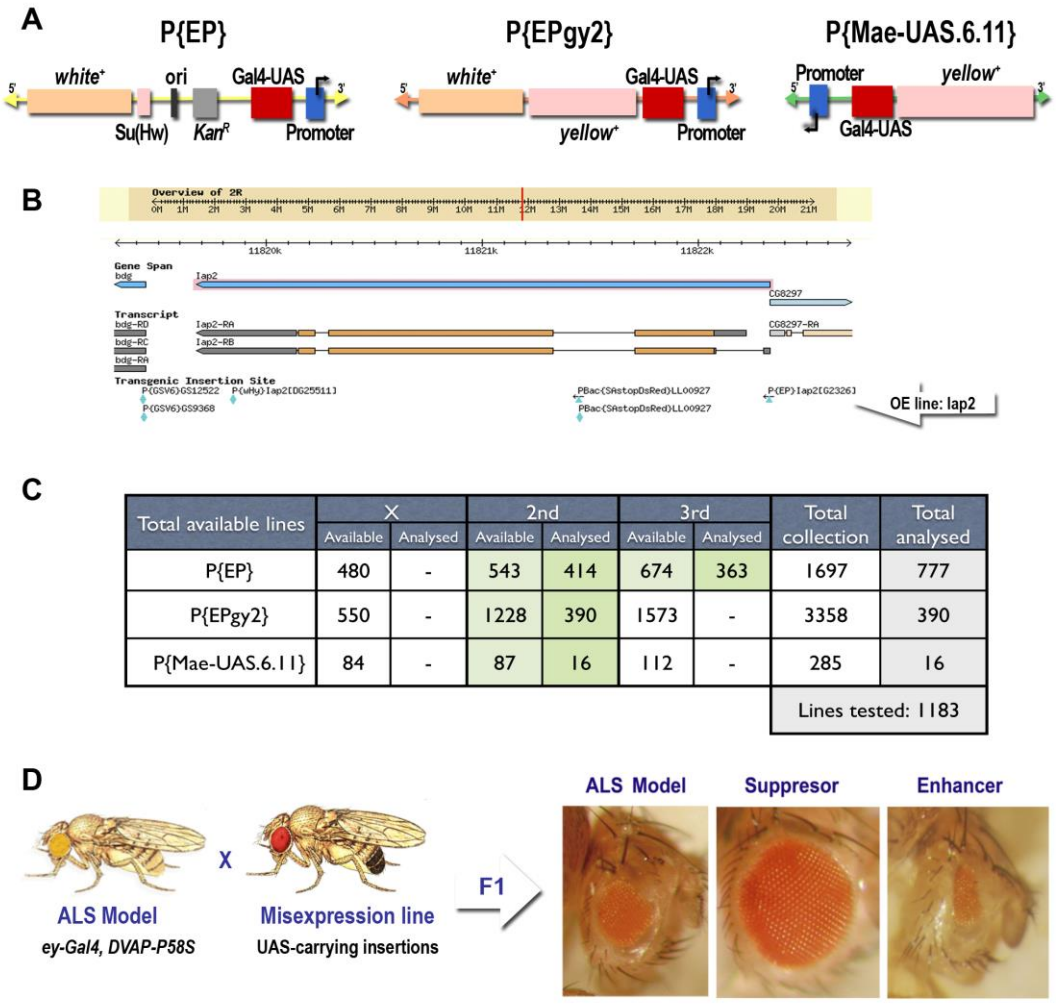

Total available lines	X		2nd		3rd		Total collection	Total analysed
	Available	Analysed	Available	Analysed	Available	Analysed		
P{EP}	480	-	543	414	674	363	1697	777
P{EPgy2}	550	-	1228	390	1573	-	3358	390
P{Mae-UAS.6.11}	84	-	87	16	112	-	285	16
							Lines tested: 1183	

Figure 11. *Drosophila* misexpression stocks used in this study. (**A**) Schemes of the three stock collections available in Bloomington *Drosophila* Stock Center used in this study. All of them carry a GAL4-binding UAS site (red) and a promoter (blue) to start the transcription of neighbour genes. (**B**) Genomic map of the region where is inserted the line DIAP2^{G2326}. The element insertion (blue triangle), in a correct direction and location at the regulatory region of the gene, ensures an increased transcription of the target gene. (**C**) Stocks used in this study. In green are highlighted the collections used, from the second and third chromosome. Available lines not included in the analysed category include lines with a potential loss-of-function effect and redundant lines already tested. A total of 1183 lines were screened. (**D**) General scheme of the genetic screen. Female virgins expressing DVAP-P58S in the eye were crossed with males from the misexpression collection and their offspring can present either no effect in the ALS model phenotype or a modification to the phenotype suppressing or enhancing the DVAP-P58S-linked neurodegeneration.

(Figure 11A). The constructs can start the transcription of a neighbour gene if they are inserted in the correct orientation within 2kb upstream of a transcription unit (Figure 11B) (Bellen *et al.*, 2004). These parameters were used to filter the original collection and discard lines that were less likely to overexpress the target gene.

Stocks not considered included lines with insertion in the middle or the 3' end of a gene, stocks in which the direction of transcription of the transgenic promoter was in the opposite direction than the orientation of the target gene, and stocks inserted in a genomic region without close neighbour genes. In addition, when more than one stock was available to target one gene, the best located insertion according to the previous parameters was selected for analysis.

As a long-term project, in our group we believe that the best way to understand completely DVAP mechanisms and toxicity is to screen the whole genome and analyse all the possible available overexpression stocks. In this study, we presented the first step to this aim, with the analysis of 1183 potential overexpression lines available in BDSC (Figure 11C). These lines include all the available lines inserted in the second chromosome, curated to test potential overexpression stocks from the previously mentioned three collections. Additionally, we tested all the potential overexpression stocks from the P{EP}collection in the third chromosome, an extra set of 363 lines.

These stocks were carefully tested and repeated three times when results showed either significant or inconclusive modification. In this way, the first stage of the screen consisted of a cross of female virgins *ey-Gal4,DVAP-P58S* with males of misexpression stocks received from BDSC, to analyse the offspring and quantify their eye size in order to select modifiers (Figure 11D). This stage, the most time-consuming part of the study, included an estimated amount of over 1500 crosses, before the next steps of validations and further characterisation discussed later. A flow chart detaling this stage and posterior experiments performed to reach a final group of high-confidence modifiers is displayed in the Figure 12.

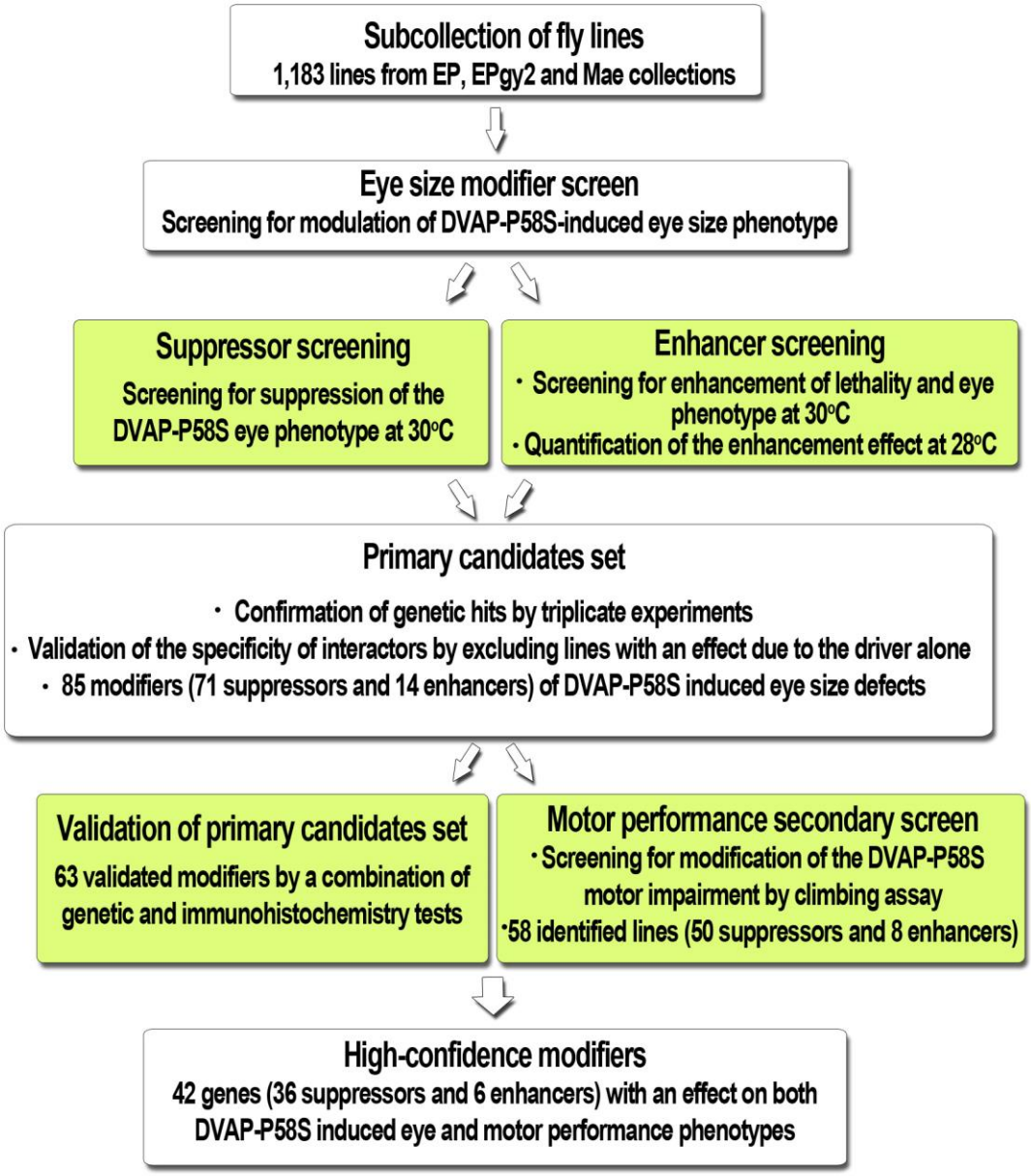

Figure 12. Flow chart of the genetic screen. Flow chart illustrating pipeline of DVAP-P58S-modifiers identification. Starting from an initial set of 1183 misexpression collection, we obtained a set of 42 high confidence modifiers of DVAP-P58S linked neurodegeneration.

4.6 Ninety seven lines were identified as modifiers of DVAP-P58S-induced neurodegeneration in the eye

In order to carry out the screen, the methodology was highly coordinated. A constant collection of *ey-GAL4,DVAP-P58S* female virgins allowed to perform up to 50 crosses per week. 10-12 female virgins were crossed to 8-10 males from each misexpression line and were left at room temperature for 48 hours before transferring the vials to a 30ºC water bath. A duplicate vial was used to increase the offspring number and reduce the chance of failed crosses. Offspring was then collected and analysed under the microscope to look for phenotypic differences between each cross and the respective control. Pictures of female flies were taken to quantify the average eye area surface of each cross using ImageJ. Crosses without a clear change in eye size were also captured but not quantified. Crosses with potential modification effect were confirmed through this quantitative analysis and the stock was crossed again two more times to confirm the phenotype and then kept for further studies. Stocks that failed to modify the phenotype were discarded. Throughout this process, the stocks were treated blindly and identified only by their stock number and not by their gene name, to avoid introducing any bias in data processing.

Lines with suppressor modifier effect (reduced DVAP-P58S-linked neurodegeneration in the eye with an increase in its area, from now on "Suppressors") were detected and later confirmed through quantification (Figure 13). For lines with an enhancement effect (lines that increased DVAP-P58S toxicity reducing even more the eye size, from now on "Enhancers") the detection was less straightforward, as previously discussed, with an already small, damaged eye in the tester line (*ey,DVAP-P58S*). Therefore, we selected lines that enhanced the degeneration in the eye and the lethality linked to DVAP-P58S, and these stocks were kept for further tests and crosses repetition at 28ºC.

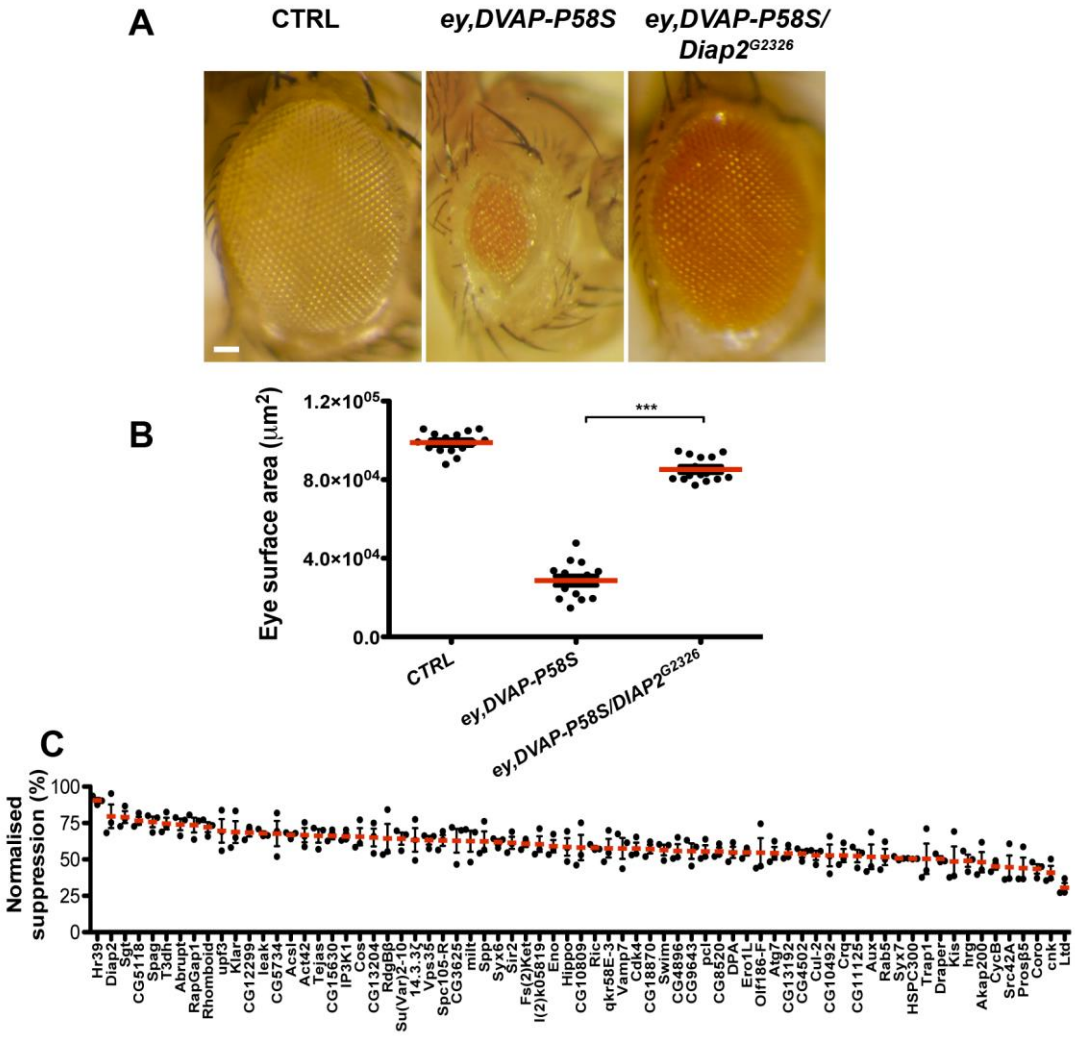

Figure 13. Genetic suppressors of DVAP-linked neurodegeneration in the eye. (**A**) Stereo microscope images of control (*ey-Gal4/+*), *ey,DVAP-P58S (ey-GAL4,DVAP-P58S/+*) *and ey,DVAP-P58S/DIAP*^{G2326} *(ey-GAL4,DVAP-P58S/ DIAP*^{G2326}) adult fly eyes. Scale bar = 50 um. (**B**) Quantification of the eye surface area of adults flies. The population average size (red line) in the co-expression of *DVAP-P58S* and the representative suppressor EP line is drastically increased ($P<0.001$, One-way ANOVA) to levels closer to wild type, suppressing the degenerative phenotype of the tester line. (**C**) List of suppressor misexpression lines detected in the screen. Each point represents the average surface area from one experiment, normalised to the size of its control *ey,DVAP-P58S* eye. Average of three independent experiments is displayed as a red line. Significant suppression of DVAP-P58S neurodegeneration was observed in 71 misexpression lines.

After the analysis of almost 1200 lines, we obtained 97 lines with a potential modification effect. With these candidate modifiers we started an exhaustive validation round of assays (detailed in the next section) to discard additional false positive lines. These analyses include a more specific test for enhancer lines, genetic controls of P-element insertions and phenotypic analysis of the modifier lines without the DVAP-P58S expression. After these validation assays, we completed a final list with 85 confirmed modifiers. In the Tables 5 and 6 are reported the complete lists of validated modifiers together with the average percentage of modification, name of the allele used and molecular activities associated, according to the PANTHER classification system (Mi *et al.*, 2013). Table 7 describes the modification effect of each independent experiment, and the statistical difference compared to their controls. Also, variation between the three replicas was analysed using a one sample t-test, comparing their average to the hypothetical value of modification (no modification effect, value = 0). The average of all the independent triplicates was significantly different than the hypothetical value. This list of 71 suppressors and 14 enhancers indicates a successful approach in the search of DVAP-P58S-modifier genes and it will be the core of the next steps of this study.

Gene Name - Suppressors	Gene Symbol	Modifying allele	Stock ID	% Sup	Protein class	Biological process	Cellular component
Hormone receptor-like in 39	Hr39	P{EPgy2}Hr39^{EY04579}	20152	90.55	Hormone receptor	regulation of transcription, DNA-dependent female meiosis chromosome segregation ecdysone-mediated induction of cell autophagic cell death activation of cysteine-type endopeptidase activity involved in apoptotic process spermathecum morphogenesis regulation of gene silencing steroid hormone mediated signaling pathway regulation of transcription, DNA-dependent male courtship behavior, veined wing generated song production	nucleus
Inhibitor of apoptosis 2	Iap2	P{EP}Iap2^{G2326}	26986	79.62	Protease inhibitor	sensory organ development defense response to Gram-negative bacterium endopeptidase activity involved in apoptotic process negative regulation of apoptotic process peptidoglycan recognition protein signaling pathway positive regulation of protein import into nucleus	-
Small glutamine-rich Tetratricopeptide containing protein	Sgt	P{EPgy2}^{EY02712}	15587	79.12	Chaperone	neuromuscular synaptic transmission	-
CG5118	CG5118	P{EPgy2} CG5118^{EY18569}	16541	76.58	-	-	-
Spaghetti	Spag	P{EPgy2}spag^{EY11196}	20274	75.79	Chaperone	cell proliferation imaginal disc growth imaginal disc development imaginal disc fusion, thorax closure	-
Type III alcohol dehydrogenase	T3dh	P{EPgy2}T3dh^{EY09338}	17559	74.65	Dehydrogenase	oxidation-reduction process	-

Abrupt	ab	P{EPgy2}ab^{EY09709}	16949	74.02	Nucleic acid binding	sensory organ development synaptic target recognition muscle attachment axon choice point recognition dendrite morphogenesis neuron development muscle organ development border follicle cell migration mushroom body development	nucleus
Rap GTPase activating protein 1	RapGAP1	P{EPgy2}^{EY01137}	15062	73.59	G-protein modulator	inter-male aggressive behavior activation of Rap GTPase activity regulation of small GTPase mediated signal transduction	germ plasm
Rhomboid	rho	P{EP}rho^{EP3704}	17276	72.15	Serine-protease	brain development learning or memory cytokinesis epidermal growth factor receptor signaling pathway salivary gland development axonogenesis behavioral response to ethanol negative regulation of gene expression stem cell fate commitment proteolysis	plasma membrane Golgi apparatus integral to membrane apical part of cell
Upf3	Upf3	P{EPgy2}Upf3^{EY03241}	16558	69.62	Nucleic acid binding	nuclear-transcribed mRNA catabolic process, nonsense-decay	-
Klarsicht	klar	P{EP}EP3104^{EP3104}	6413	68.83	Hydrolase	microtubule-based movement nuclear migration lipid particle transport along microtubule compound eye morphogenesis cellular membrane organization lipid transport organelle localization larval visceral muscle development flight locomotion	dynein complex nuclear envelope lipid particle perinuclear region cytoplasm cytoplasmic microtubule
CG12299	CG12299	P{EPgy2} CG12299^{EY01579}	15520	68.45	KRAB box transcription factor	-	-

Leak	lea	P{EP}lea^{EP2582}	17071	67.86	Receptor	axon guidance ventral cord development tracheal outgrowth, open tracheal system neuron migration positive regulation of cell-cell adhesion cardioblast cell fate specification mushroom body development central complex development gonad development synaptic target recognition	plasma membrane axon
CG5734	CG5734	P{EPgy2} CG5734^{EY05560}	15456	67.76	Phosphatidyl inositol binding	-	-
Acyl-CoA synthetase long-chain	Acsl	P{EPgy2}Acsl^{EY07112}	19860	66.87	Ligase	positive regulation of sequestering of triglyceride axon guidance nervous system development synaptic transmission segmentation neurogenesis long-chain fatty acid metabolic process	lipid particle cytoplasm endoplasmic reticulum
Actin 42A	Act42A	P{Epgy2} Act42A^{EY05608}	15460	66.67	Motor protein	cytoskeleton organization phagocytosis mitotic cytokinesis	actin filament microtubule associated complex
Tejas	tej	P{Epgy2}tej^{EY20088}	22361	66.19	Signal transduction	karyosome formation negative regulation of transposition	P granule
CG15630	CG15630	P{Epgy2}EY20668	22414	66.18	Cell adhesion family	-	-
Inositol 1,4,5-triphosphate kinase 1	IP3K1	P{Mae-UAS.6.11} IP3K1^{UY530}	6769	65.77	Kinase	response to oxidative stress	cytoplasm

Costa	cos	P{Epgy2}cos^{EY08735}	19759	65.64	Motor protein	ovarian follicle cell development positive regulation of hh target transcription factor activity negative regulation of transcription factor import into nucleus microtubule-based movement regulation of proteolysis smoothened signaling pathway imaginal disc-derived wing morphogenesis regulation of protein stability negative regulation of sequence-specific DNA binding transcription factor activity cytoplasmic sequestering of transcription factor	cytoplasm kinesin complex microtubule associated complex Hedgehog signaling complex plasma membrane vesicle membrane
CG13204	CG13204	P{Epgy2} CG13204^{EY11838}	21076	65.03	Nucleic acid binding	-	-
Retinal degeneration B beta	rdgBβ	P{EP}rdgBβ^{G8057}	27975	64.37	Transporter	signal transduction transport	cytoplasm
Suppressor of variegation 2-10	Su(var)2-10	P{Epgy2} Su(var)2-10^{EY01453}	19642	64.25	Ligase	chromosome condensation imaginal disc growth hemopoiesis regulation of JAK-STAT cascade regulation of protein catabolic process compound eye development chromosome organization neurogenesis mitotic G2 DNA damage checkpoint positive regulation of innate immune response	cytoplasm nuclear lamina nucleoplasm nucleus polytene chromosome
14-3-3ζ	14-3-3ζ	P{Epgy2} 14-3-3ζ^{EY06147}	19919	63.42	Chaperone	Ras protein signal transduction activation of tryptophan 5-monooxygenase activity olfactory learning chromosome segregation mitotic cell cycle, embryonic learning or memory cell proliferation protein folding compound eye photoreceptor cell differentiation thermosensory behavior	nucleus germline ring canal microtubule associated complex

Vacuolar protein sorting 35	Vps35	P{Epgy2} Vps35^{EY14200}	20913	63.20	Membrane trafficking protein	vesicle-mediated transport endocytosis retrograde transport, endosome to Golgi protein transport	endosome late endosome retromer complex
Spc105-Related	Spc105-R	P{EP}G4635	28884	63.09	-	mitotic spindle organization kinetochore assembly neurogenesis	condensed chromosome outer kinetochore
CG3625	CG3625	P{Epgy2} CG3625^{EY07089}	16406	62.88	-	-	integral to membrane
Milton	milt	P{Mae-UAS.6.11} milt^{LA00951}	22198	62.52	Mitochondrial trafficking protein	axon transport of mitochondrion mitochondrion distribution Nebenkern assembly sperm mitochondrion organization axon transport of mitochondrion	mitochondrion
Signal peptide peptidase	spp	P{EP}G2086	27455	62.40	Protease	open tracheal system development cellular response to unfolded protein signal peptide processing	endoplasmic reticulum membrane
Syntaxin 6	Syx6	P{Epgy2}Syx6^{EY14508}	20941	61.91	SNARE protein	neurotransmitter secretion vesicle-mediated transport synaptic vesicle docking involved in exocytosis Golgi vesicle transport	plasma membrane SNARE complex
Silent information regulator 2	Sir2	P{EP}Sir2^{EP2300}	24859	61.43	Acetylase	histone deacetylation chromatin silencing regulation of histone acetylation determination of adult lifespan response to nutrient regulation of apoptotic process behavioral response to ethanol regulation of transcription, DNA-dependent positive regulation of feeding behavior	cytoplasm nucleus nucleoplasm
Female sterile (2) Ketel	Fs(2)Ket	P{EPgy2} Fs(2)Ket^{EY06666}	15967	60.73	Transporter	mitosis chorion-containing eggshell formation | protein import into nucleus actin filament organization regulation of cell shape	nuclear pore cytoplasm nuclear envelope lipid particle microtubule

Lethal (2) k05819	l(2)k05819	P{EPgy2}EY03384	20150	60.55	-	-	-
Enolase	Eno	P{EPgy2}Eno^{EY23161}	22610	59.08	Enolase	glycolysis	lipid particle phosphopyruvate hydratase complex
Hippo	hpo	P{EP}hpo^{G3315}	27105	58.58	Kinase	protein phosphorylation apoptotic process cell proliferation response to ionizing radiation negative regulation of neuron apoptotic process stem cell proliferation retinal cell programmed cell death eye development organ growth negative regulation of transcription, DNA-dependent	-
CG10809	CG10809	P{EP}CG10809^{G4564}	27161	58.17	-	-	-
Ras which interacts with calmodulin	Ric	P{EP}Ric^{G2693}	27003	58.10	Small GTPase	response to oxidative stress response to starvation response to heat response to osmotic stress small GTPase mediated signal transduction GTP catabolic process	plasma membrane
Quaking related 58E-3	qkr58E-3	P{EPgy2} qkr58E-3^{EY02038}	15086	57.68	Transcription factor	apoptotic process regulation of alternative mRNA splicing, via spliceosome	nucleus nuclear speck
Vesicle-associated membrane protein 7	Vamp7	P{EP}Vamp7^{G7738}	28488	57.56	SNARE protein	intracellular protein transport autophagic vacuole maturation vesicle fusion endosome to lysosome transport autophagic vacuole fusion	plasma membrane integral to membrane late endosome membrane SNARE complex

Cyclin-dependent kinase 4	Cdk4	P{EPgy2}Cdk4^{EY09330}	19891	57.55	Kinase	protein phosphorylation cell proliferation regulation of cell growth mitochondrion organization JAK-STAT cascade blastoderm segmentation open tracheal system development regulation of cell cycle mitotic cell cycle	-
CG18870	CG18870	P{EPgy2} CG18870^{EY06926}	15981	57.14	-	-	-
Secreted Wg-interacting molecule	Swim	P{EPgy2} Swim^{EY09931}	17622	56.49	Protease	positive regulation of Wnt receptor signaling pathway immune response proteolysis	chorion extracellular space
CG4896	CG4896	P{EPgy2} CG4896^{EY01431}	19814	55.85	-	-	-
CG9643	CCG9643	P{EPgy2} CG9643^{EY07345}	16815	55.72	Methyltransferase	-	-
Polycomblike	Pcl	P{EPgy2}Pcl^{EY08457}	19876	55.49	-	transcription, DNA-templated multicellular organismal development chromatin modification neurogenesis defense response to fungus	chromosome nucleus
CG8520	CG8520	P{EPgy2} CG8520^{EY09481}	17573	55.43	Hydrolase	-	-
Disc proliferation abnormal	dpa	P{EPgy2}dpa^{EY04015}	15922	54.86	DNA helicase	DNA replication mitotic spindle organization	nucleus MCM complex
Ero1-like protein	Ero1L	P{EP}Ero1L^{G18511}	29300	54.83	Oxidoreductase	chaperone mediated protein folding requiring cofactor oxidation-reduction process	endoplasmic reticulum
Olf186-F	olf186-F	P{EPgy2} olf186-F^{EY01467}	20119	54.67	Signaling molecule	positive regulation of NFAT protein import into nucleus positive regulation of calcium ion transport nervous system development store-operated calcium entry	integral to membrane

Autophagy-specific gene 7	Atg7	P{EPgy2}Sec6^{EY10058}	17635	54.22	Transfer protein ligase	regulation of autophagy macroautophagy larval midgut cell programmed cell death determination of adult lifespan regulation of defense response to virus positive regulation of macroautophagy cellular response to starvation oogenesis	cytoplasm
CG13192	CG13192	P{EPgy2} CG13192^{EY07746}	17400	54.20	G-protein coupled receptor	-	-
Ubiquitin-conjugating enzyme E2Q-like	CG4502	P{EPgy2} CG4502^{EY07938}	17415	53.95	Ligase	-	-
Cullin-2	Cul-2	P{EPgy2}Cul-2^{EY09124}	19883	52.79	Ubiquitin-protein ligase	neurogenesis growth of a germarium-derived egg chamber regulation of synaptic growth at neuromuscular junction ubiquitin-dependent protein catabolic process	nuclear ubiquitin ubiquitin ligase complex
CG10492	CG10492	P{EPgy2} CG10492^{EY10125}	17640	52.75	-	-	-
Croquemort	crq	P{EPgy2}crq^{EY14489}	20939	52.71	Receptor	phagocytosis phagocytosis, engulfment defense response immune response autophagic cell death apoptotic process macrophage activation salivary gland cell autophagic cell death cell adhesion	plasma membrane membrane
CG11125	CG11125	P{EP}CG11125^{G18969}	26951	52.37	-	-	-
Auxillin	Aux	P{EP}aux^{G6787}	30174	51.85	Transcription factor	protein phosphorylation synaptic vesicle uncoating Notch signaling pathway compound eye morphogenesis sperm individualization protein phosphorylation	Golgi stack

Rab5	Rab5	P{EPgy2}Rab5^{EY10619}	20193	51.73	Membrane trafficking regulatory protein	chromatin organization mitosis endocytosis negative regulation of cell proliferation endosomal vesicle fusion axonogenesis protein transport Rab protein signal transduction vesicle-mediated transport Notch receptor processing	early endosome lipid particle synapse neuronal cell body vesicle
Syntaxin 7	Syx7	P{EP}Syx7^{G6457}	28476	50.75	SNARE protein	neurotransmitter secretion vesicle-mediated transport synaptic vesicle docking involved in exocytosis negative regulation of cell proliferation positive regulation of endocytosis endosomal vesicle fusion pupariation multicellular organism growth plasma membrane to endosome transport vesicle fusion	early endosome plasma membrane SNARE complex
Syntaxin Interacting Protein 1	HSPC300	P{EP}HSPC300^{G19021}	26953	50.54	-	regulation of cell shape central nervous system morphogenesis regulation of synaptic growth at neuromuscular junction positive regulation of filopodium assembly positive regulation of lamellipodium assembly	-
Trap1	Trap1	P{EPgy2} Trap1^{EY10238}	19974	50.43	Chaperone	protein folding response to oxidative stress	lipid particle mitochondrion
Draper	drpr	P{EP}drpr^{EP522}	17175	50.41	Receptor/signaling molecule	cell adhesion larval locomotory behavior phagocytosis cell competition in a multicellular organism apoptotic cell clearance salivary gland cell autophagic cell death neuron remodeling wing disc dorsal/ventral pattern formation defense response to bacterium engulfment of apoptotic cell	intrinsic to membrane

Kismet	kis	P{EPgy2}kis^{EY12846}	21391	49.16	DNA helicase	determination of adult lifespan segment specification antimicrobial humoral response axon guidance positive regulation of organ growth negative regulation of transcription, DNA-dependent short-term memory locomotion neuron remodeling peroxisome organization	nucleus microtubule associated complex
Hiiragi	hrg	P{EPgy2}hrg^{EY10340}	17668	49.15	Adenylyltransferase	mRNA polyadenylation	nucleus
A kinase anchor protein 200	Akap200	P{EP}Akap200^{EP2254}	17037	48.14	Kinase	protein localization negative regulation of Ras protein signal transduction autophagic cell death salivary gland cell autophagic cell death behavioral response to ethanol regulation of establishment of planar polarity	lipid particle
Cyclin B	CycB	P{EPgy2}CycB^{EY08217}	19870	45.23	Kinase activator	cytokinesis mitotic chromosome movement towards spindle pole mitotic cytokinesis attachment of spindle microtubules to kinetochore embryonic development via the syncytial blastoderm G2/M transition of mitotic cell cycle cellular process response to DNA damage stimulus regulation of chromatin binding regulation of cyclin-dependent serine/threonine kinase activity	pole plasm chromosome cytoplasm spindle nuclear cyclin-dependent protein kinase holoenzyme complex spindle midzone nucleus
Src oncogene at 42A	Src42A	P{EPgy2} Src42A^{EY08937}	19763	44.66	Transmembrane receptor	tricarboxylic acid cycle protein phosphorylation transmembrane receptor protein tyrosine kinase signaling pathway JNK cascade multicellular organismal development axon guidance open tracheal system development regulation of cell proliferation apoptotic cell clearance innate immune response	cytoplasm plasma membrane adherens junction

Proteasome subunit beta 5	Prosβ5	P{EPgy2}EY00934	14870	43.98	Proteasome	centrosome organization mitotic spindle organization mitotic spindle elongation cell proliferation neurogenesis proteolysis involved in cellular protein catabolic process proteasomal ubiquitin-dependent protein catabolic process	proteasome core complex
Coronin	coro	P{EP}coro^{GE15547}	26894	43.51	Non-motor actin binding	defense response to fungus actin cytoskeleton organization adult somatic muscle development	actin cytoskeleton mitotic spindle
Connector enhancer of ksr	cnk	P{EPgy2}cnk^{EY06675}	20160	40.89	Kinase modulator	signal transduction Ras protein signal transduction compound eye photoreceptor cell differentiation imaginal disc-derived wing morphogenesis anterior/posterior axis specification, embryo torso signaling pathway tracheal outgrowth, open tracheal system imaginal disc-derived wing vein morphogenesis	apical part of cell cytoplasm plasma membrane cell-cell adherens junction
Lightoid	ltd	P{EPgy2}ltd^{EY07166}	20166	30.51	GTPase activity	ommochrome biosynthetic process learning or memory olfactory learning eye pigment precursor transport protein transport Rab protein signal transduction vesicle-mediated transport compound eye pigmentation regulation of lipid storage regulation of autophagy	synapse recycling endosome vesicle lysosome autophagic vacuole

Table 5. List of suppressors of DVAP-P58S-associated toxicity in the eye. For each modifier gene found in the screen, the average modification effect is displayed after three independent experiments, performed at 30ºC. Statistical analysis of each experiment is detailed in Table 7. *Stock ID* represents the Bloomington *Drosophila* stock center annotation for the line carrying the specific *Allele*. *Protein class* was obtained from the classification database PANTHER. *Biological process* and *Cellular component* GO terms were obtained from FlyBase.

Gene Name - Enhancers	Gene Symbol	Modifying allele	Stock ID	%Enhance		Protein class	Biological process	Cellular component
				Eye	Let			
Scabrous	sca	P{EPgy2}EY00639	20095	57.14	41.18	Signaling molecule	chaeta morphogenesis nervous system development female meiosis chromosome segregation ommatidial rotation nervous system development lateral inhibition regulation of R8 cell spacing in compound eye compound eye development imaginal disc-derived wing margin morphogenesis response to alcohol	fibrinogen complex extracellular region
Myocyte-specific enhancer factor 2	Mef2	P{EP}Mef2^{EP2002a}	17230	40.80	58.77	Transcription factor	transcription from RNA polymerase II promoter mesoderm development regulation of transcription, DNA-dependent heart development muscle fiber development myoblast fusion locomotor rhythm antimicrobial humoral response lipid storage carbohydrate storage	nucleus
Peroxisome biogenesis factor 10	Pex10	P{EP}Pex10^{G5094}	27176	24.59	53.24	Transporter	peroxisome organization spermatid development primary spermatocyte growth male meiosis cytokinesis spermatocyte division protein import into peroxisome matrix protein import into peroxisome membrane very long-chain fatty acid catabolic process peroxisome organization	integral to peroxisomal membrane peroxisome
Smooth	sm	P{EPgy2}sm^{EY07191}	19727	23.01	20.30	Splicing factor	adult feeding behavior axon guidance determination of adult lifespan	ribonucleoprotein complex
CG9153	CG9153	P{EP}CG9153^{G5486}	27181	22.60	47.63	Ubiquitin-protein ligase	protein ubiquitination involved in ubiquitin-dependent protein catabolic process	cytoplasm nucleus

Mitochondrial carrier homolog 1	Mtch	P{EP}Mtch^{G8642}	27981	20.49	46.35	Mitochondrial carrier protein	-	mitochondrion
CG7324	CG7324	P{EP}CG7324^{G8800}	27480	20.07	60.05	Hydrolase	regulation of Rab GTPase activity	-
Malate dehydrogenase	Mdh1	P{EPgy2} Mdh1^{EY08761}	16435	18.04	29.28	Dehydrogenase	lateral inhibition cellular carbohydrate metabolic process malate metabolic process	cytoplasm lipid particle cytosol peroxisome
Longitudinals lacking	lola	P{EPgy2} lola^{EY10040}	27480	17.37	40.28	Nucleic acid binding	axon guidance antimicrobial humoral response brain morphogenesis startle response locomotion involved in locomotory behavior inter-male aggressive behavior nurse cell apoptotic process regulation of transcription, DNA-dependent neurogenesis gonad development	nucleus
Dynamin associated protein 160	Dap160	P{EP}Dap160^{EP2543}	19582	14.70	28.93	Membrane trafficking protein	protein localization synaptic growth at neuromuscular junction synaptic vesicle endocytosis positive regulation of protein kinase activity positive regulation of neuroblast proliferation negative regulation of Notch signaling pathway	presynaptic membrane cytoplasm apical cortex plasma membrane synaptic vesicle
Alanyl-tRNA synthetase	Aats-ala	P{EP}Aats-ala^{G3500}	27111	13.45	41.18	RNA binding protein	alanyl-tRNA aminoacylation	cytoplasm
Dreadlocks	dock	P{EPgy2}EY08327	19871	12.87	24.47	Signaling molecule	axon guidance insulin receptor signaling pathway axonogenesis regulation of insulin receptor signaling pathway myoblast fusion	cytoplasm
CG30456	CG30456	P{EP}EP2185	17237	12.25	52.06	Signaling molecule	imaginal disc-derived leg morphogenesis positive regulation of Rho protein signal transduction	-
Calcium-binding protein 1	CaBP1	P{EPgy2} CaBP1^{EY12345}	20346	11.06	34.99	Isomerase	cell redox homeostasis glycerol ether metabolic process positive regulation of apoptotic cell clearance	lipid particle endoplasmic reticulum

Table 6. List of enhancers of DVAP-P58S-associated toxicity in the eye. For each modifier gene found in the screen, the average modification effect is displayed after three independent experiments, performed at 28ºC. Statistical analysis of each experiment is detailed in Table 7. In addition, lethality changes were measured in triplicate for these enhancers. *Stock ID* represents the Bloomington *Drosophila* stock center annotation for the line carrying the specific *Allele*. *Protein class* was obtained from the classification database PANTHER. *Biological process* and *Cellular component* GO terms were obtained from FlyBas

Suppressors	R1	P	S	R2	P	S	R3	P	S	OST (P)
Hr39	87.67	< 0.0001	***	93.61	< 0.0001	***	90.38	< 0.0001	***	0.0004
Diap2	75.25	< 0.0001	***	68.31	< 0.0001	***	95.31	< 0.0001	***	0.0102
Sgt	86.72	< 0.0001	***	72.72	< 0.0001	***	77.91	< 0.0001	***	0.0027
CG5118	81.93	< 0.0001	***	72.69	< 0.0001	***	75.13	< 0.0001	***	0.0013
Spag	80.11	< 0.0001	***	78.72	< 0.0001	***	68.53	< 0.0001	***	0.0023
T3dh	82.51	< 0.0001	***	72.53	< 0.0001	***	68.91	< 0.0001	***	0.003
Abrupt	78.84	< 0.0001	***	77.05	< 0.0001	***	66.16	< 0.0001	***	0.0029
RapGap1	63.79	< 0.0001	***	80.56	< 0.0001	***	76.41	< 0.0001	***	0.0047
Rhomboid	65.83	< 0.0001	***	77.21	< 0.0001	***	73.4	< 0.0001	***	0.0021
CG3625	72.06	< 0.0001	***	70.01	< 0.0001	***	46.57	0.0006	***	0.0165
CG12299	63.52	< 0.0001	***	72.25	< 0.0001	***	69.59	< 0.0001	***	0.0014
upf3	69.02	< 0.0001	***	83.9	< 0.0001	***	55.95	< 0.0001	***	0.0132
Klar	65.04	< 0.0001	***	58.16	< 0.0001	***	83.28	< 0.0001	***	0.0117
leak	66.19	< 0.0001	***	70.88	< 0.0001	***	66.5	< 0.0001	***	0.0005
CG5734	81.92	< 0.0001	***	69.42	< 0.0001	***	51.93	< 0.0001	***	0.0161
Acsl	64.2	< 0.0001	***	68.41	< 0.0001	***	67.99	< 0.0001	***	0.0004
Act42	65.86	< 0.0001	***	75.41	< 0.0001	***	58.75	< 0.0001	***	0.0052
Tejas	71.52	< 0.0001	***	70.11	< 0.0001	***	56.95	< 0.0001	***	0.0049
IP3K1	63.82	< 0.0001	***	63.15	< 0.0001	***	70.34	< 0.0001	***	0.0012
Cos	77.29	< 0.0001	***	58.43	< 0.0001	***	61.19	< 0.0001	***	0.0079
CG13204	66.01	< 0.0001	***	75	< 0.0001	***	54.09	< 0.0001	***	0.0086
RdgBβ	55.49	0.0001	***	84.3	< 0.0001	***	53.32	< 0.0001	***	0.0232
Su(Var)2-10	67.01	< 0.0001	***	69.7	< 0.0001	***	56.03	< 0.0001	***	0.0042
14.3.3ζ	77.46	< 0.0001	***	49.41	< 0.0001	***	63.4	< 0.0001	***	0.0159
Vps35	66.33	< 0.0001	***	65.89	< 0.0001	***	57.39	< 0.0001	***	0.0021
CG15630	70.37	< 0.0001	***	62.65	< 0.0001	***	65.51	< 0.0001	***	0.0012
Spp	56.64	< 0.0001	***	54.32	0.0005	***	76.23	< 0.0001	***	0.0122
milt	68.72	< 0.0001	***	48.24	< 0.0001	***	70.6	< 0.0001	***	0.0129
Syx6	63.58	< 0.0001	***	57.88	< 0.0001	***	64.28	< 0.0001	***	0.0011
Sir2	69.02	< 0.0001	***	60.61	0.0002	***	54.67	< 0.0001	***	0.0046
CG1599	43.61	0.0002	***	61.56	< 0.0001	***	67.52	0.0002	***	0.0152
Fs(2)Ket	56.75	< 0.0001	***	64.07	< 0.0001	***	61.36	< 0.0001	***	0.0012
l(2)k05819	57.01	< 0.0001	***	53.57	< 0.0001	***	71.08	< 0.0001	***	0.0077

Hippo	48.52	< 0.0001	***	69.34	< 0.0001	***	57.89	0.0002	***	0.0104
CG10809	53.15	< 0.0001	***	75.2	< 0.0001	***	46.16	< 0.0001	***	0.0219
Ric	56.72	< 0.0001	***	60.42	< 0.0001	***	57.17	< 0.0001	***	0.0004
Spc105R	69.28	< 0.0001	***	63.50	< 0.0001	***	56.46	< 0.0001	***	0.0034
qkr58E-3	54.56	0.0001	***	70.01	< 0.0001	***	48.48	< 0.0001	***	0.0121
Cdk4	65.42	< 0.0001	***	54.06	< 0.0001	***	53.17	< 0.0001	***	0.0047
CG18870	62.22	< 0.0001	***	57.29	0.0001	***	51.91	< 0.0001	***	0.0027
Swim	49.22	< 0.0001	***	60.38	< 0.0001	***	59.86	< 0.0001	***	0.0041
CG9643	58.52	< 0.0001	***	63.18	< 0.0001	***	45.47	0.0008	***	0.0089
CG4896	51.75	< 0.0001	***	65.17	< 0.0001	***	50.62	< 0.0001	***	0.0069
Pcl	63.84	< 0.0001	***	50.61	< 0.0001	***	52.02	< 0.0001	***	0.0057
CG8520	60.83	< 0.0001	***	52.12	< 0.0001	***	53.35	< 0.0001	***	0.0024
hrg	55.89	< 0.0001	***	49.97	< 0.0001	***	41.59	< 0.0001	***	0.007
DPA	54.51	< 0.0001	***	48.4	< 0.0001	***	61.67	< 0.0001	***	0.0049
Ero1L	57.88	< 0.0001	***	50.66	< 0.0001	***	55.95	< 0.0001	***	0.0015
Olf186-F	74.52	< 0.0001	***	45.42	< 0.0001	***	44.07	< 0.0001	***	0.0315
Atg7	62.61	< 0.0001	***	48.42	< 0.0001	***	51.64	< 0.0001	***	0.0062
CG13192	50.84	< 0.0001	***	59.91	< 0.0001	***	51.85	< 0.0001	***	0.0028
CG4502	55.84	< 0.0001	***	57.35	< 0.0001	***	48.65	< 0.0001	***	0.0025
Cul-2	55.71	< 0.0001	***	46.38	< 0.0001	***	56.29	< 0.0001	***	0.0037
CG10492	40.12	0.0015	**	52.15	< 0.0001	***	65.99	< 0.0001	***	0.0195
Crq	61.47	< 0.0001	***	50.21	< 0.0001	***	46.44	0.0005	***	0.0073
CG11125	58.51	< 0.0001	***	44.11	< 0.0001	***	54.5	< 0.0001	***	0.0066
Aux	68.63	< 0.0001	***	45.26	< 0.0001	***	41.66	0.0014	**	0.0256
Rab5	50.01	< 0.0001	***	62.15	< 0.0001	***	43.03	< 0.0001	***	0.0115
Akap200	61.81	< 0.0001	***	42.95	< 0.0001	***	39.67	< 0.0001	***	0.0199
Syx7	50.61	< 0.0001	***	52.07	< 0.0001	***	49.57	< 0.0001	***	0.0002
HSPC300	50.8	< 0.0001	***	50.51	< 0.0001	***	50.32	< 0.0001	***	< 0.0001
Trap1	71.12	< 0.0001	***	42.51	0.0117	*	37.65	0.0005	***	0.0403
Draper	48.36	0.0010	**	49.01	0.0002	***	53.87	< 0.0001	***	0.0012
Kis	69.23	< 0.0001	***	38.76	0.0418	*	37.63	0.0001	***	0.0395
Eno	56.46	< 0.0001	***	67.36	< 0.0001	***	53.41	< 0.0001	***	0.0051
CycB	49.21	< 0.0001	***	41.61	< 0.0001	***	44.86	< 0.0001	***	0.0024
Src42A	60.79	< 0.0001	***	36.93	0.0007	***	36.25	< 0.0001	***	0.0311
Prosβ5	36.62	0.0052	**	58.68	< 0.0001	***	36.64	0.0003	***	0.0268

Coro	48.22	0.0002	***	45.08	0.0019	**	37.22	0.0055	**	0.0056
cnk	50.24	< 0.0001	***	36.98	< 0.0001	***	35.46	0.0003	***	0.0129
Ltd	27.17	0.0002	***	36.95	< 0.0001	***	27.41	0.0008	***	0.011

Enhancers	R1	P	S	R2	P	S	R3	P	S	OST (P)
Pex10	22.15	< 0.0001	***	31.44	0.0002	***	20.17	0.0001	***	0.0194
Dap160	11.63	0.0224	*	12.28	0.0005	***	20.21	< 0.0001	***	0.0334
Mef2	23.74	< 0.0001	***	56.03	< 0.0001	***	42.63	< 0.0001	***	0.0489
9153	29.32	0.0018	**	19.16	0.0001	***	19.33	< 0.0001	***	0.0214
30456	14.97	< 0.0001	***	10.29	0.0171	*	11.5	0.0002	***	0.0128
Mtch	16.62	0.0005	***	29.75	< 0.0001	***	15.11	0.0075	**	0.0478
Dock	14.52	< 0.0001	***	12.05	0.0005	***	12.04	0.0314	*	0.0041
sca	65.83	< 0.0001	***	50.45	< 0.0001	***	55.15	< 0.0001	***	0.0039
Sm	27.08	< 0.0001	***	32.04	< 0.0001	***	10.18	0.0037	**	0.0402
7324	20.95	< 0.0001	***	16.75	0.0009	***	22.51	0.0003	***	0.0011
Mdh1	23.24	0.0079	**	17.39	0.0002	***	13.5	0.0035	**	0.0073
CaBP1	9.62	0.0028	**	11.26	0.002	**	12.31	0.0314	*	0.0439
lola	24.49	0.0051	**	16.11	0.0003	***	11.52	0.0026	**	0.0296
Aat-Ala	10.17	0.004	**	12.63	0.002	**	17.55	0.0453	*	0.011

Table 7. Statistical analysis of the modifying effect of DVAP-P58S interacting genes. Independent experiments were quantified and compared to their control using a two-tailed student t-test. All replicas for the 85 modifiers were significantly different than observed control values. This difference is stronger for the case of the suppressor lines. In the case of enhancer lines, modification results were also supported with a decrease in the viability of these lines. R1,R2,R3 = Replica 1, 2 and 3. P = P-value for the Student t-test. S represents the significance level of each test. OST (P) = P-value for the one-sample t-test. *** P <0.001, **P <0.01, *P <0.05.

4.7 Genetic validations of the DVAP-P58S-neurodegeneration modifier lines

4.7.1 Enhancer lines were confirmed at a lower temperature

As previously discussed, selection of experimental temperature at 30ºC improves the search of suppressors but affected the detection of enhancers. UAS-GAL4 system has been a key genetic tool in *Drosophila* studies especially for its flexibility in modulating the expression of a transgene of interest. We characterised in the previous chapter a less dramatic eye phenotype when mutant DVAP allele was expressed at 28ºC. Therefore, we used this difference to confirm the enhancer effect of selected stocks. We repeated the crosses at this lower temperature and quantified the significant reduction of eye surface area.

Originally, 26 lines were selected as potential enhancers at 30ºC, after a decrease in the eye size and a reduction of the expected number of eclosed flies. Most lines (19 stocks) maintained this modification even at 28 ºC (Figure 14A), At this lower temperature, the crosses were performed in triplicate and consequently, the eye size and viability was quantified (Figure 14C). Seven lines (stocks with insertions in genes *egl*, *alc, lilli, Capu, CG9318, gbb* and *cdc14*) were discarded after this step because their phenotype was not significantly different than controls. The confirmed positive modifiers were now tested for the next set of validations assays, altogether with the suppressor lines.

4.7.2 Identication of false positive modifying effects after exhibiting neurodegeneration independently of *DVAP-P58S* expression

Expression of DVAP-P58S in the eye has been already linked to neurodegeneration (Forrest *et al.*, 2013) and our search for modifiers in this screen is based on the genetic interaction that other genes may present with DVAP. Changes in eye size observed in crosses with lines overexpressing a specific target gene are an indication

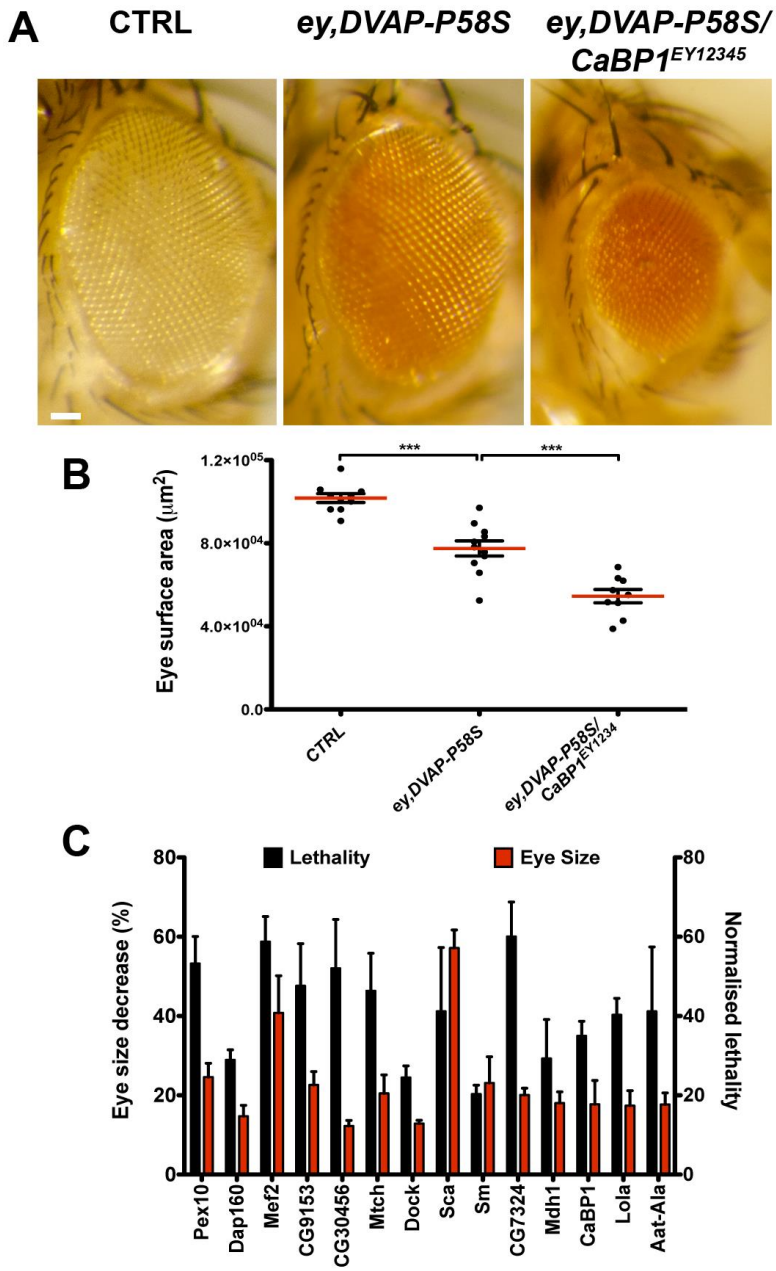

Figure 14. Genetic enhancers of DVAP-linked neurodegeneration in the eye. (**A**) Stereo microscope images of control (*ey-Gal4/+*), *ey,DVAP-P58S (ey-GAL4,DVAP-P58S/+*) *and ey,DVAP-P58S/CaBP1*^{EY12345} *(ey-GAL4,DVAP-P58S/ CaBP1*^{EY12345}) adult fly eyes. Scale bar = 50 um. (**B**) Quantification of the eye surface area of adult flies expressing the previous alleles. Co-expression of *DVAP-P58S* and the P-element insertion in the eye reduced even more the population average size (red line), enhancing the degenerative phenotype of the ALS model. (**C**) List of enhancers found in the primary screen, showing reduction in eye size (red) and viability (black) normalised to their control (*ey-Gal4,DVAP-P58S/+*). The plot represents the average of three independent experiments performed at 28ºC. Increase in DVAP-P58S- linked neurodegeneration and viability was found in 14 misexpression lines. Scale Bar = 50 um. *** P < 0.001 (One-way ANOVA).

that DVAP toxicity mechanism is affected by this overexpressed gene. However we must consider the option that the new gene may have an effect in the eye by its own, meaning that overexpression of this gene can increase or reduce the eye size, independently of DVAP-P58S expression. To address this question, we crossed all the potential modifier lines with the ey-GAL4 driver (not recombined with DVAP-P58S). We expected an eye size comparable to controls, and any change in the eye size meant a DVAP-independent effect.

From the remaining 90 stocks, most of them consistently showed the same eye size than control flies *ey-GAL4/+* (representative examples shown in Figure 15). Only in 5 cases, we observed neurodegeneration in these crosses. The lines carrying insertion in genes *wee, wech, debra, CG10444* and *elF3-S9* were discarded from further analysis. The remaining 85 lines were tested and validated in the next analyses.

4.7.3 The excision of the P-elements suggested that the phenotype was linked to the insertion

The basis of the screen is the use of misexpression lines carrying a P-Element inserted in a specific site of the genome. If the transgenic promoter of the element is altering the expression of a target gene, any modification phenotype of these lines should be caused exclusively by this P-Element insertion. Therefore, we can assume that removing this element, we should restore the original DVAP mutant phenotype from the initial cross. To test this hypothesis, we analysed four lines using a classic genetic strategy based on the excision of the P-element.

P-elements used in this study contain in their structure a 31-bp terminal inverted repeat and an 11-bp subterminal inverted repeat sequences (O'Hare & Rubin, 1983). These regions may become target of transposition and recombination from different genetic elements. A transgenic line carrying one of these elements, the P{Δ2-3} line, was characterised as an stable recombinase source (Robertson *et al.*, 1988). It could mobilise at high frequencies different elements in the genome but at

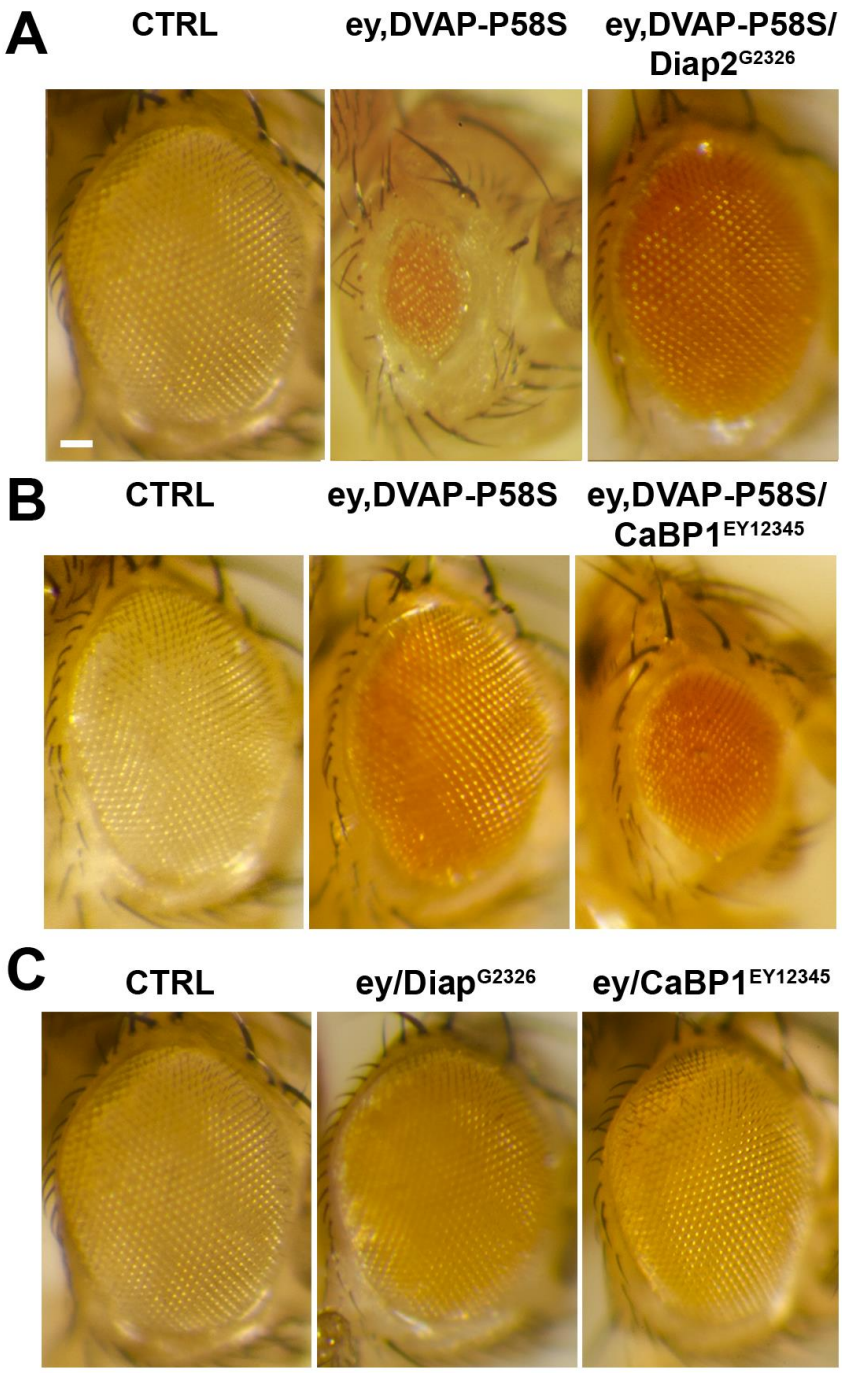

Figure 15. Genetic modification of DVAP-P58S phenotype is specific to its interaction with modifier lines. Representative suppressor (A) and enhancer (B) lines displaying its phenotype at 30ºC and 28ºC respectively. (C) Their effect in DVAP-P58S neurodegeneration was specific to the interaction, as the alleles failed to show an increase or reduction of the eye size after crossing the original misexpression lines with the ey-GAL4 driver alone. Scale bar = 50 um.

the same time, it was stable and was not affected by its own activity. This line, lacking the 2-3 intron of the P-element transposase and therefore, missing the 66kDa repressor form of the protein, became an important tool to create new deletion lines and improve transformation techniques to move elements around the genome (Robertson *et al.*, 1988).

If we remove the P-element from modifier lines, we should lose their effect in the ey,DVAP-P58S line. We tested this hypothesis in the lines over expressing the genes *DIAP2, HSPC300, Rdgbß* and *Rhomboid*. Males from the initial offspring, carrying the P-element and the transposase source *in trans*, were independently crossed with virgin females with trackable markers. This process was performed in 100 different crosses, considering the low probability of the excision event. The selected offspring from these crosses following the correct markers, were tested with the ALS model *ey-GAL4,DVAP-P58S* to observe the loss of suppression phenotype. No more than 2 positive excised lines were obtained from the original crosses. They showed a clear loss of the modification effect when compared to controls and the original misexpression stock (representative example in Figure 16). This phenotype, altogether with the marker trail observed in the genetic scheme, suggest us that the phenotype of these lines was exclusively caused by the P-element insertion. We can not confirm with this experiment however, that the suppression effect was caused by an insertion in the expected reported gene. The possibility of an insertion in another unknown gene can not be discarded with this technique. A better alternative would imply the confirmation of the effect with an independently generated overexpression allele of the same studied gene. For this reason, this classic genetic process was tested only in these initial 4 lines after obtaining the confirmation of our proposed hypothesis. However, we cannot discard the idea of using this technique as a potential source of mutants and new alleles for selected modifiers if we need further research for a specific gene.

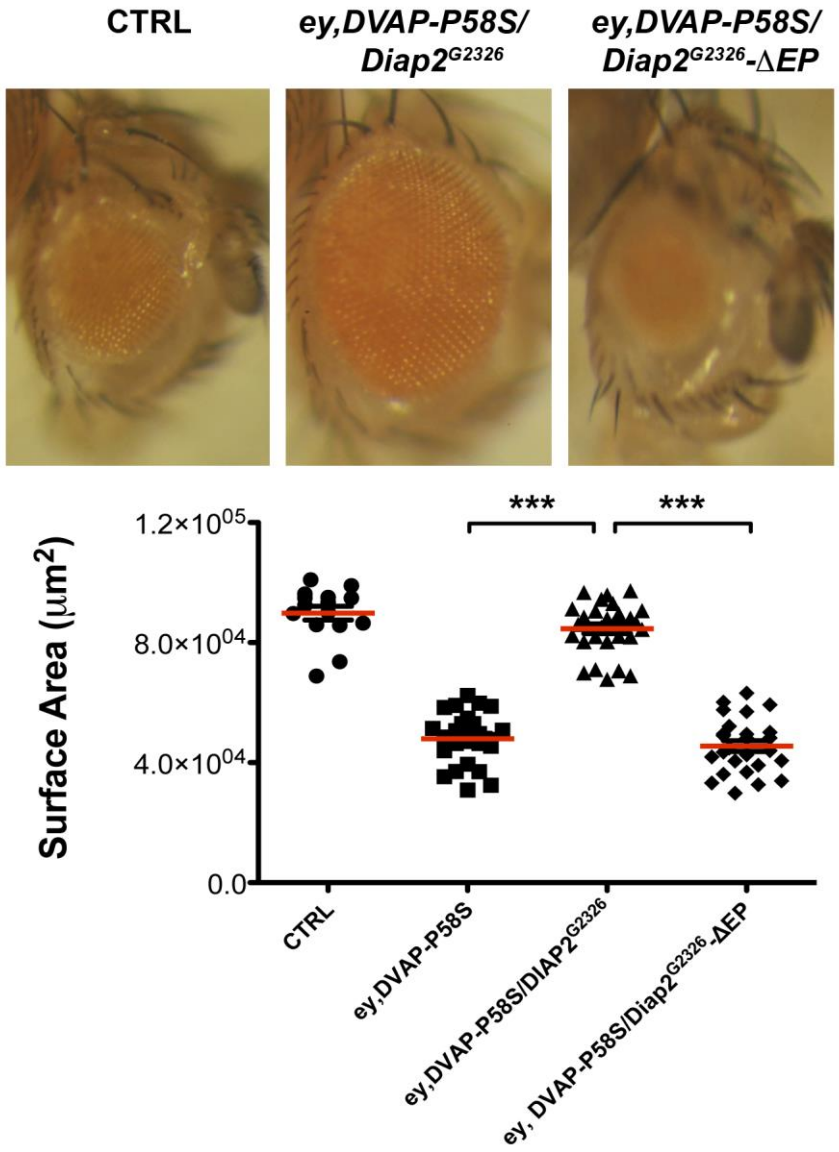

Figure 16. P-element excision from the modifier line recovers original DVAP-P58S phenotype in the eye. (**A**) Stereo microscope images of adult fly eyes of controls (*ey-Gal4/+*), *ey,DVAP-P58S/Diap2*^{G2326} (*ey-GAL4,DVAP-P58S/DIAP*^{G2326}) and *ey,DVAP-P58S/Diap2*^{G2326}*ΔEP* (*ey-GAL4,DVAP-P58S/Diap2*^{G2326}*ΔEP*) line created by the excision of the P{EP} (see results for details). Suppression in eye size toxicity of *DVAP-P58S*-expressing flies is lost without the presence of the EP element, confirming the specificity of this technique. (**B**) Quantification of eye surface area of flies carrying these alleles shows a return to original *ey,DVAP-P58S* eye size after the lack of the EP element. *** $P < 0.001$ (One-way ANOVA).

4.7.4 Exact location of the element insertion was confirmed using plasmid rescue

Besides the collaborative effort to generate misexpression collections, also has been instrumental the posterior analysis and characterisation of each stock performed by the *Drosophila* community and the Gene Disruption project (Bellen *et al.*, 2004). These analyses include not only phenotypes and affected genes, but also importantly, the exact location of each element insertion. This key information to understand and predict gene expression should be normally reliable. However with scenarios like stock mislabeling or P-element mobilization under the presence of a transposase source becomes relevant to double-check the reported information.

For this purpose, we confirmed the exact location of the element insertion using the plasmid rescue technique. This approach allowed us to calculate the exact position of the genomic region containing the P-Element and the target neighbours affected gene, by cloning this genomic segment and comparing the size of the fragment with the sequence information reported in FlyBase. From the three used collection, only the P{EP} carries the complete cassette needed for this purpose (Figure 11A, details in Chapter 2.4). This cassette includes a bacterial origin of replication for its maintenance in prokaryotic cells, kanamycin resistance as a bacterial marker for the plasmid purification, and an *Eco*RI site, which will be used as the first end of the purified restriction fragment. The second *Eco*RI site is located in the target gene, and the distance from the first site will determine the size of the purified fragment. This size of this restriction fragment is then analysed in a DNA electrophoresis and compared with the predicted size of the fragment obtained by the sequenced genomic region available in FlyBase.

From the list of modifier genes, 17 of the 27 modifiers available from the P{EP} collection were used in this study. DNA was extracted and processed for all these stocks and cloning and following restriction analysis confirmed the reported location in all of them. Results from 10 representative lines are presented in Figure 17A and the plasmid sizes from all the tested lines are displayed in Figure 17B. To

A

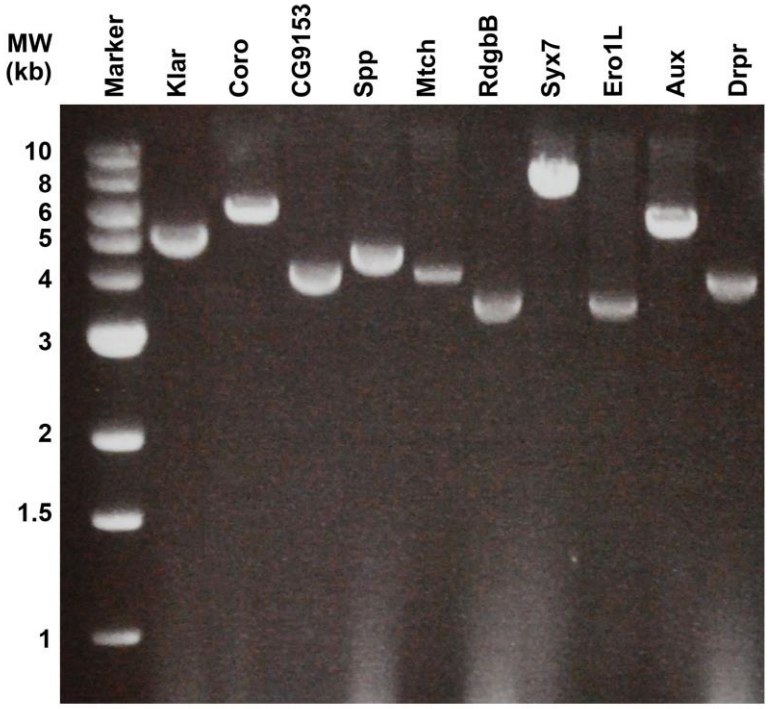

B

Gene Name	Gene Symbol	Stock number	Plasmid size (bp)
Inhibitor of apoptosis 2	Iap2	26986	7138
Ras which interacts with calmodulin	Ric	27003	8979
Peroxisome biogenesis factor 10	Pex10	27176	3887
Retinal degeneration B beta	Rdgbβ	27975	3667
Syntaxin Interacting Protein 1	HSPC300	26953	7074
Syntaxin 7	Syx7	28476	9120
Myocyte-specific enhancer factor 2	Mef2	17230	3779
Klarsicht	klar	6413	5641
Auxillin	Aux	30174	6919
CG9153	CG9153	27181	4455
Ero1-like protein	Ero1L	29300	3885
Draper	drpr	17175	3724
CG30456	CG30456	17237	6151
Signal peptide peptidase	Spp	27455	5116
Mitochondrial carrier homolog 1	Mtch	27981	5162
Coronin	Coro	26984	6875
Dynamin associated protein 160	Dap160	19582	8208

Figure 17. Plasmid rescue analysis of DVAP-P58S genetic modifiers (A) Determination of the rescued plasmid size from ten representative P{EP} lines. Each DNA fragment purified after the plasmid rescue protocol was digested with EcoRI and compared with the DNA ladder (1 kb DNA ladder, New England Biolabs). **(B)** Seventeen analysed P{EP} stocks and the size of the predicted purified plasmids obtained from their genome. Plasmid size was calculated using the bioinformatic tool NEB cutter 2.0 and compared to the observed size of the digested fragments.

obtain this result at least three clones per line were analysed, and where differences in size were observed, further analysis showed that clones with larger fragments correspond to *Eco*RI restriction sites in other location of the target gene. A most definitive confirmation of these results can be obtained sequencing the cloned fragments and compare them with the *Drosophila* genome sequence. However, we did not find major discrepancies between the predicted fragment sizes and the cloned fragments analysed, making the DNA sequencing dispensable.

This analysis included a selection from only one of the three collections studied, but the positive results proved correct and reliable the information reported in FlyBase, with no lines showing major discrepancies. For the other two collections, lacking the cassette necessary for cloning, other techniques such as inverse PCR are available to prove the same concept. However we decide to focus in next assays after confirming the information already reported in the databases for the total of analysed lines. These results were obtained together with the honour students Alistair Rocke and Mohammed Al-kharfan.

4.7.5 Independent alleles for the DVAP modifiers strongly validated the original result observed with misexpression lines

Having tested all the potential modifier lines under different validation assays, we were able to filter based on relevant controls obtaining a set of 85 potential modifiers of the DVAP toxicity (Tables 5 and 6). However, another crucial validation is to analyse whether the gene misexpressed in the modifier stock is the real causative for this phenotype. For this purpose, we aimed to test an independent allele for each of these 85 genes and corroborate with these new stocks the real effect of the former ones.

This stage is far from straightforward, if we consider the different types of alleles available, but especially the lack of solid overexpressing alternatives in the public stock centers. Considering that mostly our stocks corresponded to misexpression lines that overexpress target genes, the most direct independent alleles

are transgenic overexpression lines carrying an upstream activator sequence (UAS). However, largely these lines are not publicly available or even not constructed because some of these genes have not been fully studied yet. We tried to contact several groups from the *Drosophila* community, and were able to obtain overexpressing lines for a minor part of our set of modifiers. For this reason we decided to explore other available stocks and test as an alternative to the overexpression, other EP lines affecting the same genes but not tested initially.

Considering both alternatives, we found 14 lines, covering less than the 20% of our genes. We used as a third option, RNAi lines that down-regulate the expression of target genes. In the last years, most *Drosophila* genome has been covered with these stocks, available publicly in centers in Kyoto (NIG-FLY), Harvard (Exelixis), Vienna (VDRC) and Bloomington (TRiP collection). With the last two collections we could cover mostly our potential modifiers, testing the hypothesis that if the overexpression of target genes modifies the neurodegeneration phenotype associated with DVAP-P58S, the down regulation of the same genes should produce the opposite phenotype, altering eye size and viability in the inverse direction.

Lines acquired for this validation assay (Table 8) were tested under the same conditions as original stocks, and same parameters (eye size, viability) were measured in an identical way. For downregulation lines of original suppressor-overexpressing genes, the crosses against the model expressing *ey-Gal4,DVAP-P58S* were performed at 28ºC to expect an enhancer effect with the new allele. Also, for loss-of-function lines, it was considered a positive confirmation if the independent allele affected either eye size or ratio of viable adult flies; covering in this way any minor effect that could be missed under a more strict condition. After this analysis, we found 48 of 60 RNAi lines that were consistent with our original observation using misexpression lines. Specifically, 39 suppressor genes were confirmed by an RNAi line that has an enhancement effect in DVAP-P58S-linked eye phenotype, and 7 enhancer genes were confirmed by the suppressor effect of their RNAi lines. Additionally we were lucky to obtain from Prof. David Gilder an antibody that specifically recognises the modifier Syx7. Initially, we observed a suppression of the

Validation of modifiers with a suppressor effect by using RNAi alleles				
Gene name	**Gene symbol**	**Stock ID**	**Validation**	**% Enhancement**
Disc proliferation abnormal	dpa	v44484	Eye + Lethality	36.45 ; 44.56
Rab5	Rab5	t34832	Eye + Lethality	27.53 ; 78.97
Acyl-CoA synthetase long-chain	Acsl	v3222	Eye + Lethality	24.33 ; 37.55
Actin 42A	Act42A	v12456	Eye + Lethality	38.63 ; 39.26
Kismet	kis	v46685	Eye + Lethality	14.31 ; 62.46
Milton	milt	v41508	Lethality	33.88
Vesicle-associated membrane protein 7	Vamp7	v13316	Lethality	39.27
Croquemort	crq	v45883	Lethality	31.79
Small glu-rich tetratricopeptide protein	sgt	v22002	Lethality	39.26
CG3625	CG3625	v40855	Lethality	48.16
Hormone receptor-like in 39	Hr39	v37694	Lethality	19.18
CG13192	CG13192	v32157	Lethality	38.41
Lethal (2) k05819	l(2)k05819	v13555	Lethality	36.74
CG10809	CG10809	v38407	Lethality	38.75
CG5734	CG5734	v43798	Lethality	34.05
CG10492	CG10492	v12356	Lethality	32.82
CG12299	CG12299	v102146	Lethality	16.95
Quaking related 58E-3	qkr58E-3	v26242	Lethality	27.17
Lightoid	ltd	v104348	Lethality	25.54
14-3-3ζ	14-3-3ζ	v48724	Lethality	36.33
Ero1-like protein	Ero1L	v51169	Lethality	39.29
CG11125	CG11125	v18413	Lethality	46.71
Cyclin B	CycB	v43772	Lethality	11.77
Signal peptide peptidase	spp	v7247	Lethality	39.27
Leak	lea	v11823	Lethality	13.52
Autophagy-specific gene 7	Atg7	v27432	Lethality	39.28
Suppressor of variegation 2-10	Su(var)2-10	v30709	Lethality	18.59
Hiiragi	hrg	v42283	Lethality	36.48
Upf3	Upf3	v31444	Lethality	30.71
Secreted Wg-interacting molecule	swim	v6617	Lethality	38.42
CG18870	CG18870	v3471	Lethality	34.51
Src oncogene at 42A	Src42A	v17643	Lethality	28.55
CG13204	CG13204	t31913	Lethality	14.28
CG8520	CG8520	v36546	Lethality	19.41
Spaghetti	spag	v31253	Lethality	31.59
Cyclin-dependent kinase 4	Cdk4	v40576	Lethality	50.23
Proteasome subunit beta 5	Prosβ5	v38659	Lethality	100.00
Spc105-Related	Spc105-R	t35466	Lethality	100.00
Vacuolar protein sorting 35	Vps35	v22180	Eye	17.53

Validation of modifiers with an enhancer effect by RNAi lines				
Gene name	**Gene symbol**	**Stock ID**	**Validation**	**%Suppression**
CG30456	CG30456	v21186	Eye	41.38
Scabrous	sca	v44527	Eye	65.51
Smooth	sm	v28117	Eye	27.84
Dreadlocks	dock	v37524	Eye	60.97
Calcium-binding protein 1	CaBP1	v43148	Eye	55.11
Myocyte-specific enhancer factor 2	Mef2	v15550	Eye	38.19
CG9153	CG9153	t37220	Eye	43.57

Validation of modifiers with a suppressor effect caused by a loss–of-function				
Gene name	**Gene symbol**	**Stock ID**	**Validation**	**%Suppression**
Syntaxin Interacting Protein 1	HSPC300	t35051	Eye	46.34
Hippo	hpo	t27661	Eye	90.73
Klarsicht	klar	Klar ^{YG3}	Eye	62.89

Validation of modifiers with a suppressor effect by an overexpressing allele				
Gene name	**Gene symbol**	**Allele**	**Validation**	**%Suppression**
Inhibitor of apoptosis 2	Iap2	UAS-DIAP2	Eye	71.08

Ras which interacts with calmodulin	Ric	UAS-Ric	Eye	57.44
Silent information regulator 2	Sir2	UAS-Sir2	Eye	77.32
Rhomboid	rho	UAS-Rho	Eye	69.77
Draper	drpr	UAS-Drp	Eye	50.81
Retinal degeneration B beta	rdgBβ	P{EP}rdgBβ^{EP2360}	Eye	84.30
A kinase anchor protein 200	Akap200	P{EPgy2}Akap200^{EY01150}	Eye	61.81
Polycomblike	Pcl	P{EP}Pcl^{GE15295}	Eye	50.60

Validation of modifiers with a suppressor effect by a loss-of-function allele				
Gene name	**Gene symbol**	**Allele**	**Validation**	**%Enhancement**
Costa	cos	P{lacW}cos^{k16101}	Eye + Lethality	26.62 ; 48.82
Rap GTPase activating protein 1	RapGAP1	P{Mae-UAS.6.11}RapGAP1^{LA00889}	Eye + Lethality	24.12 ; 34.15
Type III alcohol dehydrogenase	T3dh	Mi{ET1}T3dh^{MB09825}	Lethality	40.86

Validation of modifiers with a enhancer effect by an loss-of-function allele				
Gene name	**Gene symbol**	**Allele**	**Validation**	**%Suppression**
Alanyl-tRNA synthetase	Aats-ala	P{EPgy2}Aats-ala^{EY01137b}	Eye	73.59
Dynamin associated protein 160	Dap160	Dap160Δ1	Eye	66.82

Validation of modifiers with a suppressor effect by immuno-staining			
Gene name	**Antibody**	**Tissue**	**Reference**
Syntaxin 7	rabbit anti-syx7	Brains - eye discs	Lu and Bilder, 2005

Unconfirmed modifiers		
Gene Name	**Gene symbol**	**Stock ID**
Coronin	coro	v44671
Inositol 1,4,5-triph kinase 1	IP3K1	t35296
Enolase	eno	t26300
Auxillin	aux	v16182
Trap1	Trap1	v108300
Connector enhancer of ksr	cnk	v107746
Cullin-2	Cul-2	v19297
Malate dehyrogenase	Mdh1	v27398
Longitudinals lacking	lola	v12573
Syntaxin 6	Syx6	v1501
Mitochondrial carrier homolog 1	Mtch	t16644
Peroxisome biogenesis factor 10	Pex10	v46613
CG7324	CG7324	v31063
CG15630	CG15630	v37842
Female sterile (2) Ketel	Fs(2)ket	v22348
Ub-conjugating enzyme E2Q-like	CG4502	v34855
CG4896	CG4896	v26652
Tejas	tej	v24181
Olf186-F	Olf186-F	v12221
Abrupt	ab	v41005
CG9643	CG9643	v24081
CG5118	CG5118	v34963

Table 8. Independent alleles used for validation of modifiers. Original modification effect of each gene was confirmed using an independent line that affects its expression either by up- or down-regulation. Each subtable indicates which kind of line was used and their final effect in the modifiers. Confirmation effect was observed in eye size or lethality ratios, and their modification degree was quantified and normalised to their control flies (*ey-Gal4,DVAP-P58S/+*). 62 of the 85 modifiers were confirmed with these independent lines and an extra line (Syx7) was confirmed using immunostaining assays. However, the negative 22 lines cannot be discarded as they include unavailable lines or potential weak lines unable to confirm the original effect.

DVAP-P58S neurodegenerative phenotype in the eye when we down-regulated the expression of Syx7. This implies that in a damaged DVAP-P58S tissue, the expression of Syx7 might be up-regulated. We stained DVAP-P58S tissue and indeed, observed an up-regulation of the signal specific for Syx7 compared to controls (Figure 18), validating in this way the original loss of function allele. Together, positive independent alleles from the 4 approaches (63 of 85 lines, 74% of the total) provide us the strongest genetic confirmation of our results and at the same time, validate the ALS model and our project as a valid way to search novel interactors of the mutant DVAP allele. Indeed, we can be confident about these 63 genes confirmed, but we do not have enough arguments to discard the remaining 22 lines. Some of the non-validated lines may not be dose-dependent in opposite directions, and they may lack a phenotype when down-regulated but still present the modifier phenotype when overexpressed. Conversely, the tested RNAi alleles generated only a weak hypomorph that only partially inactivates the target gene, missing the expected phenotype. Moreover, these negative results include lines not tested due to lack of an independent allele or problems in the stock when they were shipped from the stock centres. We can not discard that these lines may present a positive confirmation if we are able to test them against the ALS model or we are able to test other independent alleles.

Taken together, these assays supply us strong evidence about the initial screen and validate these genes as *bonafide* candidates for DVAP-P58S modifiers. Most importantly, these time-consuming assays are often avoided or disregarded in previously reported genetic screens, where basically most efforts of these studies are focused on a specific modifier (Franciscovich *et al.*, 2008; Couthois *et al.*, 2011; Wang *et al.*, 2013). In our case, we can propose a stronger set of modifiers, which potentially can lead to the study of different ways of action of DVAP-P58S toxicity. We consider this fact, together with the functional nature of the screen, as a strong advantage of our project compared to others attempts done in the research of ALS. Also, this gives us confidence to continue with a secondary screen and the bioinformatic analysis of these lines to understand even more these potential candidates.

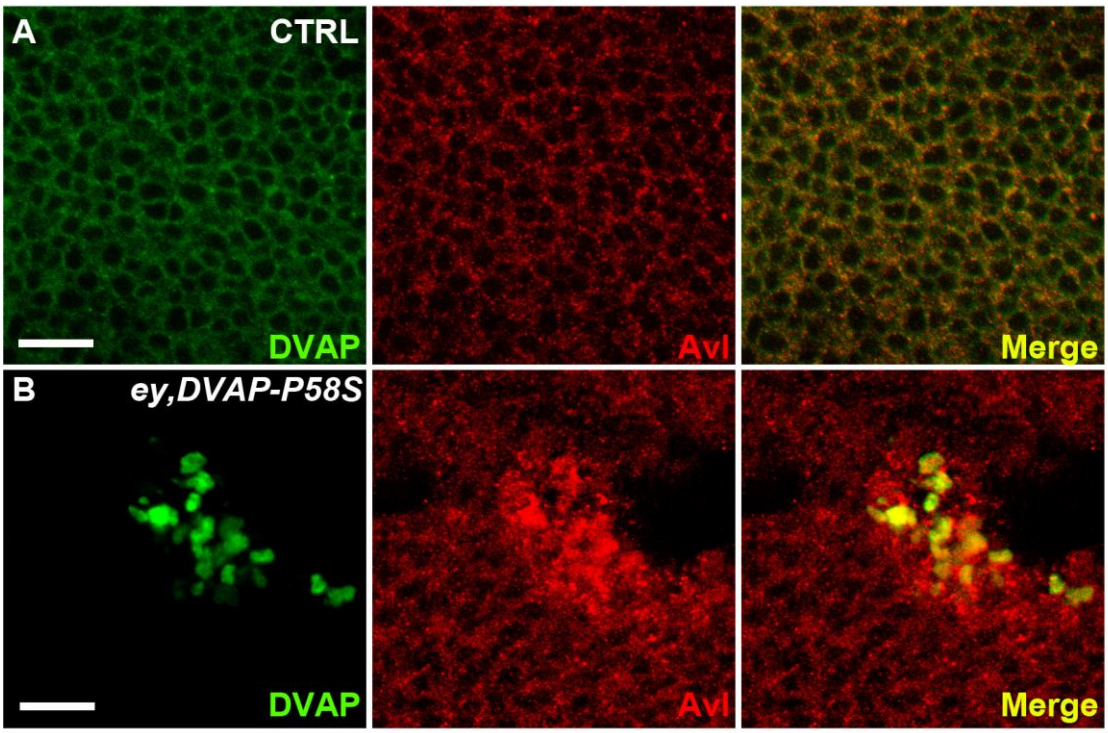

Figure 18. Syntaxin 7/Avalanche is up-regulated in *DVAP-P58S* eye imaginal discs. Control (A) and *DVAP-P58S* expressing eye imaginal discs *(ey-GAL4,DVAP-P58S/+*) (B) immuno-stained with anti-DVAP and anti-Avl antibodies. Both proteins are homogenously distributed throughout the cytoplasm, however Avl appears up-regulated in DVAP-P58S expressing cells and as part of the DVAP-positive large aggregates. Scale bar: 10μm.

Chapter 5: DVAP-P58S genetic interactors modify viability and motor performance defects.

5.1 Introduction

To correlate the previously validated DVAP-P58S genetic modifiers with common hallmarks of ALS, we studied their phenotype when expressed in the nervous system under the control of *elav-GAL4* driver. For this, we looked for changes in lethality and motor performance defects in flies co-expressing DVAP-P58S and the misexpressed alleles. These two extra readouts helped us to filter even more our potential candidate genes and validate the results obtained in the primary screen.

5.2 Lethality screen

The data presented so far indicate that DVAP-P58S expression in the eye causes a significant neurodegeneration. This phenotype was used to obtain novel DVAP-P58S genetic interactors that can provide us clues to understand ALS pathomechanism. In humans, disease's hallmarks are mostly related to loss of motor activity due to death of motor neurones. Even though we obtained *bona fide* DVAP candidates looking at the *Drosophila* eye, we asked whether we could see the same modification effects in the rest of the nervous system. With this, we tried to mimic some of the most important symptoms of patients with ALS, validating the modifier genes in a disease-related context.

We already reported in the chapter 3.7 a characterisation of the expression of *DVAP* mutant allele in the whole nervous system under the control of *elav-GAL4* driver. We observed an increase in lethality of flies expressing *DVAP-P58S* compared to control. Additionally, for the first time we presented a progressive loss in the motor performance of DVAP-P58S-expressing surviving flies that leads to a total paralysis in temperature-dependent time range (Figure 4). Over the last years, lethality screens have been used to find genes able to modify toxic activities from relevant proteins (Zhang *et al.*, 1999, Graham *et al.*, 2011, Bates *et al.*, 2014). These screens are based on the hypothesis that neurodegeneration can be suppressed or enhanced by coexpression of the toxic protein and genetic modifiers. With these studies, several genes have been found and the assay has been validated as a strong

way to find the modifiers. Therefore, we planned to use a lethality assay as a secondary screen for the DVAP-genetic interactors found in the previous chapter and strengthen their potential effect in ALS pathogenesis.

A line carrying both *elav-GAL4* driver and *DVAP-P58S* allele was constructed for this assay (*elav-GAL4/elav-GAL4; DVAP-P58S/CyO-GFP*). Virgin females from this line were crossed with males from the same misexpression lines used in the primary screen. These 85 lines shown significant modification effect in the eye and were already validated by different assays. Embryos were laid for 48 hours at room temperature to then increase *DVAP-P58S* expression transferring them at 28ºC. This temperature was selected after initial optimisation as the point where *DVAP-P58S* presented a difference in viability with controls and flies displayed a clear motor performance curve, point to be discussed later. Parental flies from the crosses were transferred to another vial to create a replica of the cross and then removed after two days laying at room temperature.

A degree of variability can be observed in two different crosses. Factors affecting the food such as cooking, dryness or humidity can alter offspring number and phenotypes. For this reason is desirable to obtain an internal control, which is obtained from the same vial than the experimental cross. We selected this option for our assays comparing the experimental flies expressing *DVAP-P58S* and normal wings (*elav-GAL4/+;DVAP-P58S/P{EP}*) with the control flies obtained from the same cross carrying the dominant marker Cy (*elav-GAL4/+; P{EP}/CyO-GFP*). Therefore, the offspring was collected and classified in two groups according their wing phenotype. These groups were counted and the viability ratio was calculated as the difference with the controls (details in Materials & Methods).

After testing each modifier in three independent experiments, 47 of 85 modifiers presented a strong modification effect, with a normalised viability larger than 0.5 times the values from control flies. In figure 19, a two-axis plot correlates the normalized viability of each modifier with their effect in the DVAP-P58S-induced neurodegeneration in the eye observed in the primary genetic screen. Forty-

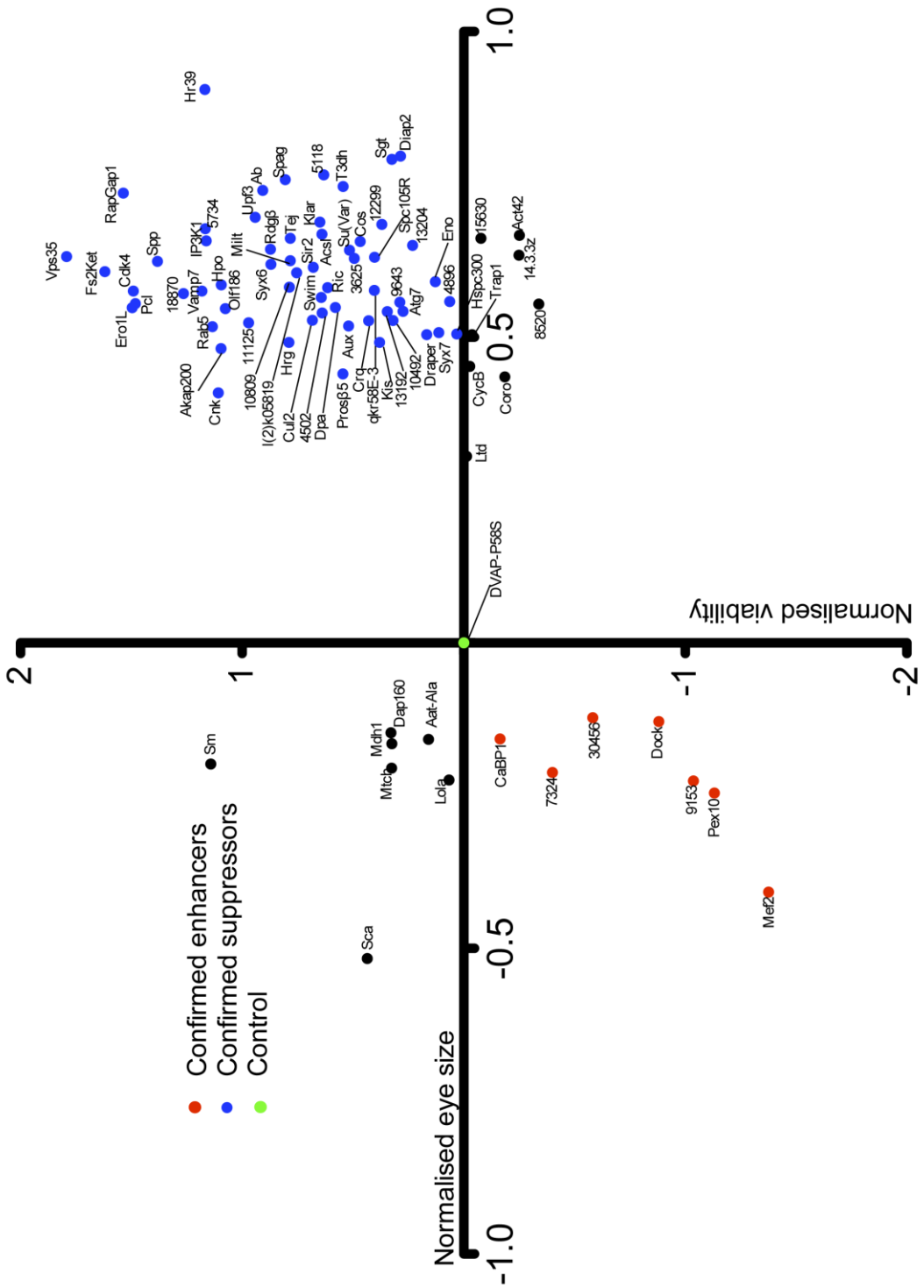

Figure 19. Secondary lethality screen. Two-axis plot expressing the correlation between eye size modification (X axis) and viability modification (Y axis) for 82 lines found in the primary screen. Each point represents the average of three independent experiments for both axes. Values were normalised by comparing with their control (DVAP-P58S, in green). Most modifiers are confirmed suppressors (blue) but there is a small group of modifiers that did not show the same phenotype in both assays (black).

one lines that were suppressors of DVAP-neurodegeneration in the eye were able to decrease the DVAP-linked lethality when co-expressed in the nervous system. Five genetic modifiers that enhanced the eye phenotype were able to reduce even more the number of flies co-expressing both genes. Only one of the 47 lines (19727 - *Smooth*) presented the modification effect in the opposite direction than the original screen. Even considering that these results could support the previous analyses, unfortunately they can not confirm them and can not be used as an independent assay. The small difference between the percentage of expected and observed flies, plus the number of repetitions (n=3) made that less than half of these positive results were statistically significant (19 of 46, two-way Student's T-test, $p<0.05$, results in Table 9), indicating not the degree of modification but only how spread the averages were. The tendency observed for most of them could potentially support as an extra readout the modification effects obtained originally in the eye. However further analyses are needed to confidently use these data. A strong alternative could be a rescue of a fully penetrant DVAP-linked lethality after an increase of temperature, but in this case we preferred to perform this experiment at the same temperature than the motor performance assay, using the same flies for both experiments.

From the original 85 lines, three stocks showed complete pupae lethality at the tested temperature. Lines overexpressing the genes Rhomboid, Leak and Src42 crossed with the line elav;DVAP-P58S were lethal at different stages of larval development and were unable to produce a significant number of viable adults. When these three lines were crossed with the driver elav-Gal4 on its own, also showed decrease in viability in a similar way. This means that they already presented a phenotype, and DVAP co-expression only could make that phenotype stronger. Probably, the observed lethality can be caused for different reasons and the study of these genes could be possible at lower temperatures. However, we did not try other conditions in this study as we focused on the main group of positive modifiers, avoiding further optimisation for specific genes. We cannot discard however, the study of these three genes if they appear to be connected to DVAP pathology.

	P1	P2	P3	Avr	M1	M2	M3	Avr	Signif
Vps35	85.71	117.86	148.65	117.41	0.529	2.030	2.820	1.793	
Fs2Ket	113.43	116.67	107.87	112.65	1.896	1.656	1.310	1.620	**
RapGap1	101.18	114.29	115.00	110.16	1.042	1.728	1.840	1.537	**
Ero1L	118.03	105.88	107.69	110.54	1.919	1.212	1.359	1.497	**
Cdk4	107.69	121.05	98.04	108.93	1.338	2.272	0.866	1.492	*
Pcl	155.77	80.00	111.94	115.90	2.841	0.213	1.394	1.482	
Spp	99.03	113.89	108.57	107.16	0.935	1.778	1.437	1.383	**
18870	78.95	126.76	100.00	101.90	0.250	2.544	1.000	1.265	
CG1599	87.50	95.00	136.84	106.45	0.292	0.803	2.450	1.182	
Hr39	109.68	96.10	100.00	101.93	1.645	0.862	1.000	1.169	*
5734	119.05	94.00	95.35	102.80	2.143	0.637	0.721	1.167	
IP3K1	116.28	97.96	92.06	102.10	1.904	0.882	0.703	1.163	*
Sm	131.25	98.51	114.29	114.68	2.375	0.946	0.104	1.142	
Rab5	93.10	109.09	104.70	102.30	0.772	1.463	1.170	1.135	**
cnk	107.60	109.33	88.57	101.84	1.456	1.560	0.309	1.108	*
Akap200	117.24	106.67	81.82	101.91	1.977	1.403	-0.091	1.096	
Hippo	110.20	102.44	92.31	101.65	1.578	1.136	0.573	1.095	
Olf186-F	110.68	108.33	85.11	101.37	1.381	1.504	0.345	1.076	
CG11125	88.24	108.75	92.60	96.53	0.581	1.598	0.733	0.971	
upf3	86.05	102.33	103.03	97.13	0.503	1.141	1.182	0.942	
ab	129.23	78.65	89.29	99.06	2.656	-0.290	0.357	0.908	
RdgBb	89.36	83.08	113.33	95.26	0.409	0.441	1.769	0.873	
Syx6	100.00	98.11	94.38	97.50	1.000	0.938	0.676	0.871	*
spag	85.71	87.23	111.63	94.86	0.491	0.229	1.698	0.806	
hrg	95.40	92.31	100.00	95.90	0.836	0.535	1.000	0.790	*
10809	93.33	100.00	89.60	94.31	0.738	1.000	0.625	0.787	**
milt	89.58	97.06	100.00	95.55	0.542	0.809	1.000	0.783	*
tej	128.68	80.60	80.00	96.43	2.721	-0.172	-0.200	0.783	
l(2)k05819	85.00	98.92	97.39	93.77	0.465	0.945	0.854	0.755	*
Cul-2	76.47	91.67	105.56	91.23	0.161	0.672	1.219	0.684	
Sir2	94.03	96.15	87.27	92.49	0.666	0.795	0.580	0.680	*
klar	88.06	75.41	107.50	90.32	0.606	-0.082	1.425	0.650	
Swim	100.00	92.73	84.06	92.26	1.000	0.561	0.372	0.644	
acsl	92.00	101.23	83.54	92.26	0.520	1.049	0.352	0.640	
4502	83.52	97.74	93.18	91.48	0.413	0.885	0.618	0.639	
5118	93.96	76.19	99.10	89.75	0.785	0.156	0.956	0.632	
Ric	100.00	94.74	77.27	90.67	1.000	0.696	0.150	0.615	
DPA	83.95	112.05	88.89	94.96	-0.070	1.451	0.359	0.580	
prosB5	87.41	87.88	88.89	88.06	0.551	0.523	0.563	0.546	***
T3dh	95.10	93.33	87.50	91.98	0.674	0.660	0.300	0.545	*
Aux	82.05	82.76	95.00	86.60	0.293	0.431	0.835	0.520	*
Su(Var)2-10	73.61	97.92	106.12	92.55	-0.759	0.908	1.398	0.516	
3625	88.89	75.93	105.56	90.12	0.604	-0.455	1.333	0.494	
Cos	61.40	112.00	106.93	93.44	-1.573	1.528	1.451	0.468	

sca	79.37	90.20	101.75	90.44	-0.376	0.614	1.069	0.436	
crq	84.62	90.32	96.51	90.48	0.077	0.452	0.761	0.430	
qkr58E-3	91.57	90.67	83.17	88.47	0.531	0.651	0.029	0.404	
Spc105R	82.00	81.32	93.33	85.55	0.362	0.086	0.759	0.403	
Kis	81.60	87.50	87.10	85.40	0.344	0.363	0.432	0.380	*
12299	95.08	71.43	90.37	85.63	0.705	-0.018	0.422	0.370	
13192	81.18	83.61	77.14	80.64	0.329	0.459	0.246	0.345	**
Dap160	90.91	78.00	87.18	85.36	0.394	0.220	0.373	0.329	
Mtch	77.42	72.73	102.70	84.28	-0.279	0.100	1.156	0.326	
Mdh1	93.62	83.01	73.33	83.32	0.773	0.253	-0.050	0.325	
Sgt	95.65	76.00	89.86	87.17	0.739	-0.385	0.620	0.325	
10492	78.20	84.21	94.87	85.76	0.223	0.046	0.692	0.320	
9643	83.33	81.48	89.36	84.73	0.406	0.057	0.404	0.289	
Diap2	90.53	85.71	83.82	86.69	0.220	0.529	0.110	0.286	
Atg7	83.33	83.08	80.00	82.14	0.344	0.199	0.278	0.274	*
13204	69.47	81.75	98.08	83.10	-0.088	-0.103	0.885	0.231	
Draper	65.19	92.86	101.18	86.41	-0.973	0.412	1.065	0.168	
Aat-Ala	80.00	81.72	88.89	83.54	-0.367	0.280	0.563	0.159	
eno	96.35	65.12	74.70	78.72	0.757	-0.373	0.004	0.129	
Syx7	79.17	83.72	98.41	87.10	-0.958	0.359	0.938	0.113	
lola	83.76	70.59	62.16	72.17	0.421	0.029	-0.249	0.067	
4896	75.44	97.96	66.67	80.02	-0.484	0.878	-0.203	0.064	
HSPC300	106.25	72.00	69.74	82.66	1.347	-0.586	-0.664	0.032	
Ltd	85.37	77.55	80.99	81.30	0.171	-0.144	-0.064	-0.012	
CycB	95.45	51.16	74.42	73.68	0.850	-0.923	-0.007	-0.027	
Trap1	84.56	80.70	61.33	75.53	0.450	-0.114	-0.447	-0.037	
15630	61.54	87.27	78.40	75.72	-0.371	0.352	-0.212	-0.077	
CaBP1	75.00	76.92	70.40	74.11	-0.416	0.091	-0.165	-0.163	
Coro	80.88	60.43	71.43	70.91	0.322	-0.935	0.057	-0.185	
14.3.3z	85.71	82.42	63.64	77.26	0.206	0.227	-1.181	-0.249	
Act42	72.73	63.83	67.92	68.16	-0.291	-0.305	-0.158	-0.251	
8520	53.66	81.82	78.95	71.47	-0.652	-0.099	-0.263	-0.338	
7324	81.36	63.01	85.71	76.69	-0.118	-1.219	0.137	-0.400	
CG30456	91.14	76.69	51.85	73.23	0.686	-0.140	-2.291	-0.582	
dock	46.15	66.67	59.50	57.44	-1.549	-0.630	-0.462	-0.880	*
CG9153	67.53	74.42	28.57	56.84	-1.165	-0.366	-1.578	-1.036	
Pex10	62.34	80.00	36.36	59.57	-1.259	-0.333	-1.800	-1.131	
Mef2	30.91	78.08	57.95	55.65	-3.606	0.137	-0.656	-1.375	

Table 9. Viability ratios observed in DVAP-P58S flies co-expressing the modifier alleles. P, Percentage of flies observed, normalised by the number of flies expected for each cross. M, Modification ratio expressed by the difference between observed and expected percentage P and controls C, (P-C)/(100-C). Significance level calculated after unpaired, two-tailed Student's t-test for P1, P2 and P3 and their controls. From 82 tested modifiers, 49 showed a viability modification consistent with the primary screen, but only 20 of these were statistically significant although.*** $p<0.001$, ** $p<0.01$, * $p<0.05$.

5.3 Motor performance assay

In the previous section we observed a modification in the lethality when misexpression lines were crossed with flies expressing DVAP-P58S in the nervous system. We tested the offspring from these crosses to analyse whether they displayed as well neurodegenerative phenotype over time. Previously, we observed that the expression of DVAP-P58S in the nervous system produced a late-onset progressive motor dysfunction that was dependent on the temperature of the system (Figure 7). Expression of the gene at higher temperatures resulted in a shorter time-curve with a steep decrease in the climbing ability, which made difficult to observe any modification with another genetic interactor. The same assay performed at lower temperatures produced a time-curve twice as long and with a slower decline in the motor performance and an increased variability between points. For these reasons, we determined the optimal temperature as 28ºC, where we obtained a conveniently short time-curve but with enough space to observe phenotypic changes.

The climbing assay has been used in previous genetic screens in *Drosophila* (Miller *et al.*, 2012; Kaltenbach *et al.*, 2007). They can provide a strong phenotype that is related specifically with neurodegeneration and at the same time, can be used at large scale to search for modifiers. In our case we tested the 82 modifiers (not including the lethal lines *Rho, Leak* and *Src42*) to search for modification in the DVAP-P58S-induced motor performance decline. For this purpose, sets of 10 flies were challenged each two days to see whether they were able to climb 8 centimeters in 15 seconds. The average of 10 trials was compared to the performance of controls and time points were analysed statistically using two-way ANOVA.

From the 82 DVAP genetic interactors tested, 58 showed a significant modification in at least one point of the curve, which confirmed the same modification effect observed in the primary screen. According their degree of significance, suppressor lines were grouped in strong (showing modification effect in most part of the time curve), intermediate (with a significance difference with controls in two time points) and weak modifiers (showing modification in one time

point). From the 50 confirmed suppressors, 30 showed a strong effect, 14 an intermediate and 6 a weak one. In the case of the enhancers, the modification of the 8 positive lines was observed only at the beginning of the curve, as the performance of the control *elav;DVAP-P58S* was at minimum levels after 8 days and an enhancing of this phenotype was no longer possible. The group of 24 negative results includes 15 lines that did not show any difference compared to the control and 9 lines that displayed a slight opposite effect to that exhibited by the phenotype in the eye neurodegeneration, indicating that a more complex interaction may be present between DVAP-P58S and these modifiers. Table 10 presents statistical classification of the modifier lines and Figure 20 individual results of each modifier tested.

After the analysis of these results, different aspects can be mentioned. Considering that allele- and dose-dependent effects may be present in some of the negative results, further optimisation of the conditions can lead to an increase of the number of confirmed lines. Just as in the case of the validation with independent alleles, we can not discard however, the negative results as real DVAP interactors. Another possibility is a different interaction of the modifiers in the nervous system and imaginal discs, where their specific relation with DVAP is yet to be elucidated. Nevertheless, it is remarkable the important group of genes confirmed by all means, even if we do not consider the supporting results from the viability assay. Starting from 1183 misexpression stocks, we isolated 85 potential modifiers and at least half of them also were validated by two independent assays (Figure 21). This group of genes not only validates our project but also increases the potential mechanisms and pathways associated with DVAP pathomechanism. As previously mentioned, a further study of each one of these genes is mandatory to understand their function in DVAP biology and their link with current gaps in the ALS study. However, as an initial step, the current list of genetic modifiers is a promising start to further analyse their connection with known information, not only by bioinformatic analyses but also with the mentioned characterisation of some of these genetic modifiers.

Suppressors - Strong effect	TP1	TP2	TP3	TP4	TP5	Overall
Cyclin B	***	***	***	***	-	1.000
Ras which interacts with calmodulin	***	***	***	***	-	1.000
Inhibitor of apoptosis 2	***	***	***	**	-	0.917
CG4896	***	***	***	***	ns	0.800
Hippo	**	***	***	***	***	0.933
CG5734	ns	***	***	***	***	0.800
Small glu-rich tetratricopeptide protein	ns	***	***	**	*	0.600
Lightoid	***	***	***	ns	-	0.750
Tejas	**	***	***	***	ns	0.733
Secreted Wg-interacting molecule	**	***	***	***	ns	0.733
Abrupt	ns	***	***	**	-	0.667
CG10492	***	***	***	*	ns	0.667
CG13204	***	***	***	*	ns	0.667
Auxillin	ns	***	***	***	ns	0.600
Klarsicht	*	***	***	*	ns	0.533
CG15630	***	***	***	ns	ns	0.600
Croquemort	***	***	***	ns	ns	0.600
Olf186-F	ns	*	***	***	**	0.600
Vesicle-associated membrane protein 7	ns	***	***	***	ns	0.600
CG5118	ns	***	***	***	ns	0.600
Proteasome subunit beta 5	ns	**	***	***	*	0.600
Hiiragi	ns	***	***	***	ns	0.600
Cyclin-dependent kinase 4	***	***	ns	***	ns	0.600
Acyl-CoA synthetase long-chain	ns	***	***	ns	**	0.533
Disc proliferation abnormal	ns	*	***	***	*	0.533
Draper	***	***	ns	ns	-	0.500
Enolase	ns	***	***	ns	-	0.500
CG18870	ns	**	***	**	ns	0.470
A kinase anchor protein 200	*	***	*	ns	-	0.420
Actin 42A	ns	*	***	**	ns	0.400
Suppressors - Intermediate effect	TP1	TP2	TP3	TP4	TP5	Overall
Connector enhancer of ksr	ns	***	***	ns	ns	0.400
CG13192	(**)	***	***	ns	ns	0.400
Female sterile (2) Ketel	ns	ns	***	***	ns	0.400
Vacuolar protein sorting 35	ns	ns	***	***	ns	0.400
Milton	ns	***	***	ns	ns	0.400
Inositol 1,4,5-triphosphate kinase 1	ns	ns	***	***	ns	0.400
Syntaxin interacting protein 1	ns	ns	ns	***	***	0.400
CG9643	ns	***	***	ns	ns	0.400
Upf3	ns	***	***	ns	ns	0.400
CG11125	ns	**	ns	***	*	0.400
CG8520	(***)	ns	***	ns	*	0.267
Trap1	ns	ns	*	***	ns	0.267

Ero1L	ns	*	***	ns	ns	0.267
Quaking related 58E-3	ns	*	***	ns	ns	0.267
Suppressors - Weak effect	TP1	TP2	TP3	TP4	TP5	Overall
Syntaxin 6	**	*	*	ns	ns	0.267
Spc105-related	ns	ns	***	ns	ns	0.200
Autophagy-specific gene 7	ns	*	*	ns	-	0.170
Signal peptide peptidase	ns	***	ns	ns	-	0.250
Type III alcohol dehydrogenase	ns	***	ns	ns	-	0.250
lethal (2) k05819	ns	ns	**	ns	ns	0.133
Enhancers	TP1	TP2	TP3	TP4	TP5	Overall
Myocyte-specific enhancer factor 2	***	***	ns	ns	-	0.500
CG9153	***	***	ns	ns	-	0.500
scabrous	***	*	*	ns	ns	0.333
longitudinals lacking	ns	***	ns	ns	-	0.250
Smooth	***	***	***	ns	ns	0.600
Malate dehyrogenase	ns	ns	***	***	ns	0.400
Dreadlocks	(**)	***	***	ns	ns	0.400
Alanyl-tRNA synthetase	ns	***	*	ns	ns	0.270
Suppressors - No effect	TP1	TP2	TP3	TP4	TP5	Overall
Suppressor of variegation 2-10	ns	**	ns	ns	-	0.167
Retinal degeneration B beta	ns	ns	***	ns	ns	0.200
CG10809	ns	ns	**	ns	ns	0.130
Costa	ns	**	ns	ns	ns	0.130
Rab5	ns	ns	ns	ns	ns	0.000
Cullin-2	ns	ns	ns	ns	ns	0.000
spaghetti	ns	ns	ns	ns	ns	0.000
Polycomblike	ns	ns	ns	ns	ns	0.000
CG3625	ns	ns	ns	ns	ns	0.000
Suppressors - Opposite effect	TP1	TP2	TP3	TP4	TP5	Overall
Rap GTPase activating protein 1	ns	*	(**)	ns	ns	0.070
Hormone receptor-like in 39	(***)	(***)	ns	ns	ns	0.000
kismet	ns	ns	(***)	(***)	ns	0.000
Syntaxin 7	(***)	(***)	ns	ns	ns	0.000
14-3-3ζ	ns	ns	ns	ns	ns	0.000
Coronin	ns	(***)	(*)	ns	ns	0.000
CG12299	ns	ns	ns	(***)	ns	0.000
Ub-conjugating enzyme E2Q-like	ns	ns	(***)	ns	ns	0.000
Silent information regulator 2	(***)	ns	ns	ns	-	0.000
Enhancers – No effect	TP1	TP2	TP3	TP4	TP5	Overall
Dynamin associated protein 160	(***)	(***)	(***)	(***)	-	0.000
Peroxisome biogenesis factor 10	ns	ns	ns	ns	-	0.000
CG30456	ns	ns	*	ns	ns	0.070
calcium-binding protein 1	ns	***	ns	ns	ns	0.200
Mitochondrial carrier homolog 1	*	ns	ns	ns	-	0.083
CG7324	ns	ns	ns	ns	ns	0.000

Table 10. Motor performance assay tested on the DVAP-P58S genetic modifiers. TP, Time point tested. Overall column express relative significance level though out the different time points. Strong modifiers are significantly different from controls at most part of the curve. Intermediate lines show two points significantly different from the control and weak modifiers include alleles which are significantly different in at least one time point but with a curve closer to the one observed in controls. A group of modifiers presented an opposite effect to the one observed in the primary screen; their significance level is presented in brackets. 58 modifiers discovered in our primary screen were confirmed using this assay. *** $p<0.001$, ** $p<0.01$, * $p<0.05$, ns $p>0.05$ (Two-way ANOVA).

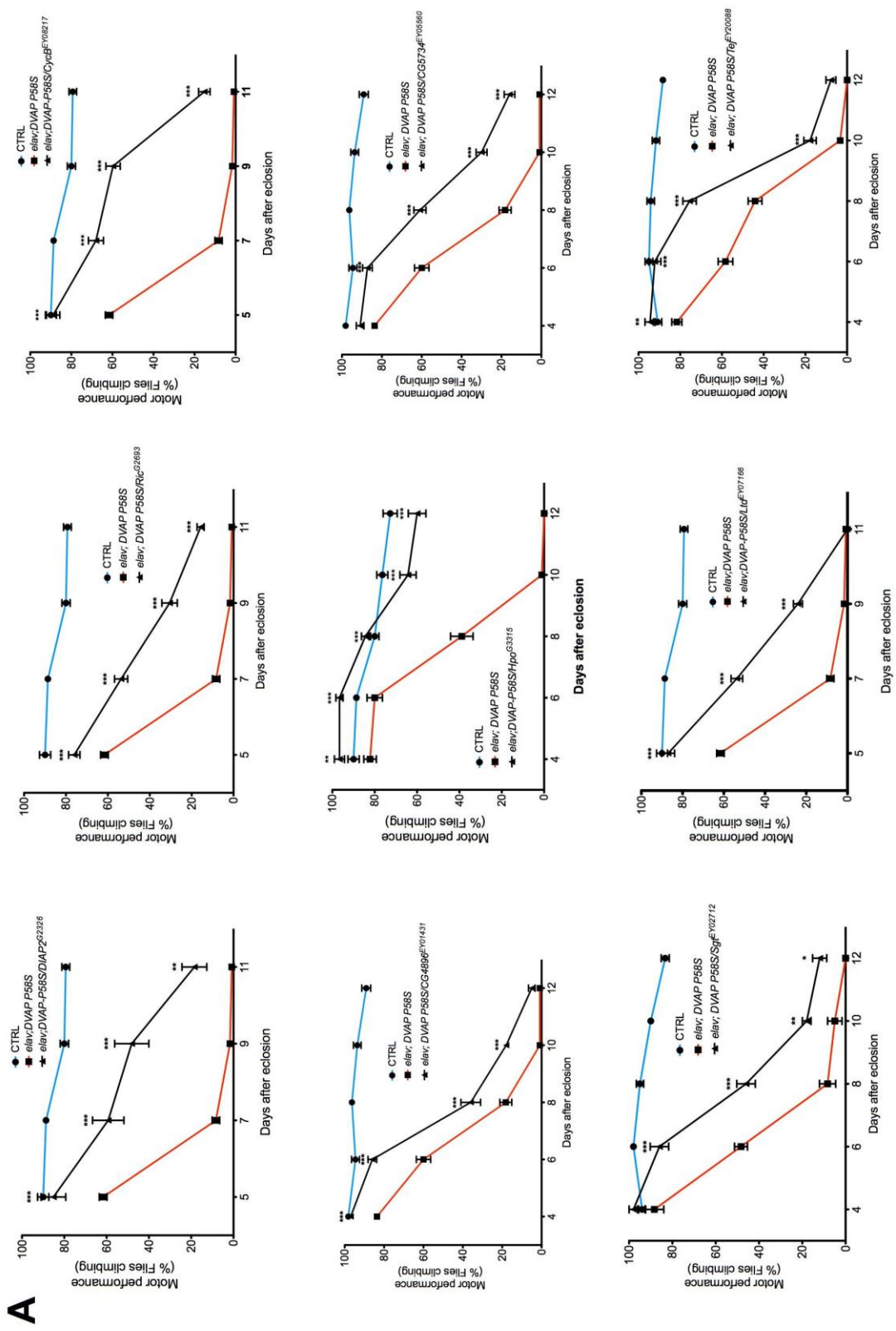
A
CTRL
elav;DVAP P58S
elav;DVAP-P58S/DIAP2^G2326
elav;DVAP P58S/CG4896^EY01431
elav;DVAP P58S/Sgf^EY02712
elav; DVAP P58S/Ric^G2693
elav;DVAP-P58S/Hpo^G3315
elav;DVAP P58S/Lic^EY07166
elav;DVAP P58S/CycE^EY09217
elav; DVAP P58S/CG5734^EY05560
elav; DVAP P58S/Tej^EY20088
Motor performance (% Flies climbing)
Days after eclosion

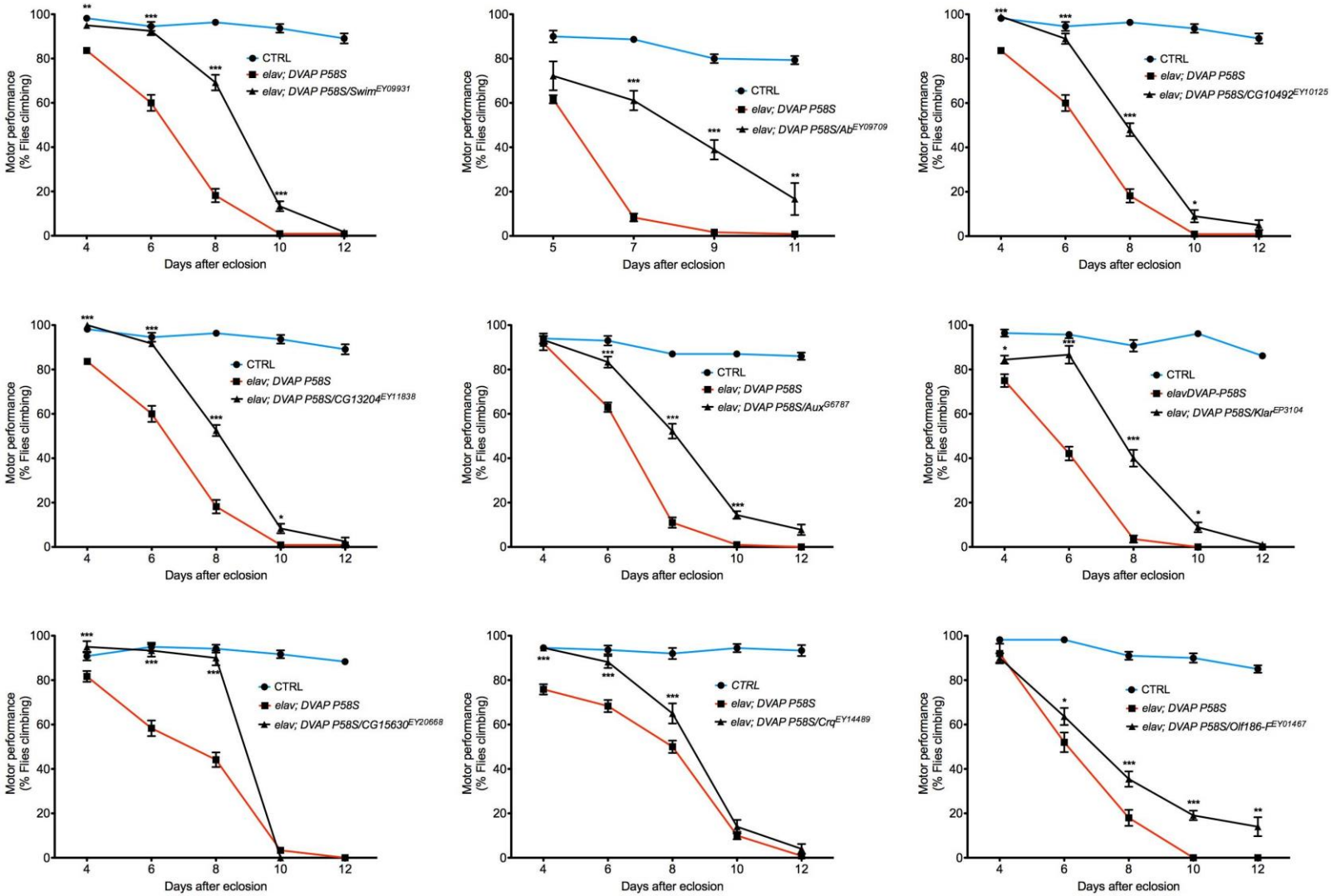
Motor performance (% Flies climbing)
Days after eclosion
CTRL
elav; DVAP P58S
elav; DVAP P58S/Swim EY09931
elav; DVAP P58S/Ab EY09709
elav; DVAP P58S/CG10492 EY10125
elav; DVAP P58S/CG13204 EY11838
elav; DVAP P58S/Aux G6787
elavDVAP-P58S
elav; DVAP P58S/Klar EP3104
elav; DVAP P58S/CG15630 EY20668
CTRL
elav; DVAP P58S
elav; DVAP P58S/Crq EY14489
elav; DVAP P58S/Olf186-F EY01467

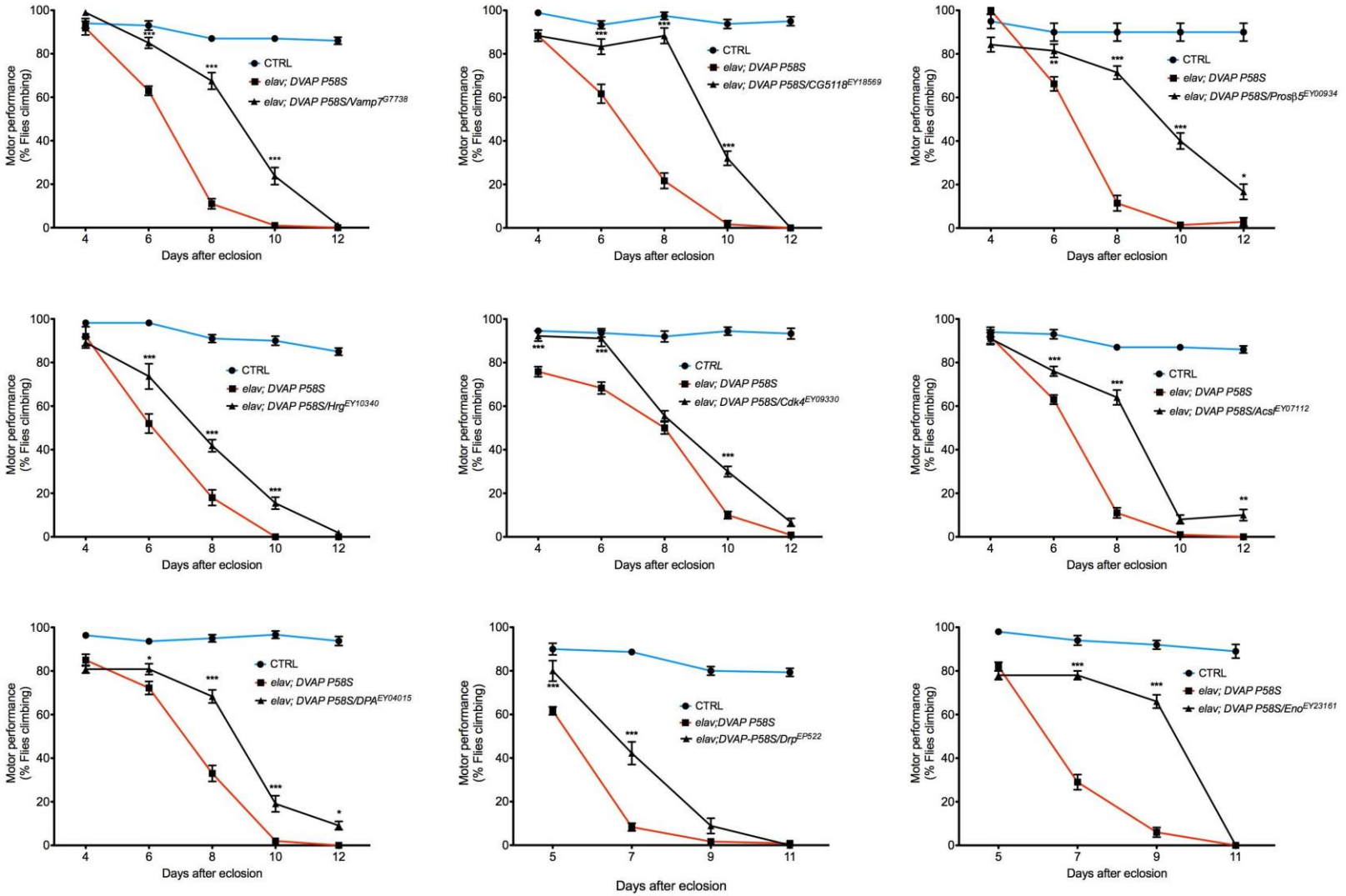
Motor performance (% Flies climbing)
Days after eclosion
CTRL
elav; DVAP P58S
elav; DVAP P58S/Vamp7G7738
elav; DVAP P58S/CG5118EY18569
elav; DVAP P58S/Prosβ5EY00934
elav; DVAP P58S/HrgEY10340
elav; DVAP P58S/Cdk4EY09330
elav; DVAP P58S/AcslEY07112
elav; DVAP P58S/DPAEY04015
elav;DVAP P58S
elav;DVAP-P58S/DrpEP522
elav; DVAP P58S/EnoEY23161

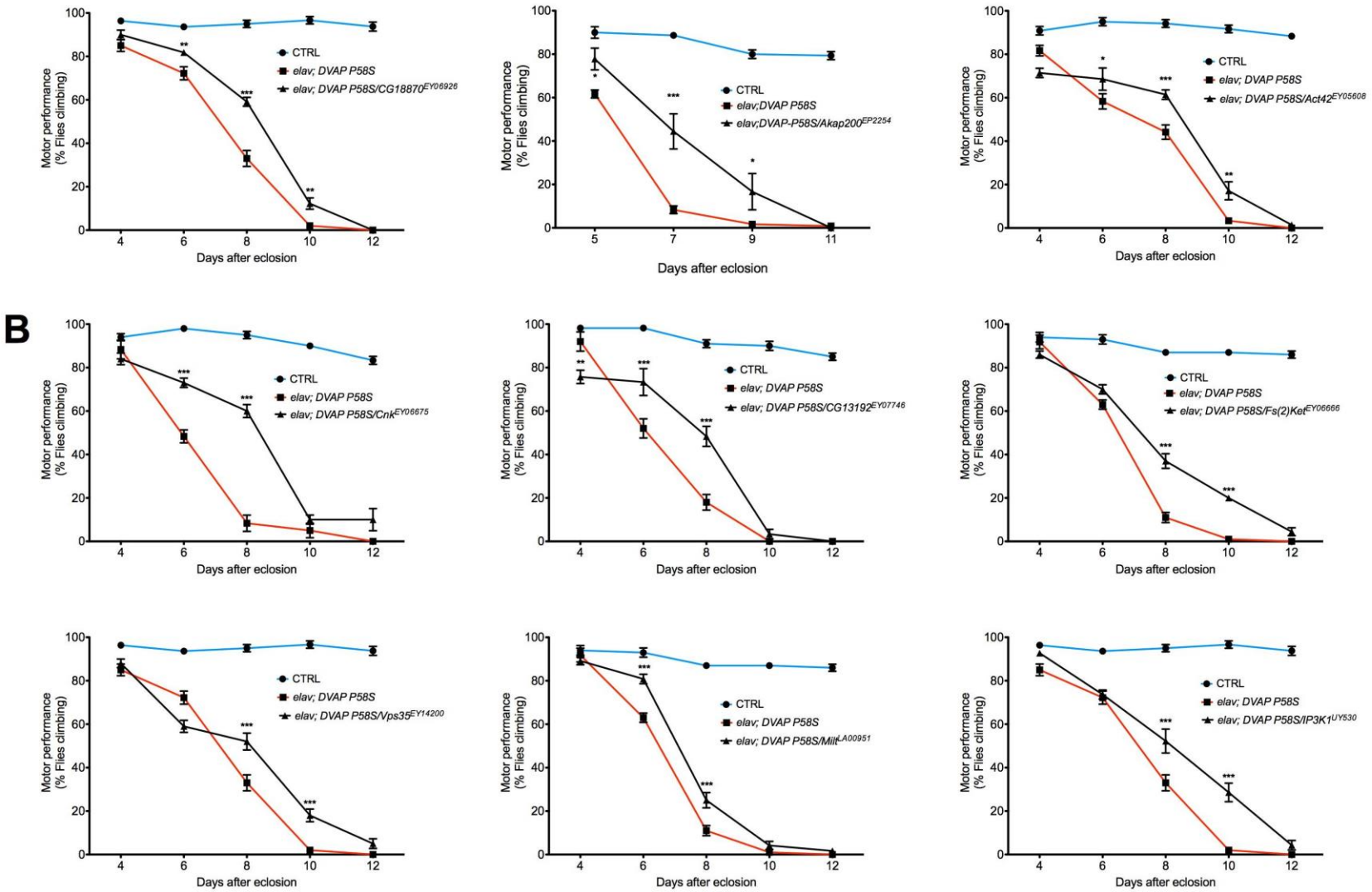
B
Motor performance (% Flies climbing)
Days after eclosion
CTRL
elav; DVAP P58S
elav; DVAP P58S/CG18870EY06926
elav;DVAP-P58S/Akap200EP2254
elav; DVAP P58S/Act42EY05608
elav; DVAP P58S/CnkEY06675
elav; DVAP P58S/CG13192EY07746
elav; DVAP P58S/Fs(2)KelEY06666
elav; DVAP P58S/Vps35EY14200
elav; DVAP P58S/MiltLA00951
elav; DVAP P58S/IP3K1UY530

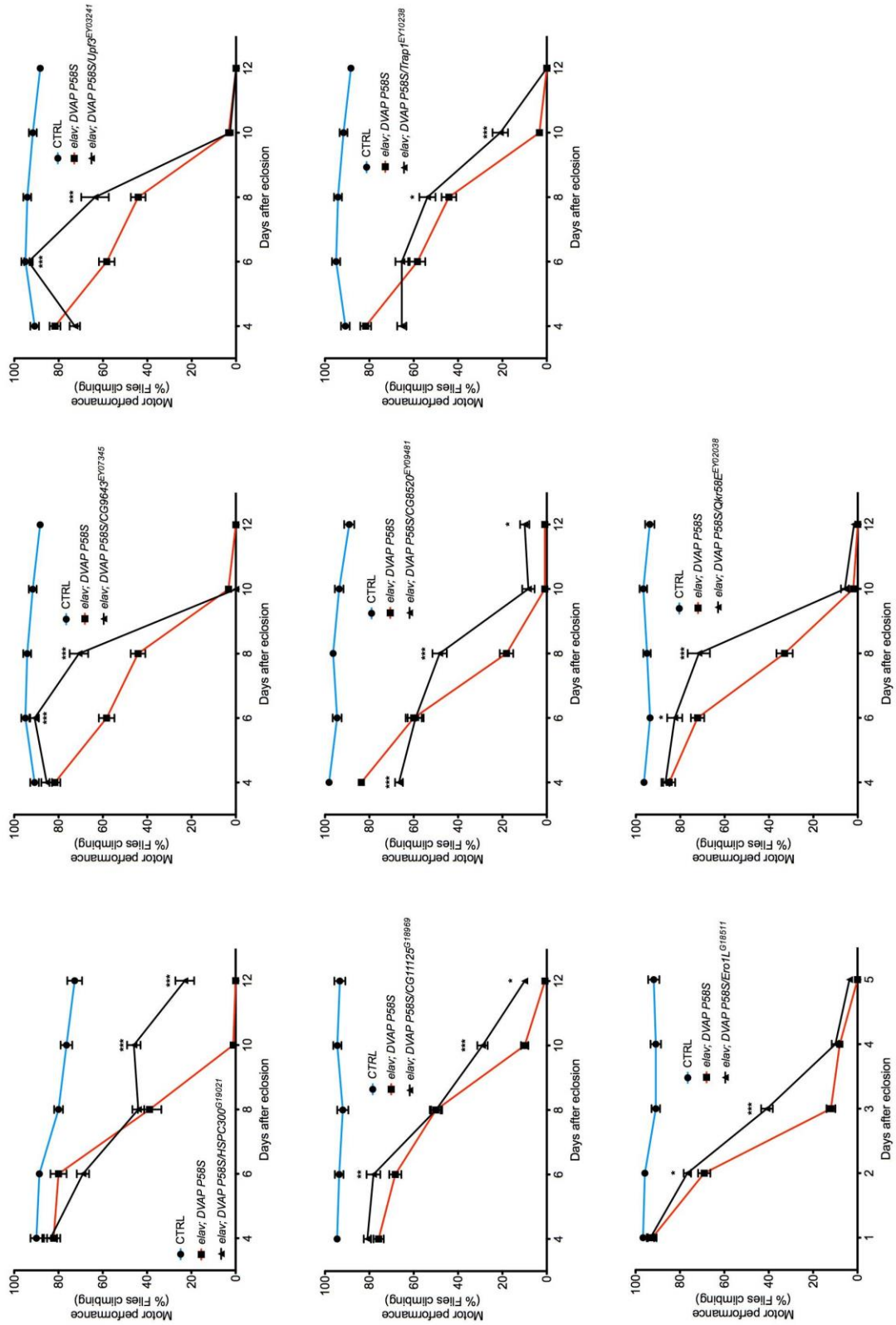
Motor performance (% Flies climbing)
Days after eclosion
CTRL
elav; DVAP P58S
elav; DVAP P58S/Upf3E703241
elav; DVAP P58S/CG9643E707345
elav; DVAP P58S/CG8520EY09481
elav; DVAP P58S/Qkr58EEY02038
elav; DVAP P58S/Trap1EY10238
elav; DVAP P58S/HSPC300G19021
elav; DVAP P58S/CG11125G18969
elav; DVAP P58S/Ero1LG18511

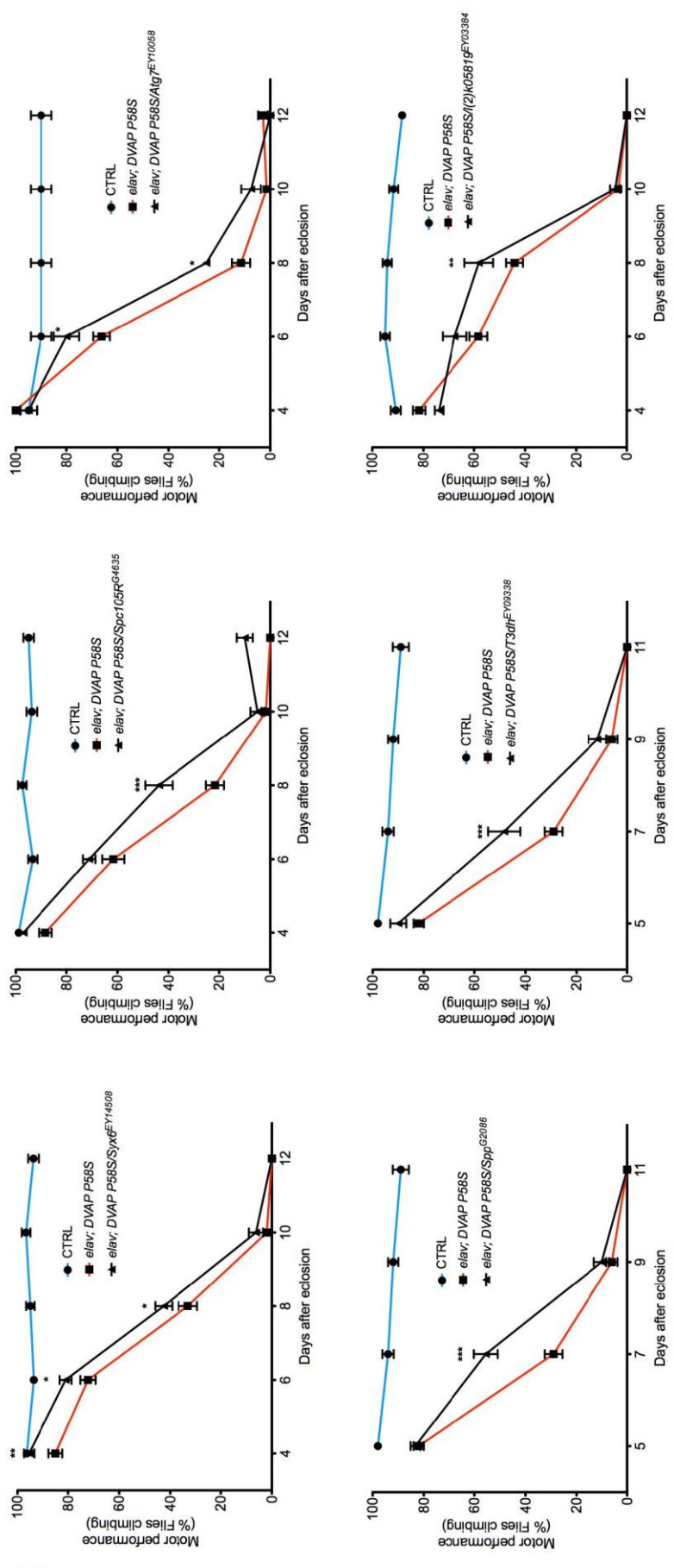
C
Motor performance
(% Flies climbing)
Days after eclosion
CTRL
elav; DVAP P58S
elav; DVAP P58S/Atg7EY10058
elav; DVAP P58S/l(2)k05819FY03384
elav; DVAP P58S/T3dhrEY09338
elav; DVAP P58S/Spc105REG4635
elav; DVAP P58S/SpdG2086
elav; DVAP P58S/SyxδEY14508

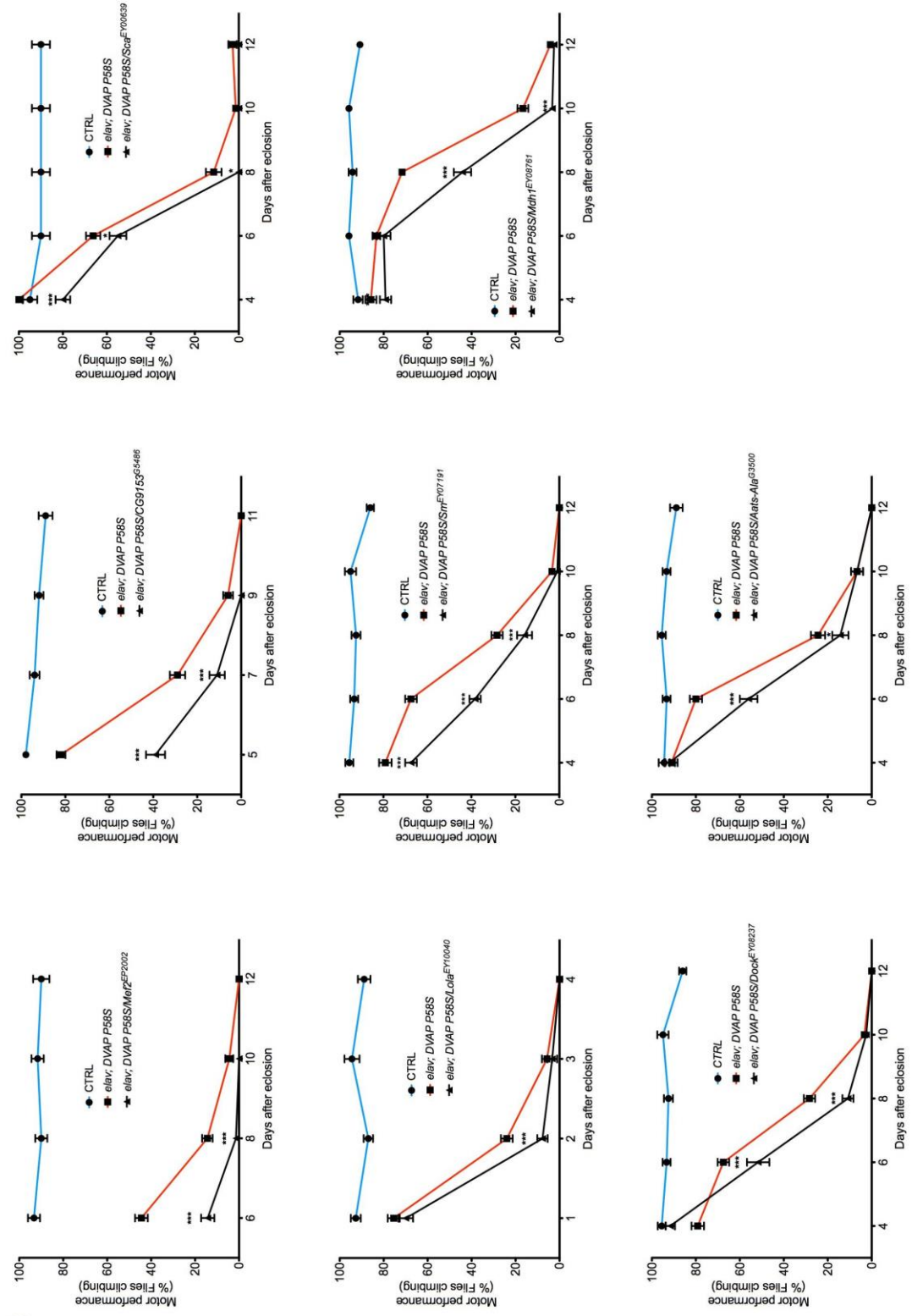
D
Motor performance (% Flies climbing)
Days after eclosion
CTRL
elav; DVAP P58S
elav; DVAP P58S/Mef2EP2002
elav; DVAP P58S/CG9153S5486
elav; DVAP P58S/Lola FY10040
elav; DVAP P58S/Sif FY07191
elav; DVAP P58S/Aats-Ala G3500
elav; DVAP P58S/Dock FY08237
elav; DVAP P58S/Scaf FY00639
elav; DVAP P58S/Mdh1 EY08761

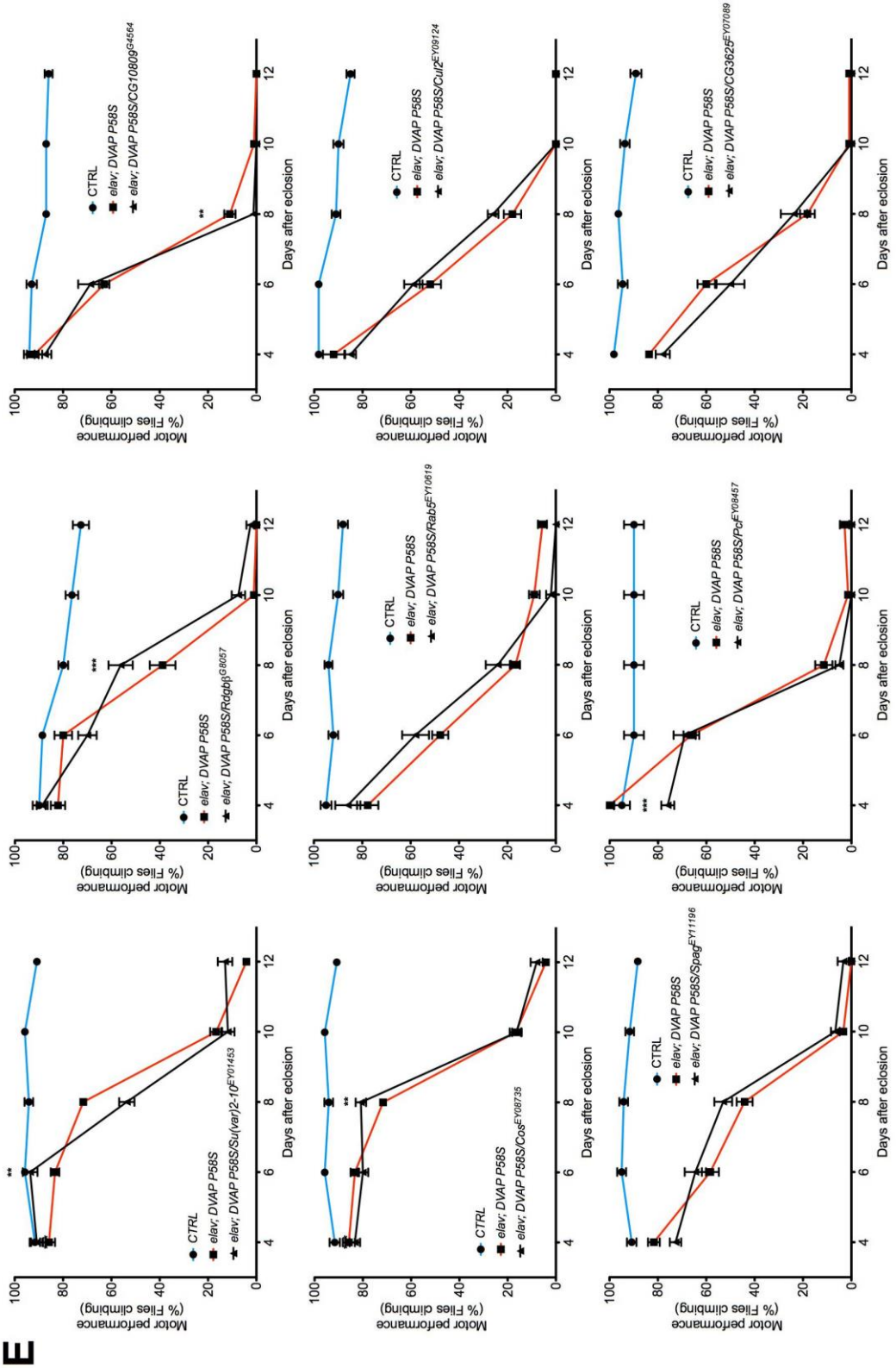
E
Motor performance (% Flies climbing)
Days after eclosion
CTRL
elav; DVAP P58S
elav; DVAP P58S/CG10809G4564
elav; DVAP P58S/Cul2EY09124
elav; DVAP P58S/CG3622SEY07089
elav; DVAP P58S/Su(var)2-10EY01453
elav; DVAP P58S/RdgbβG8057
elav; DVAP P58S/Rab5EY10619
elav; DVAP P58S/PcEY08457
elav; DVAP P58S/CosEY08735
elav; DVAP P58S/SpagEY11196

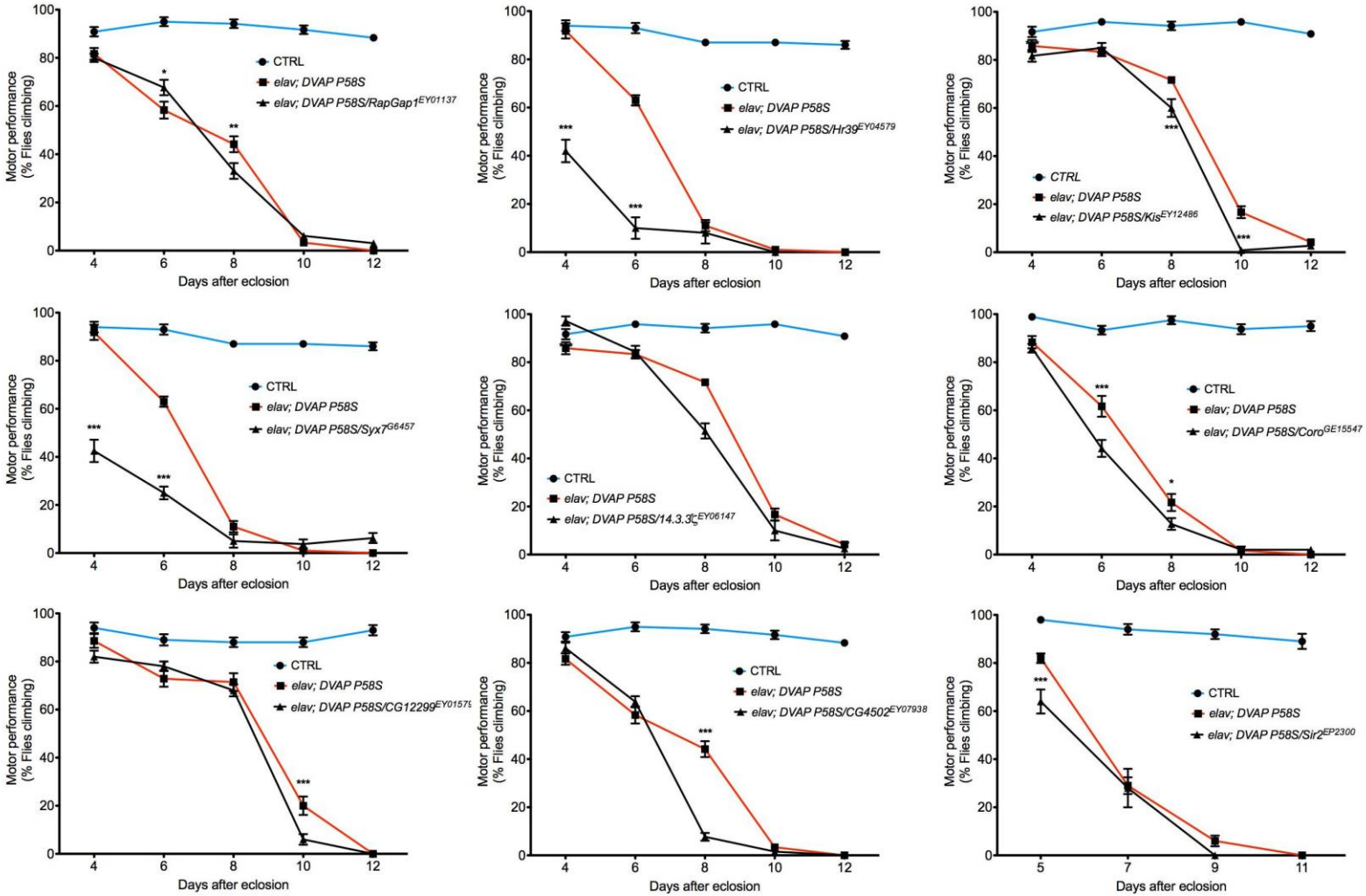
Motor performance (% Flies climbing)
Days after eclosion
CTRL
elav; DVAP P58S
elav; DVAP P58S/RapGap1EY01137
elav; DVAP P58S/Hr39EY04579
elav; DVAP P58S/KisEY12486
elav; DVAP P58S/Syx7G6457
elav; DVAP P58S/14.3.3ζEY06147
elav; DVAP P58S/CoroGE15547
elav; DVAP P58S/CG12299EY0157
elav; DVAP P58S/CG4502EY07938
elav; DVAP P58S/Sir2EP2300

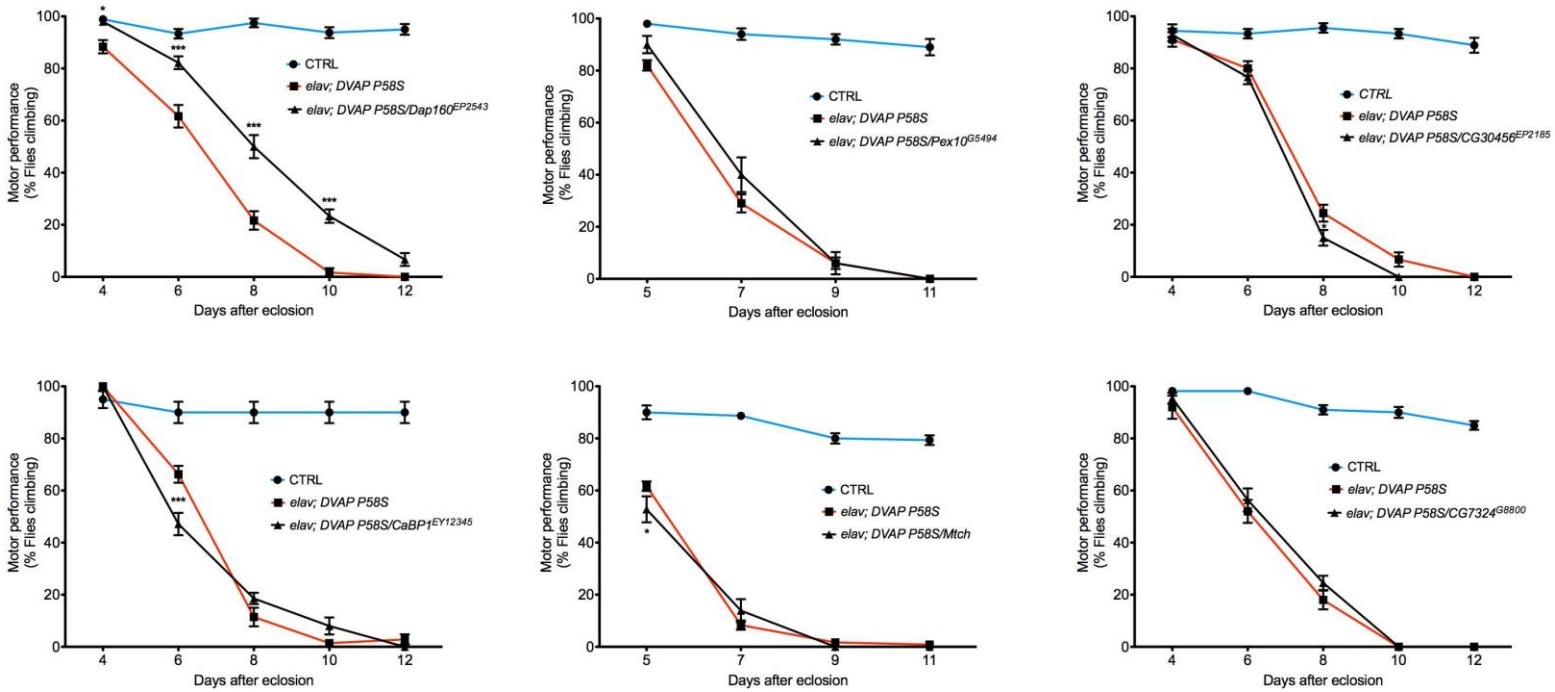
Motor performance (% Flies climbing)
Days after eclosion
CTRL
elav; DVAP P58S
elav; DVAP P58S/Dap160EP2543
elav; DVAP P58S/Pex10G5494
elav; DVAP P58S/CG30456EP2185
elav; DVAP P58S/CaBP1EY12345
elav; DVAP P58S/Mtch
elav; DVAP P58S/CG7324G8800

Figure 20. Motor performance behaviour of each of the DVAP-P58S genetic modifiers. Climbing assay was performed in flies co-expressing in the nervous system *DVAP-P58S* and each one of the genetic modifiers. Modification output in this assay was classified as suppressors showing a strong (A), intermediate (B) or weak modification effect (C), enhancers (D) and lines that did not present any effect compared to controls or did not confirm the effect observed in the primary eye screen (E). Each experimental line (black line) is compared to the tester line (red line: *(elav-GAL4/+; DVAP-P58S/+*) and to the control (blue line: *elav-GAL4;+/+*). *** $P < 0.001$, ** $P < 0.01$, * $P < 0.05$ (Two-way ANOVA).

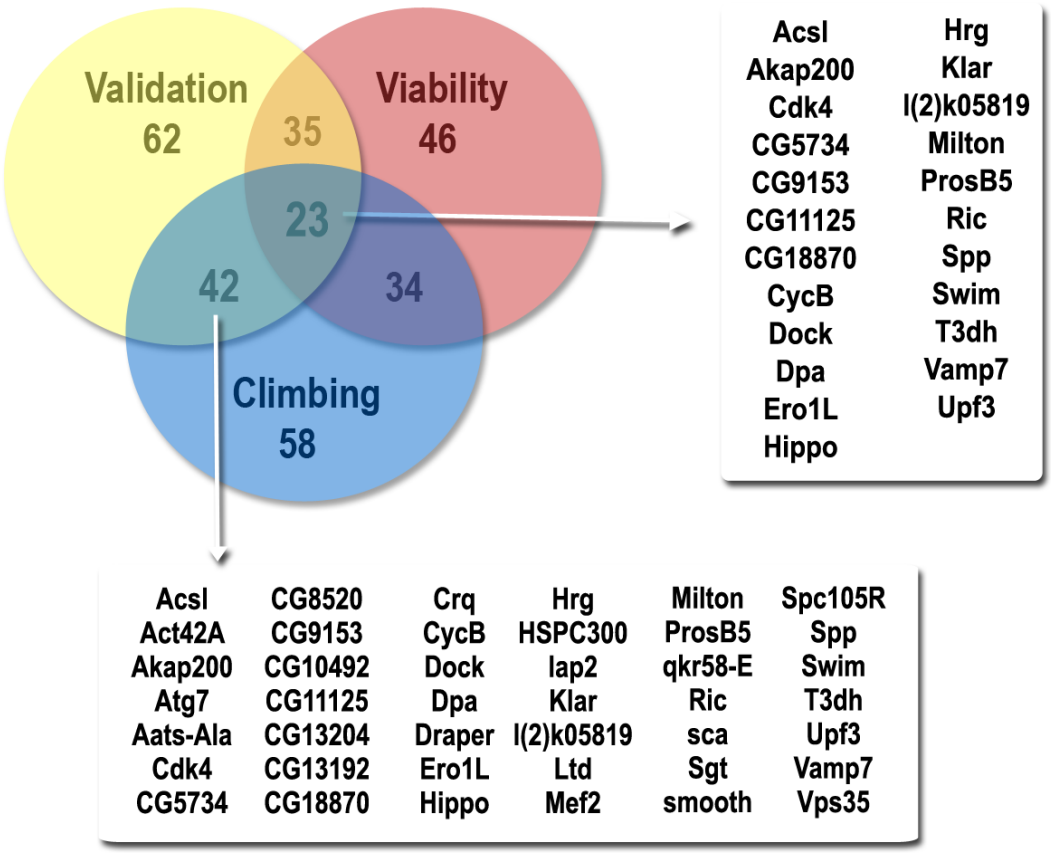

Figure 21. Summary scheme of screens and validations results. The number of positive modifiers is displayed for each of the independent allele (yellow), viability (red) and climbing assays (blue). Intersection between two circles represents the number of lines that showed positive modification in those two readouts. From an initial set of 85 modifiers, 23 were confirmed also by these three methods (white box, right). Considering the two stronger methods, 42 *bona fide* modifiers of DVAP-P58S toxicity were identified (white box, bottom).

Chapter 6: Bioinformatic analysis of the DVAP-P58S-toxicity modifier genes

6.1 Introduction

The aim of the following analyses was to further characterise the confirmed list of genetic modifiers using different bioinformatic approaches. We searched for predicted and known functions of each modifier gene, potential interactions between them and DVAP, and if these connections were translated into human orthologs of the modifiers. *In-silico* analyses are a central component of previously published genetic screens and with these approaches, we were able to connect DVAP-P58S-toxicity modifiers with relevant functional pathways.

6.2 Human orthologs and functional categories were found for most of the modifying genes

A central step in our analysis is to understand the nature of each modifier and its function in the cell. In theory, if different researchers try several unrelated approaches to study and classify the function of genes, a disorganised amount of divergent data would be potentially useless. To address this problem, the Gene Ontology consortium was created to provide a controlled vocabulary of terms to describe functions and characteristics of each gene (Ashburner *et al.*, 2000). These GeneOntology (GO) terms are grouped in three categories: *Biological process*, describes the protein's biological activity or the pathways where it is involved; *Molecular function,* referred to the biochemical nature of the protein and *Cellular component*, or the specific location of the protein inside the cell (Robinson *et al.*, 2004)

After this publication, several approaches have applied this data source to address different questions in a practical way. To study the specific gene function and protein family classification, we used the classification data base PANTHER (Protein ANalysis THrough Evolutionary Relationships), part of the GeneOntology consortium (Table 5 and 6). Through this database, we associated protein categories to each modifier gene according the function they are performing in the cell. Only 12 modifiers (13.3%) are not linked with a protein function, primarily corresponding to

non-studied Computed Genes (CG lines). Although some information regarding these genes is available and can potentially link them to relevant functional pathways, the specific nature of the proteins still remains unknown. From these categories, the presence of trafficking and SNARE proteins highlight as one the most represented groups. Also we could find an important number of kinases, which potentially can be target of chemical modulation for potential therapeutic approaches.

PANTHER also informs the best available human ortholog of the confirmed DVAP-P58S-neurodegeneration modifiers. However, several other tools have been developed over the last years to predict ortholog genes based in different approaches such as phylogeny, sequence similarity or protein-protein interaction (Hu *et al.*, 2011). The use of different algorithms can be difficult to handle and the specificity of the results can be hard to compare between all the approaches. To avoid that, we used DRSC Integrative Ortholog Prediction Tool (DIOPT), an approach that integrates all these several prediction tools and predicts the best ortholog based on the number of independent algorithms that yielded the same result (Hu *et al.*, 2011). In this case, we obtained a score showing the number of positive algorithms for that specific ortholog (Table 11). From the 85 modifiers, 77 exhibit a significant human ortholog found in at least two of the ten different algorithms. Overall these lines display a human version according most tested algorithms, giving us a strong support of the possible function of the modifiers in humans and expanding the available studies that characterise these genes. For this approach however, we took into consideration only the best human ortholog for each *Drosophila* gene according this software. Bearing in mind that more than one paralog can be found in humans for one *Drosophila* gene, the selection of only one of them under DIOPT's parameters can represent an incomplete picture of the genetic networks. However, for the following analyses the presence of this only ortholog could provide enough information to the relation of VAPB and its genetic modifiers. Most importantly, the presence of a human ortholog indicates that our data obtained in *Drosophila* can be translated into a mechanism of ALS in humans.

Drosophila Gene Name	*Drosophila* Symbol	Human Symbol	DIOPT score	Human Gene Name	Human Gene ID
Suppressors					
Hormone receptor-like in 39	Hr39	NR6A1	2	nuclear receptor subfamily 6, group A member 1	2649
Inhibitor of apoptosis 2	Iap2	BIRC2	9	baculoviral IAP repeat containing 2	329
Small glutamine-rich tetratricopeptide containing protein	Sgt	SGTB	10	small glutamine-rich tetratricopeptide repeat (TPR)-containing, alpha	6449
CG5118	CG5118	-	-	-	-
Spaghetti	Spag	RPAP3	10	RNA polymerase II associated protein 3	79657
Type III alcohol dehydrogenase	T3dh	ADHFE1	10	alcohol dehydrogenase, iron containing, 1	137872
Abrupt	ab	-	-	-	9278
Rap GTPase activating protein 1	RapGAP1	RAP1GAP2	6	RAP1 GTPase activating protein 2	23108
Rhomboid	rho	RHBDL3	5	rhomboid veinlet-like 3	162494
CG3625	CG3625	AIG1	10	androgen-induced 1	51390
CG12299	CG12299	ZNF366	3	zinc finger protein 366	167465
Upf3	Upf3	UPF3B	10	UPF3 regulator of nonsense transcripts homolog B	65109
Klarsicht	klar	-	-	-	-
Leak	lea	ROBO1	5	roundabout 1	6091
CG5734	CG5734	SNX17	10	sorting nexin 17	9784
Acyl-CoA synthetase long-chain	Acsl	ACSL3	9	acyl-CoA synthetase long-chain family member 3	2181
Actin 42A	Act42A	ACTB	6	actin, beta	60
Tejas	tej	TDRD5	3	tudor domain containing 5	1635
Inositol 1,4,5-triphosphate kinase 1	IP3K1	ITPKA	2	Inositol-trisphosphate 3-kinase A	3706
Costa	cos	KIF7	4	Kinesin family member 7	374654
CG13204	CG13204	-	-	-	-
Retinal degeneration B β	rdgBβ	PITPNC1	9	phosphatidylinositol transfer protein cytoplasmic 1	26207
Suppressor of variegation 2-10	Su(var)2-10	PIAS1	9	protein inhibitor of activated STAT, 1	8554
14-3-3ζ	14-3-3ζ	YWHAZ	9	tyrosine 3-monooxygenase/tryptophan 5-monooxygenase activation protein, zeta	7534
Vacuolar protein sorting 35	Vps35	VPS35	10	vacuolar protein sorting 35 homolog	55737
Spc105-Related	Spc105R	-	-	-	-
CG15630	CG15630	NCAM1	2	neural cell adhesion 1	4684
Signal peptide peptidase	spp	HM13	9	histocompatibility (minor) 13	81502
Milton	milt	TRAK1	10	trafficking protein, kinesin binding 1	22906
Syntaxin 6	Syx6	STX6	10	Syntaxin 6	10228
Silent information regulator2	Sir2	SIRT1	8	sirtuin 1	23411
Vesicle-associated membrane protein 7	Vamp7	VAMP7	9	vesicle-associated membrane protein 7	6845
Female sterile (2) Ketel	Fs(2)Ket	KPNB1	10	karyopherin (importin) beta 1	3837
lethal (2) k05819	l(2)k05819	KIAA0195	9	KIAA0195	9772
Hippo	hpo	STK3	9	serine/threonine kinase 3	6788
CG10809	CG10809	ANKRD54	6	ankyrin repeat domain 54	129138
Ras which interacts with calmodulin	Ric	RIT2	9	Ras-like without CAAX 2	6014
quaking related 58E-3	qkr58E-3	KHDRBS1	4	KH domain containing, RNA binding, signal transduction associated 1	10657
Cyclin-dependent kinase 4	Cdk4	CDK6	9	cyclin-dependent kinase 6	1021
CG18870	CG18870	-	-	-	-
Secreted Wg-interacting molecule	Swim	TINAGL1	9	tubule-interstitial nephritis antigen-like	64129
CG9643	CG9643	METTL10	6	methyltransferase like 10	399818
CG4896	CG4896	RBM5	8	RNA binding motif protein 5	10181
Polycomblike	Pcl	MTF2	8	Metal response element binding transcription factor 2	22823
CG8520	CG8520	LACE1	10	lactation elevated 1	246269
hiiragi	hrg	PAPOLG	8	poly(A) polymerase gamma	64895
disc proliferation abnormal	dpa	MCM4	9	minichromosome maintenance complex component 4	4173
Ero1-like protein	Ero1L	ERO1LB	7	ERO1-like beta	56605

Drosophila Gene Name	*Drosophila* Symbol	Human Symbol	DIOPT score	Human Gene Name	Human Gene ID
olf186-F	olf186-F	ORAI1	10	ORAI calcium release-activated calcium modulator 1	84876
Autophagy-specific gene 7	Atg7	ATG7	10	autophagy related 7	10533
CG13192	CG13192	GNB1L	9	guanine nucleotide binding protein, beta polypeptide 1-like	4584
Ubiquitin-conjugating enzyme E2Q-like	CG4502	UBE2QL1	7	ubiquitin-conjugating enzyme E2Q family-like 1	134111
Cullin-2	Cul-2	CUL2	10	cullin 2	8453
CG10492	CG10492	ZCCHC2	2	zinc finger, CCHC domain containing 2	54877
Croquemort	crq	SCARB1	3	scavenger receptor class B, member 1	949
CG11125	CG11125	ENKD1	7	enkurin domain containing 1	84080
Auxilin	Aux	GAK	10	cyclin G associated kinase	2580
Rab5	Rab5	RAB5A	9	RAB5A, member RAS oncogene family	5868
A kinase anchor protein 200	Akap200	-	-	-	65108
Syntaxin 7	Syx7	STX7	9	syntaxin 7	8417
Syntaxin interacting protein 1	HSPC300	BRK1	6	BRICK1, SCAR/WAVE actin-nucleating complex subunit	55845
Trap1	Trap1	TRAP1	10	TNF receptor-associated protein 1	10131
Draper	drpr	MEGF11	9	multiple EGF-like-domains 11	84467
kismet	kis	CHD7	9	chromodomain helicase DNA binding protein 6	55636
Enolase	Eno	ENO1	9	enolase 1, (alpha)	2023
Cyclin B	CycB	CCNB1	6	cyclin B1	891
Src oncogene at 42A	Src42A	FRK	9	Fyn-related kinase	2444
Proteasome subunit beta 5	Prosβ5	PSMB5	10	proteasome (prosome, macropain) subunit beta, type, 5	5693
Coronin	coro	CORO1C	8	coronin, actin binding protein, 1C	23603
connector enhancer of ksr	cnk	CNKSR2	7	connector enhancer of kinase suppressor of Ras 2	22866
Lightoid	ltd	RAB32	6	member RAS oncogene family 32	10981
Enhancers					
scabrous	sca	FGA	2	fibrinogen alpha chain	2243
Smooth	sm	HNRPL	8	heterogeneous nuclear ribonucleoprotein L	3191
longitudinals lacking	lola	-	-	-	-
Myocyte-specific enhancer factor 2	Mef2	MEF2A	7	myocyte enhancer factor 2A	4205
CG7324	CG7324	TBC1D9	8	TBC1 domain family, member 9	23158
Mitochondrial carrier homolog 1	Mtch	MTCH2	10	mitochondrial carrier 2	23788
Peroxisome biogenesis factor 10	Pex10	PEX10	10	peroxisomal biogenesis factor 10	5192
calcium-binding protein 1	CaBP1	PDIA6	10	protein disulfide isomerase family A, member 6	10130
Dynamin associated protein 160	Dap160	ITSN1	9	intersectin 1 (SH3 domain protein)	6453
Malate dehyrogenase	Mdh1	MDH1	10	malate dehydrogenase 1, NAD (soluble)	4190
Alanyl-tRNA synthetase	Aats-ala	AARS	10	alanyl-tRNA synthetase	16
CG9153	CG9153	HERC4	9	HECT and RLD domain containing E3 ubiquitin protein ligase 4	26091
Dreadlocks	dock	NCK1	10	NCK adaptor protein 1	4690
CG30456	CG30456	PLEKHG4	2	pleckstrin homology domain containing, family G, member 4	25894

Table 11. Human orthologs of the DVAP-P58S genetic modifiers.

6.3 GeneOntology terms enrichment associates DVAP toxicity with cell death, vesicle recycling and other biological process

Over the last years, several genomic and proteomic studies in *Drosophila* have provided data that link genes to functional pathways and highlight interactions between proteins. To generate hypotheses regarding potential functions of the confirmed modifiers, we used two different approaches. The Database for Annotation, Visualization and Integrated Discovery (DAVID) is a NIH-based database that provides a comprehensive set of tools to analyse and integrate GeneOntology terms (Huang *et al.*, 2008). Through DAVID, we were able to discover enriched functional groups and GO terms, starting from a gene set. GeneMANIA on the other hand is another tool based on the GeneOntology consortium (Warde-Farley *et al.*, 2010). This tool collects 60 *Drosophila* data sets from other databases (BioGRID, Gene Expression Omnibus, Pathways Commons and I2D) to create connections between fly genes using their gene functions and reported interactions, determining the most enriched categories in a specific data set. Firstly we studied the most enriched functional categories using DAVID.

We analysed the 85 DVAP-P58S-toxicity modifiers with this database and found 41 significant, non-redundant GeneOntology (GO) functional categories, including 3 Molecular Function terms and only 2 Cell Compartment term: Lipid Particle and Endosome. Interestingly, the best ranked, non-redundant categories are related with Vesicle metabolism, signaling and development (Figure 22). When this analysis was performed with GeneMANIA, similar results were obtained, with the same most enriched categories reported. Notably the most enriched annotation cluster, an analysis used to filter out redundant terms, also predicts Endosome and Cell signaling as the most important category found in the screen. Relevant genes part of this group are the vacuolar protein sorting *Vps35*, syntaxins *Syx6* and *Syx7*, the signal transducer *scabrous* and the vesicle and RAS-related protein *Rab5*.

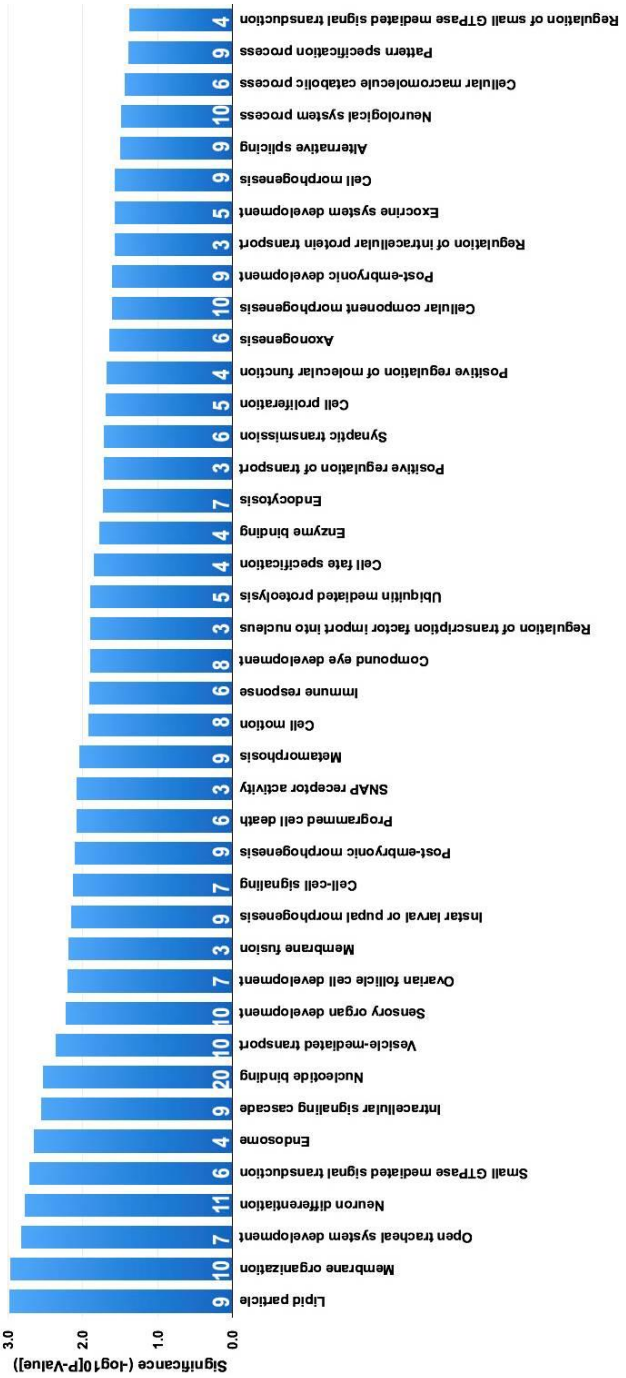

Figure 22. Functional categories overrepresented in the genetic modifiers list. GeneOntology terms associated with all the genes found in the screen were analysed with the bioinformatic database DAVID. A total of 41 significantly enriched terms were found with a significance cutoff of 0.05, where the significance is expressed as the $-\log_{10}$ (P values). Numbers in white represent the number of genes in each specific category. Most enriched categories are related to vesicle trafficking, lipids and development.

6.4 Gene network analyses reveal known interaction between the modifiers and predict potential involved pathways

A comprehensive gene network was built with all the DVAP-P58S-modifier genes, based on the co-localisation, physical, genetic and predicted interaction *Drosophila* datasets integrated in the GeneMANIA database and visualized with the software Cytoscape (Shannon *et al.*, 2003) (Figure 23). Only a small group of significant interactions linked DVAP with its genetic modifiers. Nevertheless, important previously reported links were found, associating genes with significant GO functions and DVAP. These interactions can potentially lead to describe the way the modifiers can alter DVAP-induced neurodegeneration.

By further exploring this gene network, we observed that seven of the modifiers physically interact with DVAP. This group of genes (CG7324, Syx7, Ero1L, Rab5, CG5118, rho and Spp) shows a stronger evidence of a potential interaction with DVAP, considering that we are now adding a second connection with the genetic interaction found in the screen.

To confirm the results observed in this gene network and at the same time, predict novel genes that can potentially interact with the modifier genes and DVAP, we used as a parallel approach STRING. This is another database that predicts and report protein interactions, based on high-throughput experiments and genomic context (Jensen *et al.*, 2009). In the created network, DVAP appears connected with Autophagy, vesicle recycling and Cell proliferation clusters, including several predicted new interactors. Other significant clusters involve Proteasome activity, Translational initiation and the Notch pathway (Figure 24).

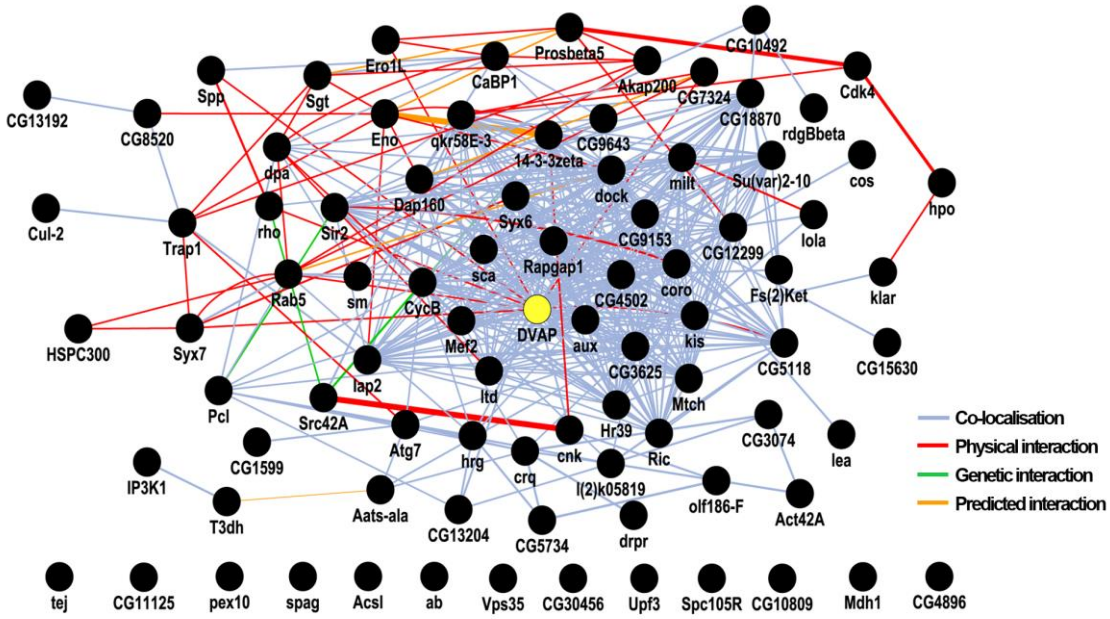

Figure 23. Interaction network of DVAP-P58S modifier genes. All the DVAP-genetic modifiers were connected using previously reported *Drosophila* data sets with GeneMANIA. Genetic modifiers were connected using previous available co-localisation (blue), physical (red), genetic (green) or predicted (orange) interaction data. In the network, DVAP (yellow circle) corresponds to a node already connected to some of its modifiers. A group of 13 modifiers do not present previously reported interaction information. Strength of the interaction was automatically weighted by the software and it is graphically displayed with different thickness of the connecting lines.

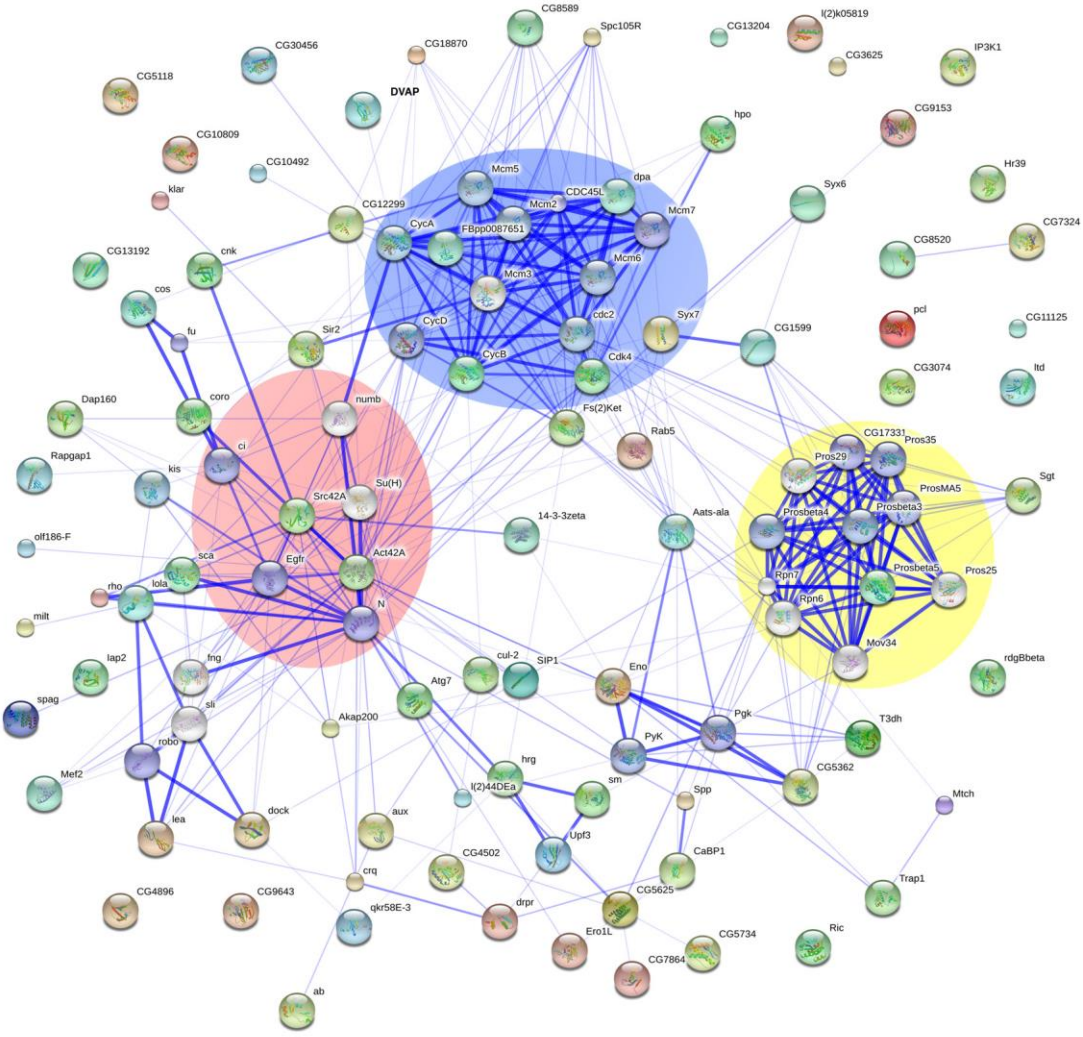

Figure 24. Interaction network of DVAP-neurodegeneration modifier genes and predicted candidate interactors. Interaction network based on high-throughput *Drosophila* data sets collected by the database STRING. Interactions between DVAP-modifier proteins and predicted interactors are displayed as components of this network. These connections gather predicted and observed modifiers in relevant protein clusters, including Notch (red area), Proteasome (yellow) and Cell cycle regulation (blue) pathways.

6.5 Ingenuity pathway analysis suggests that functions and interactions of DVAP genetic modifiers are conserved in humans

These bioinformatic analyses of *Drosophila* modifiers gave us several new paths to understand DVAP-linked toxicity. To further explore the implications of these connections among genes but in a higher context, we used Ingenuity Pathway Analysis (IPA). This software is based on previously reported data of human proteins and the way they associate to diseases, mechanisms and functions. In this way, the relation between our modifier set and disease-related pathways was studied with more detail and supporting information. From the original 85 *Drosophila* modifiers, 77 human orthologs were found (Table 11) and were used to the IPA analysis.

Functional categories analysis provided the most enriched pathways found in the screen and the genes that are part of them. Significance level and number of subcategories involved are also displayed in the Table 12. Consistent with what we observed in the *Drosophila* bioinformatic analyses, the most enriched pathways are related to Cell death, assembly and organization, with specific relevance of Fusion of vesicles, endosomes and lysosomes, as well as apoptosis and autophagosomes. Also are mentioned as significant categories Protein trafficking, Cell growth and Development.

To gather further information about our genes and pathways, we looked for predicted upstream regulators of our modifiers and their pathways. Significant transcription factors as TP53, FOS and several kinase inhibitors and chemicals drugs are predicted as potential modifiers of the DVAP-genetic interactors. Interestingly, SOD1, another ALS-causative gene, is an upstream regulator of four DVAP modifiers and its human ortholog, VAPB (Table 13). These factors can potentially affect DVAP relation with its modifiers but it is an important starting point to test novel pharmaceutical targets to affect VAPB toxicity and ALS pathogenesis.

Functional Category	Sub	P-value range	Molecules	NM
Cancer	21	3.97E-3 - 4.03E-2	ACSL3,AIG1,ATG7,BIRC2,CCNB1,CDK6,CHD7, ENO1,FGA,FRK,HM13,HNRNPL,ITSN1,KHDRBS1, KIF7,MCM4,MDH1,MEF2A,MTCH2,NCAM1,NCK1, ORAI1,PAPOLG,PDIA6,PIAS1,PSMB5,RBM5, RHBDL3,RIT2,ROBO1,SCARB1,SIRT1,TBC1D9, TRAK1,TRAP1,UPF3B,VPS35,YWHAZ	38
Carbohydrate Metabolism	9	3.97E-3 - 4.66E-2	ITPKA,PITPNC1,RAB5A,SCARB1,SIRT1,VAMP7	6
Cardiovascular System Development and Function	12	9.12E-4 - 4.77E-2	BIRC2,CDK6,MEF2A,NCK1,NR6A1,SCARB1, SIRT1,STK3,STX6,STX7,YWAHZ	11
Cell Cycle	17	3.97E-3 - 4.66E-2	CCNB1,CDK6,ITSN1,MCM4,MTCH2,PSMB5,SIRT1, TDRD5	8
Cell Death and Survival	48	1.28E-5 - 4.97E-2	AARS,ACTB,ATG7,BIRC2,CCNB1,CDK6,CUL2, ENO1,FGA,ITSN1,KHDRBS1,MDH1,MEF2A, NCAM1,NCK1,ORAI1,PIAS1,RAB32,RAB5A,RBM5, SCARB1,SIRT1, STK3, TDRD5,TRAP1,VAPB,YWHAZ	27
Cell Morphology	40	8.34E-4 - 4.69E-2	ACTB,ATG7,BIRC2,CDK6,FRK,IPTKA,ITSN1,KPNB1, NCAM1,NCK1,ORAI1,PLEKHG4,RAB5A,RIT2, ROBO1,SCARB1,SIRT1,STX6,TBC1D9,TDRD5, VAMP7,YWHAZ	22
Cell-To-Cell Signaling and Interaction	24	3.97E-3 - 3.63E-2	ATG7,BIRC2,FGA,IPTKA,NCAM1,RAB5A,SCARB1, SIRT1,VAMP7	9
Cellular Assembly and Organization	74	6.51E-5 - 4.69E-2	ACTB,ATG7,BRK1,CCNB1,CDK6,CHD7,CORO1C, FGA, FRK,GAK,ITPKA,ITSN1,KPNB1,MCM4,MEF2A, NCAM1,NCK1,PEX10,PLEKHG4,RAB32,RAB5A, RIT2,ROBO1,SCARB1,SIRT1,STX6,STX7,VAMP7, YWAHZ	29
Cellular Compromise	8	3.97E-3 - 3.90E-2	ATG7,KPNB1,NCAM1,SCARB1,SIRT1,VAMP7	6
Cellular Development	46	5.49E-4 - 4.69E-2	ACTB,ANKRD54,ATG7,BIRC2,CDK6,CHD7,ENO1, FGA,GAK,HERC4,HNRNPL,ITSN1,KHDRBS1,KIF7, MEF2A,NCAM1,NCK1,NR6A1,ORAI1,PIAS1,PSMB5, RBM5,RIT2,ROBO1,SCARB1,SIRT1,STK3,TDRD5, VAMP7,VAPB	31
Cellular Function and Maintenance	58	9.89E-5 - 4.69E-2	ACTB,ATG7,BIRC2,BRK1,CCNB1,CORO1C,FGA, GAK,HNRNPL,ITPKA,ITSN1,KPNB1,MDH1,NCAM1, NCK1,ORAI1,PEX10,PLEKHG4,RAB5A,RIT2,ROBO1, SCARB1, SIRT1,SNX17,STX6,STX7,TBC1D9,VAMP7	28

Functional Category	Sub	P-value range	Molecules	NM
Cellular Growth and Proliferation	24	3.72E-3 - 4.66E-2	AARS,ACTB,ATG7,BIRC2,BRK1,CCNB1,CDK6, CUL2,ENO1,ERO1LB,FRK,GAK,HNRNPL,ITSN1, KHDRBS1,MCM4,NCAM1,NCK1,NR6A1,ORAI1, PIAS1,RBM5,ROBO1,SCARB1,SIRT1,STK3,STX6, TRAP1	28
Cellular Movement	22	1.68E-3 - 4.19E-2	ACTB,BRK1,CCNB1,CDK6,CORO1C,FGA,FRK, HNRNPL,ITPKA,ITSN1,KHDRBS1,MTCH2, NCAM1,NCK1,ORAI1,RAB5A,ROBO1,SCARB1, SIRT1,SNX17,STX6,STX7,YWHAZ	23
Connective Tissue Development and Function	11	5.49E-4 - 4.66E-2	ACTB,CCNB1,CDK6,CHD7,GAK,ITSN1,KHDRBS1, MCM4,NCK1,PIAS1,SIRT1,SNX17	12
Developmental Disorder	23	3.41E-3 - 4.66E-2	ACTB,ATG7,CCNB1,CHD7,FGA,KIF7,ORAI1,PEX10, PSMB5,SCARB1,SIRT1,TDRD5,UPF3B	13
Embryonic Development	27	4.28E-4 - 4.69E-2	ATG7,BIRC2,CDK6,CHD7,HERC4,ITSN1,NCAM1, NR6A1,ROBO1,SCARB1,SIRT1,STK3,TDRD5,VAMP7	14
Hematological Disease	13	3.97E-3 - 3.90E-2	ACTB,CDK6,CHD7,ENO1,FGA,MCM4,NCAM1, PDIA6, PSMB5,SCARB1,STK3,YWHAZ	12
Hereditary Disorder	23	8.20E-4 - 4.66E-2	AARS,ACTB,FGA,GNB1L,KIF7,MCM4,MDH1, MEF2A,NCAM1,ORAI1,PEX10,PSMB5,RAB32,RIT2, ROBO1, SIRT1,TDRD5,TRAK1,UPF3B,VAPB,VPS3	21
Infectious Disease	10	1.58E-2 - 3.90E-2	ACTB,ATG7,FGA,GAK,ITPKA,KHDRBS1,KPNB1, PDIA6,RAB32,RAB5A,RBM5,RIT2,SCARB1,SIRT1, UPF3B,VAPB	16
Inflammatory Response	17	3.97E-3 - 4.66E-2	ACTB,ATG7,BIRC2,CORO1C,ENO1,FGA,NCAM1, RAB5A,SCARB1,SIRT1,VAMP7	11
Lipid Metabolism	49	8.03E-4 - 4.95E-2	ACSL3,ATG7,MDH1,NCAM1,PIAS1,PITPNC1, RAB5A, SCARB1,SIRT1,VAMP7	10
Molecular Transport	48	9.89E-5 - 4.39E-2	ACSL3,ADHFE1,ANKRD54,ATG7,FRK,ITSN1, KHDRBS1,KPNB1,MDH1,NCAM1,ORAI1,PEX10, PITPNC1,RAB5A,SCARB1,SIRT1,STX6,STX7,TRAK1, TRAP1,VAMP7, YWHAZ	22
Nervous System Development and Function	49	9.99E-4 - 4.69E-2	ACTB,ATG7,CDK6,CHD7,FGA,FRK,GNB1L,ITPKA, ITSN1,KHDRBS1,NCAM1,NR6A1,NCK1,RAB5A, RIT2,ROBO1, SIRT1,STK3,STX7,VAMP7,YWHAZ	21
Neurological Disease	27	8.20E-4 - 4.66E-2	AARS,ACTB,AIG1,ATG7,BIRC2,CCNB1,CHD7, CNKSR2,GNB1L,KIF7,MDH1,NCAM1,PITPNC1, PSMB5,RAB5A,RAB32,RIT2,ROBO1,SCARB1,SGTB, SIRT1,TRAK1, UPF3B,VAPB,VPS35,YWHAZ	26

Functional Category	Sub	P-value range	Molecules	NM
Organismal Development	27	4.28E-4 - 4.77E-2	ATG7,BIRC2,CDK6,CHD7,HERC4,ITSN1,KHDRBS1, MEF2A,NCAM1,NR6A1,ORAI1,PIAS1,ROBO1, SCARB1, SIRT1,STK3,TDRD5	17
Organismal Injury and Abnormalities	24	3.41E-3 - 4.66E-2	AARS,AIG1,ATG7,CCNB1,CDK6,CHD7,ENO1,FGA, KHDRBS1,KIF7,MCM4,MEF2A,MTCH2,PIAS1, ROBO1,SCARB1,SIRT1,STX7,TBC1D9,TDRD5, TRAK1,YWHAZ	22
Protein Trafficking	7	5.49E-4 - 4.28E-2	KPNB1,PEX10,RAB5A,STX6,STX7,TRAK1,VAMP7	7
Reproductive System Disease	14	3.41E-3 - 4.28E-2	AIG1,ATG7,CCNB1,CDK6,CHD7,ENO1,FGA,ITTPKA, KHDRBS1,MCM4,MEF2A,MTCH2,PDIA6,PIAS1, RAB5A,RIT2,ROBO1,SCARB1,SIRT1,STX7,TBC1D9, TDRD5, TRAK1,UPF3B,YWHAZ	25
Skeletal and Muscular Disorders	13	3.97E-3 - 4.66E-2	AARS,ACTB,CHD7,FGA,KIF7,MEF2A,PSMB5,SIRT1, VAPB,VPS35	10
Small Molecule Biochemistry	58	8.03E-4 - 4.95E-2	ACSL3,ATG7,CCNB1,FRK,ITPKA,MDH1,NCAM1, PIAS1, PITPNC1,RAB5A,SCARB1,SIRT1,VAMP7	13
Tissue Development	55	4.28E-4 - 4.69E-2	ATG7,BIRC2,CDK6,CHD7,FGA,FRK,HERC4,ITPKA, ITSN1,NCAM1,NCK1,NR6A1,RAB5A,RIT2,ROBO1, SCARB1,SIRT1,STK3,TDRD5,VAMP7,YWHAZ	21

Table 12. Ingenuity pathway analysis enriched functional categories for DVAP modifiers human orthologs. *Sub* column displays the number of subcategories included in the main functional category. Significance level of each of these subcategories is between the values presented in *P-value range* column. Number of modifier human ortholog (*NM*) reflects the number found in all the significant subcategories from the enriched functional categories.

Upstream Regulator	Molecule Type	P-value	Target molecules
IL31	other	1.10E-05	CCNB1,CDK6,MCM4
miR-181a-5p (and other miRNAs w/seed ACAUUCA)	mature microRNA	5.95E-05	ATG7,CHD7,CNKSR2,ITSN1,KIAA0195,KPNB1, MEF2A,NR6A1,PAPOLG,SGTB,SIRT1,TBC1D9, TRAK1,YWHAZ
panobinostat	chemical drug	1.08E-04	CCNB1,CDK6,YWHAZ
IND S7	chemical - kinase inhibitor	1.21E-04	ACTB,ENO1,HNRNPL
TP53	transcription regulator	1.22E-04	ACSL3,ACTB,ATG7,BIRC2,CCNB1,KPNB1, MCM4,NR6A1,PDIA6,ROBO1,SGTB,SIRT1, TINAGL1,TRAP1
MEL S3	chemical - kinase inhibitor	1.35E-04	ACTB,ENO1,HNRNPL
miR-421-3p (and other w/seed UCAACAG)	mature microRNA	2.23E-04	ACSL3,CDK6,CHD7,CORO1C,FRK,PAPOLG, UBE2QL1,VAMP7
SMOC2	other	2.43E-04	CCNB1,MCM4
desmopressin	biologic drug	2.66E-04	ACTB,ENO1,STX7,YWHAZ
T3-TR-RXR	complex	3.82E-04	ENO1,FGA,SCARB1
SOD1	enzyme	4.28E-04	ACTB,GAK,PSMB5,SIRT1,VAPB
miR-190a-5p (and other w/seed GAUAUGU)	mature microRNA	7.33E-04	ATG7,CHD7,MEF2A,PAPOLG,VAPB
BAX	transporter	7.70E-04	BIRC2,CCNB1,PDIA6
NDUFA13	enzyme	8.92E-04	CCNB1,MCM4
miR-204-5p	mature microRNA	8.99E-04	ATG7,BIRC2,CORO1C,KHDRBS1,RAP1GAP2, ROBO1,SIRT1,VAPB,YWHAZ
picropodophyllin	chemical drug	1.04E-03	CCNB1,CDK6
asiatic acid	chemical reagent	1.04E-03	CCNB1,SIRT1
KITLG	growth factor	1.11E-03	ACTB,FRK,KPNB1,ORAI1,PSMB5
D-glucose	chemical - endogenous mammalian	1.53E-03	AARS,ACTB,CCNB1,ENO1,ERO1LB,PDIA6, SIRT1
ellagic acid	chemical - endogenous non-mammalian	1.54E-03	CDK6,SCARB1
FOS	transcription regulator	1.55E-03	ENO1,FGA,GAK,PIAS1,STK3,VAMP7,YWHAZ
IND S1	chemical - kinase	2.59E-03	ACTB,ENO1
nocodazole	chemical reagent	3.07E-03	CCNB1,KHDRBS1,STK3

Table 13. Significant upstream regulators of DVAP modifiers human orthologs predicted by Ingenuity Pathway Analysis.

ALS is a complex disorder that shares symptoms and mutations with other neurodegenerative diseases. If VAPB-interactors affect the function of the protein in ALS, we may think that they may also be involved in other disorders as well. To study this idea, we searched in the public databases OMIM and GWAS for the connection between human alleles and genetic disorders. Interestingly, seventeen genes are already associated with different disorders (Table 14). Among these, neurodegenerative diseases are an important group with mutations found in Parkinson's disease, multiple sclerosis and spinocerebellar ataxia 31. Curiously, AARS, the human ortholog of Aats-ala, has been associated with Charcot-Marie-Tooth disease, a disease that extensively overlaps with ALS phenotypes. These overlapping genes can represent a currently unknown link between ALS and other diseases, especially for the ones that have been associated previously with patients carrying both disorders.

Finally, human orthologs of the DVAP genetic modifiers were analysed with supporting information to create functional networks between them. The genes were processed with the highest stringency, using only non-predicted, experimental and direct interaction between them, excluding signaling and indirect interactions. This map (Figure 25) shows interaction between 32 of the human orthologs including some well-connected nodes. YWHAZ, the ortholog of 14-3-3ζ, works as a central node of a cluster that connects VAPB with STK3, human version of Hippo. This link could work as a central way to understand the connection of VAPB with the rest of its genetic modifiers. Other functions associated with this cluster include lipid metabolism and RAS signaling pathway. Also well connected we can find proteins related with vesicles and endocytosis, in the central network (RIT2, RAB5A, ITSN1) or as an independent cluster (VAMP7, STX6, STX7).

Human symbol	*Drosophila* symbol	Disease	Phenotype MIM number	Source
UPF3B	Upf3	Mental retardation, X-linked, syndromic 14	300676	OMIM
ACTB	Act42A	Baraitser-Winter syndrome 1 Dystonia, juvenile-onset	243310 607371	OMIM OMIM
KIF7	Cos	Acrocallosal syndrome Joubert syndrome 12 Hydrolethalus syndrome 2	200990 200990 614120	OMIM OMIM OMIM
PIAS1	Su(Var)2-10	Major depressive disorder	-	GWAS
YWHAZ	14-3-3 ζ	Attention deficits Hyperactivity disorder Conduct disorder	- - -	GWAS GWAS GWAS
VPS35	Vps35	Parkinson disease 17	614203	OMIM
KPNB	Fs(2)Ket	Multiple sclerosis	-	GWAS
STX6	Syx6	Progressive supranuclear palsy	-	GWAS
RIT2	Ric	Cognitive performance Parkinson's disease	- -	GWAS GWAS
MCM4	dpa	Natural killer cell and glucocorticoid deficiency with DNA repair defect	609981	OMIM
GAK	Aux	Parkinson's disease	-	GWAS
CHD7	Kis	CHARGE syndrome	214800	OMIM
ENO1	eno	Autism spectrum disorder Attention deficit Schizophrenia	- - -	GWAS GWAS GWAS
FGA	sca	Amyloidosis, hereditary renal	105200	OMIM
PEX10	Pex10	Peroxisome biogenesis disorder 1A Peroxisome biogenesis disorder 2B Peroxisome biogenesis disorder 6A	214100 202370 614870	OMIM OMIM OMIM
AARS	Aats-ala	Charcot-Marie-Tooth disease, axonal, type 2N	613287	OMIM
PLEKHG4	CG9153	Spinocerebellar ataxia 31	117210	OMIM

Table 14. Genetic disorders associated with the human orthologs of the DVAP-modifiers according to OMIM and GWAS databases.

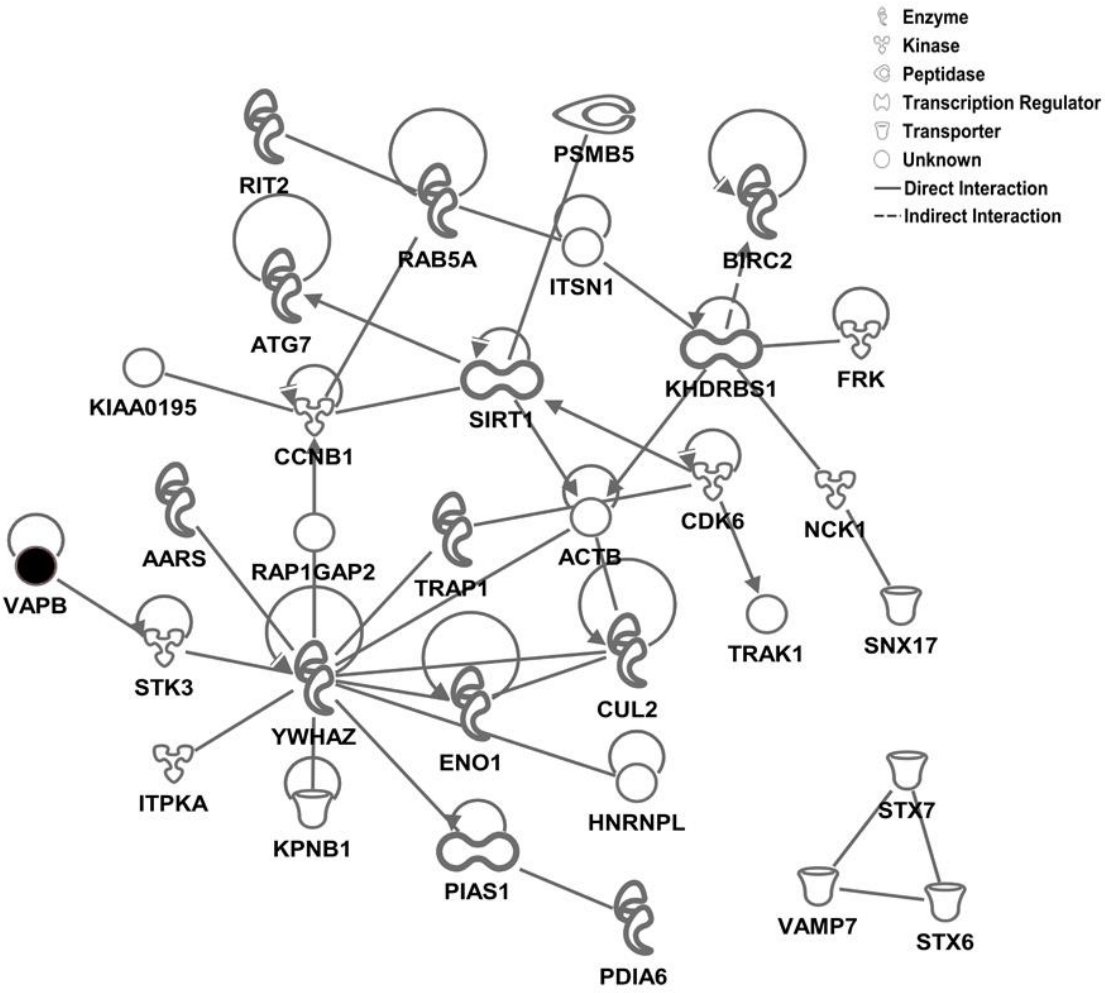

Figure 25. Ingenuity Pathway Analysis of DVAP-neurodegeneration modifiers human orthologs. Previously reported interactions between human ortholog of the DVAP-neurodegeneration modifiers found in the screen. Links include direct, indirect and self-interactions. DVAP human ortholog, VAPB, is part of the network via interaction with STK3, the human ortholog of *Hippo*. These proteins are part of a cluster with the protein YWHAZ as a central node. The vesicle related proteins VAMP7, STX6 and STX7 are interact each other but not with the rest of the studied molecules.

To expand the number of orthologs connected to VAPB and its network, we manually inserted the protein in the modifier list and then, it was connected to the rest of proteins using the "Shortest path" algorithm from IPA. Most nodes from the network were now connected using known interactions with predicted, non-DVAP-modifier proteins (Figure 26, yellow nodes). With this method, we increased in 13 the number of connected modifiers to a total of 45 nodes (green nodes). VAPB is now associated with the Vesicles cluster in a stronger way, via its interaction with STX proteins. Interestingly, other modifiers are also connected to VAPB through the central neurodegeneration-related proteins SOD1, HTT and SNCA.

These analyses gave us additional clues to understand the data obtained from the screen. Enrichment of functional clusters like cell death, lipid particle and vesicle recycling will be central in further analyses of the results from the screen.

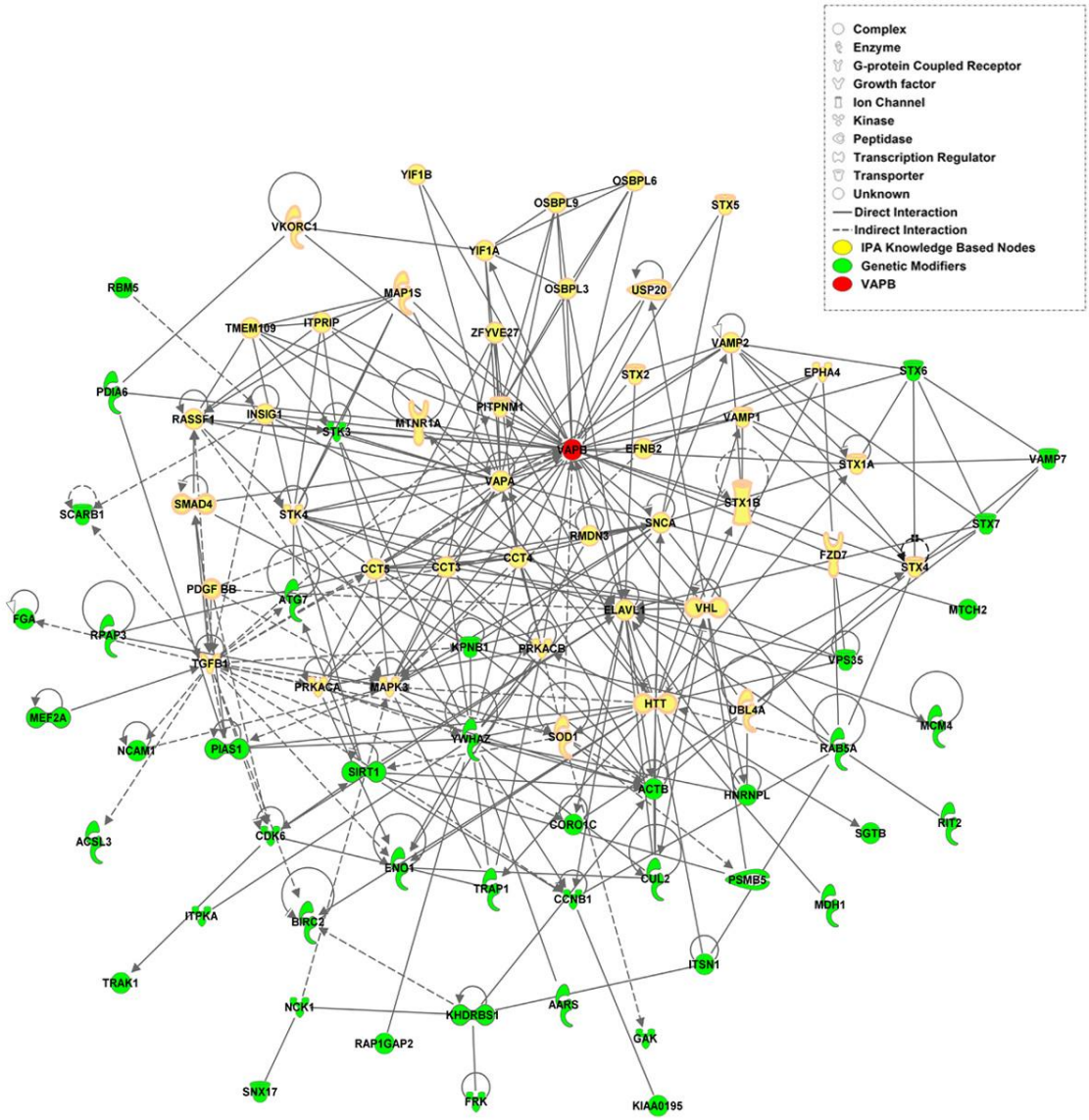

Figure 26. Expanded interaction network of DVAP-neurodegeneration modifiers human orthologs and predicted interactors. Interaction network connecting DVAP genetic modifiers and its human ortholog, VAPB. This protein is connected through known interactions with proteins not found in the screen (yellow molecules) but predicted as link with the genetic modifiers (green molecules) using the *Shortest path* algorithm. Several functional categories cluster together and are connected to VAPB through relevant predicted proteins as HTT, SNCA, VAMP and STX.

Chapter 7: Endosomal transport modifies DVAP-P58S neurodegeneration *in vivo*

7.1 Introduction

Having found and validated a novel group of DVAP genetic interactors, we were able to understand their connection using bioinformatic approaches. Among these functional categories we observed that endocytosis was one of the most represented in the genetic screen. Therefore, we plan to confirm the relation of this process with DVAP neurodegeneration studying specific endocytic genes. If our screen and the bioinformatic analysis were correct, we will be able to successfully observe modification of DVAP toxicity *in vivo* with the novel genetic modifier Rab5 and other related predicted interacting genes. Finally, we will check whether this modification is also conserved in humans.

7.2 Vesicle metabolism and endocytosis have been previously associated with neurodegeneration

The data presented so far have indicated that an important group of DVAP genetic modifiers is involved in vesicle metabolism and endocytosis. These processes, central in cell biology and neurodevelopment, are strictly regulated by complex endosomal system (Yap & Winckler, 2012). After the initial internalisation of molecules, via clathrin-dependent or -independent mechanisms, cargo molecules are stored, degraded or recycled. This process is crucial in all the cell types, but in neurons is even more specialised, considering the addition of polarisation in the endosome movement and an increased differentiation in endocytosis stages (Howe & Mobley, 2004). Therefore, endosomes in neurons regulate various central processes such as retrograde neurotrophic signaling, axonal pathfinding during development, synaptic vesicle recycling and synaptic plasticity (Yap & Winckler, 2012). Malfunction of any endocytic stage leads to a wide range of disorders, including lysosomal storage diseases and neurodegenerative disorders (Aridor & Hannan, 2002).

Previously, vesicle metabolism and endocytosis have been associated with other neurodegenerative diseases, some of them showing commonalities with ALS. In 2008, Liang and colleagues (Liang *et al.*, 2008) found that vesicle related genes modified α-syn toxicity. One of these genes, ENT3, was a conserved clathrin adapter suggesting that protein transport to vacuoles to initiate degradation may be involved in the Parkinson's pathomechanism. Another example was provided by Dimitriadi and colleagues (Dimitriadi *et al.*, 2010) with the finding of common proteins in *C. elegans* and *D. melanogaster* as modifiers of SMN. These proteins were linked to endocytosis and synaptic vesicle release, functions enriched in our screen. Last year, MacLeod and cols (MacLeod *et al.*, 2013) elegantly proved that the common mechanism between Parkinson's disease causative genes LRRK2 and PARK16 implicated retromer and lysosomal pathways. They showed that two central proteins in this process were RAB7L1 and VPS35. Interestingly these two proteins were found in our screen as DVAP-P58S-induced toxicity modifiers.

7.3 Vps35, Syx7, Ric and Rab5 are amongst the vesicle-associated genes found as DVAP-P58S modifiers

The genetic screen presented in the previous chapters revealed genes associated with vesicle metabolism; however this is the first time that they are connected to DVAP-linked neurodegeneration or ALS. From the 85 identified modifiers, 13 were functionally connected to vesicle fusion and recycling (Figure 27A). The interaction network of these proteins is highly connected as expected and DVAP also appear to be part of the cluster. Known physical interaction was found between DVAP and Ero1L, Syx7 and Rab5. On the other hand, Ric co-expresses with DVAP and co-localisation with DVAP was found in five of these proteins: Ric, Ltd, Syx6, Dap160 and Aux. However, all these data are taken from large scale *Drosophila* studies and no functional interaction has mostly been described so far between these genes and either DVAP or ALS pathogenesis. Some of these genes although, can be linked to DVAP through other known DVAP-interactors like OSBP (Rocha *et al.*, 2009) or other genetic modifiers found in this screen such as Atg7 (Figure 27B).

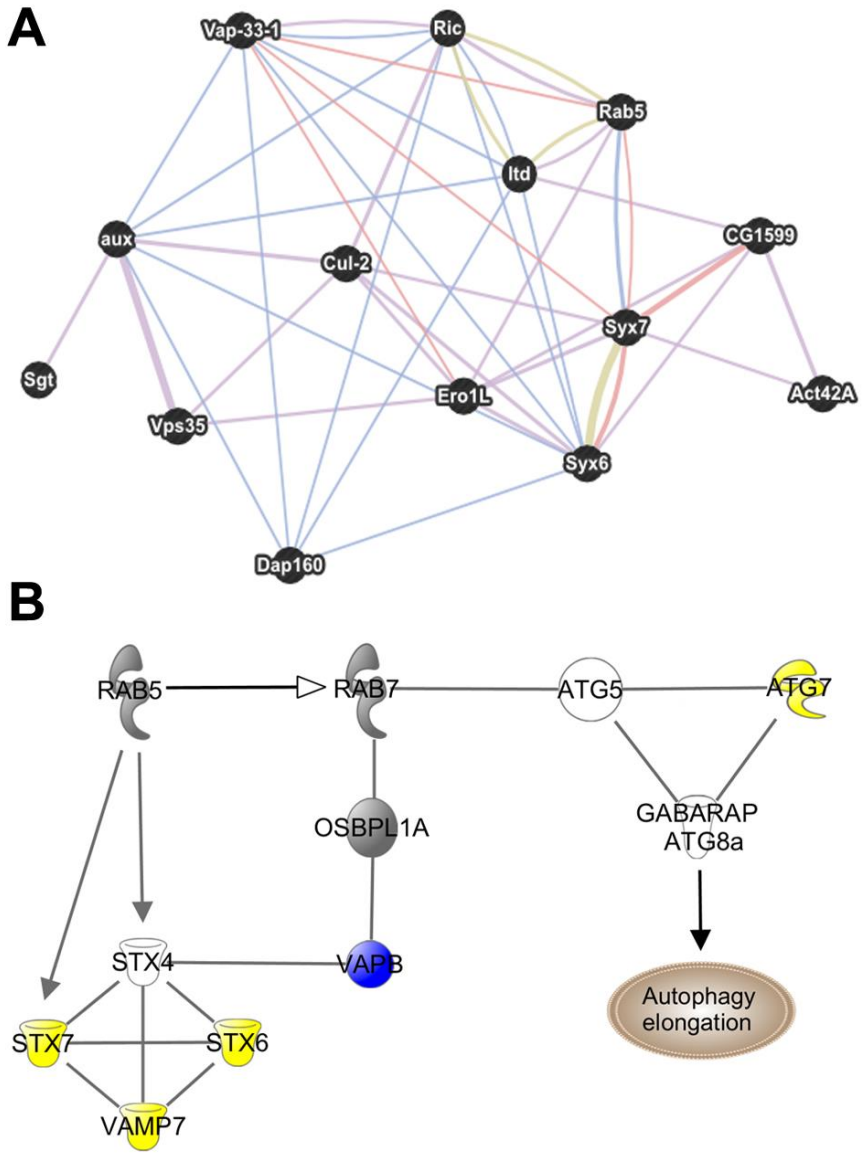

Figure 27. DVAP genetic interactors are associated with vesicle traffic. (A) Reported interactions between DVAP genetic interactors based on *Drosophila* databases compiled by GeneMANIA. DVAP presents known interactions with 7 of the 13 proteins that form the well-connected network using co-expression (purple), co-localisation (blue), physical (red) and genetic interaction data (green). (B) Diagram displaying the functional connection between some of the human orthologs associated with vesicle recycling (yellow nodes). Links represent known interactions between the proteins, including known VAPB interactors such as OSBPL1A. Vesicle recycling can regulate endocytosis and autophagy, two possible disease-related mechanisms.

From the 13 genes, 7 were in the group of 42 high-confidence modifiers confirmed by an independent allele and motor performance assay: Sgt, Vps35, Ltd, Act42A, Vamp7, Ero1L and Ric. The last three were also confirmed by the viability assay. These 7 genes are suppressors of DVAP-mediated toxicity and interestingly, all of them are connected to other modifiers or to pathways relevant to DVAP or ALS. Vps35 is a central component of the retromer complex and controls trafficking between endosome and Golgi. Its loss causes mislocalisation of endocytic proteins and defects in neuromuscular junction (Korolchuk *et al.*, 2007) and as previously mentioned, is connected with Parkinson's mechanism. In this same process but in opposite direction, are also involved other two modifiers, the syntaxin 6 and 7. The first one regulates trafficking from trans-Golgi network (TGN) to early endosomes and syntaxin 7 connects early and late endosome. The correct balance between concentrations of these proteins ensures an accurate distribution of the cargo molecules in the cell (Jung *et al.*, 2012). Interestingly, Syx6 and Syx7 are suppressors but the tested lines were loss of function for these genes. This means that the same effect is observed with the down-regulation of the anterograde transport and with the up-regulation of the reverse trafficking, suggesting that these three proteins can be involved in DVAP-toxicity in a mechanism involving transport from vesicles to Golgi.

On the other hand, Ras-related protein interacting with calmodulin, Ric, is the only *Drosophila* member of Rit subfamily of Ras-related small GTPases (Wes *et al.*, 1996). Ric regulates the p38-Akt pathway, proteins previously associated with VAPB in oxidative stress and growth control. At the same time, CG9153 is an uncharacterized DVAP modifier and its human ortholog is Herc4, an ubiquitin ligase with a Guanine nucleotide Exchange Factor (GEF) domain. This protein is the common ancestor of a family involved in vesicular transport and the same GEF domain (RCC-1-like, RLD) is found in another gene causative of ALS, alsin. As downstream effectors of alsin stand out the Ras-related protein Rab5 and syntaxin 7 (Hadano *et al.*, 2007; Morrison *et al.*, 2008), both found in our modifier genes set. The linkage between Alsin and DVAP through these endocytic genes could be

relevant to understand both pathomechanism and explain possible common molecular pathways between these two disease variants.

7.4 DVAP-P58S mediated aggregates disrupts Rab5 wild type localisation in *Drosophila* nervous system

Rab5 was one of the 13 vesicle-related genes found as a strong modifier in 3 of 4 possible readouts, failing to show a significant suppression effect only in the climbing assay. This small GTPase is involved in clathrin-mediated endocytosis from the membrane to the early endosome pool (Cavalli *et al.*, 2001) regulating important cellular processes such as postsynaptic trafficking and autophagy (Dou *et al.*, 2013; Brown *et al.*, 2005). As part of early endosomes, Rab5 concentration is recruited by an increased amount of the phosphoinosite PI3P (Zoncu *et al.*, 2009). Maturation to late endosome involves a molecular exchange from Rab5 to Rab7, activity probably controlled by Rab proteins and phosphoinositides levels (Yap & Winckler, 2012).

Protein aggregation is a common hallmark for most neurodegenerative diseases. In our group we also showed that DVAP-P58S forms aggregates that sequester the wild type form of the protein, triggering cell death (Chai *et al.*, 2008). Rab5 also has been associated with protein aggregates, decreasing the toxicity levels of aggregates formed by disease-related proteins such as huntingtin (Ravikumar *et al.*, 2008), amyloid β (Li *et al.*, 2012) and α-synuclein (Sancenon *et al.*, 2012). For this reason we wanted to study the relation between Rab5 and DVAP protein aggregation.

So far, we have shown that Rab5 down-regulation is involved in DVAP-P58S toxicity and its overexpression can suppress the neurodegeneration. To understand what happens with Rab5 in DVAP mutants and whether the protein is mislocalised, we dissected eye imaginal discs from flies expressing DVAP-P58S and stained them with Rab5-specific antibodies. In controls, both proteins showed a clear distribution, mainly in the cell contour and without any noticeable colocalisation (Figure 28A).

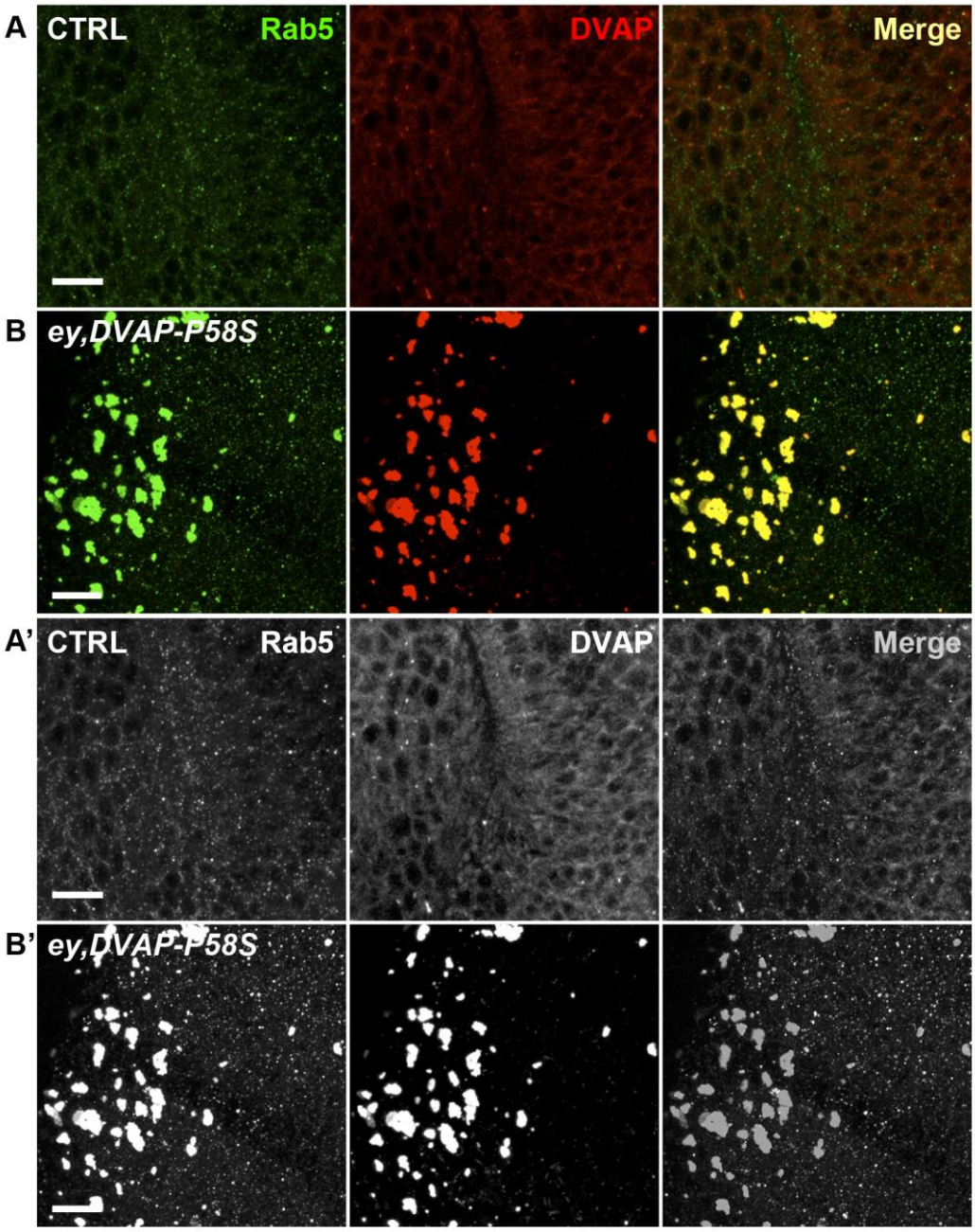

Figure 28. Rab5 colocalises with DVAP-P58S-induced aggregates. Representative confocal images from CTRL (*ey-Gal4/+*) and *ey,DVAP-P58S (ey-GAL4,DVAP-P58S/+*) eye imaginal discs stained with DVAP and Rab5 antibodies. In controls, both proteins showed a clear staining in the cell contour, but the aggregate formation caused by the overexpression of DVAP-P58S dramatically sequesters Rab5 protein. Bar = 10 um.

However in DVAP mutant imaginal discs, Rab5 and especially DVAP lost their localisation forming protein aggregates that contain both mutant and wild type forms of the protein, as we have previously reported (Chen *et al.*, 2010). Interestingly, Rab5 presents an irregular, granular distribution and is sequestered into DVAP-P58S-mediated aggregates (Figure 28B), suggesting that the depletion from wild type structures and loss of its function is caused by the formation of DVAP-P58S aggregates. This interesting finding can be further supported with a better characterization of the exact location of these proteins. The addition of nuclear (DAPI), ER (Boca), Golgi (GM130) or membrane specific markers (HRP) could clarify furthermore the exact nature of Rab5 and DVAP interaction. Additionally, the comparison on the effect between DVAP-P58S and DVAP-WT over Rab5 localisation could provide more evidence to the proposed loss-of-function mechanism.

7.5 Overexpression of the endolysosomal markers Rab7 and Rab11 also suppress DVAP-P58S linked neurodegeneration

The initial analysis of this chapter detailed 13 genetic interactors of DVAP that were associated with vesicle recycling. However, the most enriched vesicle-related functional category was endosome, a central structure for the vesicle trafficking. When we isolated the genes associated with this category and study their connection to predicted genes, we were able to make several important observations. Firstly, most genes and their connections are conserved between *Drosophila* and humans (Figure 29). This not only supports the idea that this process has a central role inside the cell, but also validates the search for novel disease-related pathways in *Drosophila.* Secondly, we observed that some predicted interactors are also conserved in both networks. Interestingly, connected to Rab5 and Vps35 we observe the presence of Rab7. This protein is another endosome-related GTPase that in its mutant form produces axonal degeneration and can cause Charcot-Marie-Tooth (CMT) disease, which is highly reminiscent to ALS and its hallmarks (McCray *et al.*, 2010). For instance, FIG4/SAC3, another vesicle-related ALS-causative gene also is associated with CMT Disease (Chow *et al.*, 2009). Interestingly, McCray *et al.* found

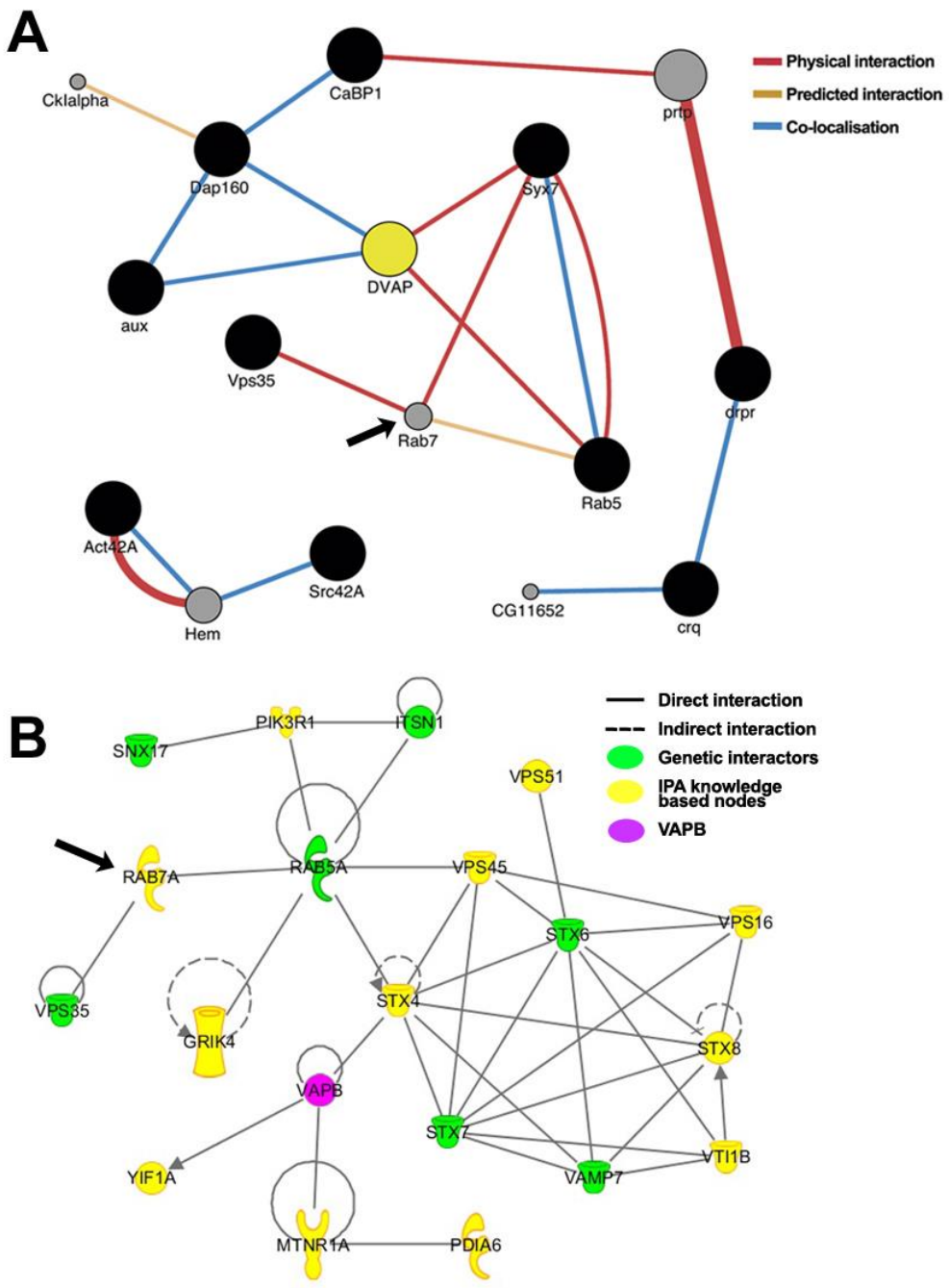

Figure 29. Rab7 is a predicted interactor of DVAP. (A) Interaction network between *Drosophila* DVAP modifiers that belong to functional categories associated with endocytosis (black nodes). The network can be strengthened with the addition of predicted interactors not found in the genetic screen (Gray nodes). (B) Interaction network between human orthologs of DVAP modifiers using the *Grow* feature of IPA. Predicted interactors in this network (yellow nodes) present previously reported interactions with the molecules found in the screen. Interestingly, Rab7 appears strongly connected in both network as a potential DVAP interactor through its interaction with the DVAP modifiers Vps35 and Rab5 (black arrows).

a physical interaction between this protein and DVAP in *Drosophila*, supporting a previously proposed mechanism linking both proteins in the regulation of microtubule trafficking of late endosomes (Rocha *et al.*, 2009).

To study whether Rab7 displays the same phenotype as the other vesicle-related DVAP genetic interactors found in the screen, we tested different Rab7 alleles to search for toxicity modification effect. Transgenic flies expressing a disease-causing mutation (L129F, Figure 30A) and a dominant negative allele (T22N) did not have any significant effect in DVAP toxicity, as they maintain the eye size of the ey,DVAP-P58S line (Figure 31). Interestingly, the overexpression of the wild type Rab7 version or an engineered constitutively active form (Q67L) showed a significant suppression of the DVAP neurodegeneration in the eye (Figure 30B,C), suggesting that the balance of DVAP and Rab7 activity can be important also for late endocytic vesicles and not only in early nucleation stages as Rab5 and other vesicle-related modifiers indicated. This effect was also confirmed in the nervous system, as the overexpression of Rab7 and its constitutively active form suppress DVAP-P58S lethality and motor performance defects (Figure 30D).

To confirm even more the implication of this pathway in DVAP-P58S-mediated neurodegeneration, we went one step further in the molecules associated with the formation of endosomes. Rab11 is the final step of the machinery that also involves Rab5 and Rab7. Rab11 is involved in the recycling of endosome back to plasma membranes, regulating the balance between these molecules (Bastin and Heximer, 2013). If we observed an important effect of Rab5 and Rab7 in DVAP toxicity, we should expect a similar effect with Rab11. Indeed, we observed a significant suppression of DVAP-P58S-mediated neurodegeneration in the eye upon Rab11 overexpression (Figure 32). In conclusion, we were able to support previously reported DVAP interaction with our model and strengthen the relation between DVAP-P58S-linked neurodegeneration and vesicles metabolism.

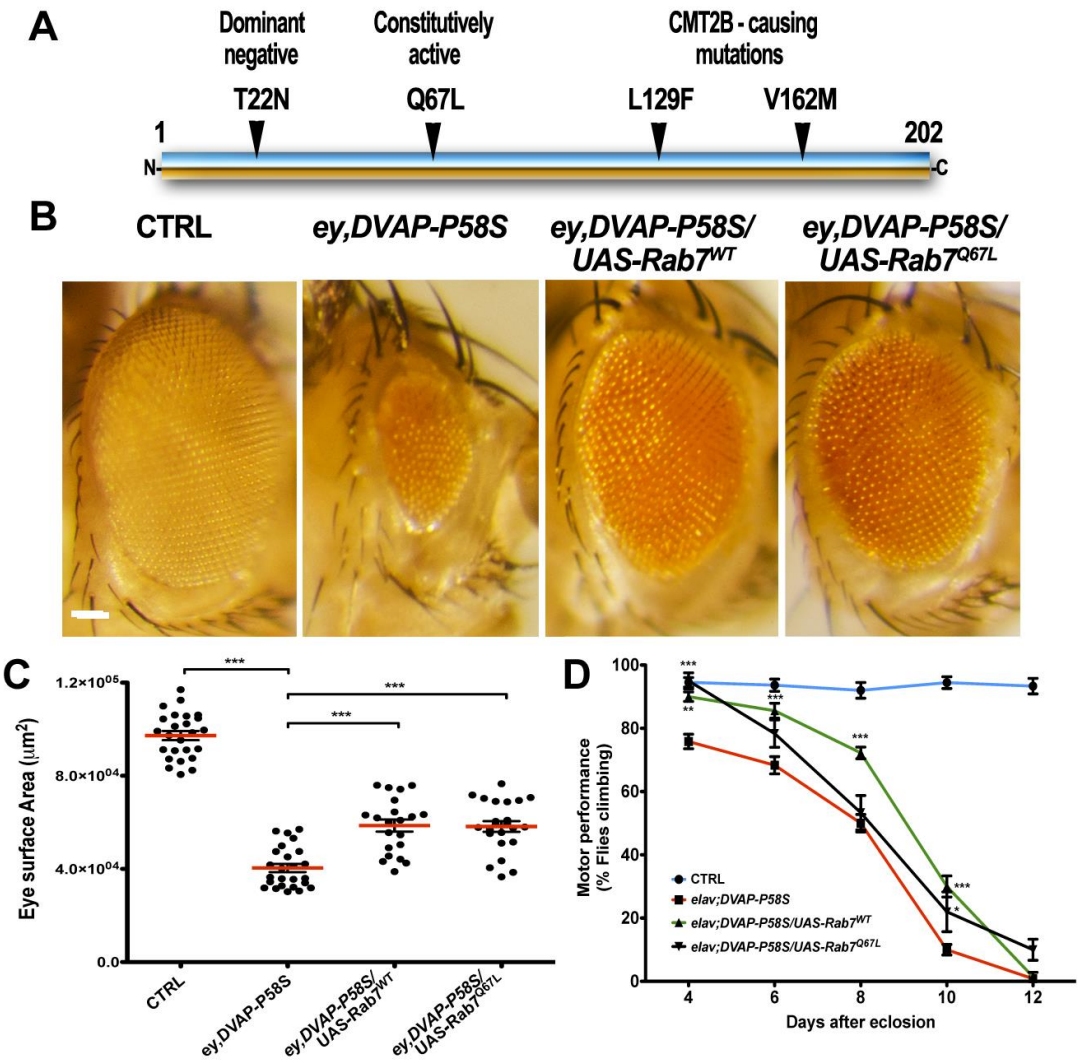

Figure 30. Suppression of DVAP neurodegeneration by upregulation of Rab7. (A) Genetic structure of *Drosophila* Rab7 gene. Two mutations associated with Charcot-Marie-Tooth disease and the dominant negative and constitutively active alleles were tested. (B) Light microscopy images of control flies (*ey-GAL4/+)* and flies expressing DVAP-P58S protein under the regulation of ey-GAL4 driver *(ey-GAL4,DVAP-P58S/+*), and Rab7 up-regulation alleles *UAS-Rab7^{WT} (ey-GAL4,DVAP-P58S/UAS-Rab7^{WT}*) and *UAS-Rab7^{Q67L} (ey-GAL4,DVAP-P58S/UAS-Rab7^{Q67L}*) A significant suppression is observed for both alleles. (C) Quantification of the eye size of the crosses performed. Both up-regulated alleles presented a significant suppression compared with the ALS model. (D) DVAP-P58S-induced motor performance defect is suppressed by the overexpression of Rab7 in the nervous system, and in a lower degree by its constitutively active form. Scale Bar = 50 um. *** P < 0.001, ** P < 0.01, * P < 0.05 (One-way ANOVA in C, Two-way ANOVA in D).

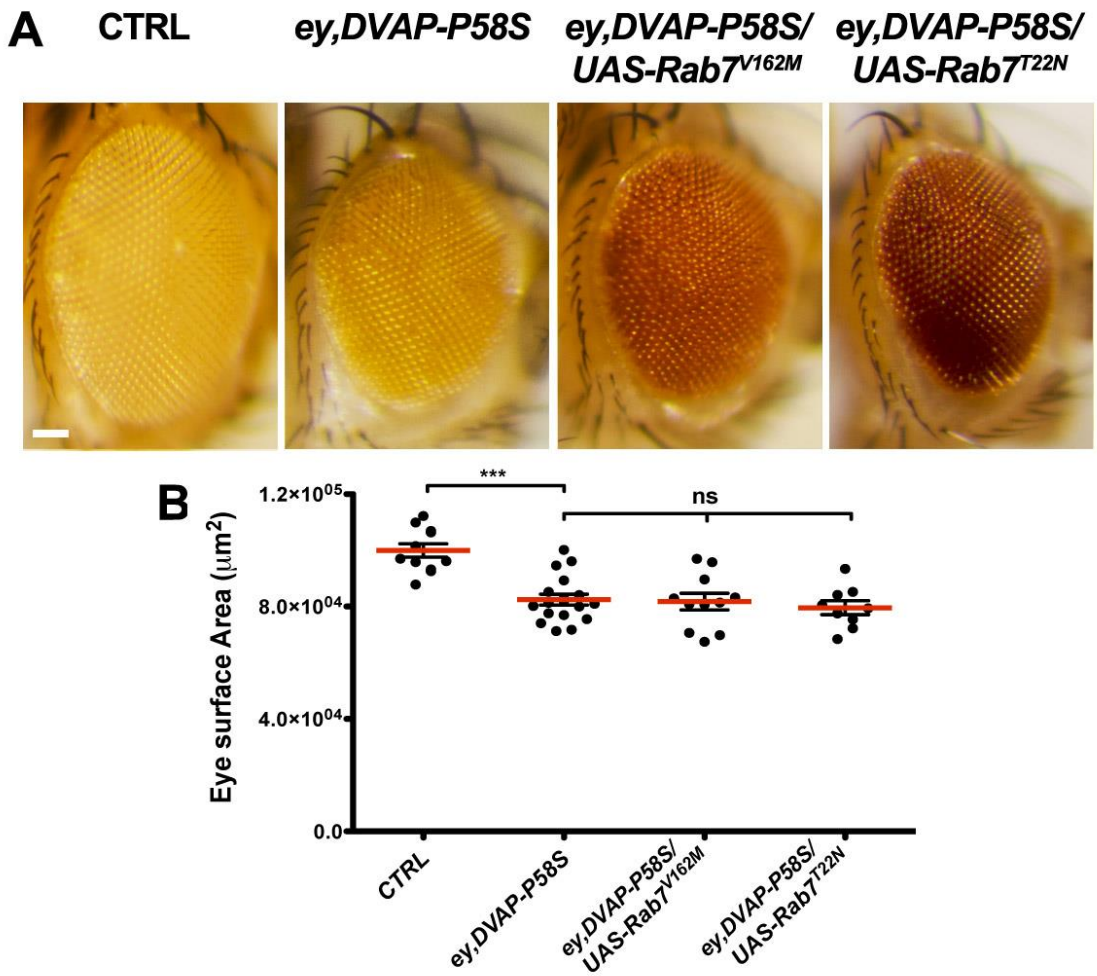

Figure 31. Down-regulation of Rab7 does not affect DVAP neurodegeneration. (A) Light microscopy images of control (*ey-GAL4/+*) and flies expressing DVAP-P58S protein under the regulation of ey-Gal4 driver *(ey-GAL4,DVAP-P58S/+*), and *Rab7* down-regulating alleles *(ey-GAL4,DVAP-P58S/UAS-Rab7^{V162M}* and *ey-GAL4,DVAP-P58S/UAS-Rab7^{T22N}*). No significant effect is observed for the alleles *UAS-Rab7^{V162M}* and *Rab7^{T22N}*. (B) Quantification of the eye size of the crosses performed. Scale Bar = 50 um. *** $P < 0.001$, ns $P > 0.05$ (One-way ANOVA).

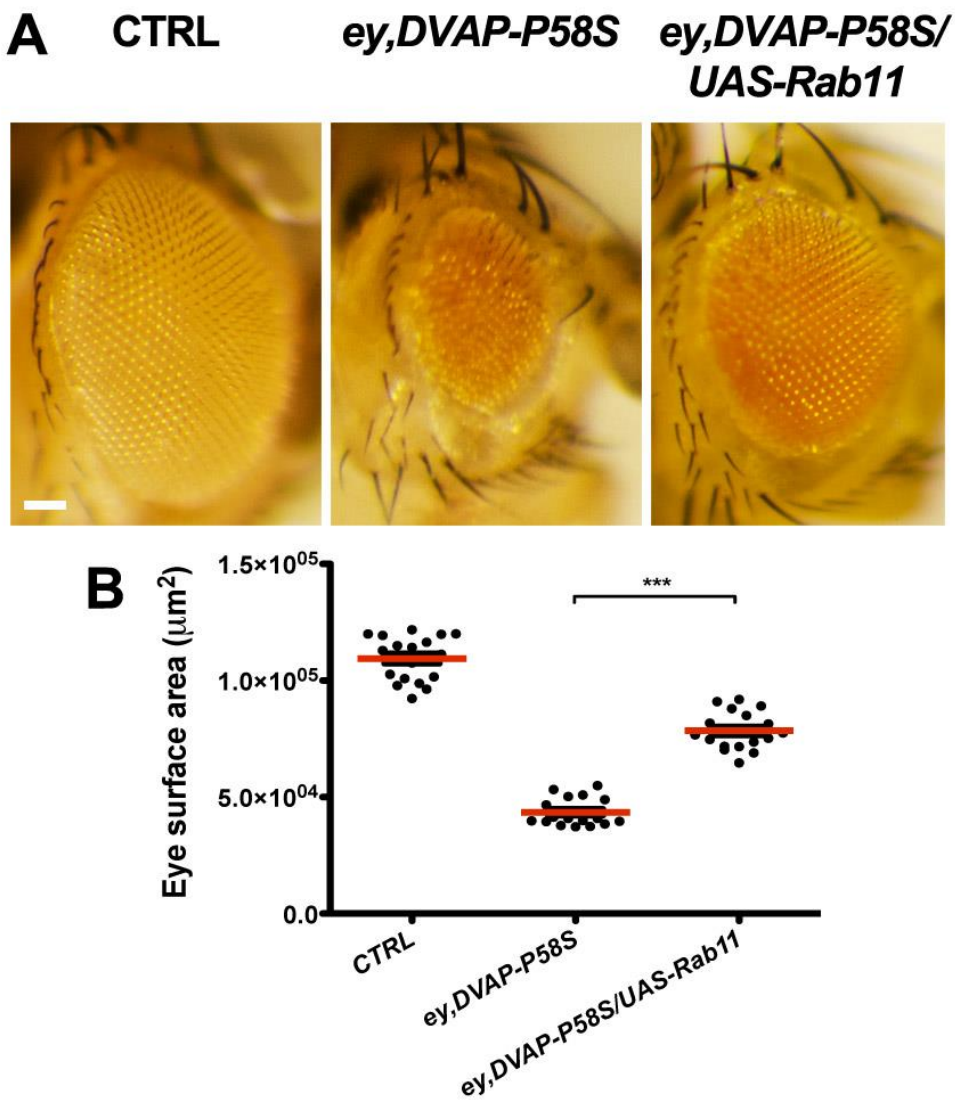

Figure 32. Suppression of DVAP neurodegeneration by upregulation of Rab11. (A) Light microscopy images of control (*ey-GAL4/+*) and flies expressing DVAP-P58S protein under the regulation of ey-Gal4 driver *(ey-GAL4,DVAP-P58S/+*), and Rab11 overexpressing allele *(ey-GAL4,DVAP-P58S/UAS-Rab11*). (B) Quantification of the eye size of the crosses performed reveals a significant suppression of the DVAP-P58S phenotype in the eye by the overexpression of Rab11. Scale Bar = 50 um. *** $P < 0.001$ (One-way ANOVA).

7.6 Rab5 mislocalisation in DVAP-P58S-expressing tissue is conserved in humans

In this genetic screen, we identified vesicle-related genes capable to modify DVAP-P58S-mediated neurodegeneration. Some of these genes were previously linked to DVAP in *Drosophila* and we observed *in-silico* that these connections were conserved in humans. To confirm this last observation and link DVAP-modifiers with ALS phenotypes in patients, we studied the levels and distribution of the endocytosis-related protein RAB5A in tissues from ALS patients. This is the ultimate assay to validate the genes found in *Drosophila* and their potential relevance in the pathomechanism of ALS. Previous screens have validated in this way their results, showing that use of genetic approach in smaller organisms can be a great way to find novel genes involved in human neurodegenerative diseases (Neumann *et al.*, 2006; Couthouis *et al.*, 2011).

Human *post-mortem* spinal cord tissue was used to do immunohistochemistry using an antibody specific to the human protein RAB5A. When we analysed tissue from healthy control individuals, RAB5A seems to distribute in the contour of circular structures, possibly related to vesicles and endosome (Figure 33). However, when we analysed tissues from two representative patients with ALS, RAB5A distribution in neurons lost the previous organization and looks to be part of multiple abnormal protein aggregates (Results provided by Dr. Colin Smith, Centre for Clinical Brain Sciences, University of Edinburgh). This result confirmed the aggregation observed in *Drosophila* tissue but more importantly, suggest that loss-of-function and aggregation of endocytic proteins could be linked to ALS pathogenesis. Taken together, our data identify potential novel ALS causative genes and their related pathways can lead to a better understanding of the mechanisms related with DVAP-P58S-associated neurodegeneration.

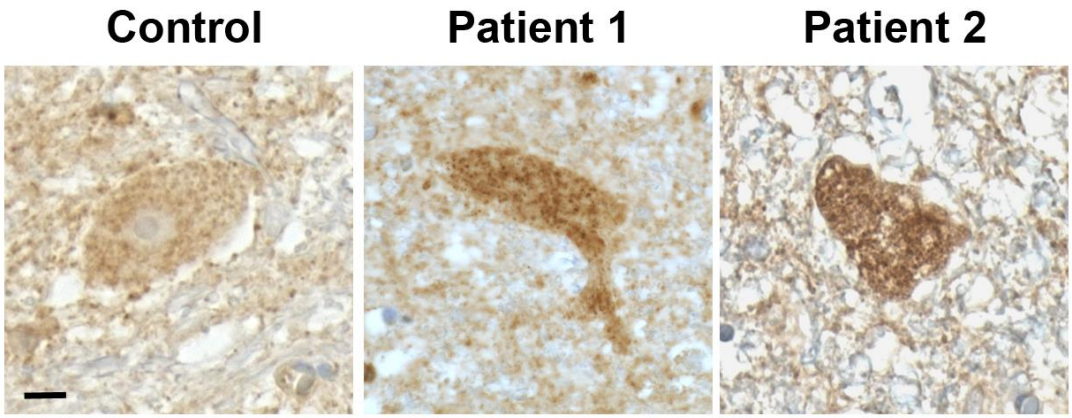

Figure 33. RAB5A mislocalises and aggregates in spinal cord neurons of patients with ALS. Representative images of immunohistochemistry of Control tissue and two different ALS patients tissue stained for RAB5A, displaying a change in the distribution of the protein. In Control individuals, RAB5A presents a defined circular staining but in tissue from two patients with ALS, an up-regulation and a dense aggregate-like structure is observed altogether with the lack of ring structures. Scale Bar = 10 um

Chapter 8:

Discussion

8.1 Overview of the project

Only over the last two decades, research in the neurodegenerative field has showed an increased development. Major characterisation of several degenerative diseases has improved the chances of finding therapies and cures for a great number of patients. ALS is not outside this group, with an impressive amount of scientific growth since the discovery of TARDBP as causative gene in 2008 (reviewed in Robberecht & Phillips, 2013; Renton *et al.*, 2014). This fact however, brings as a drawback an increasing amount of data that try to explain the whole disease without understanding the basic mechanisms of it yet. Moreover, the lack of success in several models and therapeutic trials, has led to a challenging point where it is difficult to move forward (Genc and Ozdinler, 2014). We thought that instead keep trying to understand the mechanism of the disease with the current knowledge, we needed to expand our available data and hence, explore known and novel pathways in a better way. This is useful to fill the gaps that could potentially merge two apparently dissimilar processes in a clearer one. More importantly, with the novel molecules found in this screen we are now able to study mechanisms that previously were not associated with ALS pathomechanism. Moreover, these novel molecules will potentially lead us to comprehend as well, more cases of ALS patients with a sporadic origin.

From this perspective, we could observe that our proposal of finding novel genetic interactors of the ALS-causative gene DVAP was mostly achieved. Selection of a high amount of parameters to perform a genome-wide screen is not always exempt of risks and failures. For this reason, we initially tested different parameters and decided a specific set of conditions to obtain in a clear way genetic modifiers of DVAP-induced neurodegeneration in the eye. We also covered with extra assays the more complicated search for enhancers of the DVAP-linked phenotype. Therefore, we started the screen with the aim to search for significant modifiers, minimising the risks of potential false hits. The initial discovery of 85 potential DVAP genetic interactors, and their subsequent validation and confirmation through a series of assays, confirmed the success of the selection of parameters and suggest that we are

now in a better position to understand the disease. At the same time, we can support the use of our *Drosophila* ALS model based on the expression of the mutant allele DVAP-P58S, for the search of genes using genome-wide screens. The combination of this model with classical *Drosophila* genetic techniques successfully achieved what has been also reported in other genetic screens that searched genes associated with neurodegenerative diseases over the last years (Park *et al.*, 2014; MacLeod *et al.*, 2013; Miller *et al.*, 2012).

Another positive aspect of the outcome of this project is the favourable prospect to carry on with the use of this ALS model. A group of modifiers can hypothetically be the target of studies to modulate their activities. Up- or down-regulation of the activity of these proteins can lead to potential therapeutic tests to suppress toxicity. At the same time, changes in the activity of kinases or proteins related with lipid metabolism can be assessed with the same consistent phenotypes used in this study, such as the neurodegeneration in the eye of the ALS model. Further biochemical characterization of these novel molecules opens a real possibility to understand the mechanisms associated with the disease.

8.2 Endocytosis up-regulation suppress DVAP-P58S-induced neurodegeneration

To fulfill completely the purpose of the project and find the genes involved in the ALS pathomechanism, is mandatory further characterisation of each one of the proposed genetic interactors. We selected genes linked to vesicle metabolism and endocytosis as an initial stage to validate the project and move forward in the understanding of the disease. Luckily, we were able to not only confirm the biological relevance of one of these proteins, Rab5, but to expand our search to other related Rab proteins as well. This finding provides a step forward to the relation between this molecular process and neurodegeneration, which hopefully can open novel researches in this direction. However, this also implies that similar biological assays can be used to further validate other genes found in the genetic screen. The

potential validation of other pathways will provide a bigger picture of the DVAP biology in the cell.

Rab5, an important endocytic component found in the screen, is a protein that is critical for early endosome fusion along the endocytic pathway. The native Rab5 protein is present in endosomes at synaptic terminals as well as in cell bodies (Wucherpfennig *et al.*, 2003). Both Rab5 constitutively active (CA) and dominant negative (DN) mutations affect Rab5 protein localisation, forming aggregates and less punctate signal than the wild-type in photoreceptor cells. Rab5-CA still colocalises with wild-type but DN looks more disperse, moving away from original early endosomes (Zhang *et al.*, 2007). In the present study, we confirmed the relation between Rab5 and DVAP using two different approaches. Overexpression of Rab5 was able to suppress the DVAP-P58S associated neurodegeneration in the *Drosophila* eye. Also, we observed a mislocalisation and aggregation of Rab5 in tissue from flies expressing the ALS-linked DVAP allele. These observations suggest a strong interaction between both proteins. Thus, a main consequence of DVAP aggregation and loss-of-function could be related with the loss-of-function of Rab5 and with this, deregulation of the normal endocytic balance. DVAP-P58S-induced aggregates capture Rab5-WT protein and decrease its available levels. Therefore it makes sense that with the increase of available protein overexpressing the Rab5-WT allele, we were able to suppress the toxicity. It still remains unknown whether this suppression is due to a return to normal levels of early endosomes or whether this increase would also remove the DVAP-induced protein aggregates, improving the response to protein aggregation in the cell. The confirmation of RAB5 mislocalisation phenotype in tissue from patients with ALS validates our proposed model and methodology, but more importantly suggests that this effect is a conserved VAPB-related phenotype.

The functioning of the endocytic trafficking is based on the highly coordinated spatial distribution and directionality of the vesicles. These aspects are regulated by different factors including the concentration and composition of phosphoinositides, and the sequential assembly of specific regulatory proteins or markers, such as the

Rab-GTPases (Krauss and Haucke, 2011). Bioinformatically we were able to predict marker proteins involved in this process. Rab7 appears as the next step after Rab5 early endosome control. Present as a marker for late endosomes, Rab7 continues the recycling process inside the cell (Burd, 2011). Rab11 is the final step of the endocytic control and marker of recycling endosomes (Yap and Wickner, 2012). Therefore, the experimental confirmation of the Rab5 suppression effect with the overexpression alleles of Rab7 and Rab11 was highly important. Additionally, the identification in this study of other late endosome and lysosome markers, such as VAMP7 and Syntaxin 7, underlines the involvement of this last endocytic step in VAPB-linked toxicity. This last point is highly significant considering the function of late endosomes as crossroad with autophagy and protein degradation mechanisms (Scott *et al.*, 2014), which also may play an important role in DVAP toxicity.

Another regulator of the coordinated endocytic trafficking is the concentration and composition of phosphoinositides, which can create different compartments and finally determine the fate of each structure and cargos (Yap and Wickner, 2012). We already associated phosphoinositides misregulation and DVAP neurodegeneration (Forrest *et al.*, 2013). Therefore, the connection between DVAP-mediated phosphoinositide regulation and Rab protein activity acquire a central relevance with the observed neurodegeneration. It would be interesting to study the possibility that DVAP control of membrane dynamics is due to its interaction with more endocytic proteins, working as a central scaffold protein, or whether its lipid regulation is sufficient to affect membranes and the homeostasis of endosomes. Rocha *et al.* proposed a model where VAPB controls late endosome positioning by motor proteins in a cholesterol-dependent process (Rocha *et al.*, 2009). This supports the function of VAPB yeast homologue, Scs2, as a tethering protein in the formation of multi contact sites (MCS) between ER and plasma membrane (Manford *et al.*, 2012). A disruption in the MCSs between endosomes and ER can be a potential scenario in DVAP-P58S neurons due to the lack of tethering function of this protein. An increase in the amount of Rab proteins available may compensate that loss of function and may facilitate MCSs formation to recover normal trafficking.

The link proposed here between ALS and endocytosis is not a minor one. Even though previous studies tried to explore this connection (Kasperaviciute *et al.*, 2007), we did not know major links between ALS and endocytosis. However this year, Farg *et al.* associated Rab proteins to C9orf72 patients, proposing that this novel causative gene is a regulator of several steps in the endosomal trafficking (Farg *et al.*, 2014). Here, we can now link endocytosis and the levels of Rab proteins in the DVAP-linked neurodegeneration, suggesting a VAPB role facilitating vesicular trafficking. More important is the fact that DVAP works as key protein that, despite being previously ignored as central cause of the disease's mechanism, is proven as central node for processes that now emerge as relevant for the disease.

8.3 RAS signaling pathway is the most represented mechanism amongst the DVAP genetic modifiers

From the whole set of genetic modifiers found in this study, probably the best connected each other were the molecules associated with RAS signaling pathway. This superfamily of proteins plays a role in almost every cellular process, sharing as a biochemical activity the hydrolysis and binding of GTP (Colicelli, 2004). The activated state of these proteins is caused by the binding of GTP that increases the affinity of RAS proteins to their downstream effectors. The hydrolysis of GTP or its exchange for a GDP molecule inactivates the proteins, differentially signaling in this way several processes. GTP exchange and protein activation can be accelerated by the removal of GDP molecules by the Guanine nucleotide exchange factors (GEFs) (Chardin *et al.*, 1993). In the opposite way, RAS proteins can be inactivated by the hydrolysis of bound GTP performed by the GTPase activating proteins (GAPs) (McCormick, 1998). With this complex network, several signaling pathways are down- or up-regulated, affecting the activity of an impressive amount of downstream targets and regulating in this way cellular homeostasis (Colicelli, 2004).

The superfamily is formed by at least ten different subfamilies, some of them represented in our genetic screen. RAS subfamily include the first identified member, rat sarcoma (RAS) (Harvey, 1964), which is up-regulated in different

tumour cells and therefore, has been associated with cancer, growth and cell differentiation. RAS associated with brain proteins (RABs) is another subfamily previously discussed as central outcome of our assays, with an important control in endocytosis and vesicle metabolism. This one is the largest family with 71 members, due in part to an important number of expansions and duplications, if we consider that the number of members from humans is the double than in *Drosophila* (Colicelli, 2004). RHO (Ras homolog) is a third subfamily associated with cancer and cytoskeletan remodeling (Sahai and Marshall, 2002; Fransson *et al.*, 2003), which include different Rho proteins and the motility regulator Rac1. Interestingly, the downstream target of Rac1 is Alsin, another ALS causative gene (Yang *et al.*, 2001). The Rac1-mediated relocalisation of Alsin from the cytoplasm to the membrane appears to be the most affected process damaged by ALS-linked mutations (Otomo *et al.*, 2011). Furthermore, the downstream target of Alsin is RAB5, protein that in turn is an upstream regulator of STX7 (Hadano *et al.*, 2007; Morrison *et al.*, 2008). Both of them are DVAP genetic modifiers found in our genetic screen. The impairment in the interaction between Rac1 and Alsin would lead to a lack of activation of Rab5 that would translate in a deficiency of the endocytic balances, idea already discussed in the previous section. Indeed, this was observed by Otomo *et al.*, when Alsin mutants failed to be localised by Rac1-induced macropinosomes, which lead to a loss of function of Rab5 affecting its role in endocytosis and autophagy. This relocalisation failure also may be caused by a lower affinity of the Alsin mutant protein to the macropinosomal-enriched lipid molecules PI3P and PI4P (Otomo *et al.*, 2011). Alsin presents three GEFs signaling motifs, including RCC1-like domain (RLD) which is also present in HERC ubiquitin ligases (Hochrainer *et al.*, 2005). We found in the screen CG9153, the *Drosophila* homolog of HERC4, supporting even more the involvement of this pathway. The connection between RAS pathways and endocytosis, with ALS-linked mutations in VAPB has not been associated yet and could provide novel insights into ALS pathogenesis.

Another DVAP-interactor found in the screen is "Ras interacts with calmodulin", Ric. This protein is a member of the Rit subfamily of Ras small

GTPases, which other members are Rin and Rit (Wes *et al.*, 1996). In contrast to other RAS subfamilies, Rit proteins are not well understood and even though they are connected to major MAPK cascades, their exact function is not completely characterized (Shi *et al.*, 2013). However, it is known that the MAPK p38 works as a downstream target of Ric, in an anti-apoptotic pathway that also involves Akt, mTor, Mef2 and Atg1 (Cai *et al.*, 2011; Bitting & Armstrong, 2013). The suppression of DVAP-P58S neurodegeneration caused by the overexpression of Ric suggests that a delay in apoptotic responses could protect the cell from protein aggregation or novel unknown mechanisms caused by DVAP mutant allele. Furthermore, we found in the screen RapGAP1 (Chen *et al.*, 1997), a GAP protein that inactivates RAP and RAS proteins, and potentially can be also one of the currently unidentified GAP proteins for Ric (Shao *et al.*, 1999; Shi *et al.*, 2013). The fact that we observed suppression by a loss of function allele of this protein supports the previous hypothesis. Also, it links the RAS signaling with other functional process unveiled in the screen such as vesicle trafficking and apoptosis. The relation between Akt and DVAP is known but not yet understood (Rao *et al.*, 2012); perhaps the regulation of RAS proteins is the link between that previously reported data.

Other two genes found in the screen are the oncogene Src42 and the kinase modulator Cnk. This last protein is involved in the RAS pathway modulating antagonistically RAF, the first identified RAS effector (Van Aelst *et al.*, 1993). Cnk is essential to RAF activation due to two N-terminal domains, but also presents a short C-terminal element, the RAF-inhibitory region (RIR) that avoid the normal signaling from RAF to MEK independently of RAS activation (Douziech *et al.*, 2003). The effect of this region can be suppressed although, by a binding activity of Src42 over the C-terminal region of Cnk. The binding of Src42 returns the MAPK signaling and therefore, the activation of the initial cascade. Thus, Cnk mediates RAF activity from the interaction with signals from RAS and Src42, preventing signaling leakage to MEK (Laberge *et al.*, 2005; Douziech *et al.*, 2003). Once again, it seems that an overall activation of the RAS pathway is linked with a suppression of DVAP-induced neurodegeneration. In this case, we observed that both Src42 and Cnk are suppressors with an overexpression allele, which suggests an overall

downregulation of RAF and its downstream effectors MEK and ERK in cells expressing DVAP-P58S. This also implies that in neurodegenerative cells, the RAF repressive effect over MST2 is silenced, which would lead to an increase in apoptosis. Altough recently was shown that a coordinated balance in the phosphorylation state of MST and RAF can switch between apoptosis and cell proliferation (Romano *et al.*, 2014). Interestingly, we found in our screen that the MST2 ortholog hippo is upregulated in DVAP-P58S neurons, leading to an increase in apoptosis as another potential trigger in neurodegeneration. Therefore, DVAP regulation of RAS pathways could play a key role in the strict balance between cell proliferation and neurodegeneration increase through apoptosis.

Recently, other studies have linked RAS pathways to neurodegeneration. Down-regulation of RAS-MAPK-MSK1 pathway can decrease the levels of ATXN1, the causative gene of spinocerebellar ataxia type 1 (SCA1). This down-regulation, which can be mimicked pharmaceutically, lead to a suppression of the phenotypes associated with the disease (Park *et al.*, 2013). Similar results were obtained in a screen for modifiers of huntingtin, the causative gene of Huntington's disease. Down-regulation of the RRAS pathway and its central protein related RAS viral (r-ras) oncogene homolog, suppress expanded huntingtin-associated neurodegeneration (Miller *et al.*, 2012). Both studies were genetic screens that used among other systems, *Drosophila* as a fast way to find important unappreciated pathways. In our study, again we obtain similar results that strongly support the use of the model for this kind of studies. In our case, further characterisation of DVAP interactions with RAS-related proteins could elucidate the mechanisms involved in neurodegeneration and other cellular processes affected by these interactions.

With all these details, it is interesting that in this study we were able to find out many genes involved in these signaling pathways. If we consider that proteins and regulators can be shared between pathways affecting simultaneously multiple targets (Boguski and McCormick, 1994), we can underline that most of the components of the RAS-signalling cascade are represented in the screen. We can find the initial steps with the Ric protein, its repressor RapGAP and then, the downstream target

Rab5 and potentially CG9153, which share commonalities with Alsin. Downstream effectors such as Src42, Mef2, Syx7 and 14-3-3ζ expand the mechanistic spectrum controlled potentially by DVAP. The additional evidence of the involvement of DVAP in endocytosis and lipid metabolism can give us clues about the specific function of the protein and changes associated with the ALS-linked mutations.

8.4 Hippo signaling pathway is involved in ALS pathomechanism

The relation between VAP proteins and cell proliferation is a novel and interesting research focus that could explain some of the ALS-linked phenotypes. Only recently, Rao *et al.* found an up-regulation of VAPB in metastatic breast tumor tissue that could be explained through a link with the modulation of the AKT pathway (Rao *et al.*, 2012). For this reason, it is significantly important that from the genetic modifiers found in our screen, one of the most represented functional categories was cell death. Not only a relevant number of genes from this category were found, but also some of them were confirmed by all of our validation tests, strengthening their link to VAP biology.

One of the suppressors found in this project is Hippo, a central component in the control of cell proliferation. Hippo is the ortholog of human MST1 and STK3 serine/threonine kinases (Dan *et al.*, 2001). These human proteins have been identified as tumor suppressors, activating apoptosis and decreasing cell proliferation as a normal function (Harvey *et al.*, 2003). Activation of apoptosis has also been reported with the overexpression of Hippo in *Drosophila* (Pantalacci *et al.*, 2003). In our screen, we found that two loss-of-function lines for this gene strongly suppress DVAP-P58S-associated neurodegeneration in the eye and motor performance. These results suggest that DVAP-P58S mechanism could be linked to an activation of apoptosis, and the loss-of-function of Hippo could block that process, suppressing in this way the neurodegeneration. That would be in line with data proposed by Rao *et al*. (Rao *et al.*, 2012), where DVAP-WT functions as an oncoprotein that activates the pro-survival AKT pathway. Therefore DVAP-P58S, acting through a loss-of-function mechanism, would fail to activate pro-survival pathways and could promote

instead apoptosis and cell-cycle exit, just as seen with Hippo overexpression (Pantalacci *et al.*, 2003). Thus, Hippo loss-of-function, as observed in our study, can balance the DVAP-P58S effect by decreasing its apoptotic activity. Further analyses in the interaction of these proteins are needed to understand this potential mechanism. Considering that the regulation of VAP over AKT is not known, it will likely need interaction with other proteins, as VAP does not present any kinase activity (Rao *et al.*, 2012).

Discovered initially in *Drosophila*, Hippo is the central component of the homonymous tumour suppressor pathway (Udan *et al.*, 2003; Pantalacci *et al.*, 2003). After receive positive stimulation from different regulators including the Decapentaplegic and Wingless gradients, and the cytoskeleton-binding proteins Merlin, Expanded and Kibra, Hippo is able to bind the interactor Salvador. This complex phosphorylates and activates Warts, which then phosphorylates and inhibits the transcription activator Yorkie. This inhibition translate in the down-regulation of downstream targets of the pathway such as diap1, cycE, ex and bantam, leading to an overall control of the cell growth. A mutation in any gene upstream of Yorkie will lead to a constant expression of the downstream targets and an increase in the cell proliferation (Zhao *et al.*, 2011). This pathway is highly conserved in humans, where the central components of the pathway have been linked to tumour formation and cancer. Interestingly, other genetic modifiers found in this study are Syx7/Avl and Diap2. The first one is an endocytic neoplastic tumor suppressor gene that regulates the same pathway (Robinson and Moberg, 2011). On the other hand, Diap2 and its paralog Diap1 are downstream targets of the Hippo pathway (Martin-Belomente & Perez-Moreno, 2011). We already reported that DIAP1 up-regulation strongly suppresses DVAP-P58S-linked neurodegeneration in the eye (Forrest *et al.*, 2013), so this effect is now confirmed with the suppression observed with DIAP2 overexpression. At the same time, supports the idea of DVAP-P58S causing neurodegeneration triggering apoptosis via the Hippo pathway. Additionally, hippo ortholog MST2 is a downstream target of the RAF pathway, the previously discussed anti-apoptotic pathway highly represented in our screen. Recently, the Hippo pathway was strongly associated with DVAP in a study performed by Norbert

Perrimon's group, where using mass spectrometry, DVAP was identified as part of a high-confidence *Drosophila* Hippo protein-protein interaction network (Kwon *et al.*, 2013). Curiously in this study, vesicular trafficking, a highly enriched category from our screen, highlights as one of the best linked functions to the Hippo pathway.

8.5 DVAP interaction with Klar and lipid droplets could, at least in part, explain the ALS pathomechanism

VAPB and ALS have been strongly associated with lipid metabolism over the last years. A common factor found in ALS patients is the abnormal amount of lipids in the blood or dyslipidemia (Turner *et al.*, 2009). Additionally, genes encoding proteins involved in lipid metabolism appear to be up-regulated in spinal cords of ALS patients (Malaspina *et al.*, 2001). VAPB on the other hand, interacts with several lipid related proteins such as CERT, Nir2, OSBP and Sac1 (Kawano *et al.*, 2006, Amarilio *et al.*, 2005, Ngo and Ridgway, 2009, Forrest *et al.*, 2013). A strong factor for the interaction with VAP is the presence in some of these proteins of the diphenylalanine in an acidic tract (FFAT) motif. Proteins targeted to the ER and nuclear membrane by this signaling motif include the lipid- and VAP-interacting proteins CERT and OSBP (Kaiser *et al.*, 2008, Wyles et a., 2002, Kawano *et al.*, 2006). Interaction between VAP and lipid transport proteins carrying FFAT-like motifs such as FAPP-2 supports furthermore the role of VAP in the transfer of lipids (Mikitova and Levine, 2012). Moreover, in 2006 Cermelli *et al.* purified lipid droplets from *Drosophila* embryos and using capillary liquid chromatography-tandem mass spectroscopy, they detected that DVAP was significantly representated in the lipid droplet fraction (Cermelli *et al.*, 2006). Lipid droplets store and supply lipids for different cellular processes such as energy metabolism and production of molecules derived from lipids (Pol *et al.*, 2014). All the previous evidence provides more relevance to the DVAP-modifier genes found in this study, considering that Lipid metabolism is a significant functional cathegory, based on Ingenuity Pathway analysis, and Lipid Particle is the most enriched Gene Ontology term, according to the DAVID database.

One of the components of this functional category found in our screen is Klarsicht, a protein that controls lipid droplets and nuclei dynamics (Elhanany-Tamir *et al.*, 2012). This gene, functional ortholog of the human Nesprins, presents a complex structure and regulation that comprises alternative splicing and different promoters (Kim *et al.*, 2013). The different isoforms share an N-terminal region that interacts with dynein and kinesin motors. However, the C-terminal region changes the different specificity of the protein for different cargos (Vu *et al.*, 2011). The α-isoform carries a KASH domain that regulates the interaction with the outer nuclear envelope. On the other hand, the β-isoform carries a LD domain that binds embryonic lipid droplets (Guo *et al.*, 2005). Other 3 isoforms (γ, δ, ε) are less studied but differ in the basic genetic structure, fact that expands even more the biology of the protein. In our screen, we identified as a suppressor of DVAP-P58S-toxicity the allele $Klar^{EP3104}$. To confirm the effect of this gene we obtained several *Drosophila* tools from Prof. Michael Welte, a well-known expert of this protein. We were able to confirm that a loss-of-function effect was responsible for the neurodegenerative suppression in the eye and motor performance. We observed the same phenotypic effect with the EP line and with the loss-of-function alleles YG3 (that block the expression of α and β isoforms) and $Klar^{1}$ (a truncated version of the protein that lacks the specific C-terminal domains and therefore, acts as a null allele (Welte *et al.*, 1998)). More interestingly, we detected that overexpressing the β-isoform produces an enhancement of the DVAP-P58S-toxicity in the eye and the rest of nervous system, deteriorating viability and motor performance of the tester line. These data suggest a strong interaction between DVAP and Klar and a potential common role of these proteins in ALS pathogenesis, likely mediating nuclei and lipid droplets dynamics.

Recently, other lipid droplet-associated proteins have been linked to motor neuron diseases. Mutations in the genes SPG20 and Seipin are associated with motor neuron disorders and misregulation of lipid droplets metabolism (Bakowska *et al.*, 2007; Yagi *et al.*, 2011). Additionally, these particles are associated with other neurodegenerative diseases like Parkinson's, where disease-linked mutant α-synucleins appear to lose its normal relocalisation from cytosol to lipid droplets,

altering at the same time the wild type metabolism of triglycerides in this organelle (Cole *et al.*, 2002). Klar-DVAP interaction can also explain changes in nuclei distribution that is associated with different disorders. Klar loss-of-function alleles produces nuclei mispositioning, an effect already involved in myopathies (Puckelwartz *et al.*, 2009, Zhang *et al.*, 2007). This suggests that Klar mutants can potentially be linked to other disorders as well, such as DVAP-mediated ALS. Further analysis of DVAP/Klar interaction, their relation with lipid droplets and nuclei dynamics, and their involvement in ALS-associated phenotypes would prove pivotal to understand the possible pathomechanism of the disease.

Klarsicht was only one of the eight proteins associated with lipid metabolism discovered in this study. Rdgbβ, Acsl and IP3K1 are linked to several steps of lipids and phosphoinositides production. As previously mentioned, the metabolism of phosphoinositides is already central in DVAP biology and the mechanism in which these genes are associated with it could clarify furthermore the currently known mechanism. For instance, human homologues of Acsl are associated with the formation of lipid droplets in the ER (ACSL3, Poppelreuther *et al.*, 2012) and to the axonal transport of synaptic vesicles (ACSL4, Liu *et al.*, 2011). On the other hand, Ero1L is another protein linked to lipids that works as a oxidoreductase in the ER and that has been associated with inositol 1,4,5-triphosphate receptor activity acting in the Ca^{++} release in the ER via unfolded protein response (UPR) (Li *et al.*, 2009). Curiously, this protein is a known physical interactor of DVAP (Guruharsha *et al.*, 2009) and is involved in the DVAP-linked pathway Notch (Tien *et al.*, 2008). Even though some of these data would imply a strong connection between these players, there is not a known mechanism to link them with the observed phenotypes. The participation of DVAP and these lipid-realted proteins to ALS pathomechanism is a novel possibility that should be considered.

8.6 DVAP-P58S modifier genes are correlated with MSP secretion mechanism

In 2008, Tsuda *et al.* reported that MSP fragment of VAPB is cleaved, secreted and binds to Eph receptors (Tsuda *et al.*, 2008). Using *Drosophila* and *C. elegans* they also showed that the presence of the ALS-linked mutation P56S suppresses the cleavage and promote ubiquitination and aggregation of the protein. Following works supported this model and associated the MSP secretion to mitochondria localisation (Han *et al.*, 2012) and energy metabolism in adult survival (Han *et al.*, 2013). At the moment some key aspects of this theory have not been completely elucidated, like specificity of the biochemical assays or validation in human patients. However, this model exhibits some interesting notions of a possible DVAP pathomechanism and more interestingly, a functional relevance of the ALS-linked mutation. In the present study, we found a group of DVAP-toxicity modifiers that are related with the MSP secretion hypothesis and that could provide further clues to understand this mechanism.

From our screen, five modifiers codify proteins that support this hypothesis. We found *Leak*, a gene that encodes a protein associated with axon guidance and that is part of the receptor family Roundabout (Schimmelpfeng *et al.*, 2001). Han proposed that MSP binds to the Eph receptor Lar to stabilise the mitochondria. Also, it can bind to Leak to block Lar activation. *C. elegans* VAPB mutants have mitochondrial defects, which are suppressed by the inactivation of Lar (Han *et al.*, 2012). This also may be achieved by the activation of Leak, which can explain the suppression of the DVAP-P58S toxicity by the overexpression of Leak that we observed in our screen. Additionally, the ARP2/3 complex plays a central role in the mitochondria stabilisation. This highly conserved complex is the key nucleator for the actin cytoskeleton, binding existing actin filaments to form daughter filaments. In this way, ARP2/3 complex regulates motility, cytokinesis and endocytosis (Rotty *et al.*, 2013). Interestingly, we found that two genes involved in the actin nucleation process were part of the DVAP-modifier list. HSPC300 is one of the five proteins that support ARP2 and ARP3 proteins in the complex that initiate actin nucleation,

playing a reported role in axonal and NMJ architecture as well (Qurashi *et al.*, 2007; Rotty *et al.*, 2013). We also found Act42A, a gene that encodes for one of the six *Drosophila* actin isoforms (Fyrberg *et al.*, 1981), each of them probably with a different specialized function (Jacinto & Baum, 2003). Curiously, the ARP2/3 complex was originally identified as an interacting factor for Profilin, an acting-binding protein that recently was associated with ALS after mutations in the gene encoding this protein were found in several ALS kindred (Machesky *et al.*, 1994; Wu *et al.*, 2012). Further studies in the interaction between DVAP with HSPC300, Act42A, and Leak can provide more support to the potential non-autonomous effect of the MSP domain.

However, possibly the most interesting modifier related with MSP secretion unveiled in the screen is the protease Rhomboid. Part of one of the four families of transmembrane proteases, rhomboid is present in all branches of life including endosymbiotic organelles (Urban & Dickey, 2011). It was firstly described in *Drosophila* as the activator of *Spitz*, a ligand of the epidermal growth factor (EGF) receptor (Sturtevant *et al.*, 1993). Therefore, rhomboid plays a central role in early developmental stages, hydrolyzing peptide bonds inside the cell membrane (Urban *et al.*, 2001). In human cells, the activity of rhomboid activity has been associated with cancer cells, probably related with Growth factor signaling (Etheridge *et al.*, 2013).

The *rhomboid* catalytic site includes four conserved residues responsible for the specific serine-cleavage. Some proteins lack the catalytic domain but still maintain the protein structure, therefore are called rhomboid protein (no proteases) or iRhom, and have been associated with endoplasmic reticulum-associated degradation of proteins (Christova *et al.*, 2013). In *Drosophila*, Rhomboid is located in the Golgi and initiates neighboring cell pathways cleaving Spitz. The peptide obtained from Spitz cleavage is then secreted to activate EGF pathway in other cells. This process can be a common mechanism for other proteins that could use the Rho-Spitz pathway to express its information in an EGF-like way (Urban & Dickey, 2011). Interestingly, this is highly reminiscent to the VAPB secretion proposed by Tsuda. Secreted MSP domain of VAPB binds to Eph receptor in the neighbour cells,

controlling in this way energy metabolism (Tsuda *et al.*, 2008, Han *et al.*, 2012). Despite the confirmation of this secretion and its link to a non-cell autonomous effect in the ALS pathogenesis (Han *et al.*, 2013), proteases in charge of the cleavage of the MSP domain have not been found yet.

Rhomboid active site is positioned in the lipid bilayer of the cell membrane and recognises a specific sequence in the transmembrane domain of the target proteins. Previously it was described that a helix-destabilising residue is necessary to be part of the transmembrane domain, but these residues were necessary only if the sequence is in the transmembrane domain and not if the sequence is outside of it (Strisovsky *et al.*, 2009). Considering these parameters, we can observe that VAPB aminoacid sequence presents a 25 residue long region in its transmembrane domain that potentially can be cleaved by rhomboid, fitting the proposed consensus sequence. A potential cleavage of VAPB in this region would lead to a release from its membrane localisation and fit with the secretion hypothesis. This is even more possible if we consider previous co-expression (Weber *et al.*, 2008) and physical interaction data (Guruharsha *et al.*, 2011) that link VAPB and Rhomboid.

The authors of the MSP hypothesis finally proposed that ALS-linked mutation inhibits MSP secretion, due to an increased protein accumulation and UPR activation that potentially decreases the amount of VAPB-MSP available to be cleaved. This lack of signaling in neighbour cells might affect mitochondrial localisation and muscular morphology of patients (Tsuda *et al.*, 2008, Han *et al.*, 2012). In this situation, an overexpression of the protease rhomboid could increase the amount of secreted MSP, suppressing the VAPB-P56S-linked toxicity. Indeed, this is the situation observed in our screen. The result suggests that further experiments with these two proteins such as site-directed mutagenesis and localisation studies, could potentially confirm that rhomboid plays an important role in DVAP mechanism. At the same time, this mechanism fits with the effect of the other modifiers found in the screen, located all of them downstream the MSP signaling. A decrease in Lar activity caused by an overexpression of Leak or a change in the stability of the ARP2/3

complex could lead to an improved mitochondrial stabilisation and suppression of VAPB-linked phenotype.

8.7 Ubiquitin-mediated protein clearance is confirmed as a DVAP-linked relevant process

In parallel to uncover unexpected pathways associated with DVAP pathogenesis that we have discussed previously, it was important for this study to find genes and pathways already associated with ALS and VAPB function, such as MSP-domain secretion and protein degradation (Tsuda *et al.*, 2008; Lev, 2008). Together with autophagy, the ubiquitin-proteasome system is the main pathway to degrade non-functional proteins in the cell (Ravid & Hochstrasser, 2008). In a normal cellular state, proteins must be properly folded to reach their final destination in a process regulated by proteins already linked to ALS (Blokhuis *et al.*, 2013). When this process is not perfectly performed, proteins are normally degraded by the ubiquitin-proteasome system (UPS). This system selectively tags proteins with an ubiquitin molecule, which are degraded by the proteasome. This ubiquitination process is mediated by three enzymatic classes: E1 activating enzymes bind and activate the inert ubiquitin molecule that is then transferred to an E2 ubiquitin conjugating enzyme. The final step is carried out by an E3 ubiquitin ligase that finally transfer the ubiquitin molecule from the E2 enzyme to the protein tagged for degradation (Ravid & Hochstrasser, 2008). When this process fails and proteins are not degraded immediately, the unfolded protein response (UPR) is activated. This ER-stress response is composed by three pathways, which central components are the transcription factors XBP-1 and ATF6 and the PERK kinase. These molecules activate chaperones and proteins involved in ER-degradation (Ron & Walter, 2007). Interestingly, DVAP has been previously associated with this response. The overexpression of VAPB-WT promotes UPR after an increased production of XBP1 mRNA was observed in cell culture (Kanekura *et al.*, 2006). On the other hand, the MSP domain of VAPB interacts and negatively modulates ATF6 activity, in a process that could involve membrane trafficking and ATF6 traslocation disruption (Gkogkas *et al.*, 2008).

In our genetic screen we found different genes involved in these processes. Three different genes associated with UPS's last step were found. Cul-2 is part of the Cullin family of molecular scaffolds that organise RING-E3 ubiquitin ligases. Including hundreds of components, this family is the largest ubiquitin ligase class, becoming one of the most important post-translational protein regulators (Petroski & Deshaies, 2005). Another DVAP-modifier is Su(Var)2-10, which human ortholog is E3 SUMO-protein ligase PIAS1, working as well as a transcriptional co-regulator (Liu *et al.*, 1998). A previously discussed gene is CG9153 that encodes the ortholog of HERC4. This protein carries a HECT E3-ligase domain that also binds an activated ubiquitin molecule to target proteins for degradation (Hochrainer *et al.*, 2004). Finally, the gene CG4502, a suppressor from our screen, exhibits sequence similarities to E2 ubiquitin ligases, as predicted by InterPro. Considering that we also found as a DVAP-toxicity suppressor the essential autophagy gene Atg7, which shows functional homology to E1 activating enzymes (Rabinowitz & White, 2010), it is fair to say that protein degradation genes are strongly represented in our screen, which supports previous findings linking this process with DVAP and ALS. Therefore, the potential connection between these DVAP-interactors and other known molecules involved in protein degradation can provide missing pieces of information to completely understand this pathway.

8.8 Energy metabolism may play an important role in ALS pathogenesis

SOD1 was the first gene associated with familial cases of ALS (Rosen *et al.*, 1993). As a result in the last two decades, a strong linkage has been found between ALS cases and mitochondria. In the last years, SOD1 models have failed to support any consistent mechanism but also, gene penetrance in patients has decreased in this period, explained in part by the discovery of C9orf72 as a main cause (Robberecht & Phillips, 2013). In the same time frame however, increasing evidence have linked VAPB with mitochondria defects, suggesting that mitochondria and energy metabolism can still be a central feature of ALS.

This fact is connected with the previously discussed MSP secretion, considering that VAPB affects anterograde mitochondrial movement in axons, increasing cytoplasmic Ca^{++} and affecting mitochondrial docking to tubulin (Morotz *et al.*, 2012). Additionally, VAPB interacts with mitochondrial membrane protein PTPIP51 in its junction with ER, regulating the mitochondrial uptake of Ca^{++} from the ER stores. ALS-linked mutation VAPB-P56S disrupts VAPB-PTPIP51 interaction, increasing the mitochondrial uptake of Ca^{++} (De Vos *et al.*, 2012). The connection of these interactions with the mitochondrial stabilisation proposed by Han (Han et al., 2012), suggest an active role of VAPB in mitochondrial homeostasis.

In the present study we found novel DVAP genetic interactors that regulate mitochondrial metabolism. Mtch is one of the genes that enhance DVAP-P58S phenotype. This protein is the receptor of tBID, a BCL2 protein that promotes the oligomerisation of Bax in the outer membrane of the mitochondria (Zaltsman *et al.*, 2010). This oligomerisation is related with the mitochondria fission, release of cytochrome C and activation of apoptosis. Mtch loss-of-function alleles are less effective to recruit tBID, protecting in this way the mitochondria from fission (Zaltsman *et al.*, 2010). The novel overexpression phenotype observed in our screen suggests that a possible activation of mitochondrial apoptosis could enhance DVAP-P58S neurodegeneration by a still-unknown mechanism.

Important connections can be made by this protein and other apoptosis/cell death genes associated with this and other studies. From our set of genes, draper and Atg7 are related to mitochondrial shape and cell maintenance. Changes in mitochondrial membrane and death of this organelle require a cleaning process activated by these two proteins that lead to the formation of the autophagosome and its fusion with the lysosome (McPhee *et al.*, 2010). VAPB-induced aggregates or even a loss of function of this protein at initial stages of the cleaning process would affect the final recycling of the dead cellular components. In our study, the overexpression of these two proteins suppresses the DVAP-induced toxicity, suggesting that a decline in the autophagy process could be related with DVAP effect. At the same time, they would work in an opposite direction of Mtch; an

increase in mitochondrial apoptosis or a decrease in autophagy would lead to a worsening of DVAP-induced phenotype. This would still be valid if the effect of mutant DVAP triggers mitochondrial death; the delay of this step or the increase of the recycling of cellular debris would ameliorate the toxicity in the cell. To prove this mechanism is not only necessary to confirm whether this effect is specifically due to an interaction with DVAP, but also to analyse the possible relation of other downstream targets of this mechanism and previously discussed pathways such as lipid and vesicle metabolisms.

8.9 Future perspectives

Throughout this project we have identified 85 novel modifiers of DVAP-P58S neurodegeneration. Potentially, an important number of them may be involved in ALS pathology and could link some of the unconnected known disease's mechanisms. We have not only found these genes analysing neurodegeneration in *Drosophila* eye, but also tested changes in the motor performance and confirmed these results with independent alleles. These experiments lead us to propose the list of genes as *bona fide* candidates to understand ALS mechanism in a clear way and furthermore, to point these novel modifiers as initial steps for identifying possible therapeutic targets. Surely, further studies are mandatory to prove the previous sentence, but the encouraging results support in a good way these future analyses.

To the previous reports linking VAPB to important neurodegenerative processes, we can now add a consistent and relevant list of genetic interactors that support furthermore the role of VAPB in these processes. We can propose a potential mechanism where all these novel interactors support DVAP function inside the cell, and the loss of function of tis protein through the formation of DVAP-P58S-induced aggregates disrupts the vital processes that finally lead to neurodegeneration (Figure 34). Previously discussed function of DVAP in the cell include regulation of endocytic traffic, lipids and nucleai dynamics, energy metabolism and cell proliferation. The up-regulation of several DVAP genetic interactors found in this

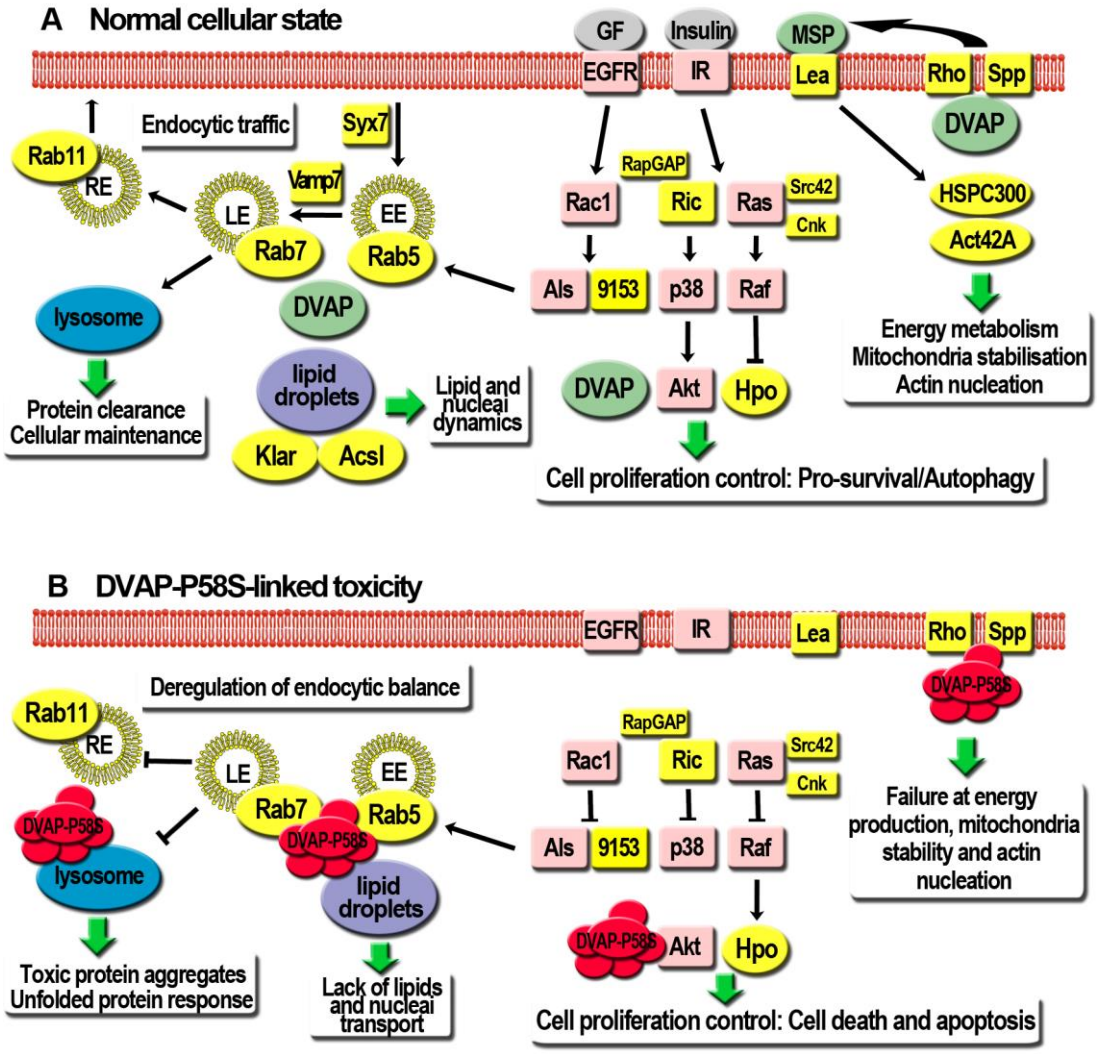

Figure 34. Proposed mechanisms involved in DVAP neurodegeneration. (A) Molecular pathways associated to DVAP activity in a normal cellular state. The correct function of this protein (green) plays an important role on regulation of endocytic traffic, lipids and nucleai dynamics, energy metabolism and cell proliferation (white boxes). Genetic interactors found in the current project (yellow) are integral part of these pathways. (B) Protein aggregates caused by the presence of DVAP-P58S (red) disrupt the described pathways leading to an overall toxicity in the cell. Lack of endocytic particles, lipid and nucleai trafficking are related to neurodegeneration that is increased by the upregulation of pro-apoptotic signaling and failure in the energy production, mitcohondria stabilization and actin ncuelation. The overexpression of the DVAP-genetic interactors (yellow) could overcome at least one of these degenerative pathways and delay cell death. Toxicity suppression could be achieved decreasing the amount of DVAP-P58S aggregates formed, their removal, or the stabilization of other damaged processes.

project (yellow nodes in Figure 34) could be sufficient to restore the normal cellular balance previously disrupted by DVAP aggregation. However, we still need to prove most of these connections and confirm that the genetic interaction just found can determine the final output of these pathways.

Originally, this study was supposed to cover the whole genome, which includes additional non-tested lines from the first and third chromosome of *Drosophila*. A better characterisation of the obtained results so far led us to hold on the progress of the screen and analyse the relation between the novel modifiers. This point is relevant as this project must be continued to cover completely the spectrum of DVAP modifiers and in this way, fill the potential gaps in the mechanisms discussed before. Undoubtedly, our progress to this date is important enough to start working on specific genes and pathways already. However, further screening of the remaining 764 potential overexpression lines from the analysed collections will provide a complete map of DVAP mechanisms in neurodegeneration.

The genetic modifiers discovered in this project are interacting with DVAP to modify neurodegeneration in our model. It would be relevant and equally useful to test these interactors with other ALS or MND causative genes. As previously discussed, some of these causative genes are already modeled in *Drosophila*, with similar neurodegenerative phenotypes to the DVAP-P58S model (Watson *et al.*, 2008; Bahadorani *et al.*, 2013; Li *et al.*, 2010). Therefore, it would be interesting to check whether DVAP-P58S modifiers also suppress the toxicity caused but mutations in TDP-43, SOD1, SMN, and C9orf72-based models in *Drosophila*. In the same way, with further collaboration with human ALS tissue centers, it would be attractive to analyse whether any of the 85 modifiers is misregulated in tissues from patients with ALS in the same way we observed for human RAB5. The success in these assays not only will advance the understanding of ALS pathomechanism, but also could help to explain the neurodegeneration observed in several patients with sporadic ALS that are not associated with any known causative gene.

Another important perspective for this work involves the novel ALS-linked VAPB mutation V234I. Last year, in a parallel project to this screen, we were able to model and characterise the *Drosophila* version of this mutant, V260I (Sanhueza *et al.*, 2013; Appendix of this study). This work yielded interesting and surprising results, specifically the confirmation of this mutation as a gain-of-function, as compared to the loss-of-function mechanism observed in DVAP-P58S. It will be important to observe the DVAP-V260I associated phenotypes under the effect of the DVAP-P58S genetic modifers found in this screen. These phenotypes include protein aggregation, activation of stress response and synaptic and nuclear abnormalities. The comparison between the modifier effects of a specific gene in the two VAPB mutant alleles can provide additional clues to explain the mechanism of VAPB neurodegeneration.

Lipid particles and metabolism became one of the most relevant functions found in this project. The relation between DVAP and the lipid-related protein Klar is being currently studied by our group. It will be necessary to confirm the levels of interaction between the two proteins and the way they associate in the lipid particles. Also it would be interesting to study their relation in the control of myonuclei and neuromuscular junction structure, which it seems to be highly regulated by their interaction. The way in which these proteins control membrane dynamics and their connection to vesicle recycling, could represent one of the strongest findings of this study.

Finally, another interesting topic found in this study is cell proliferation and cancer. The connection between DVAP and Hippo is a particularly interesting one, especially considering the biochemical nature of Hippo that makes it a perfect target for therapeutic studies involving activity modulation by chemicals and drugs (Pan, 2010). The use of our ALS model in a screen that search for chemicals able to modulate the activity of DVAP-modifiers like Hippo, could represent a great opportunity to understand in a deeper way ALS pathogenesis and translate these advances to affected patients.

References

Aguilar, P.S., Fröhlich, F., Rehman, M., Shales, M., Ulitsky, I., Olivera-Couto, A., Braberg, H., Shamir, R., Walter, P., Mann, M., Ejsing, C.S., Krogan, N.J. & Walther, T.C. (2010) A plasma-membrane E-MAP reveals links of the eisosome with sphingolipid metabolism and endosomal trafficking. *Nature Structural & Molecular Biology*, 17 (7), pp.901–908.

Al-Chalabi, A. & Hardiman, O. (2013) The epidemiology of ALS: a conspiracy of genes, environment and time. *Nature Reviews Neurology*, 9 (11), pp.617–628.

Albagha, O.M.E., Visconti, M.R., Alonso, N., Langston, A.L., Cundy, T., Dargie, R., Dunlop, M.G., Fraser, W.D., Hooper, M.J., Isaia, G., Nicholson, G.C., del Pino Montes, J., Gonzalez-Sarmiento, R., di Stefano, M., Tenesa, A., Walsh, J.P. & Ralston, S.H. (2010) Genome-wide association study identifies variants at CSF1, OPTN and TNFRSF11A as genetic risk factors for Paget's disease of bone. *Nature Genetics*, 42 (6), pp.520–524.

Amarilio, R., Ramachandran, S., Sabanay, H. & Lev, S. (2005) Differential Regulation of Endoplasmic Reticulum Structure through VAP-Nir Protein Interaction. *Journal of Biological Chemistry*, 280 (7), pp.5934–5944.

Ambegaokar, S.S. & Jackson, G.R. (2011) Functional genomic screen and network analysis reveal novel modifiers of tauopathy dissociated from tau phosphorylation. *Human Molecular Genetics*, 20 (24), pp.4947–4977.

Anagnostou, G., Akbar, M.T., Paul, P., Angelinetta, C., Steiner, T.J. & de Belleroche, J. (2010) Vesicle associated membrane protein B (VAPB) is decreased in ALS spinal cord. *Neurobiology of Aging*, 31 (6), pp.969–985.

Andersen, P.M. & Al-Chalabi, A. (2011) Clinical genetics of amyotrophic lateral sclerosis: what do we really know? *Nature Reviews Neurology*, 7 (11), pp.603–615.

Andersen, P.M., Forsgren, L., Binzer, M., Nilsson, P., Ala-Hurula, V., Keränen, M.L., Bergmark, L., Saarinen, A., Haltia, T., Tarvainen, I., Kinnunen, E., Udd, B. & Marklund, S.L. (1996) Autosomal recessive adult-onset amyotrophic lateral sclerosis associated with homozygosity for Asp90Ala CuZn-superoxide dismutase mutation. A clinical and genealogical study of 36 patients. *Brain : a journal of neurology*, 119 (4), pp.1153–1172.

Aridor, M., & Hannan, L. (2000) Traffic jam: a compendium of human diseases that affect intracellular transport processes. *Traffic*, 1, pp.836–851.

Ashburner, M., Ball, C.A., Blake, J.A., Botstein, D., Butler, H., Cherry, J.M., Davis, A.P., Dolinski, K., Dwight, S.S., Eppig, J.T., Harris, M.A., Hill, D.P., Issel-Tarver, L., Kasarskis, A., Lewis, S., Matese, J.C., Richardson, J.E., Ringwald, M., Rubin, G.M. & Sherlock, G. (2000) Gene ontology: tool for the unification

of biology. The Gene Ontology Consortium. *Nature Genetics*, 25 (1), pp.25–29.

Auluck, P.K. & Bonini, N.M. (2002) Pharmacological prevention of Parkinson disease in Drosophila. *Nature medicine*, 8 (11), pp.1185–1186.

Bahadorani, S., Mukai, S.T., Rabie, J., Beckman, J.S., Phillips, J.P. & Hilliker, A.J. (2013) Expression of zinc-deficient human superoxide dismutase in Drosophila neurons produces a locomotor defect linked to mitochondrial dysfunction. *Neurobiology of aging*, 34 (10), pp.2322–2330.

Bakowska, J., Jupille, H., Fatheddin, P., Puertollano, R. & Blackstone, C. (2007) Troyer syndrome protein Spartin is mono-ubiquitinated and functions in EGF recpetor trafficking. *Molecular biology of the cell*, 18 (5), pp.1683-1692.

Barrett, K., Leptin, M. & Settleman, J. (1997) The Rho GTPase and a putative RhoGEF mediate a signaling pathway for the cell shape changes in Drosophila gastrulation. *Cell*, 91 (7), pp.905–915.

Bartolome, F., Wu, H.-C., Burchell, V.S., Preza, E., Wray, S., Mahoney, C.J., Fox, N.C., Calvo, A., Canosa, A., Moglia, C., Mandrioli, J., Chiò, A., Orrell, R.W., Houlden, H., Hardy, J., Abramov, A.Y. & Plun-Favreau, H. (2013) Pathogenic VCP Mutations Induce Mitochondrial Uncoupling and Reduced ATP Levels. *Neuron*, 78 (1), pp.57–64.

Bastin, G & Heximer, S. (2013) Rab Family Proteins Regulate the Endosomal Trafficking and Function of RGS4. *Journal of biological chemestry*, 288 (30), pp. 21836-21849.

Bates, K., Sung, C., Hilson, L., Robinow, S. (2014) unfulfilled Interacting Genes Display Branch-Specific Roles in the Development of Mushroom Body Axons in Drosophila melanogaster. *G3*, 4 (4), pp. 693-706.

Beinert, N., Werner, M., Dowe, G., Chung, H.-R., Jackle, H. & Schafer, U. (2004) Systematic gene targeting on the X chromosome of Drosophila melanogaster. *Chromosoma*, 113 (6), pp.271–275.

Bellen, H., Lewis, R., Liao, G., He, Y., Carlson, J., Tsang, G., Evans-Holm, M., Hiesinger, P., Schulze, K., Rubin, G., Hoskins, R. & Spradling, A. (2004) The BDGP Gene Disruption Project: Single Transposon Insertions Associated With 40% of Drosophila Genes. *Genetics*, 167 (2), pp.761–781.

Bellen, H.J., Levis, R.W., He, Y., Carlson, J.W., Evans-Holm, M., Bae, E., Kim, J., Metaxakis, A., Savakis, C., Schulze, K.L., Hoskins, R.A. & Spradling, A.C. (2011) The Drosophila Gene Disruption Project: Progress Using Transposons With Distinctive Site Specificities. *Genetics*, 188 (3), pp.731–743.

Bendotti, C., Marino, M., Cheroni, C., Fontana, E., Crippa, V., Poletti, A. & De Biasi, S. (2012) Dysfunction of constitutive and inducible ubiquitin-proteasome system in amyotrophic lateral sclerosis: Implication for protein

aggregation and immune response. *Progress in Neurobiology*, 97 (2), pp.101–126.

Bilen, J. & Bonini, N. (2005) Drosophila as a Model for Human Neurodegenerative Disease. *Annual Reviews in Genetics*, pp.153–171.

Biteau, B., Karpac, J., Hwangbo, D. & Jasper, H. (2011) Regulation of Drosophila lifespan by JNK signaling. *Experimental Gerontology*, 46 (5), pp.349–354.

Bitting, R.L. & Armstrong, A.J. (2013) Targeting the PI3K/Akt/mTOR pathway in castration-resistant prostate cancer. *Endocrine Related Cancer*, 20 (3), pp.R83–R99.

Blagoveshchenskaya, A. & Mayinger , P. (2008) SAC1 lipid phosphatase and growth control of the secretory pathway. *Molecular biosystems*, 5, pp.33-42.

Blokhuis, A.M., Groen, E.J.N., Koppers, M., Berg, L.H. & Pasterkamp, R.J. (2013) Protein aggregation in amyotrophic lateral sclerosis. *Acta Neuropathologica*, 125 (6), pp.777–794.

Boguski, M & McCormick, F. (1993) Proteins regulating Ras and its relatives. *Nature*, 366 (6456), pp.643-654.

Bonini, N. (1999) A genetic model for human polyglutamine-repeat disease in *Drosophila melanogaster*. *Philos Trans R Soc Lond B Biol Sci.*, 1386, pp.1057–1060.

Branco, J., Al-Ramahi, I., Ukani, L., Perez, A.M., Fernandez-Funez, P., Rincon-Limas, D. & Botas, J. (2008) Comparative analysis of genetic modifiers in Drosophila points to common and distinct mechanisms of pathogenesis among polyglutamine diseases. *Human Molecular Genetics*, 17 (3), pp.376–390.

Brand, A.H. & Perrimon, N. (1993) Targeted gene expression as a means of altering cell fates and generating dominant phenotypes. *Development*, 118 (2), pp.401–415.

Brice, S.E., Alford, C.W. and Cowart, L.A. (2009) Modulation of sphingolipid metabolism by the phosphatidylinositol-4-phosphate phosphatase Sac1p through regulation of phosphatidylinositol in Saccharomyces cerevisiae. *Journal of Biological Chemistry*, 284 (12), 7588–7596.

Brown, T.C., Tran, I.C., Backos, D.S. & Esteban, J.A. (2005) NMDA Receptor-Dependent Activation of the Small GTPase Rab5 Drives the Removal of Synaptic AMPA Receptors during Hippocampal LTD. *Neuron*, 45 (1), pp.81–94.

Bugaut, A & Balasubramanian, S. (2012) 5'-UTR RNA G-quadruplexes: translation regulation and targeting. *Nucleic acids research*, 40 (11), pp.4727-4141.

Burd, C. (2011) Physiology and pathology of endosome-to-Golgi retrograde sorting. *Traffic,* 12 (8), pp.948-955

Cai, W., Rudolph, J., Harrison, S., Jin, L., Frantz, A., Harrison, D. & Andres, D. (2011) An evolutionarily conserved Rit GTPase–p38 MAPK signaling pathway mediates oxidative stress resistance. *Molecular Biology of the Cell*, 22, pp. 3231-3241.

Callaerts, P., Leng, S., Clements, J., Benassayag, C., Cribbs, D., Kang, Y.Y., Walldorf, U., Fischbach, K.F. & Strauss, R. (2001) Drosophila Pax-6/eyeless is essential for normal adult brain structure and function. *Journal of neurobiology*, 46 (2), pp.73–88.

Cavalli, V., Corti, M. & Gruenberg, J. (2001) Endocytosis and signaling cascades: a close encounter. *FEBS Letters*, 498 (2-3), pp.190–196.

Cermelli, S., Guo, Y., Gross, S.P., & Welte, M.A. (2006) The lipid-droplet proteome reveals that droplets are a protein-storage depot. *Current Biology*, 16, pp.1783–1795.

Chai, A., Withers, J., Koh, Y.H., Parry, K., Bao, H., Zhang, B., Budnik, V. & Pennetta, G. (2008) hVAPB, the causative gene of a heterogeneous group of motor neuron diseases in humans, is functionally interchangeable with its Drosophila homologue DVAP-33A at the neuromuscular junction. *Human Molecular Genetics*, 17 (2), pp.266–280.

Chao, J.T.-C., Foster, L.J. & Loewen, C.J.R. (2009) Identification of protein complexes with quantitative proteomics in S. cerevisiae. *Journal of Visualized Experiments*, 25, pii. 1225.

Chardin, P., Camonis, J.H., Gale, N.W., van Aelst, L., Schlessinger, J., Wigler, M.H. & Bar-Sagi, D. (1993) Human Sos1: A guanine nucleotide exchange factor for Ras that binds to GRB2. *Science*, 260, pp.1338– 1343.

Chatraryamontri, A., Breitkreutz, B.J., Heinicke, S., Boucher, L., Winter, A., Stark, C., Nixon, J., Ramage, L., Kolas, N., O'Donnell, L., Reguly, T., Breitkreutz, A., Sellam, A., Chen, D., Chang, C., Rust, J., Livstone, M., Oughtred, R., Dolinski, K. & Tyers, M. (2012) The BioGRID interaction database: 2013 update. *Nucleic Acids Research*, 41 (D1), pp.D816–D823.

Chen, F., Barkett, M., Ram, K., Quintanilla, A & Hariharan, I. (1997) Biological characterization of Drosophila Rapgap1, a GTPase activating protein for Rap1. *Proceedings of the National Academy of Sciences of the United States of America,* 94, pp.12485-12490.

Chen, H.K., Fernandez-Funez, P., Acevedo, S.F., Lam, Y.C., Kaytor, M.D., Fernandez, M.H., Aitken, A., Skoulakis, E.M.C., Orr, H.T., Botas, J. & Zoghbi, H.Y. (2003) Interaction of Akt-phosphorylated ataxin-1 with 14-3-3

mediates neurodegeneration in spinocerebellar ataxia type 1. *Cell*, 113 (4), pp.457–468.

Chen, H.J., Anagnostou, G., Chai, A., Withers, J., Morris, A., Adhikaree, J., Pennetta, G. & de Belleroche, J.S. (2010) Characterization of the Properties of a Novel Mutation in VAPB in Familial Amyotrophic Lateral Sclerosis. *Journal of Biological Chemistry*, 285 (51), pp.40266–40281.

Chen, S., Zhang, X., Song, L. & Le, W. (2012) Autophagy Dysregulation in Amyotrophic Lateral Sclerosis. *Brain Pathology*, 22 (1), pp.110–116.

Chia, R., Tattum, M.H., Jones, S., Collinge, J., Fisher, E.M.C. & Jackson, G.S. (2010) Superoxide Dismutase 1 and tgSOD1G93A Mouse Spinal Cord Seed Fibrils, Suggesting a Propagative Cell Death Mechanism in Amyotrophic Lateral Sclerosis M. B. Feany ed. *PLoS ONE*, 5 (5), p.e10627.

Chio, A., Traynor, B.J., Lombardo, F., Fimognari, M., Calvo, A., Ghiglione, P., Mutani, R. & Restagno, G. (2008) Prevalence of SOD1 mutations in the Italian ALS population. *Neurology*, 70 (7), pp.533–537.

Chou, T.B. & Perrimon, N. (1996) The autosomal FLP-DFS technique for generating germline mosaics in Drosophila melanogaster. *Genetics*, 144 (4), pp.1673–1679.

Chow, C.Y., Landers, J.E., Bergren, S.K., Sapp, P.C., Grant, A.E., Jones, J.M., Everett, L., Lenk, G.M., McKenna-Yasek, D.M., Weisman, L.S., Figlewicz, D., Brown, R.H.B. & Meisler, M.H. (2009) Deleterious Variants of FIG4, a Phosphoinositide Phosphatase, in Patients with ALS. *The American Journal of Human Genetics*, 84 (1), pp.85–88.

Christova, Y., Adrain, C., Bambrough, P., Ibrahim, A. & Freeman, M. (2013) Mammalian iRhoms have distinct physiological functions including an essential role in TACE regulation. *EMBO reports*, 14 (10), pp.884-890.

Ciura, S., Lattante, S., Le Ber, I., Latouche, M., Tostivint, H., Brice, A. & Kabashi, E. (2013) Loss of function of C9orf72 causes motor deficits in a zebrafish model of Amyotrophic Lateral Sclerosis. *Annals of Neurology*, 74 (2), pp.180-187.

Cleveland, D.W. & Rothstein, J.D. (2001) From Charcot to Lou Gehrig: deciphering selective motor neuron death in ALS. *Nature Reviews Neuroscience*, 2 (11), pp.806–819.

Cole, N., Murphy, D., Grider, T., Rueter, S., Brasaemle, D. & Nussbaum, R. (2002) Lipid binding and oligomerization properties of the Parkinson's Disease Protein a-synuclein. *Journal of biological chemestry,* 277, pp.6344-6352.

Colicelli, J. (2004) Human RAS superfamily proteins and related GTPases. *Science Stke*, 2004 (250), RE 13.

Conforti, F.L., Sprovieri, T., Mazzei, R., Ungaro, C., Tessitore, A., Tedeschi, G., Patitucci, A., Magariello, A., Gabriele, A. & Labella, V. (2006) Sporadic ALS is not associated with VAPB gene mutations in Southern Italy. *Journal of negative results in biomedicine*, 5 (7).

Cook, R.K., Christensen, S.J., Deal, J.A., Coburn, R.A., Deal, M.E., Gresens, J.M., Kaufman, T.C. & Cook, K.R. (2012) The generation of chromosomal deletions to provide extensive coverage and subdivision of the Drosophila melanogaster genome. *Genome biology*, 13 (3), p.R21.

Costanzo, M., Baryshnikova, A., Bellay, J., Kim, Y., Spear, E.D., Sevier, C.S., Ding, H., Koh, J.L.Y., Toufighi, K., Mostafavi, S., Prinz, J., St Onge, R.P., VanderSluis, B., Makhnevych, T., Vizeacoumar, F.J., Alizadeh, S., Bahr, S., Brost, R.L., Chen, Y., Cokol, M., Deshpande, R., Li, Z., Lin, Z.Y., Liang, W., Marback, M., Paw, J., San Luis, B.J., Shuteriqi, E., Tong, A.H.Y., van Dyk, N., Wallace, I.M., Whitney, J.A., Weirauch, M.T., Zhong, G., Zhu, H., Houry, W.A., Brudno, M., Ragibizadeh, S., Papp, B., Pal, C., Roth, F.P., Giaever, G., Nislow, C., Troyanskaya, O.G., Bussey, H., Bader, G.D., Gingras, A.C., Morris, Q.D., Kim, P.M., Kaiser, C.A., Myers, C.L., Andrews, B.J. & Boone, C. (2010) The Genetic Landscape of a Cell. *Science*, 327 (5964), pp.425–431.

Couthouis, J., Hart, M.P., Shorter, J., DeJesus-Hernandez, M., Erion, R., Oristano, R., Liu, A.X., Ramos, D., Jethava, N. & Hosangadi, D. (2011) A yeast functional screen predicts new candidate ALS disease genes. *Proceedings of the National Academy of Sciences of the United States of America*, 108 (52), pp.20881–20890.

Dan, I., Watanabe, N. & Kusumi, A. (2001) The Ste20 group kinases as regulators of MAP kinase cascades. *Trends in Cell Biology*, 11 (5), pp.220-230.

De Vos, K.J., Morotz, G.M., Stoica, R., Tudor, E.L., Lau, K.F., Ackerley, S., Warley, A., Shaw, C.E. & Miller, C.C.J. (2012) VAPB interacts with the mitochondrial protein PTPIP51 to regulate calcium homeostasis. *Human Molecular Genetics*, 21 (6), pp.1299–1311.

DeJesus-Hernandez, M., Mackenzie, I.R., Boeve, B.F., Boxer, A.L., Baker, M., Rutherford, N.J., Nicholson, A.M., Finch, N.A., Flynn, H., Adamson, J., Kouri, N., Wojtas, A., Sengdy, P., Hsiung, G.-Y.R., Karydas, A., Seeley, W.W., Josephs, K.A., Coppola, G., Geschwind, D.H., Wszolek, Z.K., Feldman, H., Knopman, D.S., Petersen, R.C., Miller, B.L., Dickson, D.W., Boylan, K.B., Graff-Radford, N.R. & Rademakers, R. (2011) Expanded GGGGCC Hexanucleotide Repeat in Noncoding Region of C9ORF72 Causes Chromosome 9p-Linked FTD and ALS. *Neuron*, 72 (2), pp.245-256.

Deng, H.X., Chen, W., Hong, S.T., Boycott, K.M., Gorrie, G.H., Siddique, N., Yang, Y., Fecto, F., Shi, Y., Zhai, H., Jiang, H., Hirano, M., Rampersaud, E., Jansen, G.H., Donkervoort, S., Bigio, E.H., Brooks, B.R., Ajroud, K., Sufit, R.L., Haines, J.L., Mugnaini, E., Pericak-Vance, M.A. & Siddique, T. (2011)

Mutations in UBQLN2 cause dominant X-linked juvenile and adult-onset ALS and ALS/dementia. *Nature*, 477 (7363), pp.211–215.

Dewey, C.M., Cenik, B., Sephton, C.F., Dries, D.R., Mayer, P., Good, S.K., Johnson, B.A., Herz, J. & Yu, G. (2011) TDP-43 Is Directed to Stress Granules by Sorbitol, a Novel Physiological Osmotic and Oxidative Stressor. *Molecular and Cellular Biology*, 31 (5), pp.1098–1108.

Dietzl, G., Chen, D., Schnorrer, F., Su, K.-C., Barinova, Y., Fellner, M., Gasser, B., Kinsey, K., Oppel, S., Scheiblauer, S., Couto, A., Marra, V., Keleman, K. & Dickson, B.J. (2007) A genome-wide transgenic RNAi library for conditional gene inactivation in Drosophila. *Nature*, 448 (7150), pp.151–156.

Dimitriadi, M., Sleigh, J.N., Walker, A., Chang, H.C., Sen, A., Kalloo, G., Harris, J., Barsby, T., Walsh, M.B., Satterlee, J.S., Li, C., Van Vactor, D., Artavanis-Tsakonas, S. & Hart, A.C. (2010) Conserved Genes Act as Modifiers of Invertebrate SMN Loss of Function Defects G. S. Barsh ed. *PLoS Genetics*, 6 (10), p.e1001172.

Dormann, D., Rodde, R., Edbauer, D., Bentmann, E., Fischer, I., Hruscha, A., Than, M.E., Mackenzie, I.R.A., Capell, A., Schmid, B., Neumann, M. & Haass, C. (2010) ALS-associated fused in sarcoma (FUS) mutations disrupt Transportin-mediated nuclear import. *The EMBO Journal*, 29 (16), pp.2841–2857.

Dou, Z., Pan, J.A., Dbouk, H.A., Ballou, L.M., DeLeon, J.L., Fan, Y., Chen, J.S., Liang, Z., Li, G., Backer, J.M., Lin, R.Z. & Zong, W.X. (2013) Class IA PI3K p110β Subunit Promotes Autophagy through Rab5 Small GTPase in Response to Growth Factor Limitation. *Molecular Cell*, 50 (1), pp.29–42.

Douziech, M., Roy, F., Laberge, G., Lefrancois, M., Armengod, A.V. & Therrien, M. (2003) Bimodal regulation of RAF by CNK in Drosophila. *EMBO Journal*, 22, pp.5068–5078

Drysdale, R. & FlyBase-Consortium (2008) FlyBase : a database for the *Drosophila* research community. *Methods in Molecular Biology*, pp.45–59.

Duffy, J. (2002) GAL4 System in Drosophila: a fly geneticist's Swiss army knife. *Genesis*, 34, pp.1-15.

Elden, A.C., Kim, H.-J., Hart, M.P., Chen-Plotkin, A.S., Johnson, B.S., Fang, X., Armakola, M., Geser, F., Greene, R., Lu, M.M., Padmanabhan, A., Clay-Falcone, D., McCluskey, L., Elman, L., Juhr, D., Gruber, P.J., Rüb, U., Auburger, G., Trojanowski, J.Q., Lee, V.M.Y., Van Deerlin, V.M., Bonini, N.M. & Gitler, A.D. (2010) Ataxin-2 intermediate-length polyglutamine expansions are associated with increased risk for ALS. *Nature*, 466 (7310), pp.1069–1075.

Elhanany-Tamir, H., Yu, Y.V., Shnayder, M., Jain, A., Welte, M. & Volk, T. (2012) Organelle positioning in muscles requires cooperation between two KASH proteins and microtubules. *Journal of cell biology*, 198 (5), pp. 833-846.

Etheridge, S., Brooke, M., Kelsell, D. & Blaydon, D. (2013) Rhomboid proteins: a role in keratinocyte proliferation and cancer. *Cell tissue research*. 351 (2), pp. 301-307.

Farah, C.A., Nguyen, M.D., Julien, J.P. & Leclerc, N. (2003) Altered levels and distribution of microtubule-associated proteins before disease onset in a mouse model of amyotrophic lateral sclerosis. *Journal of Neurochemistry*, 84 (1), pp.77–86.

Farg, M., Sundaramoorthy, V., Sultana, J., Yang, S., Atkinson, R., Levina, V., Halloran, M., Gleeson, P., Blair, I., Soo, K., King, A. & Atkin, J. (2014) C9orf72, implicated in amyotrophic lateral sclerosis and frontotemporal dementia, regulates endosomal trafficking. *Human molecular genetics*, 23 (13), pp.3579-3595.

Fasana, E., Fossati, M., Ruggiano, A., Brambillasca, S., Hoogenraad, C.C., Navone, F., Francolini, M. & Borgese, N. (2010) A VAPB mutant linked to amyotrophic lateral sclerosis generates a novel form of organized smooth endoplasmic reticulum. *The FASEB Journal*, 24 (5), pp.1419–1430.

Feany, M.B. & Bender, W.W. (2000) A Drosophila model of Parkinson's disease. *Nature*, 404 (6776), pp.394–398.

Feiguin, F., Godena, V.K., Romano, G., D'Ambrogio, A., Klima, R. & Baralle, F.E. (2009) Depletion of TDP-43 affects Drosophila motoneurons terminal synapsis and locomotive behavior. *FEBS Letters*, 583 (10), pp.1586–1592.

Fernandez-Funez, P., Nino-Rosales, M.L., de Gouyon, B., She, W.C., Luchak, J.M., Martinez, P., Turiegano, E., Benito, J., Capovilla, M., Skinner, P.J., McCall, A., Canal, I., Orr, H.T., Zoghbi, H.Y. & Botas, J. (2000) Identification of genes that modify ataxin-1-induced neurodegeneration. *Nature*, 408 (6808), pp.101–106.

Ferraiuolo, L., Kirby, J., Grierson, A.J., Sendtner, M. & Shaw, P.J. (2011) Molecular pathways of motor neuron injury in amyotrophic lateral sclerosis. *Nature Reviews Neurology*, 7 (11), pp.616–630.

Figlewicz, D.A., Krizus, A., Martinoli, M.G., Meininger, V., Dib, M., Rouleau, G.A. & Julien, J.P. (1994) Variants of the heavy neurofilament subunit are associated with the development of amyotrophic lateral sclerosis. *Human Molecular Genetics*, 3 (10), pp.1757–1761.

Forrest, S., Chai, A., Sanhueza, M., Marescotti, M., Parry, K., Georgiev, A., Sahota, V., Mendez-Castro, R. & Pennetta, G. (2013) Increased levels of phosphoinositides cause neurodegeneration in a Drosophila model of

amyotrophic lateral sclerosis. *Human Molecular Genetics*, 22 (13), pp.2689–2704.

Fossgreen, A., Brückner, B., Czech, C., Masters, C.L., Beyreuther, K. & Paro, R. (1998) Transgenic Drosophila expressing human amyloid precursor protein show gamma-secretase activity and a blistered-wing phenotype. *Proceedings of the National Academy of Sciences of the United States of America*, 95 (23), pp.13703–13708.

Foti, M., Audhya, A & Emr, S. (2001) Sac1 lipid phosphatase and Stt4 phosphatidylinositol 4-kinase regulate a pool of phosphatidyl-4-phosphate that functions in the control of the actin cytoskeleton and vacuole morphology. *Molecular Biology of the Cell*, 12 (8), pp.2396–2411.

Franciscovich, A.L., Mortimer, A.D.V., Freeman, A.A., Gu, J. & Sanyal, S. (2008) Overexpression Screen in Drosophila Identifies Neuronal Roles of GSK-3 /shaggy as a Regulator of AP-1-Dependent Developmental Plasticity. *Genetics*, 180 (4), pp.2057–2071.

Fransson, A., Ruusala, A. & Aspenstrom, P. (2003) Atypical Rho GTPases have roles in mitochondrial homeostasis and apoptosis. *Journal of Biological Chemestry*, 278, pp. 6495–6502.

Fratta, P., Mizielinska, S., Nicoll, A.J., Zloh, M., Fisher, E.M.C., Parkinson, G. & Isaacs, A.M. (2012) C9orf72 hexanucleotide repeat associated with amyotrophic lateral sclerosis and frontotemporal dementia forms RNA G-quadruplexes. *Scientific Reports*, 2, p.e1016.

Freeman, M. (1996) Reiterative use of the EGF receptor triggers differentiation of all cell types in the Drosophila eye. *Cell*, 87 (4), pp.651–660.

Fruman, D.A. & Rommel, C. (2014) PI3K and cancer: lessons, challenges and opportunities. *Nature Publishing Group*, 13 (2), pp.140–156.

Fyrberg, E., Bond, B., Hershey, N., Mixter, K. & Davidson, N. (1981) The actin genes of Drosophila: protein coding regions are highly conserved but intron positions are not. *Cell*, 24 (1), pp.107-116.

Funke, A., Esser, M., Krüttgen, A., Weis, J., Mitne-Neto, M., Lazar, M., Nishimura, A., Sperfeld, A., Trillenberg, P., Senderek, J., Krasnianski, M., Zatz, M., Zierz, S. & Deschauer, M. (2010) The p.P56S mutation in the VAPBgene is not due to a single founder: the first European case. *Clinical Genetics*, 77 (3), pp.302–303.

Furuta, N., Fujita, N., Noda, T., Yoshimori, T. & Amano, A. (2010) Combinational soluble N-ethylmaleimide-sensitive factor attachment protein receptor proteins VAMP8 and Vti1b mediate fusion of antimicrobial and canonical autophagosomes with lysosomes. *Molecular biology of the cell*, 21 (6), pp.1001–1010.

Gal, J., Ström, A.-L., Kwinter, D.M., Kilty, R., Zhang, J., Shi, P., Fu, W., Wooten, M.W. & Zhu, H. (2009) Sequestosome 1/p62 links familial ALS mutant SOD1 to LC3 via an ubiquitin-independent mechanism. *Journal of Neurochemistry*, 111 (4), pp.1062–1073.

Genc, B. & Ozdinler, P. (2014) Moving forward in clinical trials for ALS: motor neurons lead the way please. *Drug discovery today*, 19 (4), pp.441-449.

Gidalevitz, T., Krupinski, T., Garcia, S. & Morimoto, R.I. (2009) Destabilizing Protein Polymorphisms in the Genetic Background Direct Phenotypic Expression of Mutant SOD1 Toxicity H. Orr ed. *PLoS Genetics*, 5 (3), p.e1000399.

Giot, L., Bader, J.S., Brouwer, C., Chaudhuri, A., Kuang, B., Li, Y., Hao, Y., Ooi, C., Godwin, B. & Vitols, E. (2003) A protein interaction map of Drosophila melanogaster. *Science*, 302 (5651), pp.1727–1736.

Gkogkas, C., Middleton, S., Kremer, A., Wardrope, C., Hannah, M., Gillingwater, T. & Skehel, P. (2008) VAPB interacts with and modulates the activity of ATF6. *Human molecular genetics*, 17 (11), pp.1517-1526.

Gkogkas, C., Wardrope, C., Hannah, M. & Skehel, P. (2011) The ALS8-associated mutant VAPBP56S is resistant to proteolysis in neurons. *Journal of Neurochemistry*, 117 (2), pp.286–294.

Grad, L.I., Guest, W.C., Yanai, A., Pokrishevsky, E., O'Neill, M.A., Gibbs, E., Semenchenko, V., Yousefi, M., Wishart, D.S., Plotkin, S.S. & Cashman, N.R. (2011) Intermolecular transmission of superoxide dismutase 1 misfolding in living cells. *Proceedings of the National Academy of Sciences*, 108 (39), pp.16398–16403.

Graham, P., Yanowitz, J., Penn, J., Deshpande, G., Schedl, P. (2011) The Translation Initiation Factor eIF4E Regulates the Sex-Specific Expression of the Master Switch Gene Sxl in Drosophila melanogaster. *PLOS Genetics*, 7 (7), p.e1002185.

Greene, J.C., Whitworth, A.J., Kuo, I., Andrews, L.A., Feany, M.B. & Pallanck, L.J. (2003) Mitochondrial pathology and apoptotic muscle degeneration in Drosophila parkin mutants. *Proceedings of the National Academy of Sciences of the United States of America*, 100 (7), pp.4078–4083.

Greeve, I., Kretzschmar, D., Tschäpe, J.-A., Beyn, A., Brellinger, C., Schweizer, M., Nitsch, R.M. & Reifegerste, R. (2004) Age-dependent neurodegeneration and Alzheimer-amyloid plaque formation in transgenic Drosophila. *Journal of Neuroscience*, 24 (16), pp.3899–3906.

Gros-Louis, F., Lariviere, R., Gowing, G., Laurent, S., Camu, W., Bouchard, J.P., Meininger, V., Rouleau, G. & Julien, J.P. (2004) A Frameshift Deletion in

Peripherin Gene Associated with Amyotrophic Lateral Sclerosis. *Journal of Biological Chemistry*, 279 (44), pp.45951–45956.

Guo, Y., Jangi, S. & Welte, M. (2005) Organelle-specific control of intracellular transport: distinctly targeted isoforms of the regulator Klar. *Molecular biology of the cell*, 16 (3), pp.1406-1416.

Guruharsha, K., Rual, J., Zhai, B., Mintseris, J., Vaidya, P., Vaidya, N., Beekman, C.,Wong, C., Rhee, D., Cenaj, O., McKillip, E, Shah, S., Stapleton, M., Wan, K., Yu, C., Parsa, B., Carlson, J., Chen, X., Kapadia, B., Vijayrhavan, K., Gygi, S., Celniker, S., Obar, R. & Artavanis-Tsakonas, S. (2011) A protein complex network of Drosophila melanogaster. *Cell*, 147 (3), pp. 690-703.

Gusella, J.F. & MacDonald, M.E. (2000) Molecular genetics: unmasking polyglutamine triggers in neurodegenerative disease. *Nature Reviews Neuroscience,* 1 (2), pp.109–115.

Hadano, S., Hand, C.K., Osuga, H., Yanagisawa, Y., Otomo, A., Devon, R.S., Miyamoto, N., Showguchi-Miyata, J., Okada, Y., Singaraja, R., Figlewicz, D.A., Kwiatkowski, T., Hosler, B.A., Sagie, T., Skaug, J., Nasir, J., Brown, R.H., Scherer, S.W., Rouleau, G.A., Hayden, M.R. & Ikeda, J.E. (2001) A gene encoding a putative GTPase regulator is mutated in familial amyotrophic lateral sclerosis 2. *Nature Genetics*, 29 (2), pp.166–173.

Hadano, S., Kunita, R., Otomo, A., Suzuki-Utsunomiya, K. & Ikeda, J.E. (2007) Molecular and cellular function of ALS2/alsin: Implication of membrane dynamics in neuronal development and degeneration. *Neurochemistry International*, 51 (2-4), pp.74–84.

Hadano, S., Otomo, A., Kunita, R., Suzuki-Utsunomiya, K., Akatsuka, A., Koike, M., Aoki, M., Uchiyama, Y., Itoyama, Y. & Ikeda, J.E. (2010) Loss of ALS2/Alsin Exacerbates Motor Dysfunction in a SOD1H46R-Expressing Mouse ALS Model by Disturbing Endolysosomal Trafficking M. B. Feany ed. *PLoS ONE*, 5 (3), p.e9805.

Halder, G., Callaerts, P. & Gehring, W.J. (1995) Induction of ectopic eyes by targeted expression of the eyeless gene in Drosophila. *Science*, 267 (5205), pp.1788–1792.

Han, S.M., Oussini, El, H., Scekic-Zahirovic, J., Vibbert, J., Cottee, P., Prasain, J.K., Bellen, H.J., Dupuis, L. & Miller, M.A. (2013) VAPB/ALS8 MSP Ligands Regulate Striated Muscle Energy Metabolism Critical for Adult Survival in Caenorhabditis elegans. *PLoS Genetics*, 9 (9), p.e1003738.

Han, S.M., Tsuda, H., Yang, Y., Vibbert, J., Cottee, P., Lee, S.-J., Winek, J., Haueter, C., Bellen, H.J. & Miller, M.A. (2012) Secreted VAPB/ALS8 Major Sperm Protein Domains Modulate Mitochondrial Localization and Morphology via Growth Cone Guidance Receptors. *Developmental Cell*, 22 (2), pp.348–362.

Harvey, J.J. (1964) An unidentified virus which causes the rapid production of tumours in mice. *Nature*, 204, pp.1104–1105.

Harvey, K.F., Pfleger, C.M., Hariharan, I.K. (2003). The Drosophila Mst ortholog, hippo, restricts growth and cell proliferation and promotes apoptosis. *Cell*, 114, pp. 457-467.

Hawkins, C.J., Wang, S.L. & Hay, B.A. (1999) A cloning method to identify caspases and their regulators in yeast: identification of Drosophila IAP1 as an inhibitor of the Drosophila caspase DCP-1. *Proceedings of the National Academy of Sciences of the United States of America*, 96 (6), pp.2885–2890.

Hochrainer, K., Mayer, H., Baranyi, U., Binder, B., Lipp, J. & Kroismayr, R. (2005) The human HERC family of ubiquitin ligases: novel members, genomic organization, expression profiling, and evolutionary aspects. *Genetics*, 85 (2), pp.153-164.

Howe, C., & Mobley, W. (2004) Signaling endosome hypothesis: A cellular mechanism for long distance communication. *Journal of Neurobiology*. 58, pp.207–216.

Hu, Y., Flockhart, I., Vinayagam, A., Bergwitz, C., Berger, B., Perrimon, N., Mohr, S. (2011) An integrative approach to ortholog prediction for disease-focused and other functional studies. *BMC Bioinformatics,* 12 (357).

Huang, C., Tong, J., Bi, F., Zhou, H. & Xia, X.G. (2012) Mutant TDP-43 in motor neurons promotes the onset and progression of ALS in rats. *Journal of Clinical Investigation*, 122 (1), pp.107–118.

Huang, D., Sherman, B., Lempicky, R. (2008) Systematic and integrative analysis of large gene lists using DAVID bioinformatics resources. *Nature Protocols*, 4, pp. 44-57.

Huang, Y. & Mucke, L. (2012) Alzheimer Mechanisms and Therapeutic Strategies. *Cell*, 148 (6), pp.1204–1222.

Ingre, C., Pinto, S., Birve, A., Press, R., Danielsson, O., de Carvalho, M., Guđmundsson, G. & Andersen, P.M. (2013) No association between VAPB mutations and familial or sporadic ALS in Sweden, Portugal and Iceland. *Amyotrophic Lateral Sclerosis and Frontotemporal Degeneration*, 14 (7-8) pp.620–627.

Jackson, G.R., Salecker, I., Dong, X., Yao, X., Arnheim, N., Faber, P.W., MacDonald, M.E. & Zipursky, S.L. (1998) Polyglutamine-expanded human huntingtin transgenes induce degeneration of Drosophila photoreceptor neurons. *Neuron*, 21 (3), pp.633–642.

Jacinto, A. & Baum, B. (2003) Actin in development. *Mechanisms of Development*, 120, pp.1337-1349.

Jansen, M., Ohsaki, Y., Rita Rega, L., Bitman, R., Olkkonen, V., Ikonen, E. (2011) Role of ORPs in sterol transport from plasma membrane to ER and lipid droplets in mammalian cells. *Traffic,* 12 (2), pp.218-231.

Jensen, L.J., Kuhn, M., Stark, M., Chaffron, S., Creevey, C., Muller, J., Doerks, T., Julien, P., Roth, A., Simonovic, M., Bork, P. & Mering, von, C. (2009) STRING 8-a global view on proteins and their functional interactions in 630 organisms. *Nucleic Acids Research*, 37 (Database), pp.D412–D416.

Johnson, B.S., Snead, D., Lee, J.J., McCaffery, J.M., Shorter, J. & Gitler, A.D. (2009) TDP-43 Is Intrinsically Aggregation-prone, and Amyotrophic Lateral Sclerosis-linked Mutations Accelerate Aggregation and Increase Toxicity. *Journal of Biological Chemistry*, 284 (30), pp.20329–20339.

Johnson, J.O., Mandrioli, J., Benatar, M., Abramzon, Y., Van Deerlin, V.M., Trojanowski, J.Q., Gibbs, J.R., Brunetti, M., Gronka, S., Wuu, J., Ding, J., McCluskey, L., Martinez-Lage, M., Falcone, D., Hernandez, D.G., Arepalli, S., Chong, S., Schymick, J.C., Rothstein, J., Landi, F., Wang, Y.-D., Calvo, A., Mora, G., Sabatelli, M., Monsurrò, M.R., Battistini, S., Salvi, F., Spataro, R., Sola, P., Borghero, G., Galassi, G., Scholz, S.W., Taylor, J.P., Restagno, G., Chiò, A., Traynor, B.J. & Consortium23, T.I. (2010) Exome Sequencing Reveals VCP Mutations as a Cause of Familial ALS. *Neuron*, 68 (5), pp.857–864.

Jung, J.J., Inamdar, S.M., Tiwari, A. & Choudhury, A. (2012) Regulation of intracellular membrane trafficking and cell dynamics by syntaxin-6. *Bioscience Reports*, 32 (4), pp.383–391.

Kagiwada, S. & Zen, R. (2003) Role of the yeast VAP homolog, Scs2p, in INO1 expression and phospholipid metabolism. *Journal of biochemistry*, 133 (4), pp.515–522.

Kaiser, S., Brickner, J., Reilein, A., Fenn, T., Walter, P. & Brunger, A. (2005) Structural Basis of FFAT Motif-Mediated ER Targeting. *Structure*, 13 (7), pp.1035–1045.

Kaltenbach, L.S., Romero, E., Becklin, R.R., Chettier, R., Bell, R., Phansalkar, A., Strand, A., Torcassi, C., Savage, J., Hurlburt, A., Cha, G.-H., Ukani, L., Chepanoske, C.L., Zhen, Y., Sahasrabudhe, S., Olson, J., Kurschner, C., Ellerby, L.M., Peltier, J.M., Botas, J. & Hughes, R.E. (2007) Huntingtin Interacting Proteins Are Genetic Modifiers of Neurodegeneration. *PLoS Genetics*, 3 (5), p.e82.

Kanekura, K., Hashimoto, Y., Niikura, T., Aiso, S., Matsuoka, M. & Nishimoto, I. (2004) Alsin, the Product of ALS2 Gene, Suppresses SOD1 Mutant Neurotoxicity through RhoGEF Domain by Interacting with SOD1 Mutants. *The journal of biological chemistry*, 279, pp.19247-19256.

Kanekura, K., Hashimoto, Y., Kita, Y., Sasabe, J., Aiso, S., Nishimoto, I. & Matsuoko, M. (2005) A Rac1/Phosphatidylinositol 3-Kinase/Akt3 Anti-apoptotic Pathway, Triggered by AlsinLF, the Product of the ALS2 Gene, Antagonizes Cu/Zn-superoxide Dismutase (SOD1) Mutant-induced Motoneuronal Cell Death. *Journal of Biological Chemistry*, 280 (6), pp.4532–4543.

Kanekura, K., Nishimoto, I., Aiso, S. & Matsuoka, M. (2006) Characterization of Amyotrophic Lateral Sclerosis-linked P56S Mutation of Vesicle-associated Membrane Protein-associated Protein B (VAPB/ALS8). *Journal of Biological Chemestry*, 281 (40), pp.30223-30233.

Kasperaviciute, D., Weale, M.E., Shianna, K.V., Banks, G.T., Simpson, C.L., Hansen, V.K., Turner, M.R., Shaw, C.E., Al-Chalabi, A., Pall, H.S., Goodall, E.F., Morrison, K.E., Orrell, R.W., Beck, M., Jablonka, S., Sendtner, M., Brockington, A., Ince, P.G., Hartley, J., Nixon, H., Shaw, P.J., Schiavo, G., Wood, N.W., Goldstein, D.B. & Fisher, E.M.C. (2007) Large-scale pathways-based association study in amyotrophic lateral sclerosis. *Brain : a journal of neurology*, 130 (9), pp.2292–2301.

Kawano, M., Kumagai, K., Nishijima, M. & Hanada, K. (2006) Efficient Trafficking of Ceramide from the Endoplasmic Reticulum to the Golgi Apparatus Requires a VAMP-associated Protein-interacting FFAT Motif of CERT. *Journal of Biological Chemistry*, 281 (40), pp.30279–30288.

Kidwell, M.G., Kidwell, J.F. & Sved, J.A. (1977) Hybrid Dysgenesis in Drosophila Melanogaster: A Syndrome of Aberrant Traits Including Mutation, Sterility and Male Recombination. *Genetics*, 86 (4), pp.813–833.

Kiernan, M.C., Vucic, S., Cheah, B.C., Turner, M.R., Eisen, A., Hardiman, O., Burrell, J.R. & Zoing, M.C. (2011) Amyotrophic lateral sclerosis. *The Lancet*, 377 (9769), pp.942–955.

Kim, D., Cotton, S., Manna, D. & Welte, M. (2012) Novel isoforms of the transport regulator klar. *PLoS One*, 8 (2), p.e55070.

Kim, S., Leal, S.S., Ben Halevy, D., Gomes, C.M. & Lev, S. (2010) Structural Requirements for VAP-B Oligomerization and Their Implication in Amyotrophic Lateral Sclerosis-associated VAP-B(P56S) Neurotoxicity. *Journal of Biological Chemistry*, 285 (18), pp.13839–13849.

Koh, T.W., Korolchuk, V.I., Wairkar, Y.P., Jiao, W., Evergren, E., Pan, H., Zhou, Y., Venken, K.J., Shupliakov, O., Robinson, I.M., O'Kane, C.J. & Bellen, H.J. (2007) Eps15 and Dap160 control synaptic vesicle membrane retrieval and synapse development. *Journal of cell biology,* 178 (2), pp.309-322.

Korolchuk, V.I., Schutz, M.M., Gomez-Llorente, C., Rocha, J., Lansu, N.R., Collins, S.M., Wairkar, Y.P., Robinson, I.M. & O'Kane, C.J. (2007) Drosophila Vps35

function is necessary for normal endocytic trafficking and actin cytoskeleton organisation. *Journal of Cell Science*, 120 (24), pp.4367–4376.

Kraemer, B.C., Schuck, T., Wheeler, J.M., Robinson, L.C., Trojanowski, J.Q., Lee, V.M.Y. & Schellenberg, G.D. (2010) Loss of murine TDP-43 disrupts motor function and plays an essential role in embryogenesis. *Acta Neuropathologica*, 119 (4), pp.409–419.

Kramer, J.M. & Staveley, B.E. (2003) GAL4 causes developmental defects and apoptosis when expressed in the developing eye of Drosophila melanogaster. *Genetics and molecular research*, 2 (1), pp.43–47.

Krauss, M. & Haukce, V. (2011) Shaping membranes for endocytosis. *Reviewsof physiology, biochemistry and pharmacology*, 161, pp.45-66.

Kuijpers, M., Lou Yu, K., Teuling, E., Akhmanova, A., Jaarsma, D. & Hoogenraad, C.C. (2013) The ALS8 protein VAPB interacts with the ER & Golgi recycling protein YIF1A and regulates membrane delivery into dendrites. *The EMBO Journal*, 32 (14), pp.2056–2072.

Kunst, C.B. (2004) Complex genetics of amyotrophic lateral sclerosis. *American journal of human genetics*, 75 (6), p.933-947.

Kuwabara, P.E. (2003) The multifaceted C. elegans major sperm protein: an ephrin signaling antagonist in oocyte maturation. *Genes & Development*, 17 (2), pp.155–161.

Kwiatkowski, T.J., Bosco, D.A., Leclerc, A.L., Tamrazian, E., Vanderburg, C.R., Russ, C., Davis, A., Gilchrist, J., Kasarskis, E.J., Munsat, T., Valdmanis, P., Rouleau, G.A., Hosler, B.A., Cortelli, P., de Jong, P.J., Yoshinaga, Y., Haines, J.L., Pericak-Vance, M.A., Yan, J., Ticozzi, N., Siddique, T., McKenna-Yasek, D., Sapp, P.C., Horvitz, H.R., Landers, J.E. & Brown, R.H. (2009) Mutations in the FUS/TLS gene on chromosome 16 cause familial amyotrophic lateral sclerosis. *Science*, 323 (5918), pp.1205–1208.

Kwon, Y., Vinayagam, A., Sun, X., Dephoure, N., Gygi, S., Hong, P. & Perrimon, N. (2013) The Hippo Signaling Pathway Interactome. *Science*, 342 (6159), pp.737-740.

Laberge, G., Douziech, M. & Therrien, M. (2005) Src42 binding activity regulates Drosophila RAF by a novel CNK-dependent derepression mechanism. *EMBO Journal*, 24, pp.487-498.

Lagier-Tourenne, C., Baughn, M., Rigo, F., Sun, S., Liu, P., Li, H.-R., Jiang, J., Watt, A.T., Chun, S., Katz, M., Qiu, J., Sun, Y., Ling, S.-C., Zhu, Q., Polymenidou, M., Drenner, K., Artates, J.W., McAlonis-Downes, M., Markmiller, S., Hutt, K.R., Pizzo, D.P., Cady, J., Harms, M.B., Baloh, R.H., Vandenberg, S.R., Yeo, G.W., Fu, X.-D., Bennett, C.F., Cleveland, D.W. & Ravits, J. (2013) Targeted degradation of sense and antisense C9orf72 RNA

foci as therapy for ALS and frontotemporal degeneration. *Proceedings of the National Academy of Sciences*, 110 (47), pp. 4530–4539.

Laird, A.S., Van Hoecke, A., De Muynck, L., Timmers, M., Van Den Bosch, L., Van Damme, P. & Robberecht, W. (2010) Progranulin is Neurotrophic In Vivo and Protects against a Mutant TDP-43 Induced Axonopathy M. B. Feany ed. *PLoS ONE*, 5 (10), p.e13368.

Lam, Y.C., Bowman, A.B., Jafar-Nejad, P., Lim, J., Richman, R., Fryer, J.D., Hyun, E.D., Duvick, L.A., Orr, H.T. & Botas, J. (2006) ATAXIN-1 Interacts with the Repressor Capicua in Its Native Complex to Cause SCA1 Neuropathology. *Cell*, 127 (7), pp.1335–1347.

Lee, W.C.M., Yoshihara, M. & Littleton, J.T. (2004) Cytoplasmic aggregates trap polyglutamine-containing proteins and block axonal transport in a Drosophila model of Huntington's disease. *Proceedings of the National Academy of Sciences of the United States of America*, 101 (9), pp.3224–3229.

Lee, Y.B., Chen, H.-J., Peres, J.N., Gomez-Deza, J., Attig, J., Štalekar, M., Troakes, C., Nishimura, A.L., Scotter, E.L., Vance, C., Adachi, Y., Sardone, V., Miller, J.W., Smith, B.N., Gallo, J.-M., Ule, J., Hirth, F., Rogelj, B., Houart, C. & Shaw, C.E. (2013) Hexanucleotide Repeats in ALS/FTD Form Length-Dependent RNA Foci, Sequester RNA Binding Proteins, and Are Neurotoxic. *Cell Reports*, 5 (5), pp.1178–1186.

Levine, T.P., Daniels, R.D., Gatta, A.T., Wong, L.H. & Hayes, M.J. (2013) The product of C9orf72, a gene strongly implicated in neurodegeneration, is structurally related to DENN Rab-GEFs. *Bioinformatics*, 29 (4), pp.499–503.

Levine, T.P & Loewen, C. (2006) Inter-organelle membrane contact sites: through a glass, darkly. *Current Opinions in Cell Biology*. 18, pp.371–378

Li, J., Kanekiyo, T., Shinohara, M., Zhang, Y., LaDu, M.J., Xu, H. & Bu, G. (2012) Differential Regulation of Amyloid- Endocytic Trafficking and Lysosomal Degradation by Apolipoprotein E Isoforms. *Journal of Biological Chemistry*, 287 (53), pp.44593–44601.

Li, G., Mongillo, M., Chin, K.T., Harding, H., Ron, D., Marks, A.R. & Tabas, I. (2009) Role of ERO1-alpha-mediated stimulation of inositol 1,4,5-triphosphate receptor activity in endoplasmic reticulum stress-induced apoptosis. *Journal of cellular biology*, 186 (6), pp.783-792.

Li, Y., Ray, P., Rao, E.J., Shi, C., Guo, W., Chen, X., Woodruff, E.A., Fushimi, K. & Wu, J.Y. (2010) A Drosophila model for TDP-43 proteinopathy. *Proceedings of the National Academy of Sciences*, 107 (7), pp.3169–3174.

Liachko, N.F., Guthrie, C.R. & Kraemer, B.C. (2010) Phosphorylation Promotes Neurotoxicity in a Caenorhabditis elegans Model of TDP-43 Proteinopathy. *Journal of Neuroscience*, 30 (48), pp.16208–16219.

Liang, J., Clark-Dixon, C., Wang, S., Flower, T.R., Williams-Hart, T., Zweig, R., Robinson, L.C., Tatchell, K. & Witt, S.N. (2008) Novel suppressors of α-synuclein toxicity identified using yeast. *Human Molecular Genetics*, 17 (23), pp.3784–3795.

Ling, S., Polymenidou, M., Cleveland, D. (2013) Converging mechanisms in ALS and FTD: Disrupted RNA and protein homeostasis. *Neuron*, 79 (3), pp.416-438.

Liu, Z., Huang, Y., Zhang, Y., Chen, D. & Zhang, Y. (2011) Drosophila Acyl-CoA Synthetase Long-Chain Family Member 4 Regulates Axonal Transport of Synaptic Vesicles and Is Required for Synaptic Development and Transmission. *Journal of neuroscience*, 31 (6), pp.2052-2063.

Liu, B., Liao, J., Rao, X., Kushner, S., Chung, C., Chang, D. & Shuai, K. (1998) Inhibition of Stat1-mediated gene activation by PIAS1. *Proceedings of the national academy of sciences,* 95 (18), pp.10626-10631.

Loewen, C.J.R., Roy, A. & Levine, T.P. (2003) A conserved ER targeting motif in three families of lipid binding proteins and in Opi1p binds VAP. *The EMBO Journal*, 22 (9), pp.2025–2035.

Ludolph, A.C., Bendotti, C., Blaugrund, E., Chiò, A., Greensmith, L., Loeffler, J.P., Mead, R., Niessen, H.G., Petri, S., Pradat, P.F., Robberecht, W., Ruegg, M., Schwalenstöcker, B., Stiller, D., van den Berg, L., Vieira, F. & Horsten, von, S. (2010) Guidelines for preclinical animal research in ALS/MND: A consensus meeting. *Amyotrophic Lateral Sclerosis*, 11 (1-2), pp.38–45.

Ma, Y., Creanga, A., Lum, L. & Beachy, P. (2006) Prevalence of off-target effects in Drosophila RNA interference screens. *Nature* 443 (21), pp.359-363.

Machesky, L., Atkinson, S., Ampe, C., Vanderkerckhove, J & Pollard, T. (1994) Purification of a cortical complex containing two unconventional actins from Acanthamoeba by affinity chromatography on profiling-agarose. *Journal of Cell biology*, 127, pp.107-115.

MacLeod, D.A., Rhinn, H., Kuwahara, T., Zolin, A., Di Paolo, G., McCabe, B.D., Marder, K.S., Honig, L.S., Clark, L.N., Small, S.A. & Abeliovich, A. (2013) RAB7L1 Interacts with LRRK2 to Modify Intraneuronal Protein Sorting and Parkinson's Disease Risk. *Neuron*, 77 (3), pp.425–439.

Majounie, E., Renton, A.E., Mok, K., Dopper, E.G.P., Waite, A., Rollinson, S., Chiò, A., Restagno, G., Nicolaou, N., Simón-Sánchez, J., van Swieten, J.C., Abramzon, Y., Johnson, J.O., Sendtner, M., Pamphlett, R., Orrell, R.W., Mead, S., Sidle, K.C., Houlden, H., Rohrer, J.D., Morrison, K.E., Pall, H., Talbot, K.,

Ansorge, O., Chromosome 9-ALS/FTD Consortium, French research network on FTLD/FTLD/ALS, ITALSGEN Consortium, Hernandez, D.G., Arepalli, S., Sabatelli, M., Mora, G., Corbo, M., Giannini, F., Calvo, A., Englund, E., Borghero, G., Floris, G.L., Remes, A.M., Laaksovirta, H., McCluskey, L., Trojanowski, J.Q., Van Deerlin, V.M., Schellenberg, G.D., Nalls, M.A., Drory, V.E., Lu, C.-S., Yeh, T.-H., Ishiura, H., Takahashi, Y., Tsuji, S., Le Ber, I., Brice, A., Drepper, C., Williams, N., Kirby, J., Shaw, P., Hardy, J., Tienari, P.J., Heutink, P., Morris, H.R., Pickering-Brown, S. & Traynor, B.J. (2012) Frequency of the C9orf72 hexanucleotide repeat expansion in patients with amyotrophic lateral sclerosis and frontotemporal dementia: a cross-sectional study. *Lancet neurology*, 11 (4), pp.323–330.

Malaspina, A., Kaushik, N., & de Belleroche, J. (2001) Differential expression of 14 genes in amyotrophic lateral sclerosis spinal cord detected using gridded cDNA arrays. *Journal of Neurochemestry*, 77(1), pp.132–145.

Manford, A.G., Stefan, C.J., Yuan, H.L., MacGurn, J.A. & Emr, S.D. (2012) ER-to-Plasma Membrane Tethering Proteins Regulate Cell Signaling and ER Morphology. *Developmental Cell*, 23 (6), pp.1129–1140.

Martin-Belmonte, F. & Perez-Moreno, M. (2011) Epithelial cell polarity, stem cells and cancer. *Nature Reviews Cancer*, 12 (1), pp.23-38.

Maruyama, H., Morino, H., Ito, H., Izumi, Y., Kato, H., Watanabe, Y., Kinoshita, Y., Kamada, M., Nodera, H., Suzuki, H., Komure, O., Matsuura, S., Kobatake, K., Morimoto, N., Abe, K., Suzuki, N., Aoki, M., Kawata, A., Hirai, T., Kato, T., Ogasawara, K., Hirano, A., Takumi, T., Kusaka, H., Hagiwara, K., Kaji, R. & Kawakami, H. (2010) Mutations of optineurin in amyotrophic lateral sclerosis. *Nature*, 465 (7295), pp.223–226.

McCray, B.A., Skordalakes, E. & Taylor, J.P. (2010) Disease mutations in Rab7 result in unregulated nucleotide exchange and inappropriate activation. *Human Molecular Genetics*, 19 (6), pp.1033–1047.

McCormick, F. (1998) Going for the GAP. *Current Biology*, 8 (19), pp.673–674.

McPhee, C., Logan, M., Freeman, M. & Baehrecke, E. (2010) Activation of autophagy during cell death requires the engulfment receptor Draper. *Nature*, 465 (7301), pp.1093-1097.

Mi, H., Muruganujan, A. & Thomas, P. (2013) PANTHER in 2013: modeling the evolution of gene function, and other gene attributes, in the context of phylogenetic trees. *Nucleic Acids Res*, 41, pp. D377–D386.

Mikitova, V., & Levine, T.P. (2012) Analysis of the key elements of FFAT-like motifs identifies new proteins that potentially bind VAP on the ER, including two AKAPs and FAPP2. *Plos One,* 7, p.e30455.

Millecamps, S., Salachas, F., Cazeneuve, C., Gordon, P., Bricka, B., Camuzat, A., Guillot-Noel, L., Russaouen, O., Bruneteau, G., Pradat, P.F., Le Forestier, N., Vandenberghe, N., Danel-Brunaud, V., Guy, N., Thauvin-Robinet, C., Lacomblez, L., Couratier, P., Hannequin, D., Seilhean, D., Le Ber, I., Corcia, P., Camu, W., Brice, A., Rouleau, G., LeGuern, E. & Meininger, V. (2010) SOD1, ANG, VAPB, TARDBP, and FUS mutations in familial amyotrophic lateral sclerosis: genotype-phenotype correlations. *Journal of Medical Genetics*, 47 (8), pp.554–560.

Miller, J.P., Yates, B.E., Al-Ramahi, I., Berman, A.E., Sanhueza, M., Kim, E., de Haro, M., DeGiacomo, F., Torcassi, C., Holcomb, J., Gafni, J., Mooney, S.D., Botas, J., Ellerby, L.M. & Hughes, R.E. (2012) A Genome-Scale RNA–Interference Screen Identifies RRAS Signaling as a Pathologic Feature of Huntington's Disease. *PLoS Genetics*, 8 (11), p.e1003042.

Miller, M.A., Ruest, P.J., Kosinski, M., Hanks, S.K. & Greenstein, D. (2003) An Eph receptor sperm-sensing control mechanism for oocyte meiotic maturation in Caenorhabditis elegans. *Genes & Development*, 17 (2), pp.187–200.

Mohr, S., Bakal, C. & Perrimon, N. (2010) Genomic screening with RNAi: results and challenges. *Annual reviews of Biochemestry*, 79, pp. 37-64.

Morotz, G.M., De Vos, K.J., Vagnoni, A., Ackerley, S., Shaw, C.E. & Miller, C.C.J. (2012) Amyotrophic lateral sclerosis-associated mutant VAPBP56S perturbs calcium homeostasis to disrupt axonal transport of mitochondria. *Human Molecular Genetics*, 21 (9), pp.1979–1988.

Morrison, H.A., Dionne, H., Rusten, T.E., Brech, A., Fisher, W.W., Pfeiffer, B.D., Celniker, S.E., Stenmark, H. & Bilder, D. (2008) Regulation of early endosomal entry by the Drosophila tumor suppressors Rabenosyn and Vps45. *Molecular biology of the cell*, 19 (10), pp.4167-4176.

Munch, C., Sedlmeier, R., Meyer, T., Homberg, V., Sperfeld, A.D., Kurt, A., Prudlo, J., Peraus, G., Hanemann, C.O., Stumm, G. & Ludolph, A.C. (2004) Point mutations of the p150 subunit of dynactin (DCTN1) gene in ALS. *Neurology*, 63 (4), pp.724–726.

Nachreiner, T., Esser, M., Tenten, V., Troost, D., Weis, J. & Krüttgen, A. (2010) Novel splice variants of the amyotrophic lateral sclerosis-associated gene VAPB expressed in human tissues. *Biochemical and Biophysical Research Communications*, 394 (3), pp.703–708.

Nakatsu, F., Baskin, J., Chung, J., Tanner, L., Shui, G., Lee, S., Pirruccello, M., Hao, M., Ingolia, N., Wenk, M. & De Camilli, P. (2012) PtdIns4P synthesis by PI4KIIIα at the plasma membrane and its impact on plasma membrane identity. *Journal of Cell Biology*, 109 (6), pp. 1003-1016.

Neumann, M., Sampathu, D.M., Kwong, L.K., Truax, A.C., Micsenyi, M.C., Chou, T.T., Bruce, J., Schuck, T., Grossman, M., Clark, C.M., McCluskey, L.F.,

Miller, B.L., Masliah, E., Mackenzie, I.R., Feldman, H., Feiden, W., Kretzschmar, H.A., Trojanowski, J.Q. & Lee, V.M.Y. (2006) Ubiquitinated TDP-43 in Frontotemporal Lobar Degeneration and Amyotrophic Lateral Sclerosis. *Science*, 314 (5796), pp.130–133.

Newsome, T.P., Asling, B. & Dickson, B.J. (2000) Analysis of Drosophila photoreceptor axon guidance in eye-specific mosaics. *Development*, 127 (4), pp.851–860.

Ngo, M., and Ridgway, N.D. (2009). Oxysterol binding protein-related Protein 9 (ORP9) is a cholesterol transfer protein that regulates Golgi structure and function. *Molecular and Biological Cell* 20, 1388–1399.

Nishimura, A.L., Mitne-Neto, M., Silva, H.C., Richieri-Costa, A., Middleton, S., Cascio, D., Kok, F., Oliveira, J.R., Gillingwater, T. & Webb, J. (2004a) A mutation in the vesicle-trafficking protein VAPB causes late-onset spinal muscular atrophy and amyotrophic lateral sclerosis. *The American Journal of Human Genetics*, 75 (5), pp.822–831.

Nishimura, I., Yang, Y. & Lu, B. (2004b) PAR-1 kinase plays an initiator role in a temporally ordered phosphorylation process that confers tau toxicity in Drosophila. *Cell*, 116 (5), pp.671–682.

Nishimura, Y., Hayashi, M., Inada, H. & Tanaka, T. (1999) Molecular cloning and characterization of mammalian homologues of vesicle-associated membrane protein-associated (VAMP-associated) proteins. *Biochemical and Biophysical Research Communications*, 254 (1), pp.21–26.

Nüsslein-Volhard, C. & Wieschaus, E. (1980) Mutations affecting segment number and polarity in Drosophila. *Nature*, 287 (5785), pp.795–801.

O'Hare, K. & Rubin, G.M. (1983) Structures of P transposable elements and their sites of insertion and excision in the Drosophila melanogaster genome. *Cell*, 34 (1), pp.25–35.

O'Kane, C.J. (2003) Modelling human diseases in Drosophila and Caenorhabditis. *Seminars in cell & developmental biology*, 14 (1), pp.3–10.

O'Sullivan, N.C., Jahn, T.R., Reid, E. & O'Kane, C.J. (2012) Reticulon-like-1, the Drosophila orthologue of the Hereditary Spastic Paraplegia gene reticulon 2, is required for organization of endoplasmic reticulum and of distal motor axons. *Human Molecular Genetics*, 21 (15), pp.3356–3365.

Otomo, A., Kunita, R., Suzuki-Utsunomiya, K., Ikeda, J. & Hadano, S. (2011) Defective relocalization of ALS2/alsin missense mutants to Rac1-induced macropinosomes accounts for loss of their cellular function and leads to disturbed amphisome formation. *FEBS letters,* 585, pp. 730-736.

Paik, D., Jang, Y.G., Lee, Y.E., Lee, Y.N., Yamamoto, R., Gee, H.Y., Yoo, S., Bae, E., Min, K.-J., Tatar, M. & Park, J.-J. (2012) Misexpression screen delineates

novel genes controlling Drosophila lifespan. *Mechanisms of Ageing and Development*, 133 (5), pp.234–245.

Pak, W.L., Grossfield, J. & Arnold, K.S. (1970) Mutants of the visual pathway of Drosophila melanogaster. *Nature*, 227 (5257), pp.518–520.

Pan, D. (2010) The Hippo signaling pathway in development and cancer. *Developmental cell*, 19 (4), pp.491-505.

Pantalacci, S., Tapon, N. & Leopold, P. (2003) The Salvador partner Hippo promotes apoptosis and cell-cycle exit in Drosophila. *Nature Cell Biology*, 5 (10), pp. 921-927.

Papiani, G., Ruggiano, A., Fossati, M., Raimondi, A., Bertoni, G., Francolini, M., Benfante, R., Navone, F. & Borgese, N. (2012) Restructured endoplasmic reticulum generated by mutant amyotrophic lateral sclerosis-linked VAPB is cleared by the proteasome. *Journal of Cell Science*, 125 (15), pp.3601–3611.

Park, J., Al-Ramahi, I., Tan, Q., Mollema, N., Diaz-Garcia, J.R., Gallego-Flores, T., Lu, H.-C., Lagalwar, S., Duvick, L., Kang, H., Lee, Y., Jafar-Nejad, P., Sayegh, L.S., Richman, R., Liu, X., Gao, Y., Shaw, C.A., Arthur, J.S.C., Orr, H.T., Westbrook, T.F., Botas, J. & Zoghbi, H.Y. (2013) RAS-MAPK-MSK1 pathway modulates ataxin 1 protein levels and toxicity in SCA1. *Nature*, 498 (7454), pp.325–331.

Parkinson, N., Ince, P.G., Smith, M.O., Highley, R., Skibinski, G., Andersen, P.M., Morrison, K.E., Pall, H.S., Hardiman, O., Collinge, J., Shaw, P.J. & Fisher, E.C. (2006) ALS phenotypes with mutations in CHMP2B (charged multivesicular body protein 2B). *Neurology*, 67 (6), pp.1074–1077.

Pasinelli, P. & Brown, R.H. (2006) Molecular biology of amyotrophic lateral sclerosis: insights from genetics. *Nature Reviews Neuroscience*, 7 (9), pp.710–723.

Pasinelli, P., Belford, M.E., Lennon, N., Bacskai, B.J., Hyman, B.T., Trotti, D. & Brown, R.H. (2004) Amyotrophic lateral sclerosis-associated SOD1 mutant proteins bind and aggregate with Bcl-2 in spinal cord mitochondria. *Neuron*, 43 (1), pp.19–30.

Pennetta, G., Hiesinger, P.R., Fabian-Fine, R., Meinertzhagen, I.A. & Bellen, H.J. (2002) Drosophila VAP-33A directs bouton formation at neuromuscular junctions in a dosage-dependent manner. *Neuron*, 35 (2), pp.291–306.

Peretti, D., Dahan, N., Shimoni, E., Hirschberg, K. & Lev, S. (2008) Coordinated lipid transfer between the endoplasmic reticulum and the Golgi complex requires the VAP proteins and is essential for Golgi-mediated transport. *Molecular Biology of the Cell*,19, pp.3871–3884.

Petroski, M. & Deshaies, R. (2005) Function and regulation of cullin-RING ubiquitin ligases. *Nature reviews: Molecular cell biology*, 6, pp.9-20.

Pesah, Y., Pham, T., Burgess, H., Middlebrooks, B., Verstreken, P., Zhou, Y., Harding, M., Bellen, H. & Mardon, G. (2004) Drosophila parkin mutants have decreased mass and cell size and increased sensitivity to oxygen radical stress. *Development*, 131 (9), pp.2183–2194.

Pol, A., Gross, S. & Parton, R. (2014) Review: biogenesis of the multifunctional lipid droplet: lipids, proteins, and sites. *Journal of cell biology*, 204 (5), pp.635-646.

Polymenidou, M. & Cleveland, D.W. (2011) The Seeds of Neurodegeneration: Prion-like Spreading in ALS. *Cell*, 147 (3), pp.498–508.

Poppelreuther, M., Rudolph, B., Du, C., Grobmann, R., Becker, M., Thiele, C., Ehehalt, R.. & Fullekrug, J. (2012) The N-terminal region of acyl-CoA synthetase 3 is essential for both the localization on lipid droplets and the function in fatty acid uptake. *Journal of lipid research*, 53 (5), pp.888-900.

Prubing, K., Voigt, A., Schulz, J. (2013) Drosophila melanogaster as a model for Alzheimer's disease. *Molecular degeneration*, 8 (35), pp.1-11.

Puckelwartz, M.J., Kessler, E., Zhang, Y., Hodzic, D., Randles, K.N., Morris, G., Earley, J.U., Hadhazy, M., Holaska, J.M., Mewborn, S.K., Pytel, P. & McNally, E.M. (2009) Disruption of nesprin-1 produces an Emery Dreifuss muscular dystrophy-like phenotype in mice. *Human molecular genetics*, 18 (4), pp. 607-620.

Qin, H., Wang, W. & Song, J. (2013) ALS-causing P56S mutation and splicing variation on the hVAPB MSP domain transform its β-sandwich fold into lipid-interacting helical conformations. *Biochemical and Biophysical Research Communications*, 431 (3), pp.398–403.

Quinn, W.G., Harris, W.A. & Benzer, S. (1974) Conditioned behavior in Drosophila melanogaster. *Proceedings of the National Academy of Sciences of the United States of America*, 71 (3), pp.708–712.

Qurashi, A., Sahin, B., Cabrera, P., Gautreau, A., Schenck, A. & Giangrande, A. (2007) HSPC300 and its role in neuronal connectivity. *Neural Development*, 2 (18), pp.1-13.

Rabinowitz, J. & While, E. (2010) Autophagy and metabolism. *Science*, 330 (6009), pp.1344-1348

Rao, M., Song, W., Jiang, A., Shyr, Y., Lev, S., Greenstein, D., Brantley-Sieders, D. & Chen, J. (2012) VAMP-Associated Protein B (VAPB) Promotes Breast Tumor Growth by Modulation of Akt Activity W. Debinski ed. *PLoS ONE*, 7 (10), p.e46281.

Ratnaparkhi, A., Lawless, G.M., Schweizer, F.E., Golshani, P. & Jackson, G.R. (2008) A Drosophila Model of ALS: Human ALS-Associated Mutation in

VAP33A Suggests a Dominant Negative Mechanism D. C. Rubinsztein ed. *PLoS ONE*, 3 (6), p.e2334.

Ravid, T. & Hochstrasser, M. (2008) Diversity of degradation signals in the ubiquitin-proteasome system. *Nature reviews Molecular Cell biology*, 9 (9), pp.679-690.

Ravikumar, B., Imarisio, S., Sarkar, S., O'Kane, C.J. & Rubinsztein, D.C. (2008) Rab5 modulates aggregation and toxicity of mutant huntingtin through macroautophagy in cell and fly models of Huntington disease. *Journal of Cell Science*, 121 (10), pp.1649–1660.

Raychaudhuri, S. & Prinz, W.A. (2010) The Diverse Functions of Oxysterol-Binding Proteins. *Annual Review of Cell and Developmental Biology*, 26 (1), pp.157–177.

Razzell, W., Wood, W. & Martin, P. (2011) Swatting flies: modeling wound healing and inflammation in Drosophila. *Disease models & mechanisms*, 4, pp. 569-574.

Reiter, L.T., Potocki, L., Chien, S., Gribskov, M. & Bier, E. (2001) A systematic analysis of human disease-associated gene sequences in Drosophila melanogaster. *Genome research*, 11 (6), pp.1114–1125.

Renton, A.E., Chiò, A. & Traynor, B.J. (2013) State of play in amyotrophic lateral sclerosis genetics. *Nature Neuroscience*, 17 (1), pp.17–23.

Renton, A.E., Majounie, E., Waite, A., Simón-Sánchez, J., Rollinson, S., Gibbs, J.R., Schymick, J.C., Laaksovirta, H., van Swieten, J.C., Myllykangas, L., Kalimo, H., Paetau, A., Abramzon, Y., Remes, A.M., Kaganovich, A., Scholz, S.W., Duckworth, J., Ding, J., Harmer, D.W., Hernandez, D.G., Johnson, J.O., Mok, K., Ryten, M., Trabzuni, D., Guerreiro, R.J., Orrell, R.W., Neal, J., Murray, A., Pearson, J., Jansen, I.E., Sondervan, D., Seelaar, H., Blake, D., Young, K., Halliwell, N., Callister, J.B., Toulson, G., Richardson, A., Gerhard, A., Snowden, J., Mann, D., Neary, D., Nalls, M.A., Peuralinna, T., Jansson, L., Isoviita, V.-M., Kaivorinne, A.-L., Hölttä-Vuori, M., Ikonen, E., Sulkava, R., Benatar, M., Wuu, J., Chiò, A., Restagno, G., Borghero, G., Sabatelli, M., Heckerman, D., Rogaeva, E., Zinman, L., Rothstein, J.D., Sendtner, M., Drepper, C., Eichler, E.E., Alkan, C., Abdullaev, Z., Pack, S.D., Dutra, A., Pak, E., Hardy, J., Singleton, A., Williams, N.M., Heutink, P., Pickering-Brown, S., Morris, H.R., Tienari, P.J., Traynor, B.J. & Consortium28, T.I. (2011) A Hexanucleotide Repeat Expansion in C9ORF72 Is the Cause of Chromosome 9p21-Linked ALS-FTD. *Neuron*, 72 (2), pp.257–268.

Rezaie, T., Child, A., Hitchings, R., Brice, G., Miller, L., Coca-Prados, M., Heon, E., Krupin, T., Ritch, R., Kreutzer, D., Pitts Crick, R. & Sarfarazi, M. (2002) Adult-Onset Primary Open-Angle Glaucoma Caused by Mutations in Optineurin. *Science*, 295 (5557), pp.1077–1079.

Riemensperger, T., Issa, A.-R., Pech, U., Coulom, H., Nguyễn, M.-V., Cassar, M., Jacquet, M., Fiala, A. & Birman, S. (2013) A Single Dopamine Pathway Underlies Progressive Locomotor Deficits in a Drosophila Model of Parkinson Disease. *Cell Reports*, 5 (4), pp.952–960.

Robberecht, W. & Philips, T. (2013) The changing scene of amyotrophic lateral sclerosis. *Nature Reviews Neuroscience*, 14 (4), pp.248–264.

Ron, D. & Walter, P. (2007) Signal integration in the endoplasmic reticulum unfolded protein response. *Nature Reviews Molecular Cell Biology*, 8, pp.519–529

Pirrotta, V. (1986) Cloning Drosophila genes. In D.B.Roberts, Drosophila a practical approach. First edition. *IRL Press*.

Robertson, H.M., Preston, C.R., Phillis, R.W., Johnson-Schlitz, D.M., Benz, W.K. & Engels, W.R. (1988) A stable genomic source of P element transposase in Drosophila melanogaster. *Genetics*, 118 (3), pp.461–470.

Robinson, B. & Moberg, K. (2011) Drosophila endocytic neoplastic tumour suppresor genes regulate Sav/Wts/Hpo signaling and the c-Jun N-terminal kinase pathway. *Cell cycle*, 10 (23), pp.4110-4118.

Robinson, P.N., Wollstein, A., Bohme, U. & Beattie, B. (2004) Ontologizing gene-expression microarray data: characterizing clusters with Gene Ontology. *Bioinformatics*, 20 (6), pp.979–981.

Rocha, N., Kuijl, C., van der Kant, R., Janssen, L., Houben, D., Janssen, H., Zwart, W. & Neefjes, J. (2009) Cholesterol sensor ORP1L contacts the ER protein VAP to control Rab7-RILP-p150Glued and late endosome positioning. *The Journal of Cell Biology*, 185 (7), pp.1209–1225.

Romano, D., Nguyen, L., Matallanas, D., Halasz, M., Doherty, C., Kholodenko, B. & Kolch, W. (2014) Protein interaction switches coordinate Raf-1 and MST2/Hippo signaling. *Nature Cell biology*, 16 (7), pp.673-685.

Rosen, D.R., Siddique, T., Patterson, D., Figlewicz, D.A., Sapp, P., Hentati, A., Donaldson, D., Goto, J., O'Regan, J.P. & Deng, H.X. (1993) Mutations in Cu/Zn superoxide dismutase gene are associated with familial amyotrophic lateral sclerosis. *Nature*, 362 (6415), pp.59–62.

Ross, C.A., Aylward, E.H., Wild, E.J., Langbehn, D.R., Long, J.D., Warner, J.H., Scahill, R.I., Leavitt, B.R., Stout, J.C., Paulsen, J.S., Reilmann, R., Unschuld, P.G., Wexler, A., Margolis, R.L. & Tabrizi, S.J. (2014) Huntington disease: natural history, biomarkers and prospects for therapeutics. *Nature Reviews Neurology*, 10 (4), pp.204–216.

Rotty, J., Wu, C. & Bear, J. (2013) New insights into the regulation and cellular functions of the ARP2/3 complex. *Nature Molecular cell biology*, 14(1), pp. 7-12.

Rozas, J.L., Gomez-Sanchez, L., Tomas-Zapico, C., Lucas, J.J. & Fernandez-Chacon, R. (2011) Increased Neurotransmitter Release at the Neuromuscular Junction in a Mouse Model of Polyglutamine Disease. *Journal of Neuroscience*, 31 (3), pp.1106–1113.

Russ, W.P. & Engelman, D.M. (2000) The GxxxG motif: A framework for transmembrane helix-helix association. *Journal of Molecular Biology*, 296 (3), pp.911–919.

Russell, D.W. & Sambrook, J. (2001) Molecular cloning: a laboratory manual. *Cold Spring Harbor Laboratory Press*.

Rørth, P. (1996) A modular misexpression screen in Drosophila detecting tissue-specific phenotypes. *Proceedings of the National Academy of Sciences of the United States of America*, 93 (22), pp.12418–12422.

Sahai, E. & Marshall, C. J. (2002) RHO-GTPases and cancer. *Nature Reviews Cancer*, 2, pp.133–142.

Sancenon, V., Lee, S.A., Patrick, C., Griffith, J., Paulino, A., Outeiro, T.F., Reggiori, F., Masliah, E. & Muchowski, P.J. (2012) Suppression of -synuclein toxicity and vesicle trafficking defects by phosphorylation at S129 in yeast depends on genetic context. *Human Molecular Genetics*, 21 (11), pp.2432–2449.

Sanhueza, M., Zechini, L., Gillespie, T. & Pennetta, G. (2013) Gain-of-function mutations in the ALS8 causative gene VAPB have detrimental effects on neurons and muscles. *Biology Open*, 3 (1), pp.59-71.

Satterfield, T.F., Jackson, S.M. & Pallanck, L.J. (2002) A Drosophila homolog of the polyglutamine disease gene SCA2 is a dosage-sensitive regulator of actin filament formation. *Genetics*, 162 (4), pp.1687–1702.

Savica, R., Grossardt, B.R., Bower, J.H., Boeve, B.F., Ahlskog, J.E. & Rocca, W.A. (2013) Incidence of Dementia With Lewy Bodies and Parkinson Disease Dementia. *JAMA Neurology*, 70 (11), p.1396.

Scott, C., Vacca, F. & Gruenberg, J. (2014) Endosome maturation, transport and functions. *Seminars in cell & developmental biology*, 31, pp.2-10.

Schimmelpfeng, K., Gögel, S. & Klämbt, C. (2001) The function of leak and kuzbanian during growth cone and cell migration. *Mech Dev.* 106 (1-2), pp.25-36.

Schuldiner, M., Collins, S.R., Thompson, N.J., Denic, V., Bhamidipati, A., Punna, T., Ihmels, J., Andrews, B., Boone, C., Greenblatt, J.F., Weissman, J.S. & Krogan, N.J. (2005) Exploration of the Function and Organization of the Yeast Early Secretory Pathway through an Epistatic Miniarray Profile. *Cell*, 123 (3), pp.507–519.

Shannon, P., Markiel, A., Ozier, O., Baliga, N.S., Wang, J.T., Ramage, D., Amin, N., Schwikowski, B. & Ideker, T. (2003) Cytoscape: a software environment for integrated models of biomolecular interaction networks. *Genome Research*, 13 (11), pp. 2498-2504.

Shao, H., Kadono-Okuda, K., Finlin, B. & Andres, D. (1999) Biochemical Characterization of the Ras-Related GTPases Rit and Rin. *Archives of Biochemestry and Biophysics*, 371 (2), pp.207-209.

Shi, G., Cai, W. & Andres, D. (2013) Rit subafamily small GTPases: Regulators in neuronal differentiation and survival. *Cellular signaling*, 25, pp.2060-2068.

Shi, J., Lua, S., Tong, J.S. & Song, J. (2010) Elimination of the Native Structure and Solubility of the hVAPB MSP Domain by the Pro56Ser Mutation That Causes Amyotrophic Lateral Sclerosis. *Biochemistry*, 49 (18), pp.3887–3897.

Shulman, J.M. & Feany, M.B. (2003) Genetic modifiers of tauopathy in Drosophila. *Genetics*, 165 (3), pp.1233–1242.

Simon, M. (1994) Signal transduction during the development of the *Drosophila* R7 photoreceptor. *Developmental Biology*, pp.431–442.

Simon, M.A., Carthew, R.W., Fortini, M.E., Gaul, U., Mardon, G. & Rubin, G.M. (1992) Signal Transduction Pathway Initiated by Activation of the sevenless Tyrosine Kinase Receptor. *Cold Spring Harbor Symposia on Quantitative Biology*, 57, pp.375–380.

Skehel, P.A., Fabian-Fine, R. & Kandel, E.R. (2000) Mouse VAP33 is associated with the endoplasmic reticulum and microtubules. *Proceedings of the National Academy of Sciences of the United States of America*, 97 (3), pp.1101–1106.

Skehel, P.A., Martin, K.C., Kandel, E.R. & Bartsch, D. (1995) A VAMP-binding protein from Aplysia required for neurotransmitter release. *Science*, 269 (5230), pp.1580–1583.

Soussan, L., Burakov, D., Daniels, M.P., Toister-Achituv, M., Porat, A., Yarden, Y. & Elazar, Z. (1999) ERG30, a VAP-33-related protein, functions in protein transport mediated by COPI vesicles. *The Journal of Cell Biology*, 146 (2), pp.301–311.

Sreedharan, J., Blair, I.P., Tripathi, V.B., Hu, X., Vance, C., Rogelj, B., Ackerley, S., Durnall, J.C., Williams, K.L., Buratti, E., Baralle, F., de Belleroche, J., Mitchell, J.D., Leigh, P.N., Al-Chalabi, A., Miller, C.C., Nicholson, G. & Shaw, C.E. (2008) TDP-43 Mutations in Familial and Sporadic Amyotrophic Lateral Sclerosis. *Science*, 319 (5870), pp.1668–1672.

St Johnston, D. (2002) The art and design of genetic screens: Drosophila melanogaster. *Nature reviews. Genetics*, 3 (3), pp.176–188.

Stallings, N.R., Puttaparthi, K., Luther, C.M., Burns, D.K. & Elliott, J.L. (2010) Progressive motor weakness in transgenic mice expressing human TDP-43. *Neurobiology of Disease*, 40 (2), pp.404–414.

Staudt, N., Molitor, A., Somogyi, K., Mata, J., Curado, S., Eulenberg, K., Meise, M., Siegmund, T., Häder, T., Hilfiker, A., Brönner, G., Ephrussi, A., Rørth, P., Cohen, S.M., Fellert, S., Chung, H.-R., Piepenburg, O., Schäfer, U., Jäckle, H. & Vorbrüggen, G. (2005) Gain-of-Function Screen for Genes That Affect Drosophila Muscle Pattern Formation. *PLoS Genetics*, 1 (4), p.e55.

Steffan, J.S., Bodai, L., Pallos, J., Poelman, M., McCampbell, A., Apostol, B.L., Kazantsev, A., Schmidt, E., Zhu, Y.Z., Greenwald, M., Kurokawa, R., Housman, D.E., Jackson, G.R., Marsh, J.L. & Thompson, L.M. (2001) Histone deacetylase inhibitors arrest polyglutamine-dependent neurodegeneration in Drosophila. *Nature*, 413 (6857), pp.739–743.

Stepto, A., Gallo, J.M., Shaw, C., Hirth, F. (2014) Modelling C9ORF72 hexanucleotide repeat expansion in amyotrophic lateral sclerosis and frontotemporal dementia. *Acta Neuropathol,* 127, pp.377-389

Stofanko, M., Kwon, S.Y. & Badenhorst, P. (2008) A Misexpression Screen to Identify Regulators of Drosophila Larval Hemocyte Development. *Genetics*, 180 (1), pp.253–267.

Stowers, R.S. & Schwarz, T.L. (1999) A genetic method for generating Drosophila eyes composed exclusively of mitotic clones of a single genotype. *Genetics*, 152 (4), pp.1631–1639.

Strisovsky, K., Sharpe, H.J. & Freeman, M. (2009) Sequence-Specific Intramembrane Proteolysis: Identification of a Recognition Motif in Rhomboid Substrates. *Molecular Cell*, 36 (6), pp.1048–1059.

Sturtevant, M., Roark, M. & Bier, E. (1993) The Drosophila rhomboid gene mediates the localized formation of wing veins and interacts genetically with components of the EGF-R signaling pathway. *Genes dev*, 7 (6), pp.961-973.

Teuling, E., Ahmed, S., Haasdijk, E., Demmers, J., Steinmetz, M.O., Akhmanova, A., Jaarsma, D. & Hoogenraad, C.C. (2007) Motor Neuron Disease-Associated Mutant Vesicle-Associated Membrane Protein-Associated Protein (VAP) B Recruits Wild-Type VAPs into Endoplasmic Reticulum-Derived Tubular Aggregates. *Journal of Neuroscience*, 27 (36), pp.9801–9815.

Thomas, B.J. & Wassarman, D.A. (1999) A fly's eye view of biology. *Trends in genetics*, 15 (5), pp.184–190.

Tien, A., Rajan, A., Schulze, K., Ryoo, H., Acar, M., Steller, H. & Bellen, H. (2008) Ero1L, a thiol oxidase, is required for Notch signaling through cysteine bridge formation of the Lin12-Notch repeats in Drosophila melanogaster. *Journal of cell biology*, 182 (6), pp.1113-1125.

Tseng, A.-S.K. & Hariharan, I.K. (2002) An overexpression screen in Drosophila for genes that restrict growth or cell-cycle progression in the developing eye. *Genetics*, 162 (1), pp.229–243.

Tsuda, H., Han, S.M., Yang, Y., Tong, C., Lin, Y.Q., Mohan, K., Haueter, C., Zoghbi, A., Harati, Y., Kwan, J., Miller, M.A. & Bellen, H.J. (2008) The Amyotrophic Lateral Sclerosis 8 Protein VAPB Is Cleaved, Secreted, and Acts as a Ligand for Eph Receptors. *Cell*, 133 (6), pp.963–977.

Turner, M.R., Kiernan, M.C., Leigh, P.N., & Talbot, K. (2009) Biomarkers in amyotrophic lateral sclerosis. *Lancet Neurology*. 8, pp.94–109.

Turner, B.J. & Talbot, K. (2008) Transgenics, toxicity and therapeutics in rodent models of mutant SOD1-mediated familial ALS. *Progress in Neurobiology*, 85 (1), pp.94–134.

Udan, R., Kango-Singh, M., Nolo, R., Tao, C. & Halder, G. (2003) Hippo promotes proliferation arrest and apoptosis in the Salvador/Warts pathway. *Nature Cell Biology*, 5 (10), pp. 914-920.

Urban, S. & Dickey, S. (2011) The rhomboid protease family: a decade of progress on function and mechanism. *Genome biology*, 12 (231), pp. 1-10.

Urban, S., Lee, J. & Freeman, M. (2001) Drosophila Rhomboid-1 Defines a Family of Putative Intramembrane Serine Proteases. *Cell*, 107, pp.173-182.

Vabulas, R.M., Raychaudhuri, S., Hayer-Hartl, M. & Hartl, F.U. (2010) Protein Folding in the Cytoplasm and the Heat Shock Response. *Cold Spring Harbor Perspectives in Biology*, 2 (12), pp.a004390–a004390.

Van Aelst, L., Barr, M., Marcus, S., Polverino, A. & Wigler, M. (1993) Complex formation between RAS and RAF and other protein kinases. *Proceedings National Academy of Science USA*, 90, pp. 6213–6217.

van Blitterswijk, M., van Es, M.A., Hennekam, E.A.M., Dooijes, D., van Rheenen, W., Medic, J., Bourque, P.R., Schelhaas, H.J., van der Kooi, A.J., de Visser, M., de Bakker, P.I.W., Veldink, J.H. & van den Berg, L.H. (2012a) Evidence for an oligogenic basis of amyotrophic lateral sclerosis. *Human Molecular Genetics*, 21 (17), pp.3776–3784.

van Blitterswijk, M., van Es, M.A., Koppers, M., van Rheenen, W., Medic, J., Schelhaas, H.J., van der Kooi, A.J., de Visser, M., Veldink, J.H. & van den Berg, L.H. (2012b) VAPB and C9orf72 mutations in 1 familial amyotrophic lateral sclerosis patient. *Neurobiology of Aging*, 33 (12), pp.1–4.

Van Damme, P., Bogaert, E., Dewil, M., Hersmus, N., Kiraly, D., Scheveneels, W., Bockx, I., Braeken, D., Verpoorten, N., Verhoeven, K., Timmerman, V., Herijgers, P., Callewaert, G., Carmeliet, P., Van Den Bosch, L. & Robberecht, W. (2007) Astrocytes regulate GluR2 expression in motor neurons and their

vulnerability to excitotoxicity. *Proceedings of the National Academy of Sciences of the United States of America*, 104 (37), pp.14825–14830.

Vance, C., Rogelj, B., Hortobágyi, T., De Vos, K.J., Nishimura, A.L., Sreedharan, J., Hu, X., Smith, B., Ruddy, D., Wright, P., Ganesalingam, J., Williams, K.L., Tripathi, V., Al-Saraj, S., Al-Chalabi, A., Leigh, P.N., Blair, I.P., Nicholson, G., de Belleroche, J., Gallo, J.-M., Miller, C.C. & Shaw, C.E. (2009) Mutations in FUS, an RNA processing protein, cause familial amyotrophic lateral sclerosis type 6. *Science*, 323 (5918), pp.1208–1211.

Vanselow, B.K. & Keller, B.U. (2000) Calcium dynamics and buffering in oculomotor neurones from mouse that are particularly resistant during amyotrophic lateral sclerosis (ALS)-related motoneurone disease. *Journal of Physiology*, 525 (2), pp.433–445.

Vassar, R., Kuhn, P.H., Haass, C., Kennedy, M.E., Rajendran, L., Wong, P.C. & Lichtenthaler, S.F. (2014) Function, therapeutic potential and cell biology of BACE proteases: current status and future prospects. *Journal of Neurochemistry*, 130 (1), pp.4-28.

Vu, Y., Li, Z., Rizzo, N., Einstein, J & Welte, M. (2011) Targeting the motor regulator Klar to lipid droplets. *BMC Cell biology*, 12 (9), pp.1-15.

Wang, J., Farr, G.W., Hall, D.H., Li, F., Furtak, K., Dreier, L. & Horwich, A.L. (2009) An ALS-Linked Mutant SOD1 Produces a Locomotor Defect Associated with Aggregation and Synaptic Dysfunction When Expressed in Neurons of Caenorhabditis elegans. *PLoS Genetics*, 5 (1), p.e1000350.

Warde-Farley, D., Donaldson, S.L., Comes, O., Zuberi, K., Badrawi, R., Chao, P., Franz, M., Grouios, C., Kazi, F., Lopes, C.T., Maitland, A., Mostafavi, S., Montojo, J., Shao, Q., Wright, G., Bader, G.D. & Morris, Q. (2010) The GeneMANIA prediction server: biological network integration for gene prioritization and predicting gene function. *Nucleic Acids Research*, 38 (Web Server issue), pp.W214–W220.

Warrick, J.M., Morabito, L.M., Bilen, J., Gordesky-Gold, B., Faust, L.Z., Paulson, H.L. & Bonini, N.M. (2005) Ataxin-3 Suppresses Polyglutamine Neurodegeneration in Drosophila by a Ubiquitin-Associated Mechanism. *Molecular Cell*, 18 (1), pp.37–48.

Warrick, J.M., Paulson, H.L., Gray-Board, G.L., Bui, Q.T., Fischbeck, K.H., Pittman, R.N. & Bonini, N.M. (1998) Expanded polyglutamine protein forms nuclear inclusions and causes neural degeneration in Drosophila. *Cell*, 93 (6), pp.939–949.

Watson, M.R., Lagow, R.D., Xu, K., Zhang, B. & Bonini, N.M. (2008) A drosophila model for amyotrophic lateral sclerosis reveals motor neuron damage by human SOD1. *The Journal of biological chemistry*, 283 (36), pp.24972–24981.

Watts, G.D.J., Wymer, J., Kovach, M.J., Mehta, S.G., Mumm, S., Darvish, D., Pestronk, A., Whyte, M.P. & Kimonis, V.E. (2004) Inclusion body myopathy associated with Paget disease of bone and frontotemporal dementia is caused by mutant valosin-containing protein. *Nature Genetics*, 36 (4), pp.377–381.

Weber, K., Greenspan, R., Chicoine, D., Fiorentino, K., Thomas, M. & Knight, T. (2008) Microarray analysis of replicate populations selected against a wing-shape correlation in Drosophila melanogaster. *Genetics*, 178 (2), pp.1093-1108.

Wei, H.-C., Sanny, J., Shu, H., Baillie, D.L., Brill, J.A., Price, J.V. & Harden, N. (2003) The Sac1 Lipid Phosphatase Regulates Cell Shape Change and the JNK Cascade during Dorsal Closure in Drosophila. *Current Biology*, 13 (21), pp.1882–1887.

Weir, M.L., Klip, A. & Trimble, W.S. (1998) Identification of a human homologue of the vesicle-associated membrane protein (VAMP)-associated protein of 33 kDa (VAP-33): a broadly expressed protein that binds to VAMP. *The Biochemical journal*, 333 (2), pp.247–251.

Welte, M., Gross, S., Postner, M., Block, S. & Wieschaus, E. (1998) Developmental regulation of vesicle transport in Drosophila embryos: forces and kinetics. *Cell*, 92 (4), pp.547-557.

Wes, P.D., Yu, M. & Montell, C. (1996) RIC, a calmodulin-binding Ras-like GTPase. *The EMBO Journal*, 15 (21), pp.5839–5848.

Williamson, T.L. & Cleveland, D.W. (1999) Slowing of axonal transport is a very early event in the toxicity of ALS-linked SOD1 mutants to motor neurons. *Nature Neuroscience*, 2 (1), pp.50–56.

Wilson, J.D., Thompson, S.L. & Barlowe, C. (2011) Yet1p-Yet3p interacts with Scs2p-Opi1p to regulate ER localization of the Opi1p repressor. *Molecular biology of the cell*, 22 (9), pp.1430–1439.

Witke, W. (2004) The role of profilin complexes in cellmotility andother cellular processes. *Trends on Cell Biology*, 14, pp.461–469.

Wittmann, C.W., Wszolek, M.F., Shulman, J.M., Salvaterra, P.M., Lewis, J., Hutton, M. & Feany, M.B. (2001) Tauopathy in Drosophila: neurodegeneration without neurofibrillary tangles. *Science*, 293 (5530), pp.711–714.

Woollacott, I.O.C. & Mead, S. (2014) The C9ORF72 expansion mutation: gene structure, phenotypic and diagnostic issues. *Acta Neuropathologica*, 127 (3), pp.319–332.

Wu, C.-H., Fallini, C., Ticozzi, N., Keagle, P.J., Sapp, P.C., Piotrowska, K., Lowe, P., Koppers, M., McKenna-Yasek, D., Baron, D.M., Kost, J.E., Gonzalez-Perez, P., Fox, A.D., Adams, J., Taroni, F., Tiloca, C., Leclerc, A.L., Chafe, S.C., Mangroo, D., Moore, M.J., Zitzewitz, J.A., Xu, Z.-S., van den Berg, L.H.,

Glass, J.D., Siciliano, G., Cirulli, E.T., Goldstein, D.B., Salachas, F., Meininger, V., Rossoll, W., Ratti, A., Gellera, C., Bosco, A., Bassell, G.J., Silani, V., Drory, V.E., Brown, R.H. & Landers, J.E. (2012) Mutations in the profilin 1 gene cause familial amyotrophic lateral sclerosis. *Nature*, 488 (7412), pp.499–503.

Wucherpfennig, T., Wilsch-Bräuninger, M. & González-Gaitán, M. (2003) Role of Drosophila Rab5 during endosomal trafficking at the synapse and evoked neurotransmitter release. *The Journal of Cell Biology*, 161 (3), pp.609–624.

Wyles, J.P., McMaster, C. & Ridgway, N. (2002) Vesicle-associated Membrane Protein-associated Protein-A (VAP-A) Interacts with the Oxysterol-binding Protein to Modify Export from the Endoplasmic Reticulum. *Journal of Biological Chemistry*, 277 (33), pp.29908–29918.

Xu, T., Wang, W., Zhang, S., Stewart, R.A. & Yu, W. (1995) Identifying tumor suppressors in genetic mosaics: the Drosophila lats gene encodes a putative protein kinase. *Development*, 121 (4), pp.1053–1063.

Xu, Y., Seet, L.F., Hanson, B. & Hong, W. (2001) The Phox homology (PX) domain, a new player in phosphoinositide signalling. *The Biochemical journal*, 360 (Pt 3), pp.513–530.

Xu, Z., Poidevin, M., Li, X., Li, Y., Shu, L., Nelson, D.L., Li, H., Hales, C.M., Gearing, M., Wingo, T.S. & Jin, P. (2013) Expanded GGGGCC repeat RNA associated with amyotrophic lateral sclerosis and frontotemporal dementia causes neurodegeneration. *Proceedings of the National Academy of Sciences*, 110 (19), pp.7778–7783.

Yagi, T., Ito, D., Nihei, Y., Isihara, T. & Suzuki, N. (2011) N88S seipin mutant transgenic mice develop features of seipinopathy/BSCL2-related motor neuron disease via endoplasmic reticulum stress. *Human molecular genetics*, 20 (19), pp.3831-3840.

Yang, Y., Hentati, A., Deng, H., Dabbagh, O., Sasaki, T., Hirano, M., Hung, W., Ouahchi, K., Yan, J., Azim, A., Cole, N., Gascon, G., Yagmour, A., Ben-Hamida, M., Pericak-Vance, M., Hentati, F. & Siddique, T. (2001) The gene encoding alsin, a protein with three guanine-nucleotide exchange factor domains, is mutated in a form of recessive amyotrophic lateral sclerosis. *Nature Genetics*, 29 (2), pp.160-165.

Yang, Y.M., Gupta, S.K., Kim, K.J., Powers, B.E., Cerqueira, A., Wainger, B.J., Ngo, H.D., Rosowski, K.A., Schein, P.A., Ackeifi, C.A., Arvanites, A.C., Davidow, L.S., Woolf, C.J. & Rubin, L.L. (2013) A Small Molecule Screen in Stem-Cell-Derived Motor Neurons Identifies a Kinase Inhibitor as a Candidate Therapeutic for ALS. *Stem Cell*, 12 (6), pp.713–726.

Yannoni, Y.M. & White, K. (1997) Association of the neuron-specific RNA binding domain-containing protein ELAV with the coiled body in Drosophila neurons. *Chromosoma*, 105 (6), pp.332–341.

Yap, C.C. & Winckler, B. (2012) Harnessing the Power of the Endosome to Regulate Neural Development. *Neuron*, 74 (3), pp.440–451.

Ye, Y., Lukinova, N. & Fortini, M.E. (1999) Neurogenic phenotypes and altered Notch processing in Drosophila Presenilin mutants. *Nature*, 398 (6727), pp.525–529.

Zaltsman, Y., Shachnai, L., Yivgi-Ohana, N., Schwarz, M., Maryanovich, M., Houtkooper, R.H., Vaz, F.M., De Leonardis, F., Fiermonte, G., Palmieri, F., Gillissen, B., Daniel, P.T., Jimenez, E., Walsh, S., Koehler, C.M., Roy, S.S., Walter, L., Hajnóczky, G. & Gross, A. (2010) MTCH2/MIMP is a major facilitator of tBID recruitment to mitochondria. *Nature Cell Biology*, 12 (6), pp.553–562.

Zhan, L., Hanson, K.A., Kim, S.H., Tare, A. & Tibbetts, R.S. (2013) Identification of Genetic Modifiers of TDP-43 Neurotoxicity in Drosophila G. Tear ed. *PLoS ONE*, 8 (2), p.e57214

Zhang, Q., Bethmann, C., Worth, N.F., Davies, J.D., Wasner, C., Feuer, A., Ragnauth, C.D., Yi, Q., Mellad, J.A., Warren, D.T., Wheeler, M.A., Ellis, J.A., Skepper, J.N., Vorgerd, M., Schlotter-Weigel, B., Weissberg, P.L., Roberts, R.G., Wehnert, M. & Shanahan, C.M. (2007) Nesprin-1 and -2 are involved in the pathogenesis of Emery Dreifuss muscular dystrophy and are critical for nuclear envelope integrity. *Human molecular genetics*, 16 (23), pp.2816-2833.

Zhang, J., Schulze, K.L., Hiesinger, P.R., Suyama, K., Wang, S., Fish, M., Acar, M., Hoskins, R.A., Bellen, H.J. & Scott, M.P. (2007) Thirty-One Flavors of Drosophila Rab Proteins. *Genetics*, 176 (2), pp.1307–1322.

Zhang, Q., Zheng, Q., Lu, X. (1999) A Genetic Screen for Modifiers of Drosophila Src42A Identifies Mutations in Egfr, rolled and a Novel Signaling Gene. *Genetics*, 151 (2), 697-711.

Zoncu, R., Perera, R.M., Balkin, D.M., Pirruccello, M., Toomre, D. & De Camilli, P. (2009) A Phosphoinositide Switch Controls the Maturation and Signaling Properties of APPL Endosomes. *Cell*, 136 (6), pp.1110–1121.

Appendix: Gain-of-function mutations in the ALS8 causative gene VAPB have detrimental effects on neurons and muscles

Patients with mutations in the ALS8-causative gene VAPB were found first in Brazil ten years ago (Nishimura *et al.*, 2004) and later in United Kingdom (Chen *et al.*, 2010). These mutations, P56S and T46I respectively, were present in the MSP domain of VAPB, a highly conserved domain across the evolution (Lev *et al.*, 2008). Recently, a third VAPB mutation was found in an ALS patient that also carries an expansion in the causative gene C9orf72 (van Blitterswijk *et al.*, 2012). This novel substitution, not found in a large number of healthy subjects, was located this time in the conserved transmembrane domain, which plays an important structural function compared to the conserved VAPB-MSP domain (Appendix figure 1). No information was available about the genetic background and characteristics of this mutation. Moreover, a contradictory study refuted the proposed toxicity of the mutation (Ingre *et al.*, 2013). To understand the function of this mutation and observe the phenotypes associated with it, we constructed a *Drosophila* model expressing the ortholog of this novel mutant in flies, DVAP-V260I.

To examine the effect of the DVAP-V260I mutation in the presynaptic neurons, we expressed this transgenic allele under the control of the panneural driver elav-GAL4. Neuromuscular junctions (NMJs) stained with the neuronal marker anti-horseradish peroxidase antibody (α-HRP) were analysed counting the number and size of boutons and were compared to controls. Expression of DVAP-V260I produced a significant increase in the number of boutons compared to controls (514±3 versus 272±2, $P<0.001$) and a clear decrease in the size of the boutons (Appendix figure 2). Interestingly, this phenotype is exactly the opposite of the one observed in the ALS-linked mutants DVAP-P58S and DVAP-T48I, but is similar to the one observed in the overexpression of the wild-type form of the protein (Chai *et al.*, 2008; Chen *et al.*, 2010; Pennetta *et al.*, 2002). For this reason we studied the NMJ structure of flies overexpressing two wild-type alleles of DVAP, the weak *DVAP-WT*^{1} and *DVAP-WT*^{2}, a stronger one. We observed similar effects in these two overexpressing lines, although the effect in DVAP-V260I was more severe (Appendix figure 2).

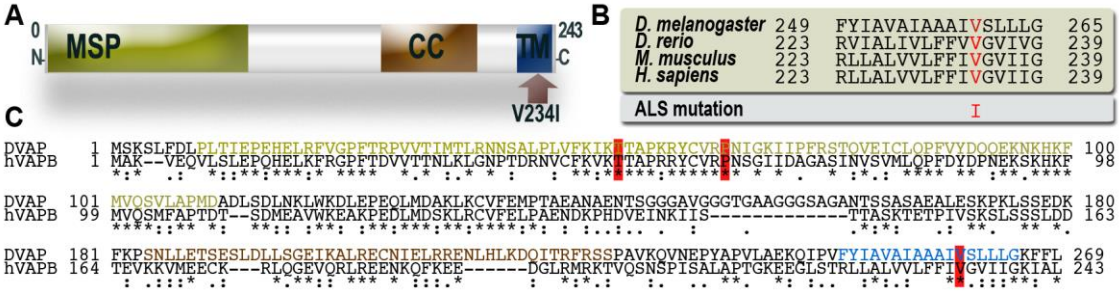

Appendix figure 1. Identification of the V234I/V260I mutation on VAP proteins. (A) Predicted functional domains in hVAPB: a transmembrane domain (blue) at the C-terminus, a coil-coiled domain (brown) in the middle and a domain (green) at the N-terminus showing a significant homology to the nematode major sperm protein (MSP). The Val234 residue (indicated by an arrow) is located within the transmembrane domain and it has been replaced by an Isoleucine in a patient with ALS. (B) High degree of conservation of the transmembrane domain in VAP proteins from different species. (C) Sequences of human VAPB (hVAPB) protein and its *Drosophila* orthologue DVAP were aligned by using the ClustalW version 1.82 alignment program available from EMBL–EBI. Asterisk indicates an identity match; colon indicates conservation between amino acids with strongly similar properties (scoring >0.5 in the Gonnet PAM 250 matrix) and period indicates a conserved substitution between amino acids with weakly similar properties (≤0.5 in the Gonnet PAM 250 matrix). Red boxes highlight the amino acid residues changed by the ALS8 causing mutations identified so far. The *Drosophila* protein (DVAP) exhibits the same functional domains as the hVAPB.

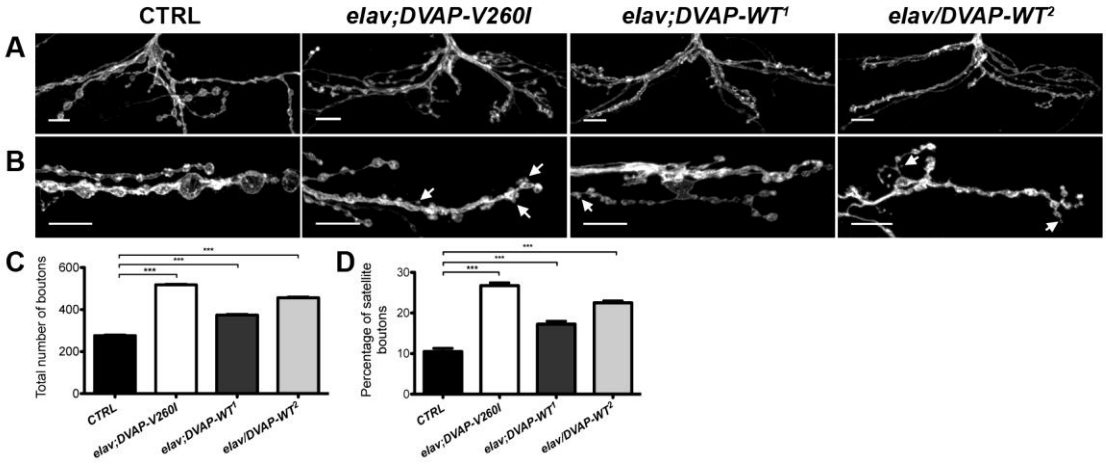

Appendix figure 2. Synaptic boutons are smaller, more numerous and clustered at NMJs expressing either *DVAP-V260I* or *DVAP-WT* transgenes. (A) Representative images of muscle 12 NMJs from abdominal segment 3 labeled with an antibody against HRP. Scale bars: 10 um. (B) Illustration of the synaptic overgrowth phenotype at HRP-stained NMJs of the indicated genotypes. In all panels arrows indicate satellite boutons. Scale bars: 10 um. (C) Quantification of the total number of boutons at muscles 12 and 13 of abdominal segment 3 and (D) quantification of satellite boutons at muscles 6/7 of the abdominal segment 3 for each indicated genotype. *elav-Gal4/+* NMJs were used as controls. *** $P < 0.001$.

These three lines presented in their NMJs many small boutons that bud off from central boutons of the synapses. This phenotype, not observed in controls, was previously associated with overgrowth synapses (Torroja *et al.*, 1999; Franco *et al.*, 2004). Quantification of these satellite boutons in the three transgenic lines resulted in a significant increase compared to control NMJs (Appendix figure 2D), although the effect in *DVAP-V260I* expressing larvae was stronger (2.6 fold compared to controls) than in the two wild-type alleles (1.7 and 2.2 fold in *DVAP-WT*^{1} and *DVAP-WT*^{2}, respectively). To discard that these previous phenotypes are due to changes in the amount of protein produced, we quantified the amount of DVAP present specifically in NMJs of larvae expressing the three constructs. Again, these alleles presented an opposite effect to DVAP-P58S and loss-of-function lines, where DVAP is observed in aggregates in the nerve and completely absent from the synapses (Appendix figure 3). Overexpression lines show a homogenous distribution in the NMJ, with higher concentration than controls. Interestingly, the levels in DVAP-V260I and DVAP-WT^{1} are similarly lower (1.7 and 1.8 fold higher than controls respectively) than the strong DVAP-WT^{2} line (2.2 fold higher). The milder phenotype observed in DVAP-WT^{1} compared to DVAP-V260I, even though they present a comparable amount of protein, suggests that the *DVAP-V260I* mutant allele acts as a hypermorphic allele in the production of an overgrowth synaptic phenotype.

Overgrowth phenotype in the *Drosophila* NMJ has been also associated with increase in number of satellite boutons and microtubule loop formation (Franco *et al.*, 2004). Changes in microtubule architecture were studied in DVAP transgenic lines staining larvae NMJs with the marker for neuronal microtubule and MAP1B homologue, Futsch (Roos *et al.*, 2000). The increase in the number of microtubule loops compared to controls was higher in the larvae expressing *DVAP-V260I* than in both lines over-expressing the wild-type allele (Appendix figure 4). The opposite effect observed in DVAP-P58S and loss-of-function lines, where futsch staining appears splayed and punctuated, is also associated with the changes in the synaptic boutons structure previously mentioned. This indicates that overexpression of *DVAP-V260I* and *DVAP-WT* affects the microtubule architecture with repercussion in the final synaptic bouton morphology.

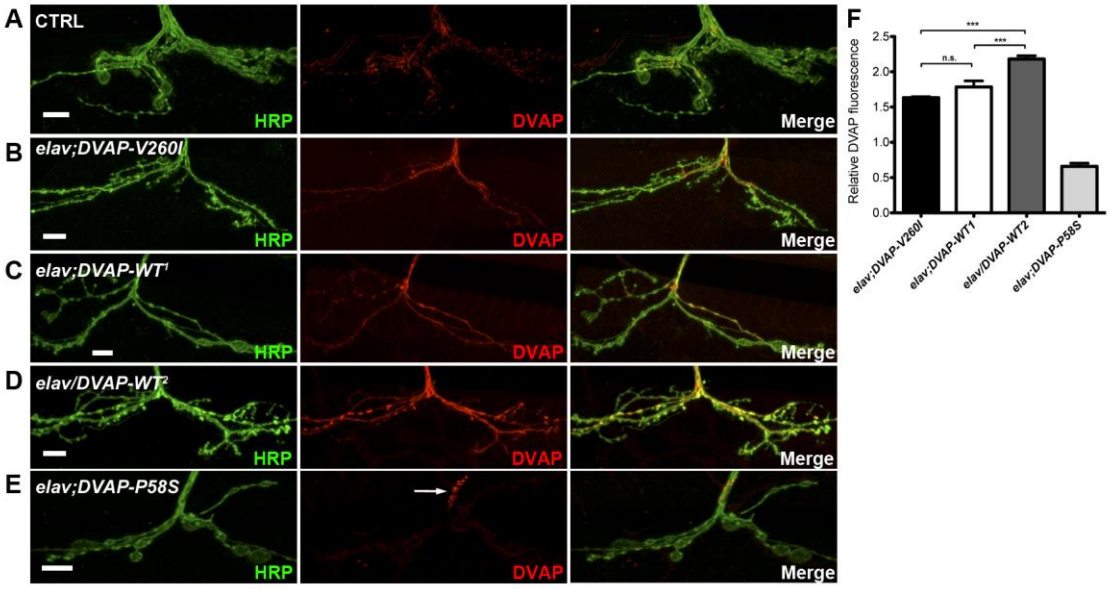

Appendix figure 3. Synaptic levels of DVAP in different genetic contexts. (A) Control *elav/+* NMJs and (B) *elav;DVAP-V260I*, (C) *elav;DVAP-WT*^{1}, (D) *elav/DVAP-WT*^{2}, (E) *elav;DVAP-P58S* NMJs stained with antibodies specific for DVAP and for anti-HRP. Scale bars: 10 um. (F) Quantification of synaptic DVAP intensity for the reported genotypes. DVAP fluorescence intensity is presented as a relative ratio of fluorescence intensity values of DVAP against those of controls. Note that in DVAP-P58S transgenic line aggregates are evident in the terminal part of the nerve (arrow in panel E) and the endogenous protein at the synapse has decreased to about 66±4% of the control value. Conversely, compared to controls DVAP levels at the synapse are significantly increased in all the other transgenic lines ($P<0.001$ in all cases). However, upregulation of DVAP levels in neurons expressing *DVAP-V260I* is comparable to that induced by the *DVAP-WT*^{1} transgene ($P>0.05$) and significantly lower than that associated with the strongest DVAP-WT overexpressing line DVAP-WT2 ($P<0.001$). The difference in DVAP levels between DVAP-WT^{1} and DVAP-WT^{2} lines was statistically significant ($P<0.001$).

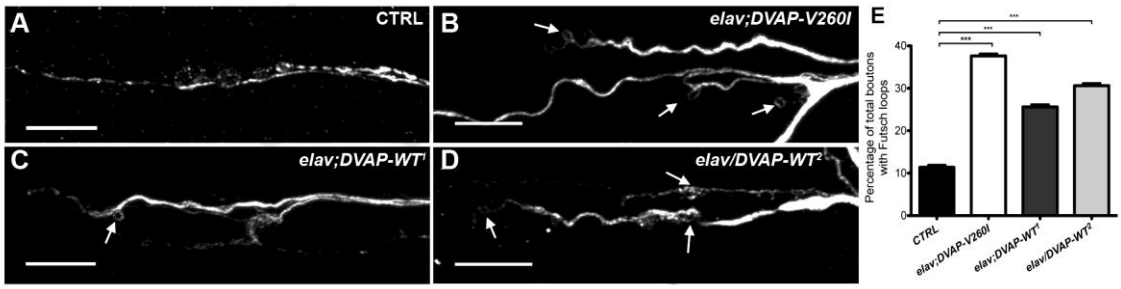

Appendix figure 4. Expression of either *DVAP-V260I* or *DVAP-WT* transgenes in neurons affects synaptic microtubule cytoskeleton. (A) Representative images of branches of NMJs of third instar *elav-Gal4/+* control larvae, (B) *elav;DVAP-V260I*, (C) *elav;DVAP-WT*^{1} and (D) *elav/DVAP-WT*^{2} larval NMJs labeled with antibodies against Futsch to show microtubule loops. Arrows in every panel indicate examples of Futsch loops. Scale bars: 10 um. (E) Quantitative assessment of Futsch-positive loops at A2 and A3 muscle 4 NMJs for each indicated genotype. The highest increase in the percentage of boutons exhibiting looped Futsch staining (relative to the total number of boutons for each NMJ) was observed when *DVAP-V260I* was expressed presynaptically. *** P<0.001.

To study whether DVAP overexpression also affects striated muscles, we expressed the alleles under the control of the muscle-specific driver BG57-GAL4. In controls, DVAP exhibit a signal throughout the muscle but in the three overexpression lines DVAP-immunopositive inclusions are observed (Appendix figure 5). This phenotype was confirmed with brain stainings from the same flies that also presented DVAP-associated inclusions (Appendix figure 6). Then, we analysed muscle nuclei morphology with the purpose of study whether nuclear defects are present in ALS as observed in Parkinson's disease (Liu *et al.*, 2012). Control NMJs present evenly spaced nuclei but in mutant lines they appear closely associated with tendency to form clusters (Appendix figure 5). Measurements of these samples show that in mutant lines, nuclei are not only closer but also longer and bigger than controls, indicating that DVAP overexpression affects neurons and muscles as well, with changes in size and positioning of nuclei. Curiously, *DVAP-V260I* overexpressing muscles presents DVAP signal predominantly inside the nucleus, a translocation previously associated with increased neurodegeneration in Parkinson's disease (Kontopoulos *et al.*, 2006).

Accumulation of protein aggregates has been associated in ALS and other diseases with upregulation of chaperone proteins and their relocation to the nucleus as a cellular response to stress (Vabulas *et al.*, 2010). We observed indeed that lines overexpressing DVAP alleles presented an increase in the accumulation of puncta immunoreactive to Hsp70 compared to control striated muscles (Appendix figure 7). Moreover, in muscles from flies expressing *DVAP-V260I*, Hsp70-positive signal was located mostly inside the nucleus, but in the two overexpressing wild-type alleles, the signal still can be observed partially cytoplasmic, with a lower signal inside the nucleus. These data suggest that DVAP overexpression triggers stress response mediated by heat-shock proteins with intensity proportional to the toxicity of the protein.

To analyse whether all these evidence are correlated to human hallmarks of the disease, we studied the phenotype of adult flies overexpressing DVAP panneurally. A significant decrease in the number of eclosed flies was observed in the three

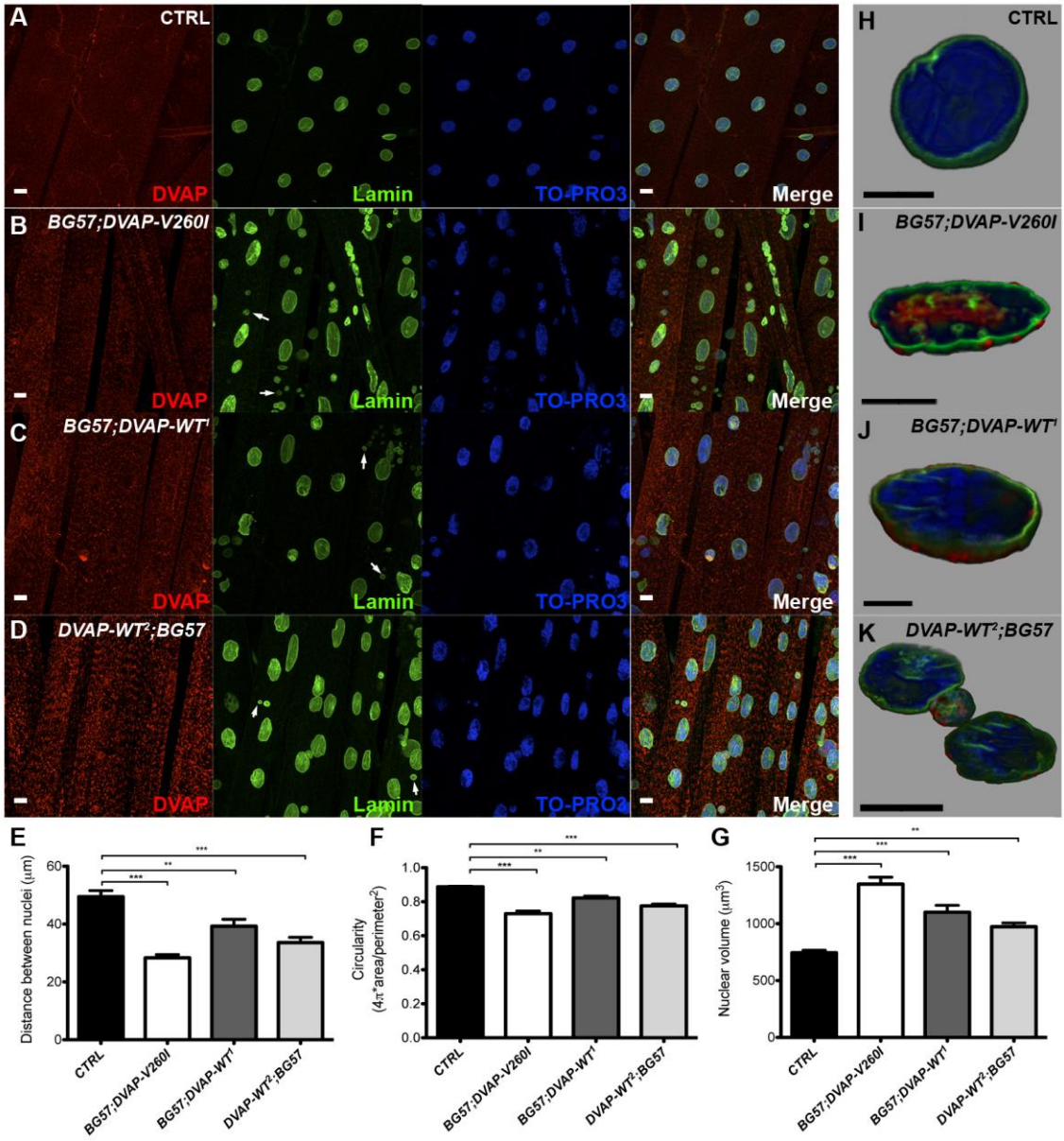

Appendix figure 5. Postsynaptic expression of either *DVAP-V260I* or *DVAP-WT* transgenes results in aggregate formation and changes in nuclear shape, size and positioning. (A) Third instar larval NMJs of *BG57-Gal4/+* control, (B) *BG57;DVAP-V260I*, (C) *BG57;DVAP-WT^{1}* and (D) *DVAP-WT^{2};BG57* NMJs expressing the indicated transgene in muscles were labeled with antibodies specific for DVAP and lamin. Nuclei were visualized with the nuclear specific marker TO-PRO3. (E) Quantification of the distance, (F) circularity and (G) volume of nuclei in randomly selected muscles for each indicated genotype. Sectioned volume renderings of representative triple-labelled nuclei of *BG57-Gal4/+* controls (H); (I) *BG57;DVAP-V260I*; (J) *BG57;DVAP-WT^{1}* and *DVAP-WT^{2};BG57* (K). Scale bars: 10 um. *** P<0.001, ** P <0.01.

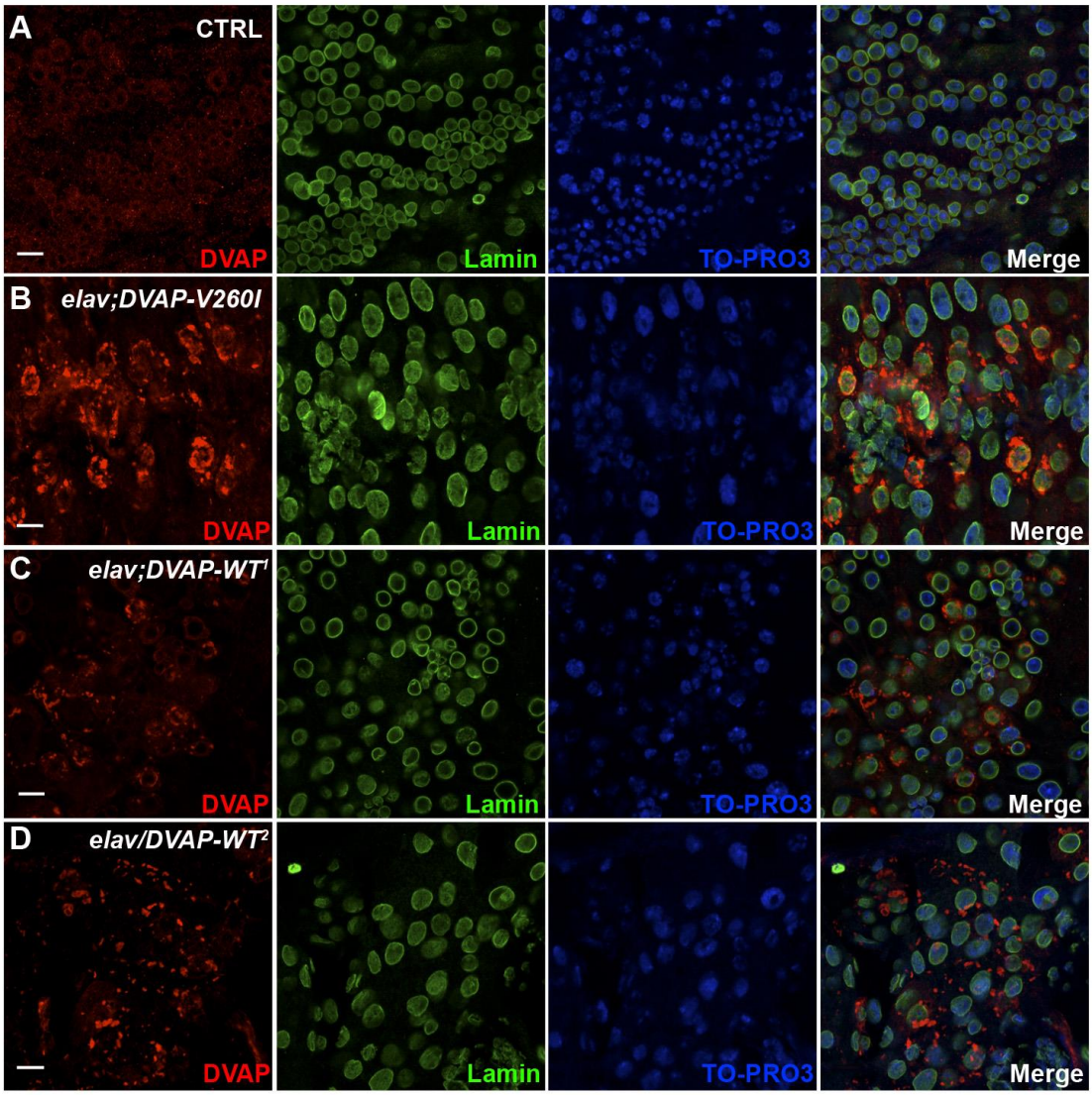

Appendix figure 6. Expression of *DVAP-V260I* and *DVAP-WT* transgenes in neurons leads to aggregate accumulation and disruption of nuclear architecture. (A) Brains of *elav-Gal4/+* control larvae and (B) *elav;DVAP-V260I*, (C) *elav; DVAP-WT*^{1}, (D) *elav/DVAP-WT*^{2} larval brains expressing their respective transgene in neurons were immunostained with antibodies specific for DVAP and Lamin. Nuclei were labeled with the nuclear marker TO-PRO3. Scale bars: 10 um.

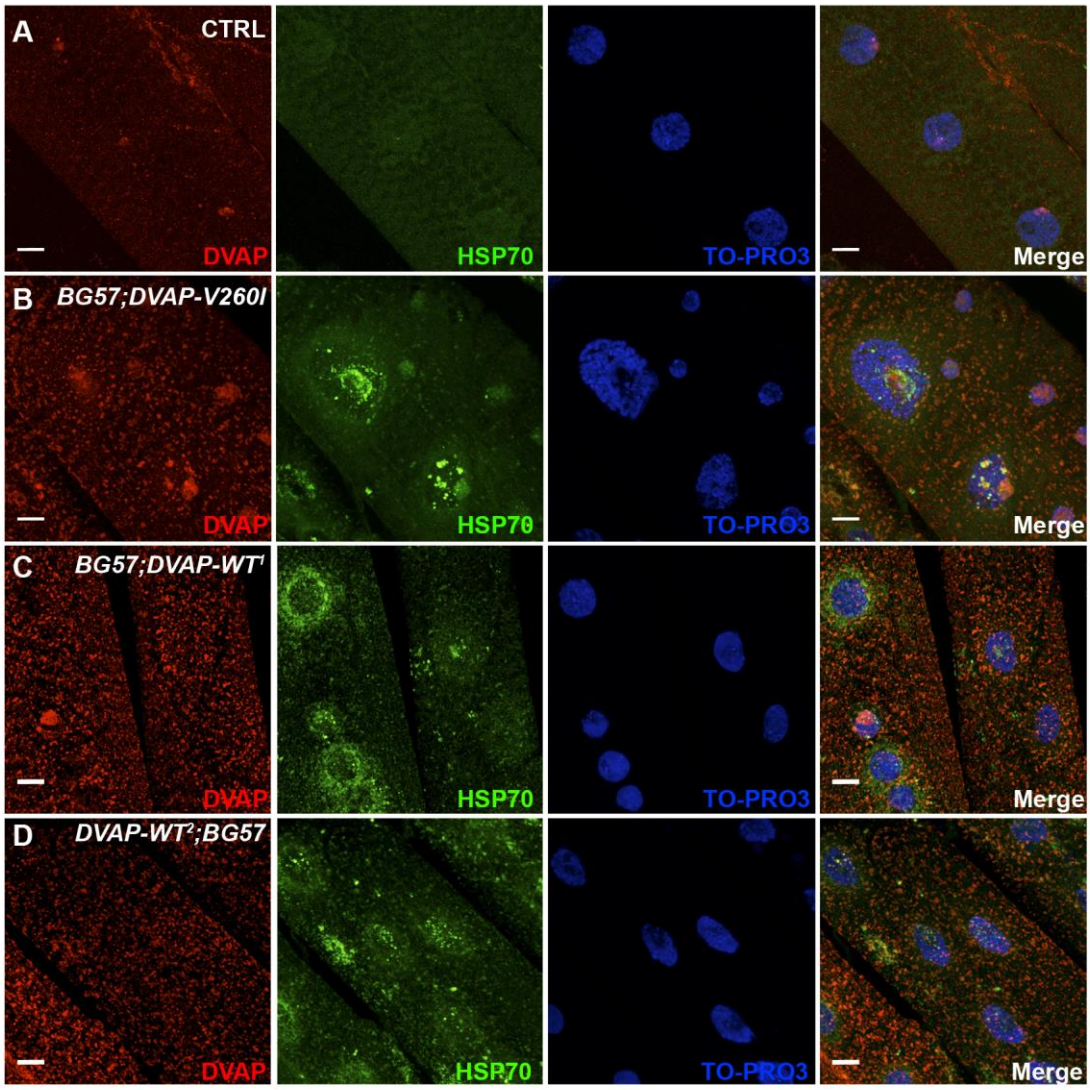

Appendix figure 7. Upregulation and subcellular relocalization of Hsp70 in striated muscles overexpressing either *DVAP-V260I* or *DVAP-WT* constructs. (A) NMJs of *BG57-Gal4/+* control larvae and (B) *BG57;DVAP-V260I*, (C) *BG57;DVAP-WT*^{1} and (D) *DVAP-WT*^{2}*;BG57* larvae expressing their respective transgene were immunolabeled with antibodies specific for DVAP and Hsp70 while nuclei were visualized with the TO-PRO3 nuclear marker. Scale bars: 10 um.

transgenic lines compared to controls, with a more severe effect in *DVAP-V260I* expressing flies (Appendix figure 8). Beside this effect, eclosed flies display postural and locomotion defects, including droopy and held-up wings (Appendix figure 8B-D) and overall uncoordination that led to adult flies to die stucked to the food. When we analysed the eyes of adult flies expressing DVAP transgenes, neurodegeneration was also observed. *DVAP-V260I* expressing flies displayed a rough and smaller eye compared to controls (Appendix figure 9), phenotype also observed in both DVAP-WT lines but in a lower degree. This neurodegeneration was confirmed with stained frontal sections of the internal structure of the eye, where photoreceptor disruption and vacuolisation was present in the three lines. These data indicate that DVAP-WT triggers neurodegeneration, with a more efficient effect from the DVAP-V260I allele.

The novel V234I mutation found in an ALS patient is located in the transmembrane domain of the protein, as compared with the two previous MSP-located VAPB mutations, P56S and T46I. This could translate in potential effects in important VAPB functions such as its interaction with the phosphoinositide phosphatase Sac1 and the ER-Golgi recycling protein YIF1A, both involved in dendritic and synaptic remodeling (Forrest *et al.*, 2013; Kuijpers *et al.*, 2013a). Here, we have linked the expression of DVAP-V260I to known human hallmarks but also to phenotypes never observed previously in the disease. Altered nuclear spacing has been related in other neurodegenerative diseases and myopathies before (Liu *et al.*, 2012; Puckelwartz *et al.*, 2009), but here we observed for the first time its correlation with the overexpression of more aggressive alleles of DVAP. Even though we observed pyknotic nuclei, classical hallmark of apoptosis, these are not present when nuclear phenotypes are already visible. Furthermore, nuclear mislocalisation could trigger apoptosis in an irreversible way (Liu *et al.*, 2012).

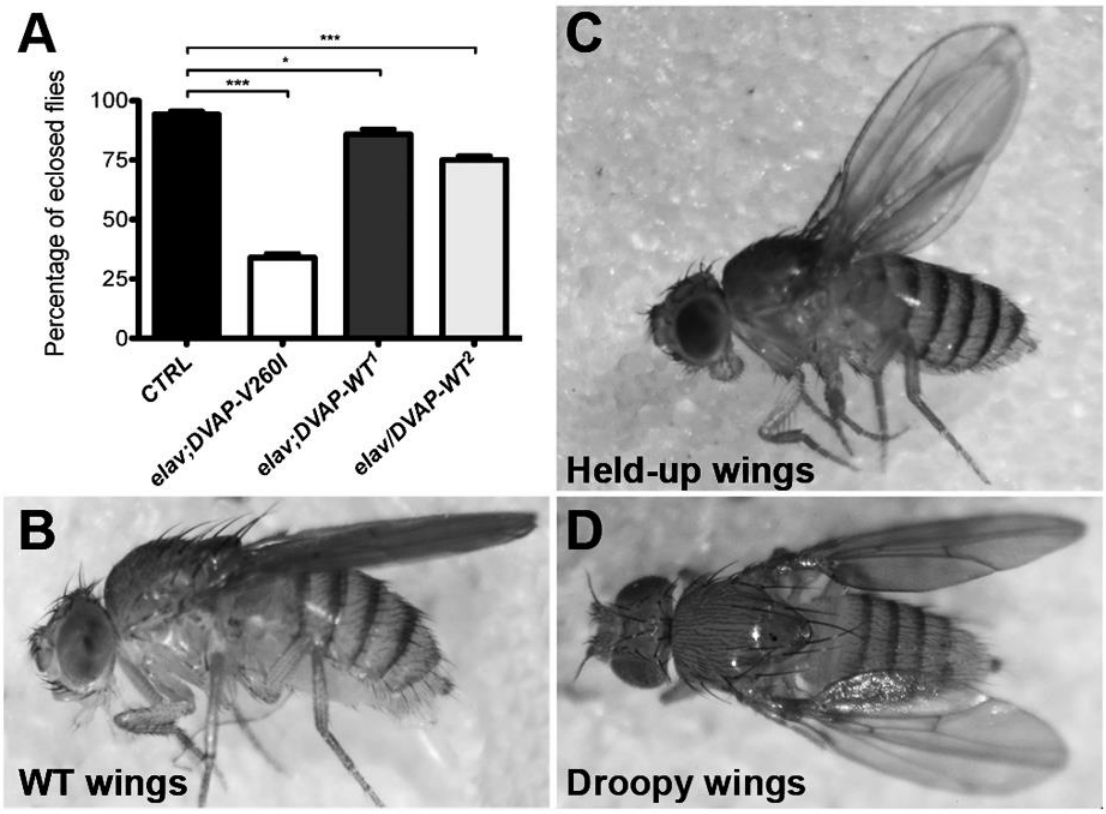

Appendix figure 8. DVAP-V260I and DVAP-WT overexpressors display reduced viability and wing postural defects. (A) Eclosion rate of flies of the designated genotype. (B) *elav-Gal4/+* control flies with a dorsal wing posture. (C) Held-up wings and (D) droopy wing flies. *** P<0.001, * P<0.05.

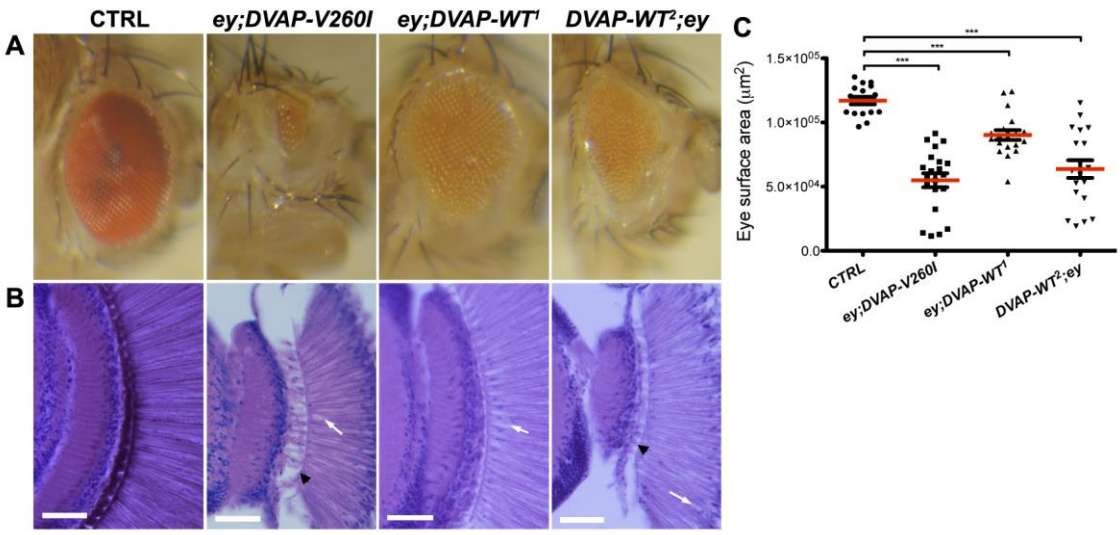

Appendix figure 9. Expression of either DVAP-V260I or DVAP-WT transgenes in adult Drosophila eyes induce neurodegeneration. (A) Stereomicroscope images of *ey-Gal4/+* control eyes and eyes of the indicated genotypes. (B) Frontal sections of control and transgenic eyes of the indicated genotypes stained with H&E. White arrows point to vacuoles in photoreceptors while the black arrowheads indicate areas of extensive tissue degeneration. (C) Quantification of the eye surface area of every genotype. Scale bars: 50 um. (*** P<0.001).

As previously characterised for DVAP-P58S and DVAP-T48I, the expression of DVAP-V260I in flies represents a solid model for the study of neurodegeneration. In this study, we observed three main phenotypes associated with its expression. Firstly, synaptic remodeling is a clear consequence of the overexpression of the three studied alleles with a greater effect in flies expressing DVAP-V260I. These phenotypes are opposite to the ones observed in DVAP-P58S, supporting the idea of a gain-of-function in the novel mutation. Secondly, the presence of DVAP-linked protein aggregates is not only observed in DVAP-P58S but also in other neurodegenerative diseases. This prion-like behaviour is increased with a protein overexpression (Eisele, 2013) and in this case, we noted that DVAP acts in this way, with an overexpression of the protein as sufficient stage to trigger prion-like aggregation of the protein. Finally, the presence of DVAP signal inside the nucleus of flies expressing the DVAP-V260I allele resembles what has been observed in Parkinson's disease (Kontoupoulos *et al.*, 2006). The neuroprotective effect of the histone deacetylase inhibitors against α-synuclein can provide innovative therapeutic alternative to ALS, considering that these inhibitors also decrease toxicity in ALS mouse models (Yoo and Ko, 2011). These three phenotypes associated with DVAP-V260I expression support the novel gain-of-function mechanism and highlight the strong dose-dependence of the phenotypes. Considering the previous loss-of-function mechanism associated with DVAP-P58S, a double mechanism seems probable as the one observed in SMN (Blauw *et al.*, 2012). This double mechanism, however, would implicate more challenging strategies for a future therapy.

Appendix references

Blauw, H. M., Barnes, C. P., van Vught, P. W., van Rheenen, W., Verheul, M., Cuppen, E., Veldink, J. H. and van den Berg, L. H. (2012) SMN1 gene duplications are associated with sporadic ALS. *Neurology* 78, pp.776-780.

Chai, A., Withers, J., Koh, Y.H., Parry, K., Bao, H., Zhang, B., Budnik, V. & Pennetta, G. (2008) hVAPB, the causative gene of a heterogeneous group of motor neuron diseases in humans, is functionally interchangeable with its Drosophila homologue DVAP-33A at the neuromuscular junction. *Human Molecular Genetics*, 17 (2), pp.266–280.

Chen, H.J., Anagnostou, G., Chai, A., Withers, J., Morris, A., Adhikaree, J., Pennetta, G. & de Belleroche, J.S. (2010) Characterization of the Properties of a Novel Mutation in VAPB in Familial Amyotrophic Lateral Sclerosis. *Journal of Biological Chemistry*, 285 (51), pp.40266–40281.

Eisele, Y.S. (2013) From Soluble Aβ to Progressive Aβ Aggregation: Could Prion-Like Templated Misfolding Play a Role? *Brain Pathology*, 23 (3), pp.333–341.

Forrest, S., Chai, A., Sanhueza, M., Marescotti, M., Parry, K., Georgiev, A., Sahota, V., Mendez-Castro, R. & Pennetta, G. (2013) Increased levels of phosphoinositides cause neurodegeneration in a Drosophila model of amyotrophic lateral sclerosis. *Human Molecular Genetics*, 22 (13), pp.2689–2704.

Franco, B., Bogdanik, L., Bobinnec, Y., Debec, A., Bockaert, J., Parmentier, M.-L. & Grau, Y. (2004) Shaggy, the homolog of glycogen synthase kinase 3, controls neuromuscular junction growth in Drosophila. *The Journal of neuroscience*, 24 (29), pp.6573–6577.

Ingre, C., Pinto, S., Birve, A., Press, R., Danielsson, O., de Carvalho, M., Guđmundsson, G. & Andersen, P.M. (2013) No association between VAPB mutations and familial or sporadic ALS in Sweden, Portugal and Iceland. *Amyotrophic Lateral Sclerosis and Frontotemporal Degeneration*, 14 (7-8), pp.620–627.

Kontopoulos, E., Parvin, J.D. & Feany, M.B. (2006) α-synuclein acts in the nucleus to inhibit histone acetylation and promote neurotoxicity. *Human Molecular Genetics*, 15 (20), pp.3012–3023.

Kuijpers, M., Lou Yu, K., Teuling, E., Akhmanova, A., Jaarsma, D. & Hoogenraad, C.C. (2013) The ALS8 protein VAPB interacts with the ER and Golgi recycling protein YIF1A and regulates membrane delivery into dendrites. *The EMBO Journal*, 32 (14), pp.2056–2072.

Lev, S., Halevy, D.B., Peretti, D. & Dahan, N. (2008) The VAP protein family: from cellular functions to motor neuron disease. *Trends in Cell Biology*, 18 (6), pp.282–290.

Liu, G.H., Qu, J., Suzuki, K., Nivet, E., Li, M., Montserrat, N., Yi, F., Xu, X., Ruiz, S., Zhang, W., Wagner, U., Kim, A., Ren, B., Li, Y., Goebl, A., Kim, J., Soligalla, R.D., Dubova, I., Thompson, J., Yates, J., III, Esteban, C.R., Sancho-Martinez, I. & Belmonte, J.C.I. (2012) Progressive degeneration of human neural stem cells caused by pathogenic LRRK2. *Nature*, 491 (7425), pp.603–607.

Nishimura, A.L., Mitne-Neto, M., Silva, H.C., Richieri-Costa, A., Middleton, S., Cascio, D., Kok, F., Oliveira, J.R., Gillingwater, T. & Webb, J. (2004) A mutation in the vesicle-trafficking protein VAPB causes late-onset spinal muscular atrophy and amyotrophic lateral sclerosis. *The American Journal of Human Genetics*, 75 (5), pp.822–831.

Pennetta, G., Hiesinger, P.R., Fabian-Fine, R., Meinertzhagen, I.A. & Bellen, H.J. (2002) Drosophila VAP-33A directs bouton formation at neuromuscular junctions in a dosage-dependent manner. *Neuron*, 35 (2), pp.291–306.

Puckelwartz, M.J., Kessler, E., Zhang, Y., Hodzic, D., Randles, K.N., Morris, G., Earley, J.U., Hadhazy, M., Holaska, J.M., Mewborn, S.K., Pytel, P. & McNally, E.M. (2009) Disruption of nesprin-1 produces an Emery Dreifuss muscular dystrophy-like phenotype in mice. *Human Molecular Genetics*, 18 (4), pp.607–620.

Roos, J., Hummel, T., Ng, N., Klämbt, C. & Davis, G.W. (2000) Drosophila Futsch regulates synaptic microtubule organization and is necessary for synaptic growth. *Neuron*, 26 (2), pp.371–382.

Torroja, L., Packard, M., Gorczyca, M., White, K. & Budnik, V. (1999) The Drosophila beta-amyloid precursor protein homolog promotes synapse differentiation at the neuromuscular junction. *Journal of Neuroscience*, 19 (18), pp.7793–7803.

Vabulas, R.M., Raychaudhuri, S., Hayer-Hartl, M. & Hartl, F.U. (2010) Protein Folding in the Cytoplasm and the Heat Shock Response. *Cold Spring Harbor Perspectives in Biology*, 2 (12), pp.a004390–a004390.

van Blitterswijk, M., van Es, M.A., Koppers, M., van Rheenen, W., Medic, J., Schelhaas, H.J., van der Kooi, A.J., de Visser, M., Veldink, J.H. & van den Berg, L.H. (2012) VAPB and C9orf72 mutations in 1 familial amyotrophic lateral sclerosis patient. *Neurobiology of Aging*, 33, p.e2950.

Yoo, Y.E. & Ko, C.P. (2011) Treatment with trichostatin A initiated after disease onset delays disease progression and increases survival in a mouse model of amyotrophic lateral sclerosis. *Experimental Neurology*, 231 (1), pp.147–159.